



HAL
open science

Synthesis of ligands and metal complexes incorporating oxyallyl patterns

Monika Tripathi

► **To cite this version:**

Monika Tripathi. Synthesis of ligands and metal complexes incorporating oxyallyl patterns. Other. Université Grenoble Alpes, 2019. English. NNT : 2019GREAV033 . tel-02488960

HAL Id: tel-02488960

<https://theses.hal.science/tel-02488960>

Submitted on 24 Feb 2020

HAL is a multi-disciplinary open access archive for the deposit and dissemination of scientific research documents, whether they are published or not. The documents may come from teaching and research institutions in France or abroad, or from public or private research centers.

L'archive ouverte pluridisciplinaire **HAL**, est destinée au dépôt et à la diffusion de documents scientifiques de niveau recherche, publiés ou non, émanant des établissements d'enseignement et de recherche français ou étrangers, des laboratoires publics ou privés.

THÈSE

Pour obtenir le grade de

DOCTEUR DE LA

COMMUNAUTÉ UNIVERSITÉ GRENOBLE ALPES

Spécialité : **Chimie Organique**

Arrêté ministériel : 25 mai 2016

Présentée par

Monika TRIPATHI

Thèse dirigée par **David MARTIN, CNRS**

préparée au sein du **Laboratoire Département de Chimie Moléculaire**
dans **l'École Doctorale Chimie et Sciences du Vivant**

Synthèse de ligands et de complexes métalliques incorporant des motifs oxyallyles

Synthesis of ligands and metal complexes incorporating oxyallyl patterns

Thèse soutenue publiquement le **11 octobre 2019**,
devant le jury composé de :

Monsieur Vincent GANDON

Professeur des Universités, ICMMO, Université Paris-Sud,
Rapporteur

Monsieur Hervé CLAVIER

Chargé de Recherche CNRS, ISM2, Université Aix-Marseille,
Rapporteur

Madame Amor RODRIGUEZ

Tenured Research Scientist, CSIC, Université de Séville (Espagne),
Examinatrice

Monsieur Yannick VALLÉE

Professeur des Universités, DCM, Université Grenoble-Alpes,
Président du jury

Monsieur David MARTIN

Directeur de Recherche CNRS, DCM, Université Grenoble-Alpes,
Directeur de thèse



Dedicated to Dr. Ram kumar Tripathi

My uncle who passed away on 26th July 2018

ACKNOWLEDGEMENTS

Firstly, I would like to thank my doctoral committee members Prof. Vincent Gandon, Dr. Hervé Clavier, Dr. Amor Rodriguez and Prof. Yannick Vallée for taking the time and effort to read, comment and evaluate this work.

My deepest acknowledgement is to my supervisor, Dr. David Martin for giving me an opportunity to be a part of his research group. The work that I have done in his team has helped me to grow from the non-synthetic chemist to a better organic chemist. I would like to thank him for his constant encouragement, guidance and advice throughout my experiments and project work. It was an amazing experience and I have learned a lot about Schlenk techniques and electrochemistry. He has always made time to meet with me & discuss science and I cannot thank him enough for that. Thank you for having me over for dinner at your place in mountains and to see your amazing family. I wish you all the best with your career in France and hope to meet you back someday.

I would like to thank my team, PhD Vianney Regnier, post-doc Christophe Lincheneau, Marc Devillard and Eder Tomas for looking after me during the preparation of this project. Thank you for all the encouragement and support that you have shown and wish you all the best for your future endeavors.

I would also like to thank Prof. Guy Royal and Florian Molton for all their help in electrochemistry. They personally assisted me with some experiments and explained the theory behind that work. I am really grateful for their help to gain a deeper understanding of electrochemistry. X-ray crystallography was an integral part of my research and therefore I would like to thank Christian Philouze and Jacques Pecaut for solving any issues

I might have had with my studies. I would like to thank my supervisor to use the NMR facilities and helping me with any new techniques I needed to use. I wish to express my gratitude towards DCM-lab, Université Grenoble-Alpes, for providing lab facilities to conduct my work. Also, to all the faculty members for the wonderful research experience and the entire lab staff for providing technical support.

I want to thank my family members for all the support they have given me during my undergraduate and graduate education. I could not have done it without you. I want to give special thanks to my parents Shyam kumar Tripathi & Manju Tripathi as well as my aunty Kalpana Tripathi for the continuous love and encouragement during the course of this work. Without your pampering this work could not be made possible. I love you all very much. Next are my very close friends: Nitika Vaish, Akanksha Kapoor and Kritika Narang. I first met them in my Masters course from India and since then we are together. Thank you Kritika for your video calls from Sweden and discussing all the problems related to chemistry and guiding me in the right direction. Thank you Nitika and Akanksha for the great time in Grenoble. I will really miss our dinner time and all the stupid jokes that we have made while being together. This work could not be made possible without your constant mental support.

Finally, I want to thank my boyfriend (now my fiancé) Harshit Bindal. During the three years of my PhD you were always there to deal with all the stress as well as the breakdowns that I accompanied. Going through something difficult as a PhD was a lot easier because of you. From our time together during the past few years, I know that you will always be there for me when I need you the most. I love you!

ABSTRACT

The stabilization of transient and non-observable oxyallyl intermediates can be achieved through the introduction of electron-donating amino substituents. The resulting 1,3-di(amino)oxyallyls are redox-active and can have up to three persistent redox forms. In particular, their radical cations are even air-persistent, as the result of “enhanced” captodative effect. This manuscript reports our efforts for the development of redox-active metal complexes featuring oxyallyl frameworks, with a particular focus on β -diketiminato (NacNac) ligands. Indeed, metal-complexes of the latter generally decompose upon ligand-centered oxidation/reduction and the design of redox-active NacNac remains a challenge.

The first chapter summarizes recent bibliography related to stabilized oxyallyl molecules and the study of redox-active ligands.

The second chapter describes the direct oxidation of vinamidines with *m*-CPBA to afford bis-imine ketone ligands. This methodology is far simpler and easier as compared to the previously described method from the literature. The coordination chemistry of these ligands and their redox behavior were also studied.

The third chapter explores an original substitution pattern on bis-imine ketones, with the introduction of electron-donating amino groups in 1,3-positions. A detailed study of the reaction of 1,3-dichloro vinamidinium salts with aniline derivatives is reported, as well as preliminary study of the metal coordination of the novel electron-rich ligand.

The last chapter presents alternatives strategies and concepts, including the use of O-protected and/or bidentates ligands.

Keywords: Organic chemistry, Ligands, Complexes, Metal-free oxidation, Redox properties.

RÉSUMÉ

Les oxyallyles sont considérés généralement comme des espèces transitoires non observables, mais peuvent être stabilisés par l'introduction de groupements aminés donateurs d'électrons. De tels 1,3-di(amino)oxyallyls sont rédox-actifs et peuvent exister sous jusqu'à trois formes redox. En particulier, leurs cations radicaux sont persistants à l'air, en raison d'un effet captodatif «extrême». Ce manuscrit décrit nos efforts pour développer des complexes métalliques redox-actifs comportant des motifs oxyallyles, avec une attention particulière pour les ligands de type β -diketimate (Nacnac). En effet, en général, les complexes de ces derniers se décomposent lors de d'une oxydation/réduction centrée sur le ligand et la conception de version redox-actives représente encore un défi.

Le premier chapitre résume la littérature récente concernant les oxyallyles stabilisés et l'étude des ligands redox actifs.

Le second chapitre décrit l'oxydation directe de vinamidines par *m*-CPBA pour former des ligands bis(imino)cétones. Cette approche synthétique représente une amélioration importante par rapport aux méthodologies précédemment décrites. La chimie de coordination et l'électrochimie de ces composés ont également été étudiées.

Le troisième chapitre explore l'introduction d'un nouveau motif di(méthyl)amino en positions 1 et 3 des bis(imino)cétones. Nous décrivons notamment une étude détaillée de la réaction des sels de 1,3-dichlorovinamidinium avec des dérivés de l'aniline, ainsi qu'une étude préliminaire de la chimie de coordination du nouveau ligand enrichi électroniquement.

Le dernier chapitre expose des stratégies et des concepts alternatifs, notamment l'utilisation de ligands O-protégés et/ou bidentés.

Mots clés: Chimie Organique, Ligands, Complexes, Oxydation sans métal, Propriétés redox.

TABLE OF CONTENTS

CHAPTER I: INTRODUCTION	1
I.1 Organic oxyallyl derivatives	3
I.1.1 Oxyallyls: the transient species	3
I.1.2 Stabilized versions of oxyallyls.....	6
I.1.3 Origin of the stability of 1,3-di(amino)oxyallyl radical cations	10
I.2 Oxyallyl-metal complexes.....	11
I.2.1 The known metal-oxyallyl compounds	11
I.2.2 Redox-active ligands.....	13
I.2.3 Oxyallyl patterns for designing redox-active NacNac ligands?	18
I.3 Overview of the project	22
CHAPTER II: BIS-IMINE KETONES (α-keto-β-diimines)	23
II.1 State of the art	25
II.1.1 Modification of β -diketiminates at central carbon ($R' \neq H$)	25
II.1.2 Applications of bis-imine ketones.....	27
II.1.3 Complexes of bis-imine ketones and the related derivatives	28
II.1.4 Synthesis of metal free bis-imine ketones	32
II.2 Results	34
II.2.1 Metal free oxidation of vinamidiniums	34
II.2.2 m-CPBA oxidation of vinamidines	36
II.2.3 Coordination chemistry of the obtained bis-imine ketone ligands.....	39
II.2.4 Oxidation of metal complexes bearing macrocyclic ligands	40
II.3 Conclusion.....	43
II.4 Experimental.....	44
CHAPTER III: BIS-IMINE KETONES INTEGRATING DIMETHYLAMINO GROUPS	51
III.1 1,3-dichlorovinamidinium precursors	53
III.2 Selectivity in the reaction of aniline with 1,3-dichlorovinamidinium salt	54
III.3 Investigation by DFT calculations	56
III.4 Limitations in the reaction of 1,3-dichlorovinamidinium with bulky anilines	61

III.5 Synthesis and study of an electron-enriched bis-imine ketone.....	63
III.6 Conclusion	67
III.7 Experimental	68
CHAPTER IV: ALTERNATIVE SYNTHETIC DESIGN & STRATEGIES.....	81
IV.1 O-protected ligands.....	83
IV.1.1 Preparation of O-protected ligands: preliminary considerations.....	84
IV.1.2 Bis(oxazoline)-based model	86
IV.2 Perspectives: alternative design for metal-based oxyallyls?	90
IV.2.1 Bis(methylbenzimidazolyl)ketone	91
IV.2.2 N,O-bidentate ligands	92
IV.3 Conclusion.....	98
IV.4 Experimental	99
CONCLUSION & PERSPECTIVES.....	113
REFERENCES.....	117
APPENDIX.....	125

CHAPTER I: INTRODUCTION

The objective of this PhD work was to produce different ligands for the synthesis of redox-active metal complexes featuring oxyallyl patterns. Initially, oxyallyls were considered as unstable intermediates that are too reactive to be isolated or to be observed but recently our research team has demonstrated that these species can be stabilized with the rational modifications of steric and electronic effects of substituents. Stable versions of oxyallyls can show redox activity by the virtue of their ability to store and deliver electrons. Therefore, the main goal of this thesis was to obtain a variety of ligand structures, the corresponding oxyallyl-metal complexes and the study of overall redox properties.

I.1 Organic oxyallyl derivatives

I.1.1 Oxyallyls: the transient species

(i) Reaction intermediates

A chemical reaction is a process in which one or more chemical compounds, the reactants, by their consumption during the reaction are converted into one or more different compounds called products that are formed as a result of the process. These reactions can sometimes go through the formation of the transient or elusive species that are known as reactive intermediates which can be formed in the preceding step and consumed in a further step to ultimately obtain the final product. These species can be classified as charged or uncharged intermediates depending on the mechanism of the reaction. The lifetime of such type of intermediates is usually short and in some cases their isolation or even observation is challenging.

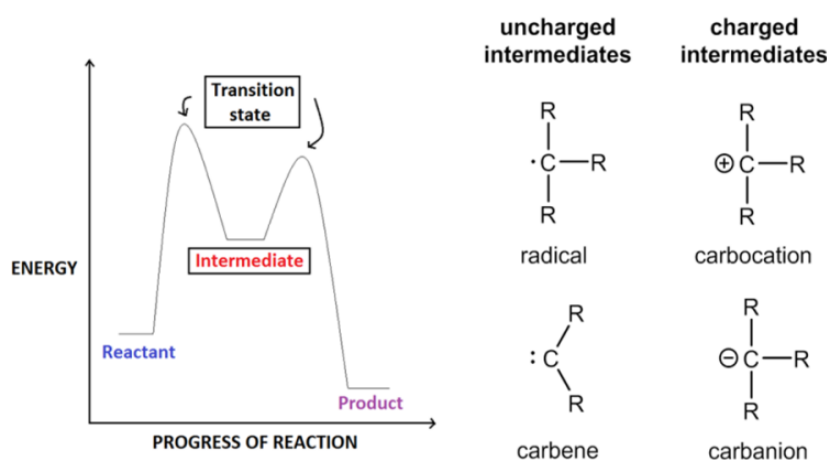


Figure 1: Energy diagram of a reaction and examples of reactive intermediates

The discovery of the stable forms of such transient species has impacted modern chemistry¹ as it has opened new opportunities for innovative concepts and applications. For instance, in 1900 Gomberg² reported a persistent radical by the treatment of tri(phenyl)methyl chloride with the zinc or silver metal. The further extension of the tri(phenyl)methyl radical structure to the formation of the first stable bi-radical specie was studied by Schlenk in 1915.³ These seminal discoveries led to the acceptance of existence of organic radicals by the scientific community and can be considered as the foundation of numerous fields in organic or polymer chemistry and also far beyond in biology, medicine and material science.⁴

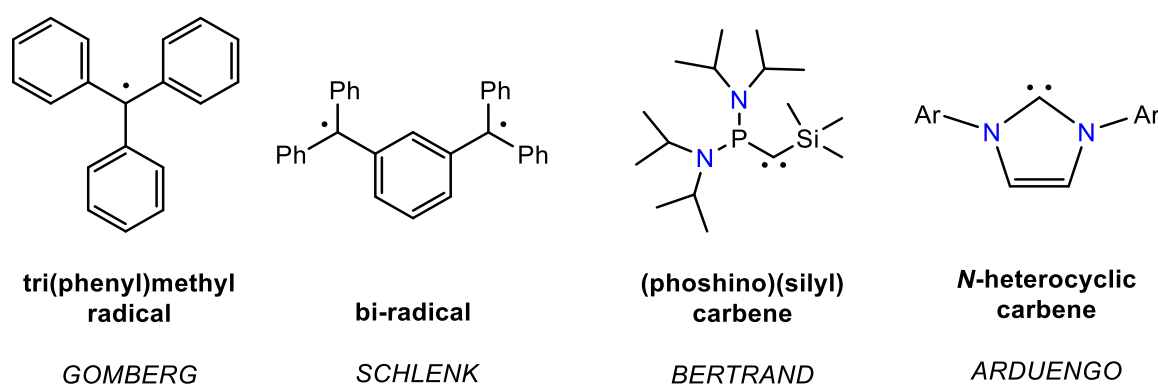


Figure 2: Stable form of intermediates

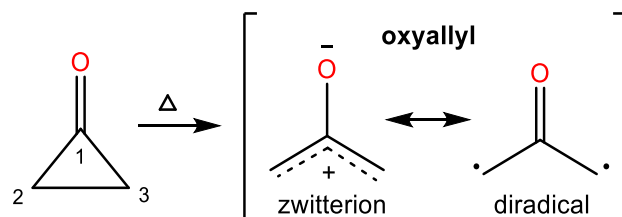
Another example is given by carbenes which had long been regarded as non-isolable intermediates. A (phosfino)(silyl) carbene was the first stable carbene generated by the photolysis of the corresponding diazo compounds⁵ by Bertrand and co-workers in 1988. In 1991, Arduengo *et al* synthesized the first N-heterocyclic carbene⁶ (NHC) that was generated by the deprotonation of the respective imidazolium chloride salt and fully characterized by X-ray diffraction study.

After these initial discoveries many stable versions of intermediates have been reported⁷ and have found applications in the field of catalysis including the design of efficient ruthenium based catalysts for olefin metathesis as well as the use of NHC-silver complexes as antimicrobials.⁸

Our research team has been interested in designing the stable versions of another kind of reactive intermediates: oxyallyls.

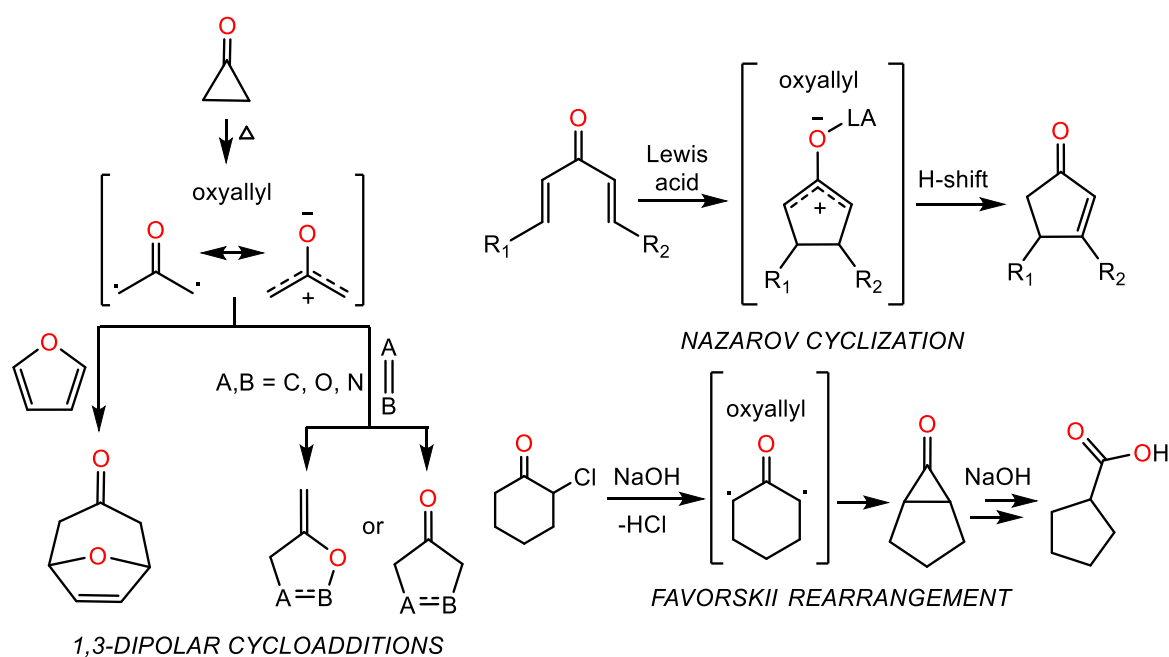
(ii) Oxyallyls as elusive intermediates

The possibility that cyclopropanone could adopt an open form by the cleavage of its C₂-C₃ bond was first stated by R. Hoffmann in 1968.⁹ These hypothetical acyclic structures are known as “oxyallyls” and belong to the class of non-Kekulé molecules. In fact, despite having an even number of electrons, their neutral π system can be described only with zwitterionic or diradical resonance forms (Scheme 1).



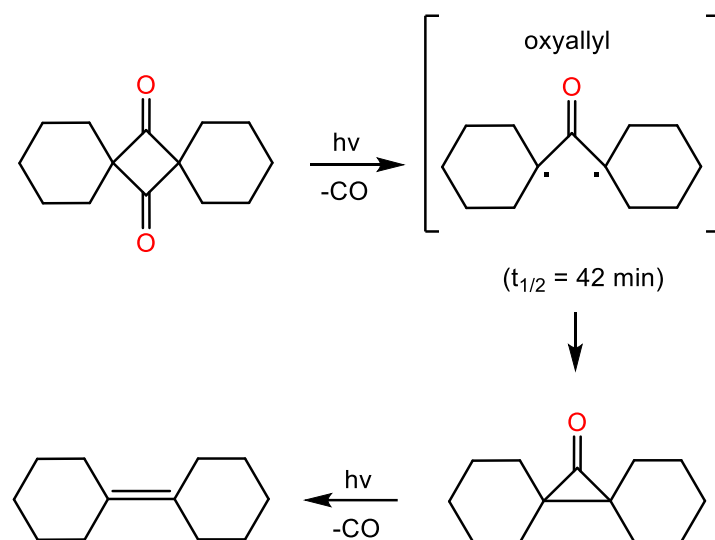
Scheme 1: The general structure of ‘oxyallyl’

These moieties had been considered as non-observable, generally too reactive and usually evade spectroscopic observation as their ring closure to give the corresponding cyclopropanone occurs within picoseconds with a negligible activation barrier.¹⁰ They have been postulated as highly reactive intermediates in several key reactions¹¹ such as 1,3-dipolar cycloadditions^{11a,e,f,i}, Nazarov cyclizations^{11g,h} and the Favorskii rearrangement^{11b} (Scheme 2).



Scheme 2: Oxyallyl derivatives as reactive intermediates

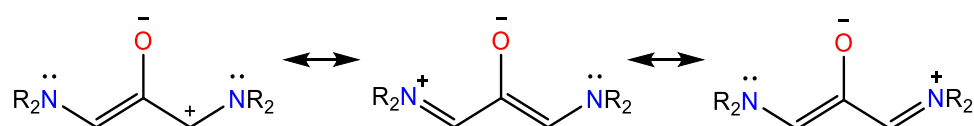
For decades despite numerous attempts,¹² even the existence of oxyallyls couldn't be proved experimentally. It is only in 2011 that Garcia-Garibay *et al* finally reported the observation of di(cyclohexyl)oxyallyl¹³ specie as a deep blue product (Scheme 3) that has a half-life of some picoseconds in solution depending on the solvent whereas 42 minutes in the solid state at room temperature. The oxyallyl ultimately decay to dicyclohexylidene by the loss of C=O group due to its decomposition under irradiation and therefore could not be isolated in the stable form.



Scheme 3: Observation of a di(alkyl)oxyallyl

I.1.2 Stabilized versions of oxyallyls

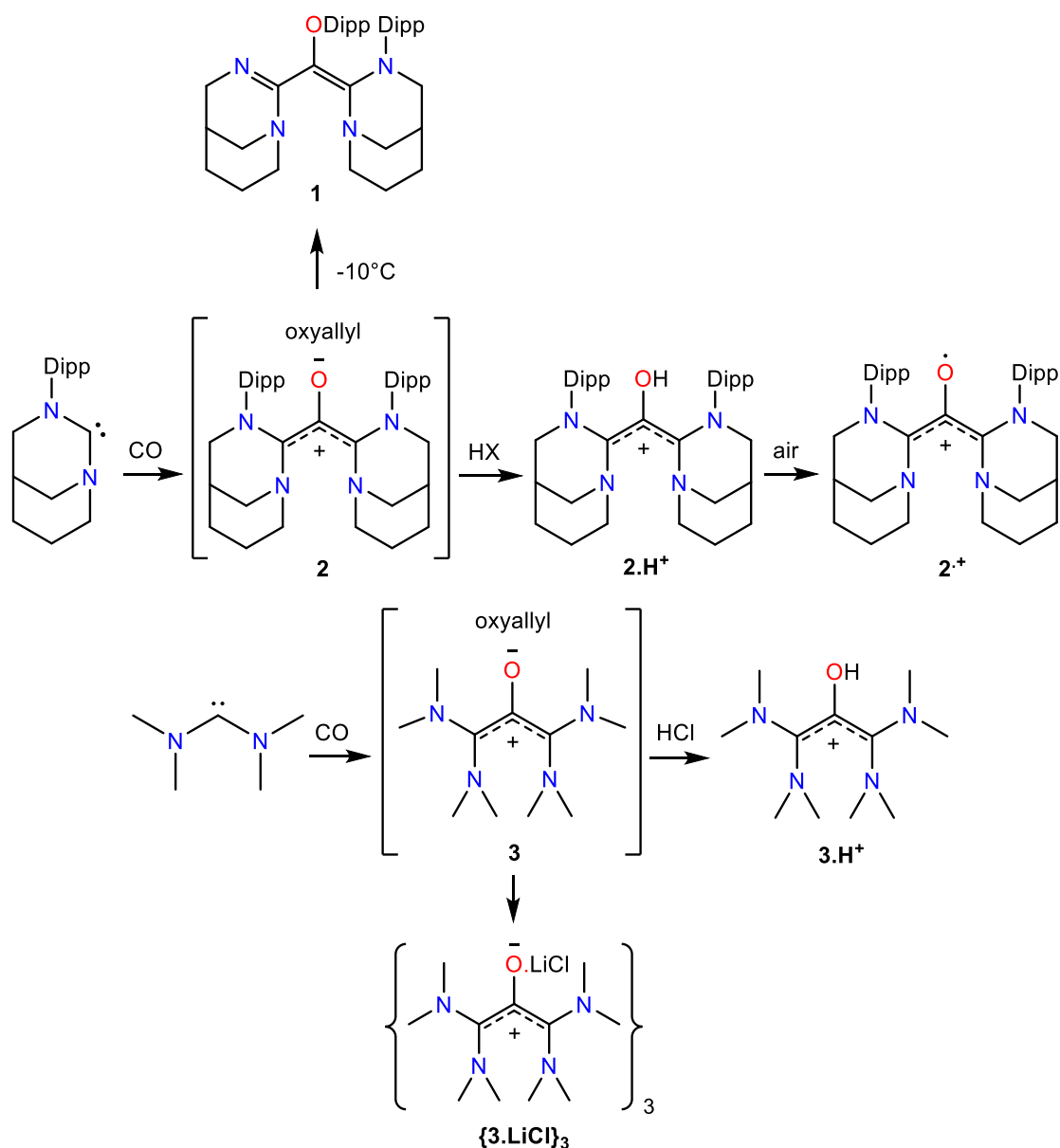
Recent results in the laboratory indicate that strong electron-donating amino substituents can dramatically stabilize oxyallyl derivatives¹⁴ due to their ability to form different mesomeric structures by the delocalization of π electrons (Scheme 4).



Scheme 4: Mesomeric forms of stabilized oxyallyls featuring 1,3-amino groups

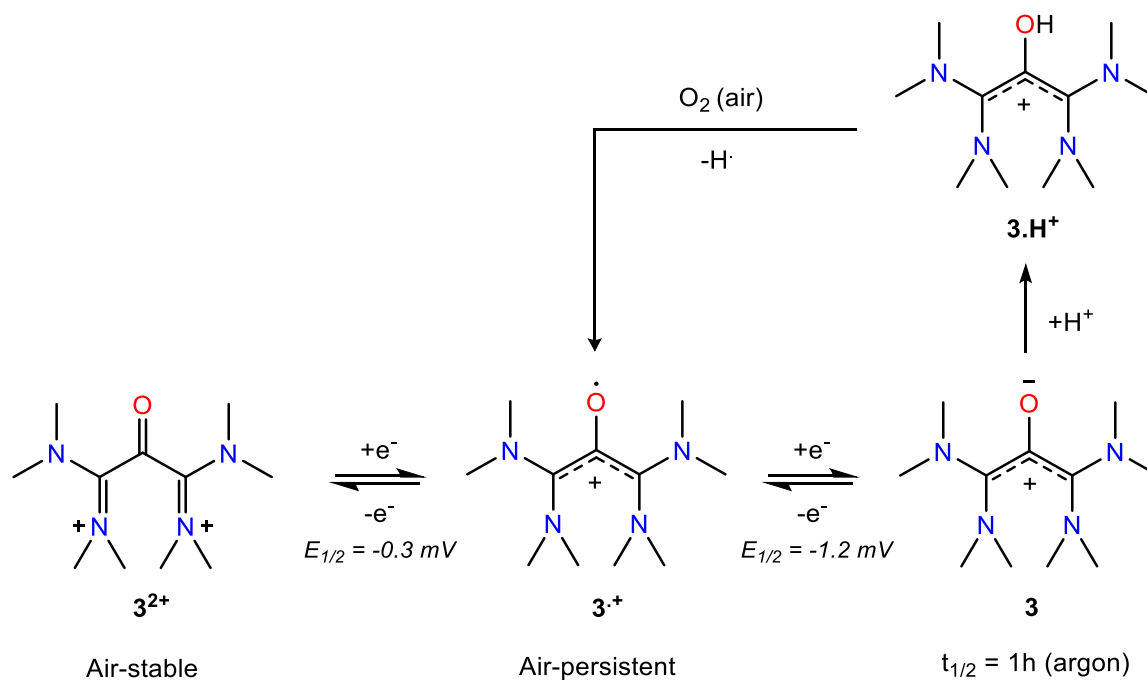
In Scheme 5, two examples of 1,3-di(amino)oxyallyls are shown which are stable enough to be observed by NMR in solution. Oxyallyl **2** was generated by the reaction of 'anti-Bredt' N-heterocyclic di(amino)carbene (NHC) with carbon monoxide (CO). It was rearranged at -10°C , avoiding its isolation, through the migration of diisopropylphenyl

(Dipp) group to yield compound **1**. In order to avoid Dipp migration, the protonated form **2.H⁺** of oxyallyl was isolated which can further behave as an **H[•]** donor to form the corresponding radical cation **2^{•+}** upon treatment with air. Similarly, the reaction between acyclic di(amino)carbene (ADAC) and CO generated oxyallyl structure **3** that can be isolated and crystallized in the form of trimeric lithium chloride adduct **{3.LiCl}₃**.



Scheme 5: Examples of reported 1,3-di(amino)oxyallyl derivatives

Our research team has reported^{14c} the isolation of oxidized dication **3²⁺** whose one-electron reduction can give the corresponding radical cation **3^{•+}** and two-electron reduction led to the corresponding oxyallyl **3** (Scheme 6).

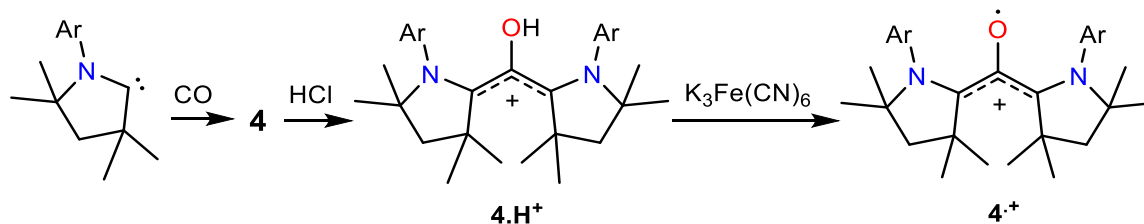


Scheme 6: Different redox states of the di-cation 3^{2+}

The similar cyclic voltammetric study was applied to oxyallyl **2** that further evidenced the formation of its four different redox-states (from 2^{2+} to $2\cdot^-$). The zwitterionic oxyallyl molecules have been characterized by NMR and can be isolated as O-coordinated metal complexes or their protonated salts. Note that these latter species are formal $\text{H}\cdot$ donors and can be easily re-oxidized into the corresponding radical cations with a soft oxidant (air, potassium ferricyanate, etc).

Hence, overall, these patterns are original reservoirs for electrons and protons. Therefore, 1,3-di(amino)oxyallyls can be considered as redox-active species for designing various ligands and metal complexes to play further with electrons (and protons).

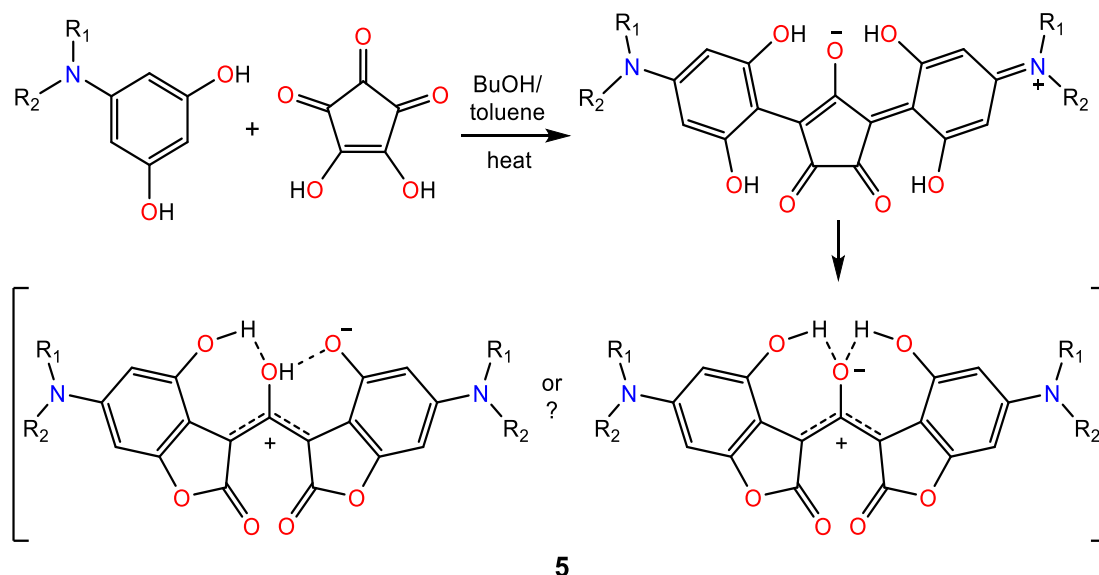
However, the stabilization of oxyallyls does not require four amino substituents surrounding their structure. As described in Scheme 7, the oxyallyl **4** features only two donating groups. It was obtained similarly by the reaction of cyclic(alkyl)(amino) carbene (CAAC) with CO^{15} and was isolated in the form of its protonated salt $4\cdot\text{H}^+$ whose further oxidation formed radical cation $4^{+\cdot}$. Both of these compounds $4\cdot\text{H}^+$ and $4^{+\cdot}$ were found to be stable towards air and moisture.



Scheme 7: Stable 1,3-di(amino)oxyallyl derivatives

In 2003, Tian *et al* reported the synthesis of compounds **5** that can be seen as examples of oxyallyl structure with two donating 4-aminophenyl groups (Scheme 8). Compounds **5** were isolated in very low yields (0.2-7.4 %) as trace impurities resulting from the condensation reaction of croconic acid with the corresponding dihydroxyaniline.^{16a} These compounds are near IR-dyes that can be used for designing non-linear optic materials due to their tendency to form J-aggregates on spin-coated films.¹⁷

Note that the genuine structure of compounds **5** is blurred by the sharing of two hydrogens by three hydroxyl groups. As a matter of fact, X-ray diffraction analysis of **5** showed similar bond lengths of all the C-O bonds present in the oxyallyl pattern and phenoxy components.^{16b}



Scheme 8: Formation of 5 in low-yields by the rearrangement of croconaines

1.1.3 Origin of the stability of 1,3-di(amino)oxyallyl radical cations

1,3-di(amino)oxyallyl radical cations constitute a new class of highly air-persistent radicals. Radicals **2⁺** and **4⁺** have been stored for more than 4 years without any evidenced decomposition whereas **3⁺** has a half-life of several hours in a well-aerated solution.

These results are remarkable as the lifetime of typical carbon centered radical species is very short because their reactions are often thermodynamically favored with low energy barriers.¹⁸ For instance, they can undergo rapid dimerization, disproportionation or hydrogen abstraction reactions. Carbon based radicals can also react with oxygen to give out peroxide radicals and the corresponding derivatives.

It is well known that the capto-dative effect¹⁹ can weaken the C-C bond of the dimer due to the combination of electron-donating, electron-withdrawing or bulky substituents that favor the formation of small amounts of monomeric radicals and can be detected in solution. A typical textbook example is 2-oxomorpholin-3-yl radical featuring the capto-dative association of an amino (donor) and a carboxy (acceptor) group. It was isolated in the solid state as the corresponding C-C dimer (Figure 3). The dissociation constant of this dimer was about 10^{-9} M at room temperature allowing the observation of a radical in de-gassed solution by EPR spectroscopy.²⁰

The first monomeric amino carboxy radical and the related bi- or tri-radicals²¹ were synthesized from cyclic (alkyl)(amino)carbenes (CAAC) which provided bulky environments that can further prevent the dimerization of the radicals. These radicals were perfectly stable under inert atmosphere but decay within few seconds when exposed to air (Figure 3). Half-lives of these radicals in air were increased up to several days by incorporating electron withdrawing substituents at the carboxy moiety. The impact of the electronic effects on their air stability was theoretically studied and interpreted as the result of “enhanced” capto-dative combination (Figure 4).¹⁵

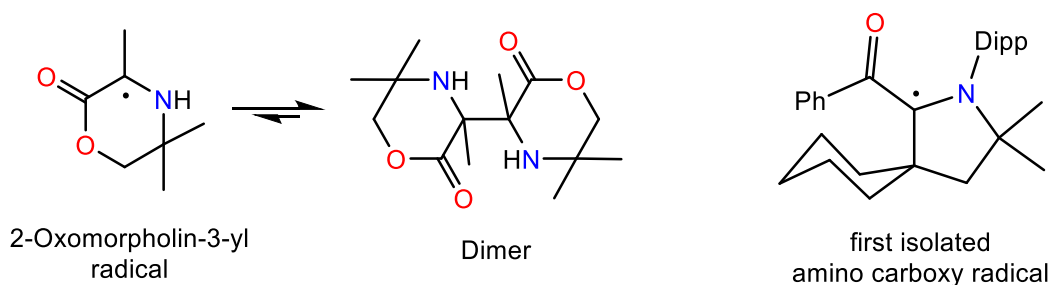


Figure 3: Observation of the C-C dimer and the first isolated amino carboxy radical

The trends observed for the stability of these monomeric amino carboxy radicals explains the air-persistency of the previously mentioned oxyallyl radical cations **2**⁺, **3**⁺ and **4**⁺. Indeed they can be also described as C-radical centers stabilized by “enhanced” capto-dative combination as they feature an electron donating amino substituent and an electron withdrawing carboxy group which is activated by an iminium moiety (Figure 4).

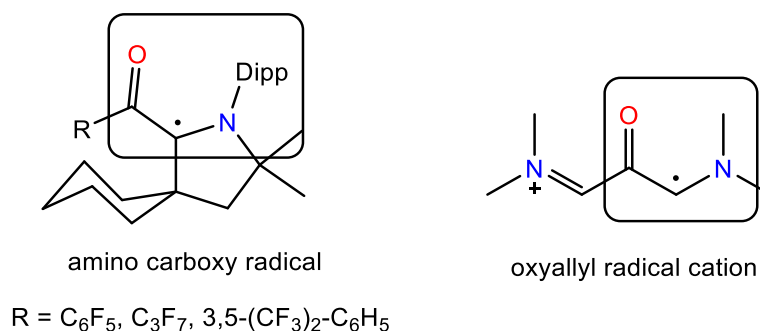


Figure 4: “Enhanced” capto-dative stabilization of radicals

I.2 Oxyallyl-metal complexes

I.2.1 The known metal-oxyallyl compounds

As discussed before, most of the stabilized class of oxyallyls were isolated in their protonated forms but the metal O-coordination of these species could also aid their isolation as stable species.

Siemeling^{14b} in 2013 reported the observation of oxyallyl **3** by the carbonylation reaction of the corresponding di(amino)carbene that was crystallized in the form of air-sensitive trimeric lithium chloride adduct **{3.LiCl}**₃ (Figure 5). Each Li atom in the complex has two O atoms and one Cl atom in its surroundings in a trigonal-planar three-

coordinate environment forming the inorganic core $[\text{Li-O}]_3$ in a regular hexagon geometry. The average bond lengths of Li-O and Li-Cl are 1.86 Å and 2.28 Å respectively which are remarkably short due to low coordination number in the complex. The formation of oxyallyl **3** was observed by the red-orange solution through in-situ NMR spectroscopy that revealed one signal in ^1H NMR and two signals in ^{13}C NMR.

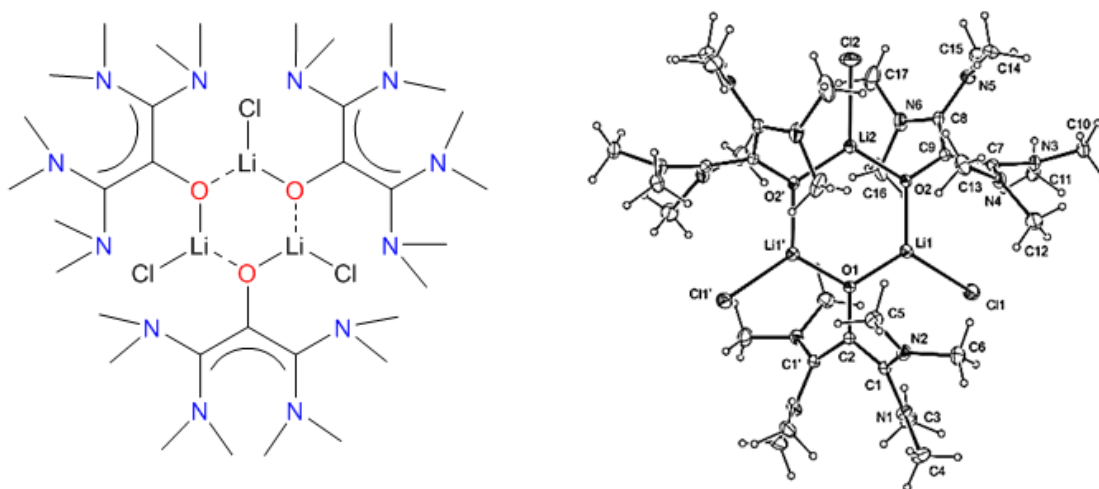
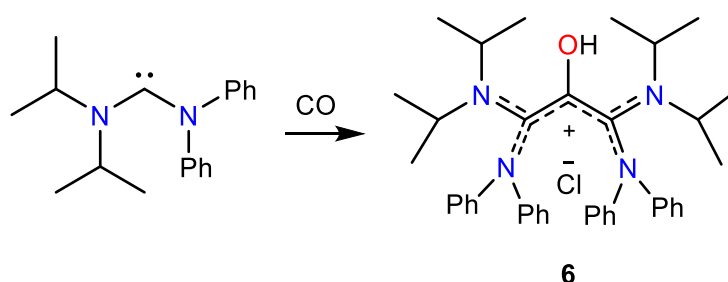


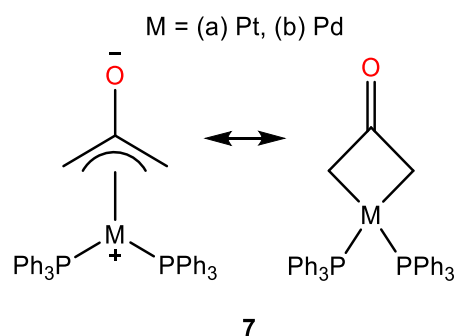
Figure 5: Crystal structure of lithium chloride adduct $\{3.\text{LiCl}\}_3$

A similar reaction was performed with a more bulky carbene in the presence of CO to afford the red hydrochloride salt **6** after acid work up which can be attributed to the structure of protonated form of oxyallyls (Scheme 9). The X-ray diffraction study confirmed that the value of C-O bond length (1.4 Å) in compound **6** and complex $\{3.\text{LiCl}\}_3$ (1.36 Å) are in the range observed for the related protonated oxyallyl derivatives (for $2.\text{H}^+$, C-O = 1.36 Å). Therefore, we can say that the structure of lithium chloride adduct $\{3.\text{LiCl}\}_3$ has an oxyallyl pattern in its backbone and can be considered similar to the protonated oxyallyl forms.



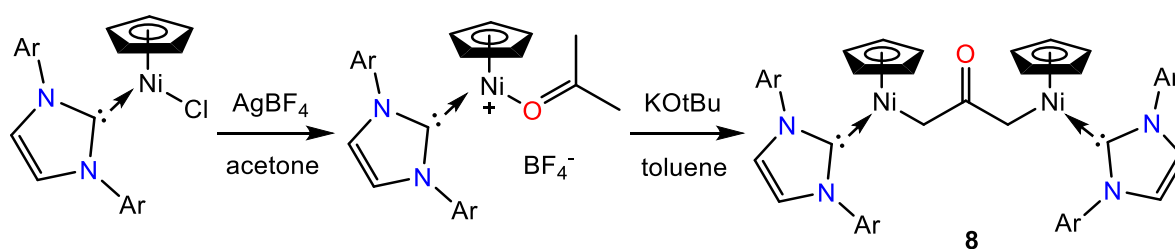
Scheme 9: Carbonylation of bulkier acyclic di(amino)carbene to form compound 6

Various organometallic compounds which can be seen as complexes of oxyallyls have been also reported in the literature.²² The platinum(II) complex **7a** possesses two relevant canonical forms, i.e., metallacyclobutanone and π -allyl. In the case of palladium(II) complex **7b**, the structural and spectroscopic studies indicate a larger contribution of the π -allylic character.^{22c}



Scheme 10: The oxyallyl-metal complexes 7

Chetcuti *et al* reported the synthesis of dinickel complex **8** by the deprotonation of cationic nickel(II) complex of acetone in which the central bridging ligand was regarded as a trapped oxyallyl (Scheme 11).^{22d} However, it is important to note that the complex **8** may be better viewed as a bis-enolate complex. Furthermore, the redox properties of the complexes **7** and **8** were not studied by the author.



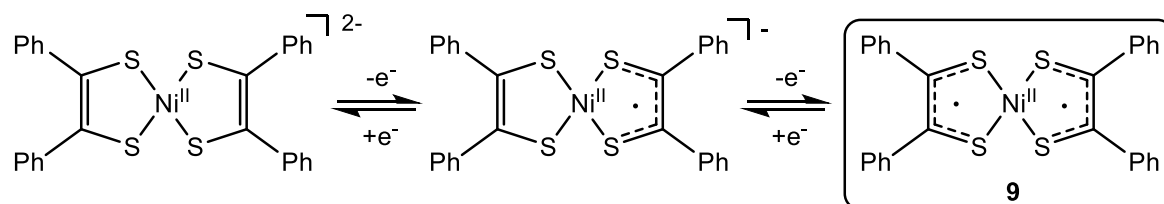
Scheme 11: Synthesis of di(metalla) ketone 8

1.2.2 Redox-active ligands

The particular category of ligands that can access multiple oxidation states in the metal complexes are known as redox-active ligands. The stepwise electrochemical or chemical one-electron oxidation or reduction can result in different oxidation states.

In Scheme 12, the oxidation state of the nickel(II) dithiolene complex $[\text{Ni}(\text{S}_2\text{C}_2\text{Ph}_2)_2]^z$ can exist in three different forms ($z = 2-, 1-, 0$) where stilbene-1,2-dithiolate acts as a redox-

active species favoring the ligand centered oxidation rather than the oxidation of the nickel metal to form the radical analogue **9** of the supporting redox-active ligand.



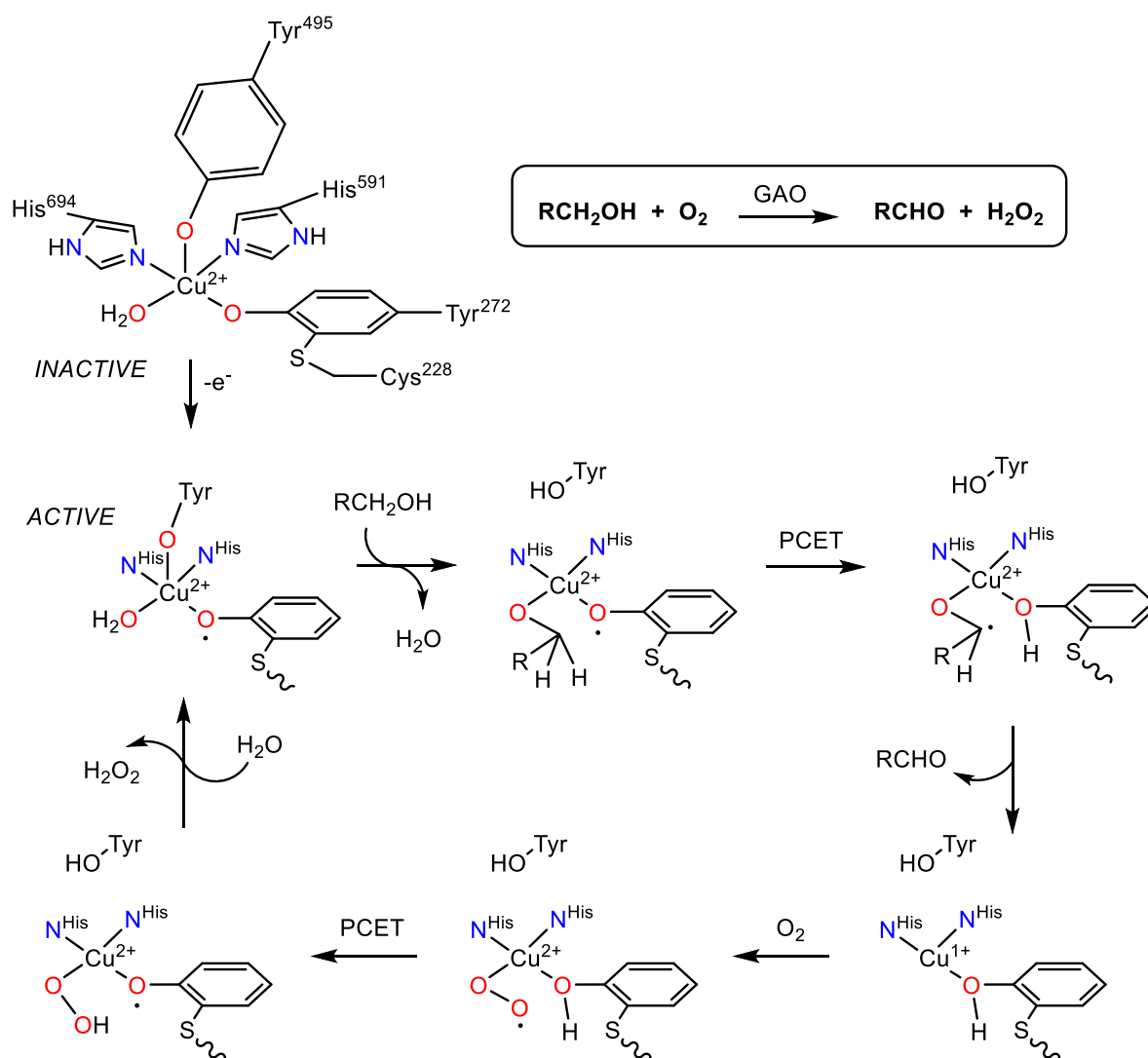
Scheme 12: Redox-active stilbene-1,2-dithiolate ligand $S_2C_2Ph_2$

Several analytical techniques are available that helps to determine the clear oxidation states of the metal ion and the redox-active ligands such as cyclic voltammetry, single crystal X-ray diffraction, UV-vis spectroscopy, EPR spectroscopy or density functional theory (DFT) calculations.²³ Apart from the redox-activity, the ligands where there is an ambiguity to assign the formal oxidation states are considered as non-innocent ligands.

The use of metal complexes with the radical structure of the redox active ligands plays a crucial role in the mechanism of catalytic processes in certain enzymatic reactions to complement the redox properties of the metalloenzymes.²⁴

Perhaps the most understood and studied example of metal-catalysis involving a redox-active ligand is the oxidation of primary alcohols to aldehydes catalyzed by the enzyme galactose oxidase (GOA).²⁵

The accepted catalytic cycle of the enzyme involves a redox-active phenolate as described in Scheme 13. The first step is the oxidation of sulfur-modified tyrosine-272 moiety to obtain the oxygen centered radical coordinated to a Cu(II) ion. The RCH_2OH group then binds through the Cu-O-Tyr-495 bond on the galactose with the release of TyrOH substituent. The radical is shifted to the galactose-alkoxide moiety by the proton-coupled electron transfer (PCET) that further reduces Cu(II) to Cu(I) with the formation of the oxidized product. The release of H_2O_2 is achieved afterwards by the reaction of the reduced enzyme with dioxygen via PCET and thus completing the cycle. There is an overall two-electron change in this catalytic cycle: one-electron oxidation is affected by the tyrosyl radical and another one-electron oxidation is performed by the Cu(II)/Cu(I) couple (Scheme 13).

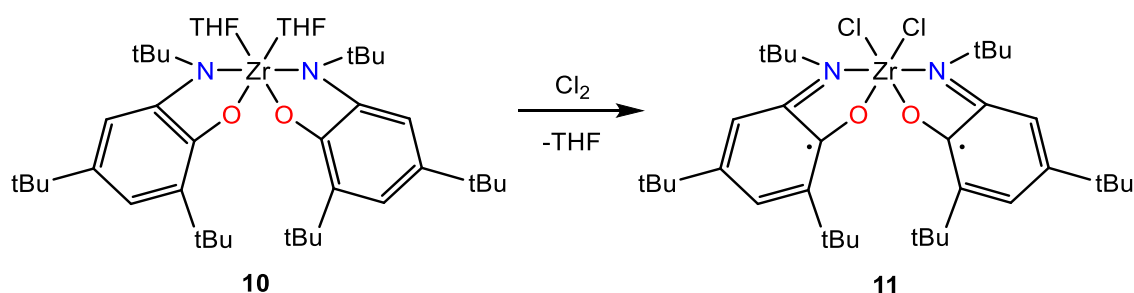


Scheme 13: Mechanism of galactose oxidase (GAO)

Several other redox-active ligands have been studied and investigated in recent times that ultimately led to useful applications in material science²⁶ and catalysis.²⁷ To date, the vast majority of efficient man-made homogeneous metal catalysts are based on noble metals which are rare and expensive (ruthenium, rhodium, palladium, platinum, etc). Their efficiency often relies on their ability to perform key elemental steps of catalytic cycles such as reductive elimination and oxidative addition, which involve two-electron redox processes. Such transformations are more difficult in the case of first-row metals. They undergo more frequently one-electron redox changes resulting in uncontrolled radical reactivities and less stable catalytic intermediates. Redox-active ligands can significantly ease two-electron processes by accepting/giving one extra

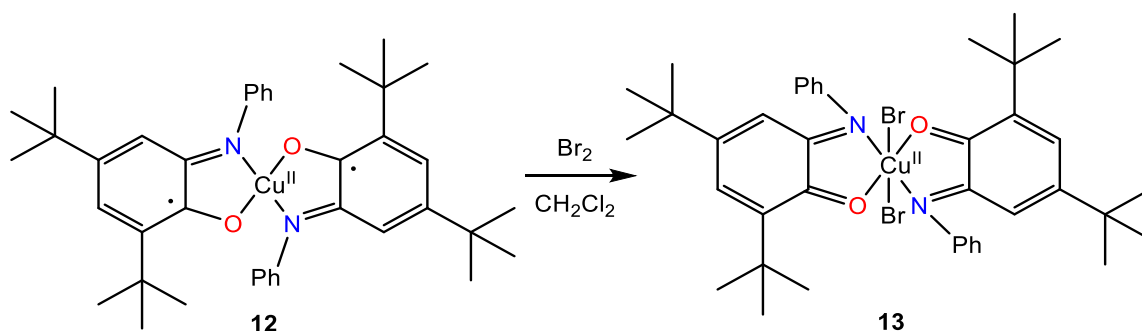
electron. In other words, they can confer nobility to cheap, earth abundant, first row metals.²⁸

One of the examples of the ligand centered oxidation was reported by the group of Heyduk.^{29a} They added molecular chlorine to a zirconium(IV) complex **10** and obtained the Zr(IV) dichloride derivative **11**. X-ray diffraction, EPR and UV-vis spectroscopy showed that the change in the oxidation state occurred at the NO-ligands and not at the metal center. Both NO-ligands proved to be redox-active: they were oxidized to their radical state by the donation of one electron each, thus allowing homolytic activation of Cl₂ upon the interaction of Zr(IV) complex **10** with molecular chlorine (Scheme 14).



Scheme 14: Ligand centered oxidative addition of chlorine to Zr(IV) complex 10

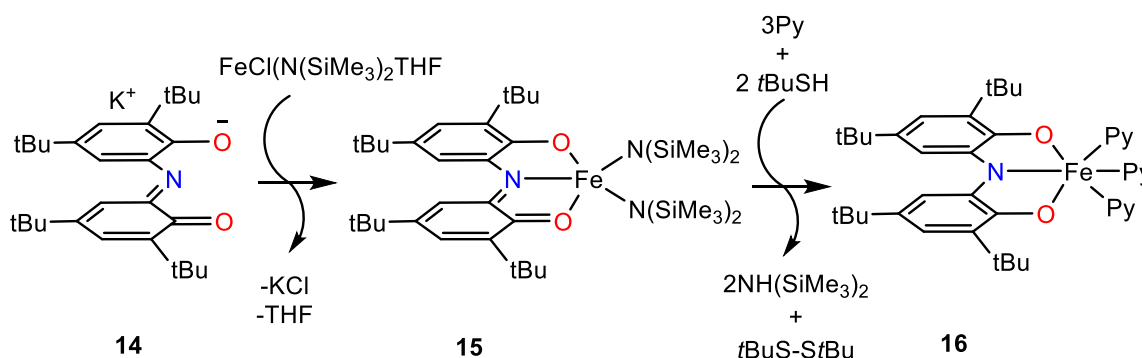
Another example of ligand assisted oxidation was reported in 2008 by the team of Chaudhuri^{29b} (Scheme 15). Upon addition of molecular bromine, the two redox-active radical amidophenolate ligands in the copper(II) complex **12** underwent one-electron oxidation to form the new hexacoordinated complex **13** in which the metal center remained untouched as a Cu(II).



Scheme 15: Ligand assisted oxidative addition of bromine to Cu(II) complex 12

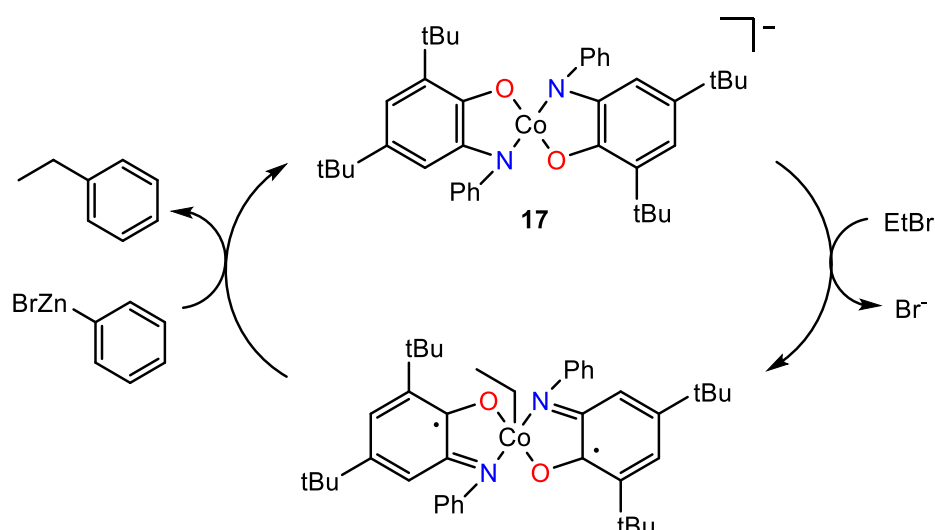
An example of a ligand assisted reductive process was also reported by Heyduk and co-workers (Scheme 16).^{29d} They first synthesized Fe(III) complex **15** by reacting the

potassium salt of the ONO ligand **14** with $\text{FeCl}(\text{N}(\text{SiMe}_3)_2)\text{THF}$. Addition of *t*-butylthiol to complex **15** in the presence of three equivalents of pyridine led to the formation of Fe(III) complex **16**. In this process, the ligand of the Fe(III) complex **15** was reduced by two-electrons.



Scheme 16: Ligand facilitated reductive elimination from Fe(III) complex 15

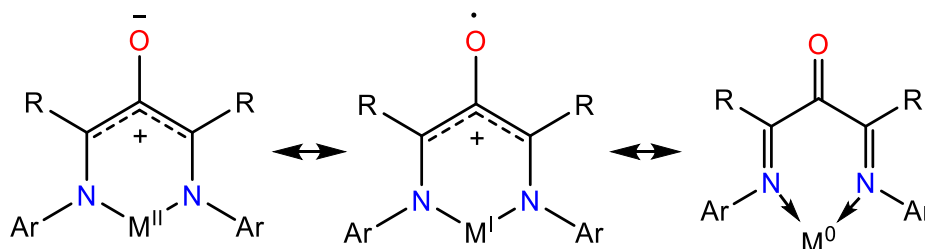
Redox-active ligands can also take part in catalytic processes. The square planar cobalt(III) complex **17** catalyzes the Negishi-like cross coupling of alkyl halides with organozinc reagents.^{29c} The catalytic cycle involves the oxidative addition of the alkylhalide, a trans-metalation with zinc and the reductive elimination leading to the final product (Scheme 17). The two NO ligands are oxidized by one electron each during the oxidative addition where the oxidation state of the metal does not change.



Scheme 17: Negishi-like cross-coupling of alkyl halides by Co(III) complex 17

I.2.3 Oxyallyl patterns for designing redox-active NacNac ligands?

The main goal of this PhD work was to explore the possibility of metal complexes with the general structure shown in Scheme 18. Due to the presence of an oxyallyl pattern, they are expected to be redox active and/or redox non-innocent.



Scheme 18: Introduction of oxyallyl patterns into NacNac structure

The structures in Scheme 18 can also be viewed as exotic redox-active versions of the very well-known 1,3-diketiminates or β -diketiminates, the so-called NacNac **18** (Figure 6) which have been a focus in coordination and organometallic chemistry for many years.³⁰ They are versatile and auxiliary ligands due to their ability to bind strongly to metals as well as their tunable and exceptional steric demands. They show a wide range of structures by changing R'' groups on the nitrogen atoms that can be hydrogen, alkyl, aryl or sometimes silyl groups. They can offer high steric protection around the metal centre by the introduction of bulkier groups (e.g. aryl groups) on the nitrogens to provide unusual coordination environment and the stabilization of highly reactive metal complexes. Their complexes have been known for most of s-, p-, d- and f-block metals, in various oxidation states. These complexes have applications in small molecule activation, novel organometallic compounds and catalysis.

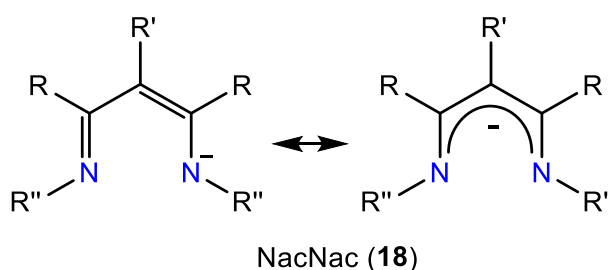
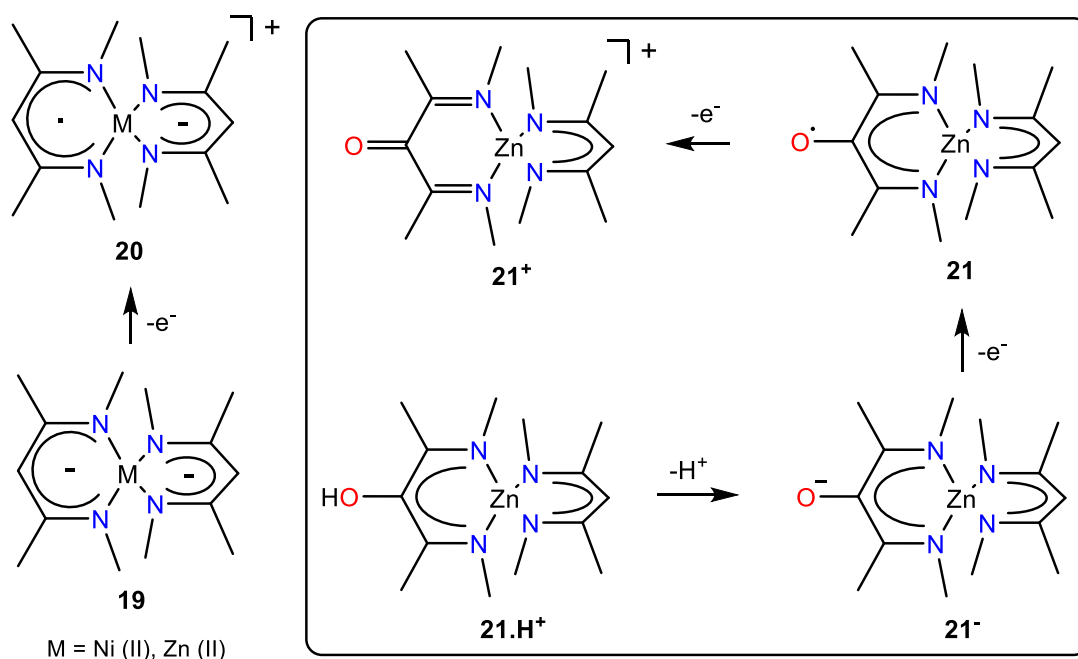


Figure 6: The general structure of NacNac 18

The presence of oxyallyl patterns in such ligands is expected to confer the redox-activity and can favor the ligand centered chemical oxidations/reductions in the formed oxyallyl-metal complexes (Scheme 18).

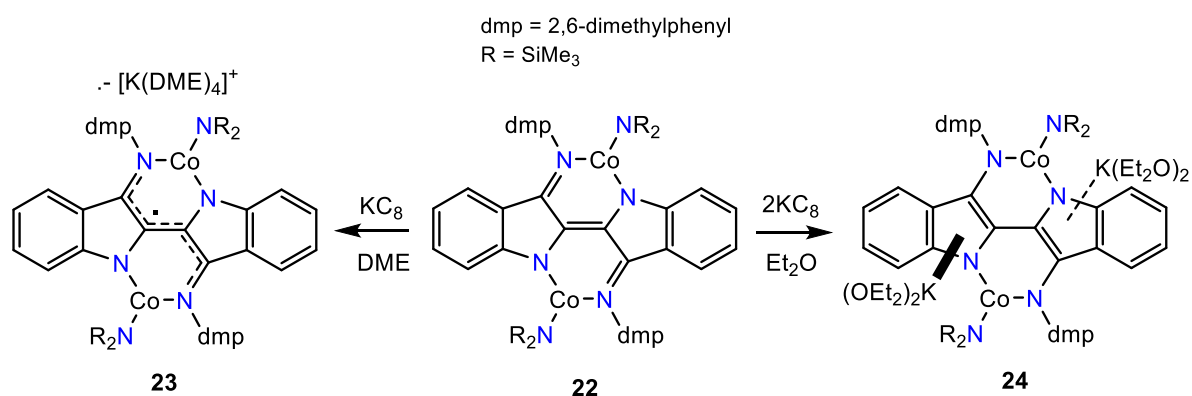
To date, the design of redox-active NacNac remains a challenge. Wieghardt *et al* in 2011 demonstrated that the NacNac ligand in complex **19**³¹ can show one electron oxidation to obtain a neutral π radical structure **20** when coordinated to high-spin Ni(II) ion (Scheme 19). The zinc analogue of **19** was also synthesized further to examine the NacNac centered oxidation that confirmed the formation of the similar π radical. However, the isolation, and even the direct observation of these radicals were not possible because they decompose within seconds.

Our proposed models are expected to be more stable, for instance Zn-complex **21** as an “oxyallyl radical equivalent” of complex **20**. Preliminary DFT calculations indicated that it is very similar to the organic air-stable oxyallyl radical cations with most of the spin density on oxygen (O = +0.44, C = +0.24 distributed over three carbon atoms) rather than on carbon atoms (+0.54) in the radical **20** that is likely the reason of its high reactivity. Complex **21** could even undergo a second ligand-centered oxidation affording the α -keto- β -diimine complex **21**⁺ (Scheme 19).



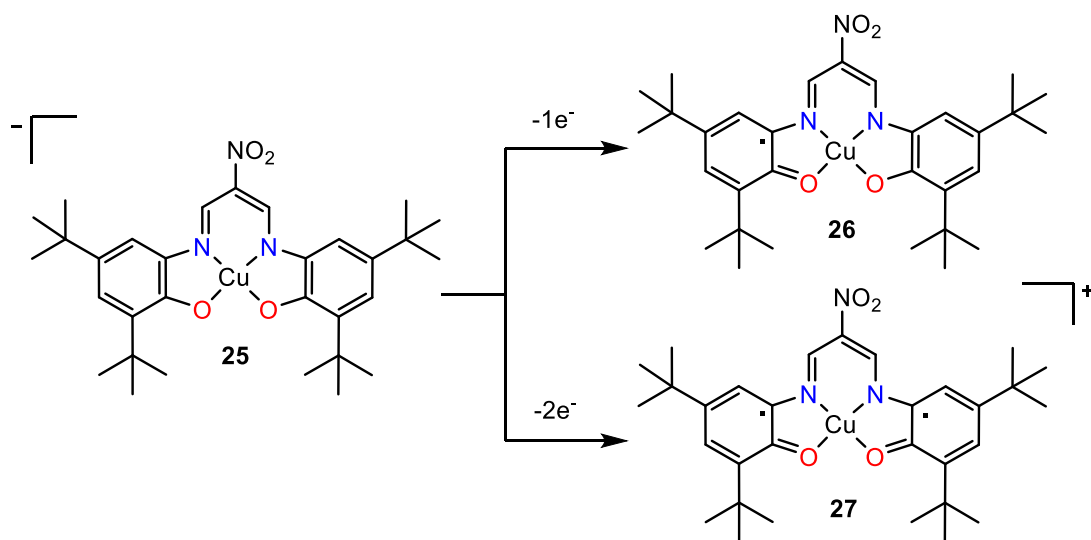
Scheme 19: The expected ligand-centered oxidation of oxyallyl-NacNac complexes

The participation of the NacNac ligand with similar redox activities is limited to a handful of examples.³² K. G. Caulton in 2012 described the use of NacNac derivatives in which two β -diketiminates moieties are combined by the central C=C bridge in the form of binucleating N,N'-diarylimine ligand (Scheme 20). The cobalt(II) complex **22** showed two reversible reductions in the cyclic voltammetry experiment. According to the solid state molecular structure, the distorted trigonal planar geometry around the cobalt center is unchanged during these reductions. In association with spectroscopic evidences, these results were consistent with the ligand centered reductions to form the corresponding radical tri-anion **23** and the tetra-anion **24** forms of the ligand.



Scheme 20: Ligand centered reduction on NacNac derivative

An example^{32b} of ligand assisted oxidation was reported by the group of S. Itoh as shown in Scheme 21. The redox-active phenol groups were incorporated within the β -diketiminato derivative to form the copper(II) complex **25**. The respective one- and two-electron oxidations of complex **25** were performed to form the expected radical **26** and the quinonoid structure **27** of the supporting ligand. The oxidized complexes **26** and **27** showed distinctive absorption spectra in the visible to NIR region that confirmed the ligand-based transitions of the oxidized organic frameworks. The crystal structure of the radical complex **26** showed the characteristic structural change in the aminophenol component of the ligand that was further in agreement with the ligand centered oxidation.



Scheme 21: Redox-activity induced in NacNac by the use of phenol groups

I.3 Overview of the project

Keeping the above discussions in mind, we wanted to contribute to the design and the organic synthesis of several ligands containing oxyallyl moieties, study the impact of different substitution patterns on their stability, the introduction of a metal center into these systems, their radical reactivity and redox properties.

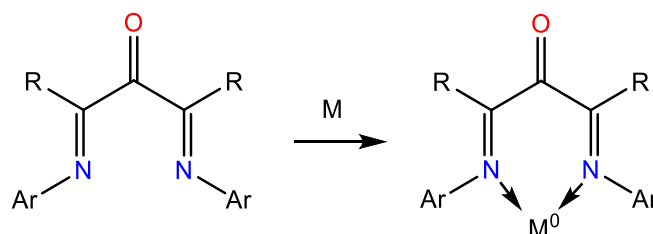
Herein, we first describe the metal-free oxidation of different vinamidines to develop several bis-imine ketones (α -keto- β -diimines), cyclic voltammetry studies of the obtained ligands and their coordination chemistry with various transition metals in **Chapter II**.

Chapter III focuses on the investigation of the full reversal of selectivity in the reaction of a 1,3-dichlorovinamidinium salt with aniline derivatives, the synthesis and the characterization of the desired electron-enriched ligand and the related complex formation.

In **Chapter IV**, new ligands with oxyallyl patterns are designed further to investigate their reactivities, the formation of metal complexes and the studies of their redox behavior are explored. Finally, this chapter presents alternative strategies and concepts as perspectives in the quest for designing redox-active NacNac structures.

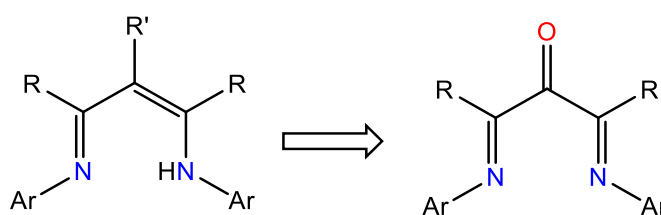
**CHAPTER II: BIS-
IMINE KETONES (α -
keto- β -diimines)**

The formation of designed metal-oxyallyl complexes can be achieved by the use of two-fold oxidized versions of β -diketiminato (NacNac) ligands, i.e., bis-imine ketones or α -keto- β -diimines (Scheme 22). The redox non-innocent behavior of these ligands is expected due to the presence of oxyallyl moieties in the metal complexes.



Scheme 22: Bis-imine ketones- precursor for desired complexes

Bis-imine ketones can be synthesized from the corresponding vinamidines (Scheme 23) but no satisfying method was available so far. Therefore, there was a need for a convenient synthetic methodology.



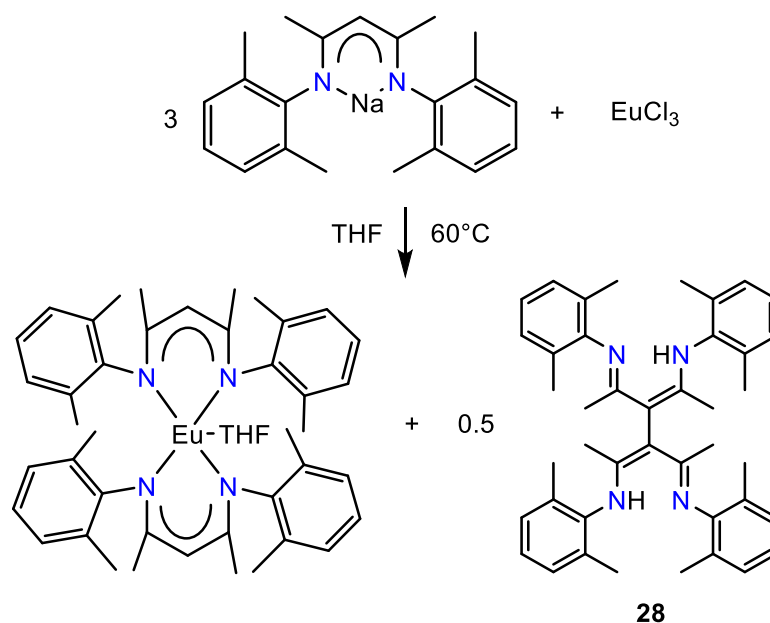
Scheme 23: Vinamidines - precursor for bis-imine ketones

II.1 State of the art

II.1.1 Modification of β -diketiminates at central carbon ($R' \neq H$)

Most of the NacNac ligands feature hydrogen atom at the central carbon ($R' = H$). Only a very few models are known with different substituents at this position.³³

Scheme 24 describes the formation of a precursor of such ligand (with $R' \neq H$): the bis-vinamidine **28**. Note that it resulted from the addition of a β -diketiminato ($R' = H$) to europium(III) chloride. Instead of the expected formation of a tris- β -diketiminato Eu(III) complex,^{33b} the ligand donated an electron reducing Eu(III) to Eu(II) ion and converted into a radical whose dimerization afforded compound **28**. This reaction is an illustration of the reactivity of the central position of NacNac ligands (when $R' = H$) which can lead to undesired side products.



Scheme 24: Formation of bis-vinamidine 28

The role of electronic effects of substituents at this central position was studied by Coates *et al.*^{33a} They synthesized a range of zinc(II) acetate complexes **29** to investigate their catalytic activity in the copolymerization of limonene oxide and carbon dioxide. Cyano-substituted ligands were found slightly underperforming when compared to their hydrogen analogues (TOF > 10 h⁻¹ (R' = H); TOF = 3-9 h⁻¹ (R' = CN)).

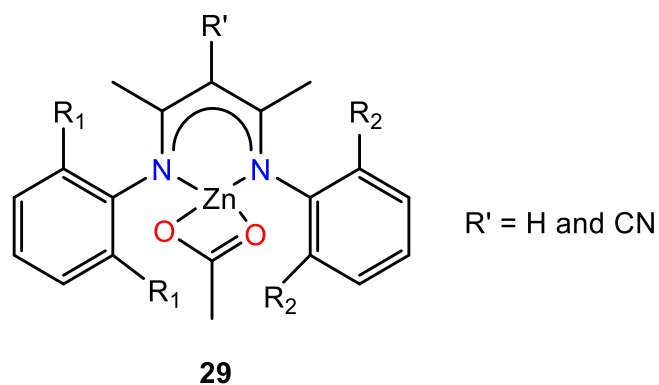
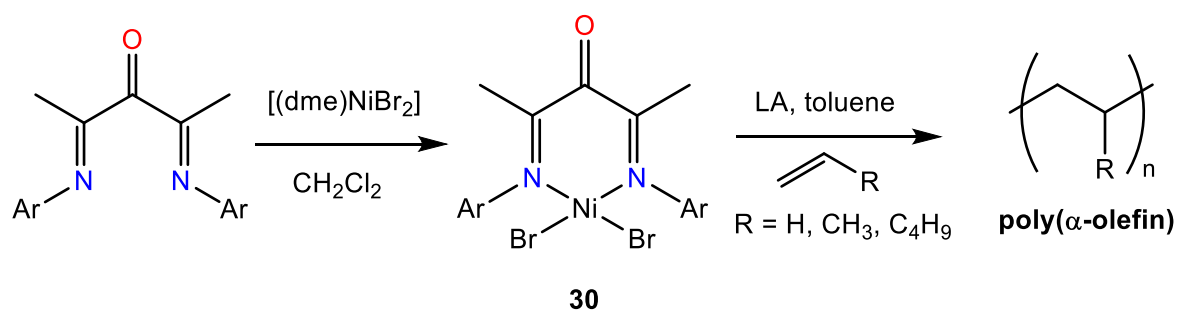


Figure 7: Example of a β -diketiminato modified structure at central carbon

The bis-imine ketones are among the rare NacNac derivatives with a remarkable modification at the central carbon (R' = O). These ligands can be used in the formation of a new type of initiator for olefin polymerization when coordinated to an appropriate metal atom.

II.1.2 Applications of bis-imine ketones

Bis-imine ketone nickel(II) complexes **30** have found applications in the polymerization of olefins as extremely active initiators.³⁴ They allowed the synthesis of high molecular weight polyethylenes and poly- α -olefins. Furthermore, the polymerization reactions were also carried out under living conditions to obtain low-disperse semi-crystalline polymers.³⁵



Scheme 25: Bis-imine ketone nickel initiators

A co-activator (a Lewis acid such as methylaluminumoxane) was required to enhance the reactivity of the initiators during the polymerization reactions. The close structural analogue (β -diimines) with respect to α -keto- β -diimines, varying only at α -position, has been used for comparative studies (Figure 8). An increase in the activity by approximately two orders of magnitude was observed for keto complex **30** in contrast to its β -diimine analogue.^{34a} The presence of carbonyl group on the ligand decreases the electron density around the nickel center and is likely the reason behind the increased rate of polymerization.

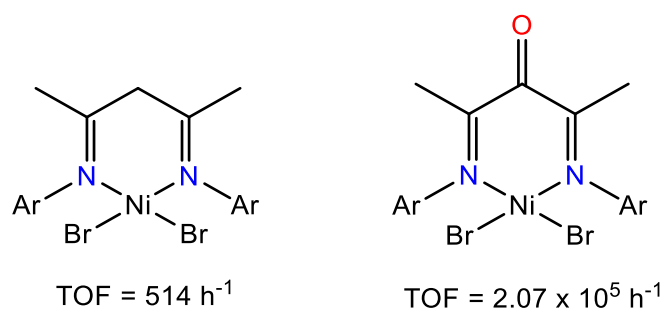
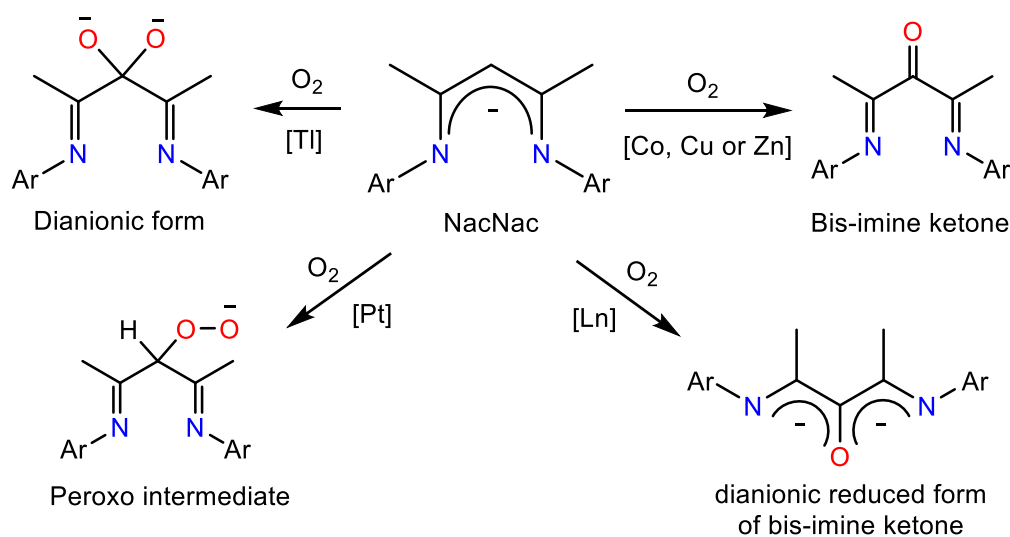


Figure 8: Structure of β -diimine (left) & bis-imine ketone (right) nickel initiators

II.1.3 Complexes of bis-imine ketones and the related derivatives

The metal complexes of α -keto- β -diimines have been known for a very long time but they were usually obtained as rare side products from the air oxidation of ligands of several unprotected NacNac complexes where central carbon atom has hydrogen atom ($R' = H$).³⁶ The process of oxidation of NacNac complexes from the reaction of molecular oxygen usually yields complex mixtures of products which can include the removal of electrons from the metal ion or from the complexed ligand, the formation of metal-oxygen adducts or the oxidative dehydrogenation of the ligand whose characterization is somehow difficult to achieve. The results reported so far indicated that this oxidation can be done in different modes (Scheme 26) to form: (i) a neutral ketone^{37a}, (ii) a dianionic gem-dioxy form^{37b}, (iii) a peroxo intermediate^{37c}, or (iv) a dianionic reduced form of the bis-imine ketone, depending upon the type of the central metal ion present in the complex.



Scheme 26: Different ways of oxidation of a NacNac

The formation of keto-macrocylic iron(II) complex **32** in high yield (> 95 %) was reported in 1997^{36e} by the oxidation of bis-macrocylic diiron compound **31** by the attack of molecular oxygen at the cross-conjugated carbon-carbon bridging double bond. The key structural data featured the corresponding signals for six different types of carbon atoms present in the β -diimine keto specie **32** (IR: $\nu = 1650$ (CO) cm^{-1} ; ^{13}C NMR: $\delta_{CO} = 187.7$, $\delta_{CN} = 176.4$, $4\delta_{CH_2} = 59.7$ to 33.3 ppm). The high yield and the observation of the reaction in solid state suggested the formation of the dioxetane intermediate for this

pathway (Figure 9). The first step formed the peroxide radical with the development of a radical in the six-membered ring by the transfer of one electron from π system to a dioxygen molecule that could be seen as other mesomeric form by the oxidation of iron(II) to iron(III) followed by the formation of dioxetane intermediate with the combination of intra-molecular radical pair that ultimately generated the keto complex **32**. The presence of β -diimine keto macrocycle **32** was also attributed by the presence of blue color in acetonitrile solution ($\lambda_{\text{max}} = 650 \text{ nm}$).

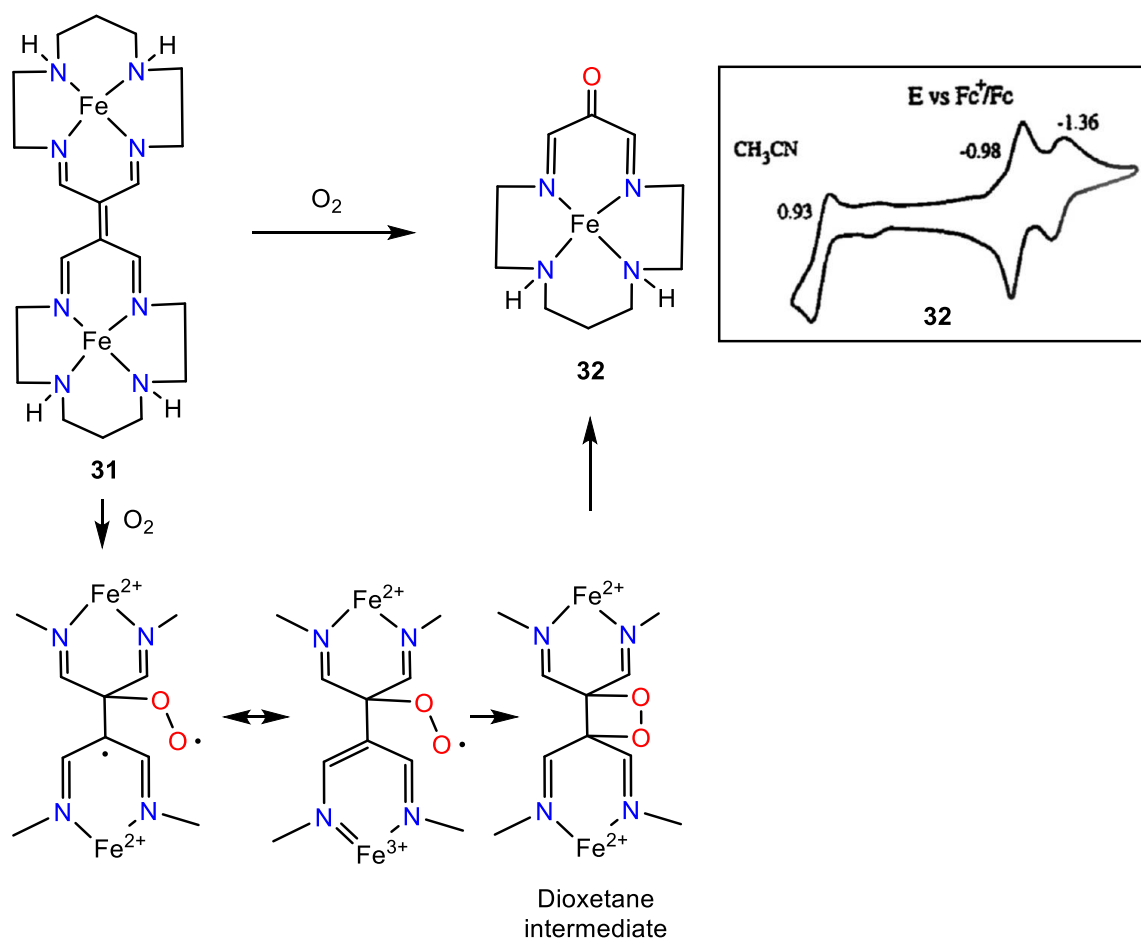
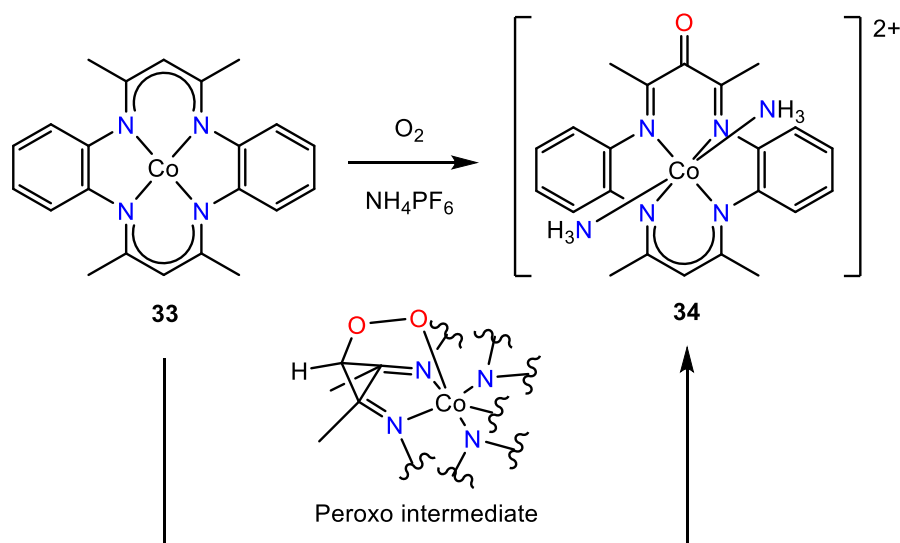


Figure 9: Keto-macrocylic Fe(II) complex **32 & its cyclic voltammogram[ref:36e]**

The cyclic voltammetry experiment (Figure 9) for the complex **32** in acetonitrile solution revealed an irreversible oxidation versus Fc/Fc^+ at 0.93 V for the oxidation of Fe^{2+} to Fe^{3+} . The iron in +2 oxidation state was relatively more stable than its +3 oxidation state due to the greater π -donor strength of Fe^{2+} . The one electron reversible reduction at -0.98 V was considered to be centered on keto- β -diimine component of the ligand. The irreversible and broader wave at -1.36 V was not understood well but it was suggested because of the pinacol reduction from the unwanted proton ions.

Another example of the β -diimine keto macrocycle was reported as the cobalt(III) complex^{36a} **34** that was formed by the oxidation of four coordinated Co(II) complex **33** in the presence of O₂. The drastic color change with a robust exothermic reaction was assumed to go through the formation of a peroxo intermediate in which one of the diiminato rings was transformed into α,β -unsaturated ketone (Scheme 27). The presence of the keto group was further confirmed by elemental analysis, IR ($\nu = 1670$ (CO) cm⁻¹) and ¹H NMR spectroscopy ($\delta_{\text{CH}_3} = 2.77$, $\delta_{\text{CH}_3} = 3.27$, $\delta_{\text{CH}} = 5.54$ ppm).



Scheme 27: Oxidation to form keto-Co(III) complex 34 intermediate

In addition to the oxidation of p- and d-block metal complexes of NacNac ligands, the complexes of lanthanides are usually known for their sensitivity in the presence of oxygen whose oxidation can lead to a variety of ligand oxygenation reactions and formation of mixed products.

An example of a controlled oxidation of NacNac-lanthanide complexes was reported in the literature^{36f} that yielded complex **35** and a C-C coupling product **36**. The general crystal structure of Er and Dy complexes which were isolated in average yields (Er = 43 %; Dy = 34 %) is represented in Figure 10. They featured eight lanthanide oxide and chloride adducts which are arranged in pairs across the molecular axis where a dianionic reduced form of a bis-imine ketone ligand bridges the two metal ions (Ln³⁺) in a tridentate fashion.

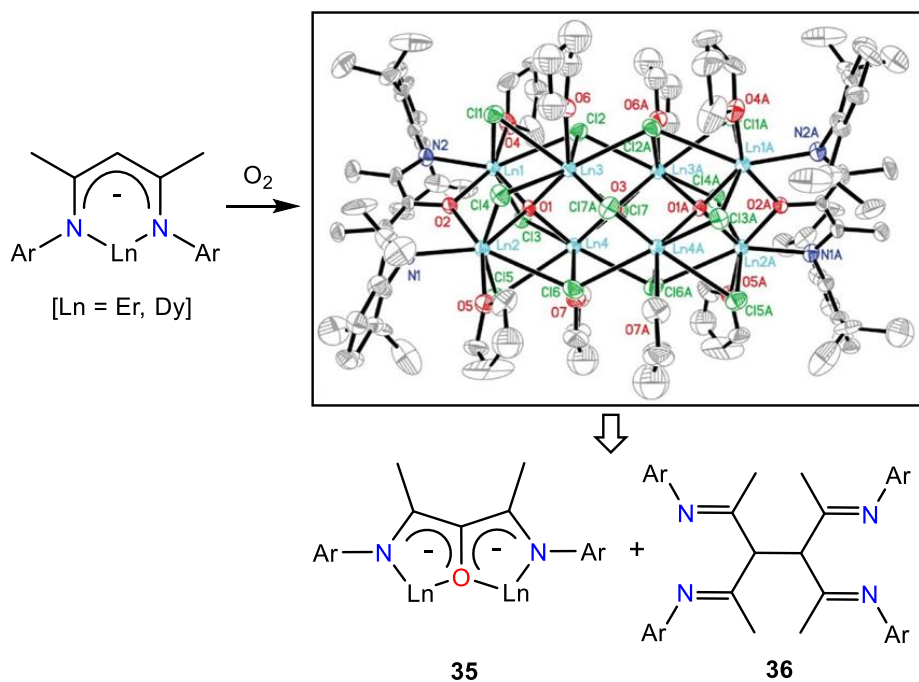


Figure 10: Crystal structure[ref:36f] of the formed Ln-cluster

While handling the highly reactive β -diketiminato-calcium cationic complex **37** for lactide polymerization, Sarazin and co-workers isolated diiminoalkoxide **38**.^{36g} The authors hypothesized that unwanted traces of moisture has resulted in the formation of this by-product **38**. However, they could not achieve the quantitative synthesis of **38** by repeating the reaction in the presence of water, dioxygen, peroxides or H_2O_2 . The X-ray analysis in Figure 11 revealed the distorted square pyramidal geometry for the complex **38** where the metal ion has the five-coordinate environment including THF molecule in their coordination sphere with nitrogen atom at axial position.

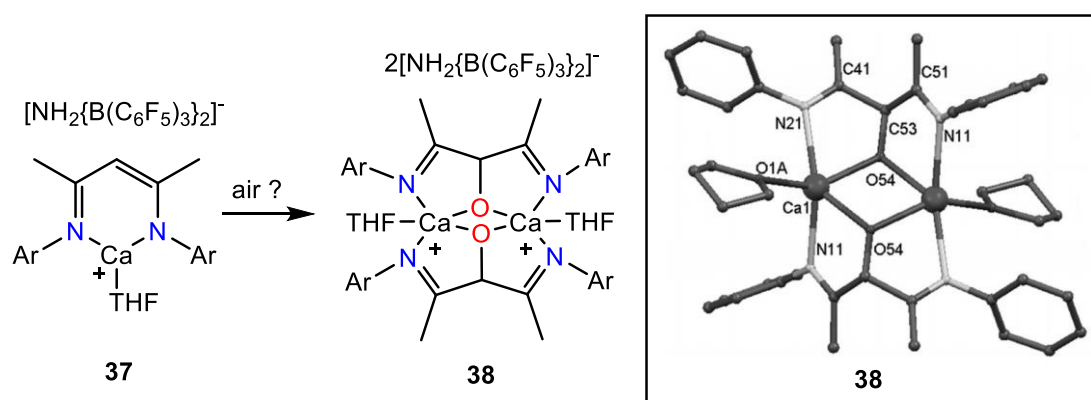
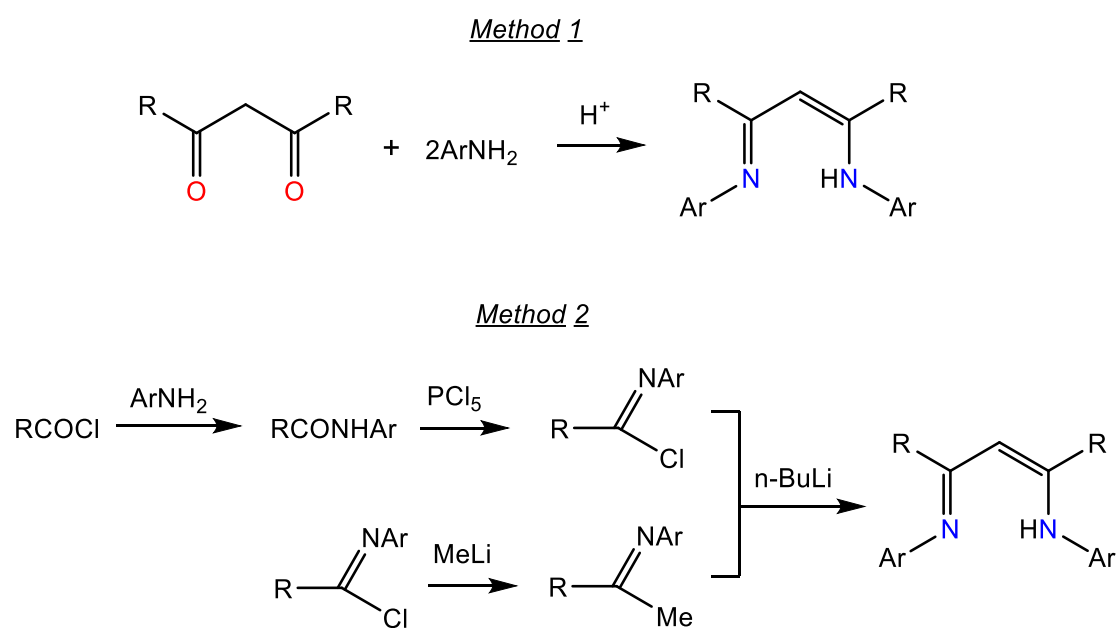


Figure 11: Crystal structure[ref:36g] of dinuclear calcium complex 38

II.1.4 Synthesis of metal free bis-imine ketones

The only available method for the synthesis of free diimine keto ligands is from the rare and selective oxygen degradation of the copper(II) and zinc(II) complexes under aerobic conditions.^{37a}

Vinamidines are the conjugated acids of NacNac ligands and therefore the obvious precursors for NacNac complexes. They can be synthesized by two different methods according to the literature (Scheme 28).³⁸ The most utilized and convenient route is the condensation of β -diketones with anilines in the presence of acid.^{38a-d} The other route is useful when the previous way of synthesis is stagnant especially in the case of bulky substituents^{38e} and allows for the synthesis of non-symmetric vinamidines.



Scheme 28: Synthesis of vinamidines

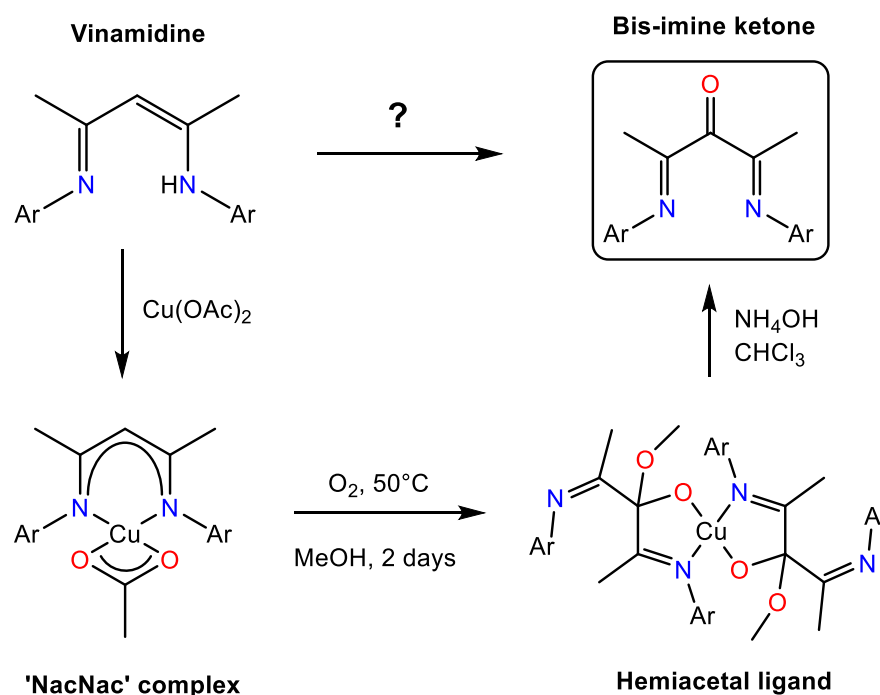
In contrast, the availability of free bis-imine ketones is far from matching the diversity of vinamidines: it is limited to very few substituting groups. This is due to the limitations of the only known method for the synthesis of metal free bis-imine ketones which was reported by Itoh *et al* in 2002.

Their procedure required three steps (Scheme 29):

(i) the formation of NaCNac-Cu(II) or NaCNac-Zn(II) complex by the treatment of vinamidine with an equivalent amount of metal (Cu or Zn) acetate at room temperature. According to the crystal structure, copper complex featured one Cu(II) with a distorted square planar geometry (in which β -diketiminate and acetate ion were bidentate ligands) whereas Zn(II) afforded a dinuclear complex with a four-coordinate tetrahedral geometry and bridging acetate and methoxide ligands between the two zinc atoms.

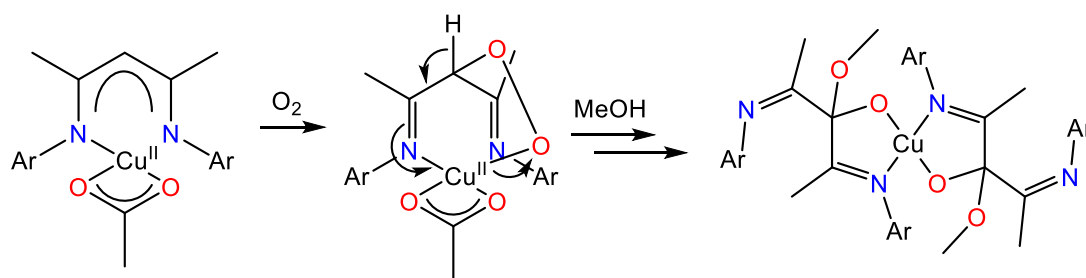
(ii) the oxidation of the Cu(II) complex with the bubbling of molecular oxygen at 50°C in methanol for at least 12 hours. A spectacular color change of the solution was observed from brown to green. This was the result of the formation of a hemiacetal derivative in which copper acquired N₂O₂ coordination within square planar geometry.

(iii) the hydrolysis and decomplexation of the resulting hemiacetal ligand using aqueous ammonia to generate the corresponding ketone diimine in 54 % overall yield.



Scheme 29: Different steps in the synthesis of bis-diimine ketones

An isotope labeling experiment with $^{18}\text{O}_2$ confirmed that dioxygen was the oxygen source during the oxidation reaction (step ii). As for the mechanism, the formation of a hydroperoxo intermediate was proposed (Scheme 30) during the oxidation step.



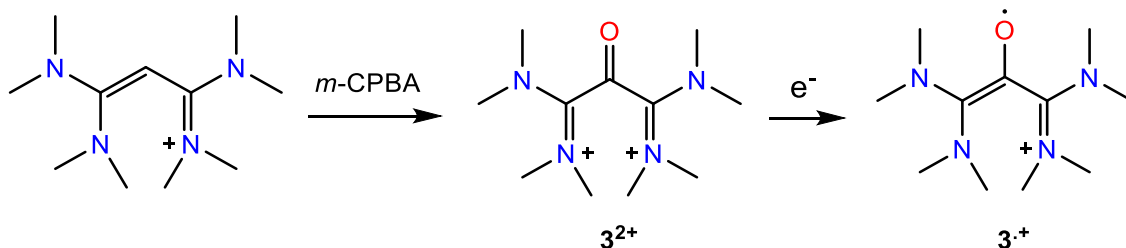
Scheme 30: Proposed hydroperoxo intermediate formed during the oxidation step

This methodology has severe limitations. Not only structure variation in the system is limited (with R = Me and a few aryl N-substituents) but its implementation is very inconvenient. The oxidation step of NaCNac-Cu(II) complex requires a continuous bubbling of pure dioxygen for around two days in a warm solution which is really troublesome and wasteful. In addition, multi-gram synthesis is impractical because it would require litres of solvent due to the low solubility of the reactants. Therefore, the synthesis of metal free bis-imine ketones was a challenge.

II.2 Results

II.2.1 Metal free oxidation of vinamidiniums

Among all the oxidation processes that we have discussed till now, our method of oxidation of vinamidiniums salts using *meta*-chloroperbenzoic acid (*m*-CPBA) is one of the simplest methodology (Scheme 31). As explained previously, the generation of an air-persistent oxyallyl radical cation³⁹ **3⁺** was achieved after oxidizing tetrakis(dimethylamino) vinamidinium using *m*-CPBA as an oxidant to form di(amidinium)ketone **3²⁺** followed by its one-electron reduction.

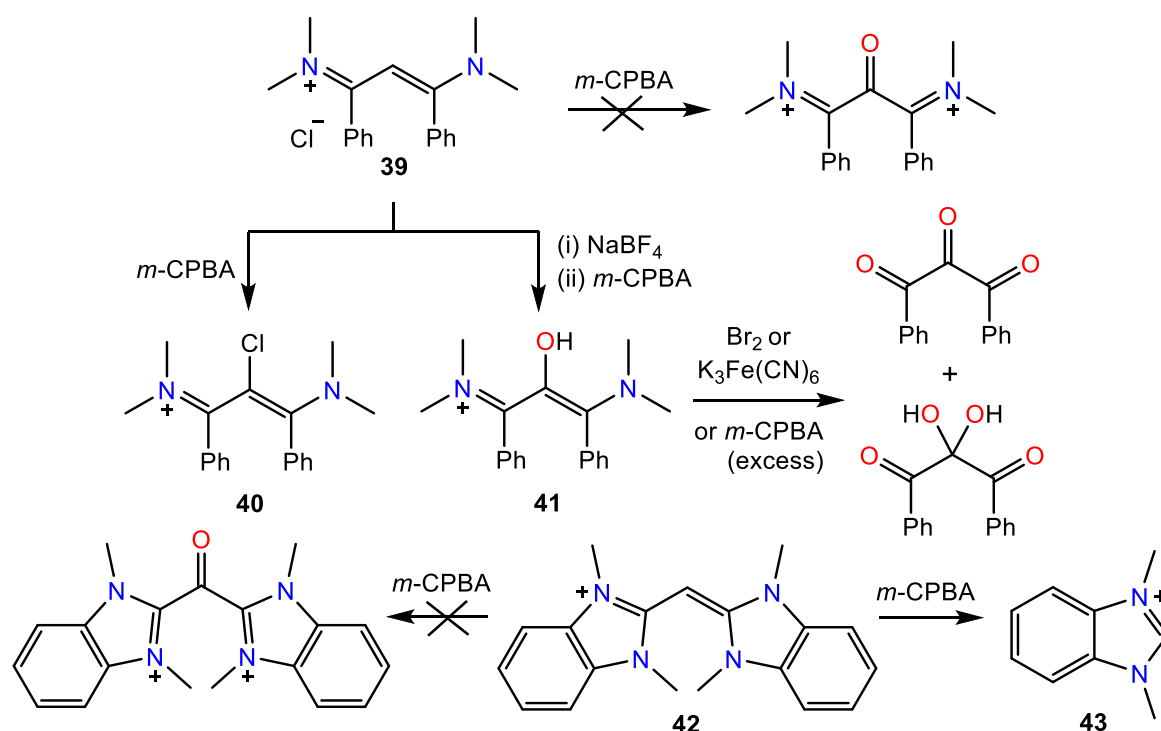


Scheme 31: Generation of oxyallyl radical cation **3⁺**

However, the result of the oxidation reaction by *m*-CPBA is highly dependent on the substitution patterns.⁴⁰ For example, the oxidation of vinamidinium **39** (Scheme 32)

afforded 2-chlorovinamidinium **40** (yield = 71 %) and not the expected keto product as the reaction of chloride counter-anions with *m*-CPBA. The same reaction was repeated with the anion metathesis of vinamidinium **39** by tetrafluoroborate and the formation of compound **41** (yield = 74 %) took place. Both of these obtained vinamidinium products **40** and **41** mainly differ at the central carbon atom according to ^{13}C NMR spectroscopy ($\delta_{40} = 94$ and $\delta_{41} = 127$ ppm) and further characterized by X-ray diffraction analysis and mass spectrometry. Of note, the reaction of vinamidinium **41** with dibromine or potassium ferricyanate or excess *m*-CPBA further formed the corresponding hydration products (trione and gem-diol) as a result of over oxidation.

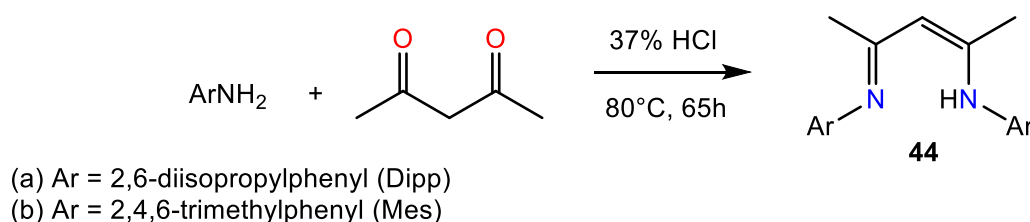
Another reaction pathway was observed in the case of mono(methine)cyanine **42** that featured an electron-rich pattern. Reaction with *m*-CPBA did not lead to the expected di-cationic keto compound but to the further oxidation and ultimately to the formation of 1,3-methyl-benzimidazolium **43**. Therefore, the oxidation of vinamidinium derivatives using *m*-CPBA, although efficient in few cases, it is not versatile and one could expect similar limitations for vinamidines.



Scheme 32: *m*-CPBA oxidation of vinamidiniums 39 and 42

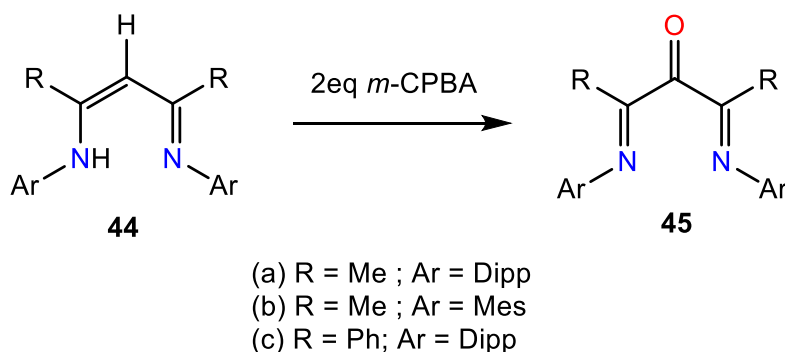
II.2.2 *m*-CPBA oxidation of vinamidines

The synthesis of vinamidines^{38d} **44a** and **44b** were done by the treatment of two equivalents of corresponding anilines (2,6-diisopropyl aniline and 2,4,6-trimethyl aniline) with pentanedione in the presence of hydrochloric acid at 80°C. Dichloromethane and water were added to the crude solids which were neutralized by adding triethylamine. After further work-up, the vinamidines were purified by crystallization in ethanol and isolated in 70-80 % yield.



Scheme 33: Synthesis of vinamidines **44a** and **44b**

Then the reaction of *m*-CPBA with the solution of vinamidine **44a** in dichloromethane was performed. According to the NMR spectroscopy, the reaction was finished in almost one hour at room temperature. The corresponding bis-imine ketone **45a** was purified by recrystallization in cyclohexane and obtained in 80 % yield.

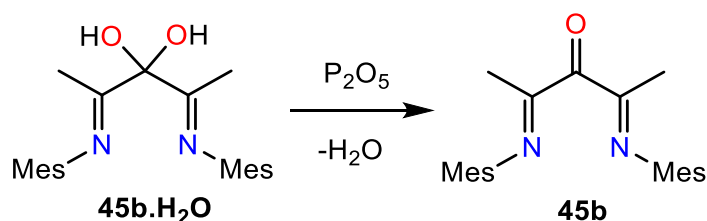


Scheme 34: One step synthesis of bis-imine ketones **45**

We started to explore the scope of this reaction which could ultimately lead to a direct and straightforward synthesis of different bis-imine ketones. We considered the similar oxidation of vinamidine **44b**.

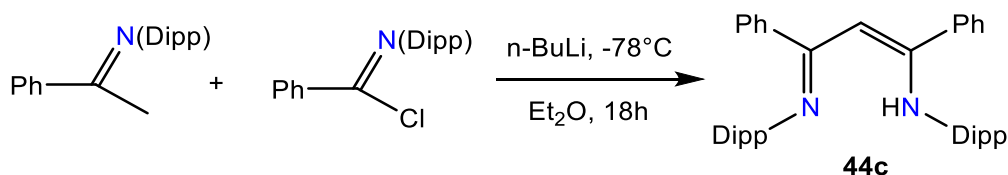
Unlike **45a**, the resulting bis-imine ketone **45b** evolved within few hours. Even freshly made crystals always contained an impurity that did not feature the respective C=O

signal at $\delta = 194$ ppm in ^{13}C NMR but instead a peak at $\delta = 94$ ppm was observed. Drying the crystals of **45b** in the presence of P_2O_5 under vacuum resulted in the pure form of diimine ketone. This supported the existence of the hydrated gem-diol form **45b.H₂O** as an impure compound.



Scheme 35: Gem-diol form of ligand 45b

To study the effect of structure variation of the backbone, vinamidine **44c** was synthesized in 82 % yield by the deprotonation of $(\text{Dipp})\text{N}=\text{CMePh}$ by one equivalent of $n\text{-BuLi}$ at -78°C followed by the addition of $(\text{Dipp})\text{N}=\text{CClPh}$ in diethylether.^{38e} The reaction mixture was refluxed overnight that formed white precipitate of the desired product and then quenched with water. The organic phase was washed with brine and extracted by dichloromethane. The crude product was purified by recrystallization from cold methanol.



Scheme 36: Formation of vinamidine 44c

Vinamidine **44c** was oxidized similarly in the presence of $m\text{-CPBA}$ to form the expected bis-imine ketone ligand **45c** in 87 % yield. Note that no synthesis was previously available for this compound.

The presence of the carbonyl was indicated by following spectroscopy (IR_{ATR} : $\nu = 1700$ cm^{-1} ($\text{C}=\text{O}$); ^{13}C NMR $\delta_{\text{CO}} = 192.5$ ppm) and confirmed by X-ray diffraction study of a single crystal (Figure 12). As a crystalline solid, ligand **45c** was found to be very stable at room temperature with no notable degradation after two years.

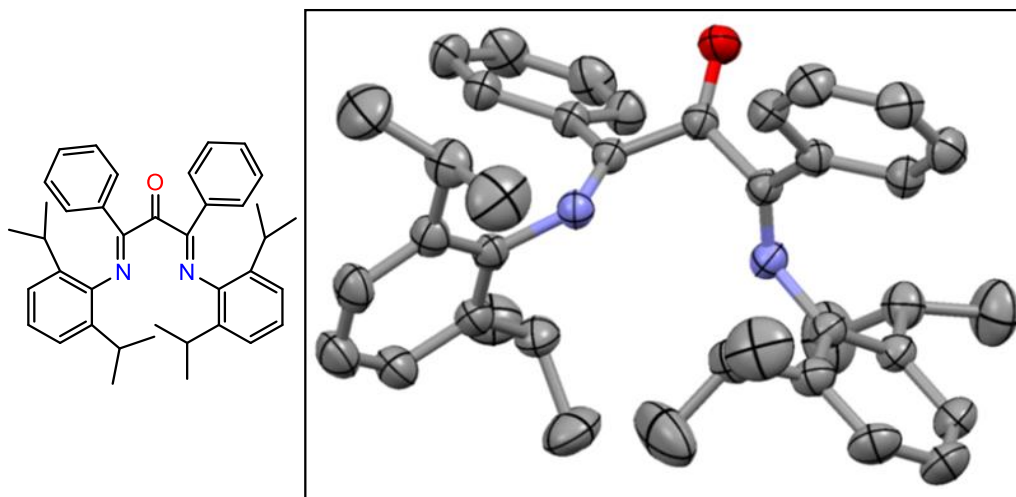


Figure 12: Crystal structure of ligand 45c (H-atoms are omitted for clarity)

The cyclic voltammetry of the bis-imine ketone ligands **45** were performed to set the bench mark for the corresponding metal complexes. The results showed one reversible reduction ($E_{1/2} = -1.9$ V for **45a** and $E_{1/2} = -1.7$ V for **45c**, see Figure 13) which was interpreted as the formation of the corresponding ketyl radical anion.

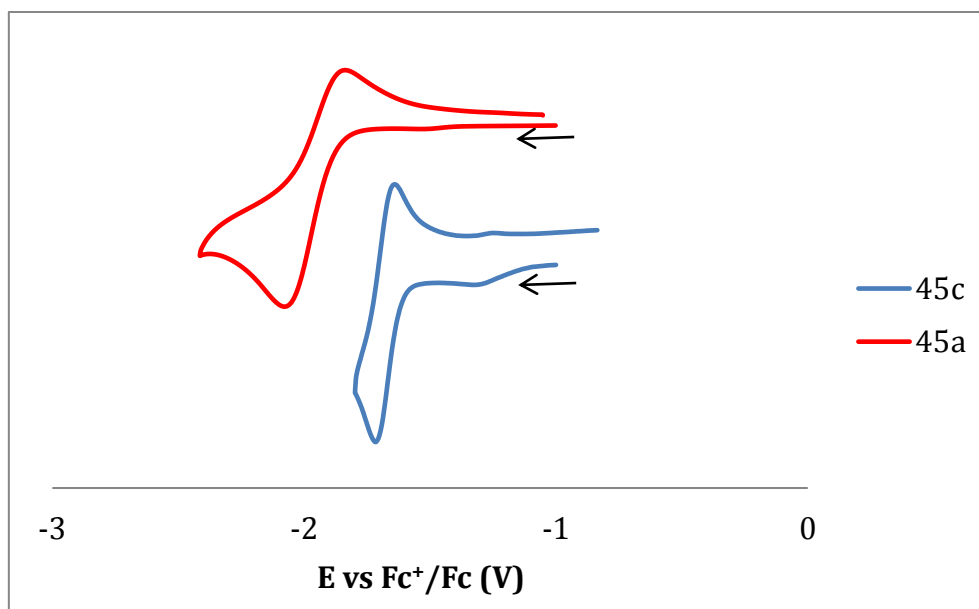
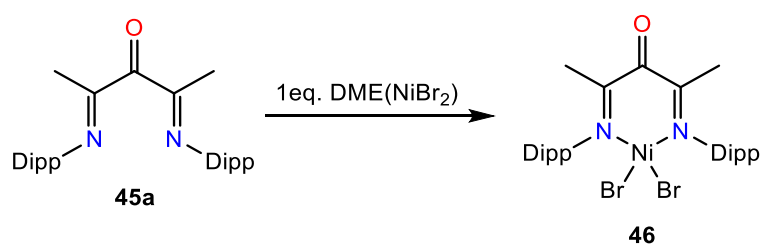


Figure 13: Cyclic voltammograms of bis-imine ketones 45a and 45c in 0.1 M solutions of TBAPF₆ in dichloromethane and acetonitrile respectively, with a scan rate of 100 mV.s⁻¹

II.2.3 Coordination chemistry of the obtained bis-imine ketone ligands

After obtaining bis-imine ketone ligands **45**, it was time to coordinate them to a metal and study the redox properties of the resulting complexes.

We started with the already published^{34c} NiBr₂-complex of ligand **45a**. The complex was synthesized by treating the ligand with one equivalent of nickel(II) bromide ethylene glycol dimethyl ether complex [(DME)NiBr₂] at room temperature in dichloromethane and isolated in 25 % yield as a highly sensitive red-brown solid (Scheme 37).



Scheme 37: Synthesis of α -keto- β -diimine nickel(II) complex **46**

According to the cyclic voltammetry experiment, complex **46** underwent an irreversible reduction at $E_{pc} = -0.9$ V indicating a fast chemical transformation upon addition of electrons. The resulting product was reversibly reduced at $E_{1/2} = -1.3$ V. However, this reduced form was not stable enough to be characterized. Indeed, after quantitative electrolysis at $E = -1.1$ V, the solution was CV- and EPR-silent.

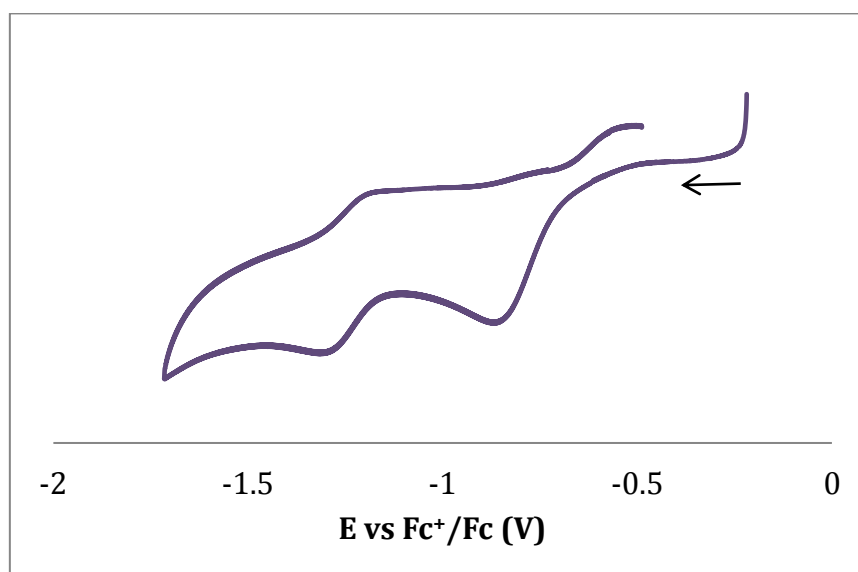
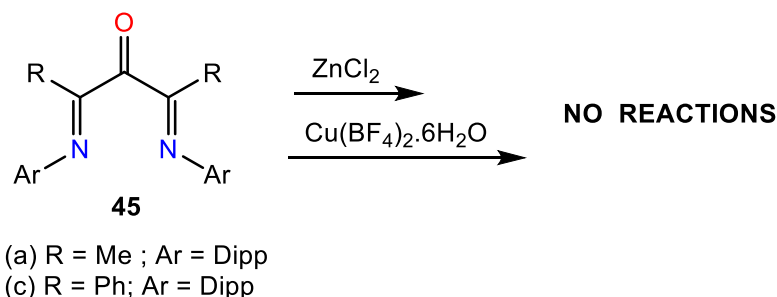


Figure 14: Cyclic voltammogram of complex **46 in 0.1 M solution of TBAPF₆ in dichloromethane with a scan rate of 100 mV.s⁻¹**

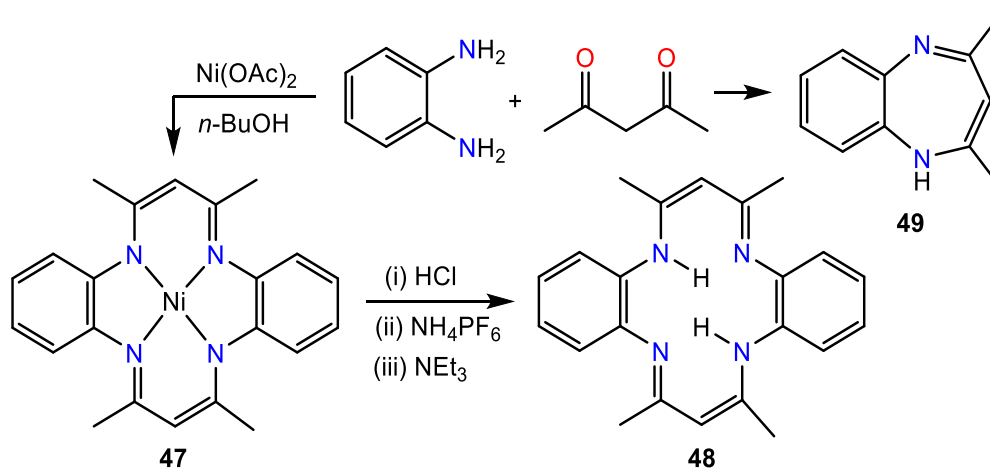
Similarly, (DME)NiBr₂ was reacted with the other ligands **45b** and **45c** but unfortunately only complex mixtures were obtained. No reaction could be evidenced when the complexation of the ligands **45a** and **45c** were tried with ZnCl₂ and Cu(BF₄)₂.



Scheme 38: Metal-complexation with ligands 45a and 45c

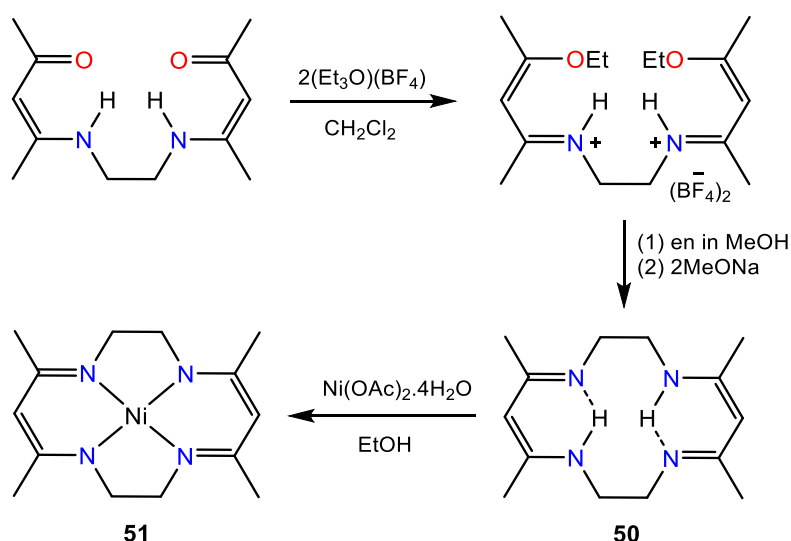
II.2.4 Oxidation of metal complexes bearing macrocyclic ligands

As bis-imine ketones **45** appeared to be poor ligands for studying coordination chemistry, we turned our attention to macrocyclic models, hoping that the issuing complexes would be more stable. We synthesized Geodken's macrocyclic ligand 2,3:9,10-dibenzo-5,7,12,14-tetramethyl-1,4,8,11-tetraazacyclotetradeca-2,4,6,9,11,13-hexaene **48** according to the literature.⁴¹ The first step was the reaction between phenylenediamine and acetylacetone in the presence of nickel acetate to afford the dark green macrocyclic Ni(II) complex **47** in 38 % yield (Scheme 39). A metal template was required: in the absence of a Ni(II) salt, 1,3-diazepine **49** was obtained. Then, the HCl gas was passed over complex **47** to form the salts of H₂**48**²⁺. Free ligand **48** was isolated in 55 % yield after the treatment with triethylamine.



Scheme 39: Preparation of macrocyclic complex 47 and corresponding ligand 48

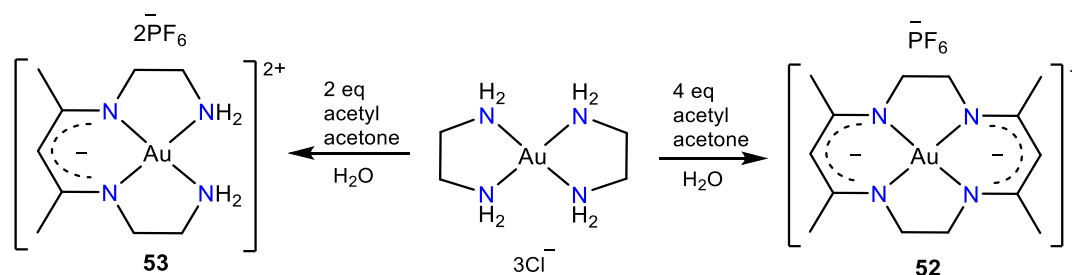
According to NMR spectroscopy, all oxidation attempts of either the macrocyclic ligand **48** or complex **47** by *m*-CPBA yielded complex mixtures. We assumed that the presence of oxidizable benzene rings was problematic and therefore we moved towards a macrocycle with no aromatic linker: 5,7,12,14-tetramethyl-1,4,8,11-tetraazacyclotetradeca-4,6,11,13-tetraene **50**. The known two-step synthesis of this ligand was straightforward and did not require a metallic template (Scheme 40).⁴² Bis(acetylaceton)ethylenediamine was reacted with triethyloxonium tetrafluoroborate in dichloromethane and further treated with ethylenediamine in methanol. The addition of sodium methoxide to the reaction mixture generated the ligand compound **50** in 43 % yield. Nickel acetate and the macrocyclic ligand **50** were refluxed in ethanol to form the corresponding macrocyclic Ni(II) complex **51** (30 % yield).^{42a}



Scheme 40: Synthesis of macrocyclic ligand **50** and its nickel (II) complex **51**

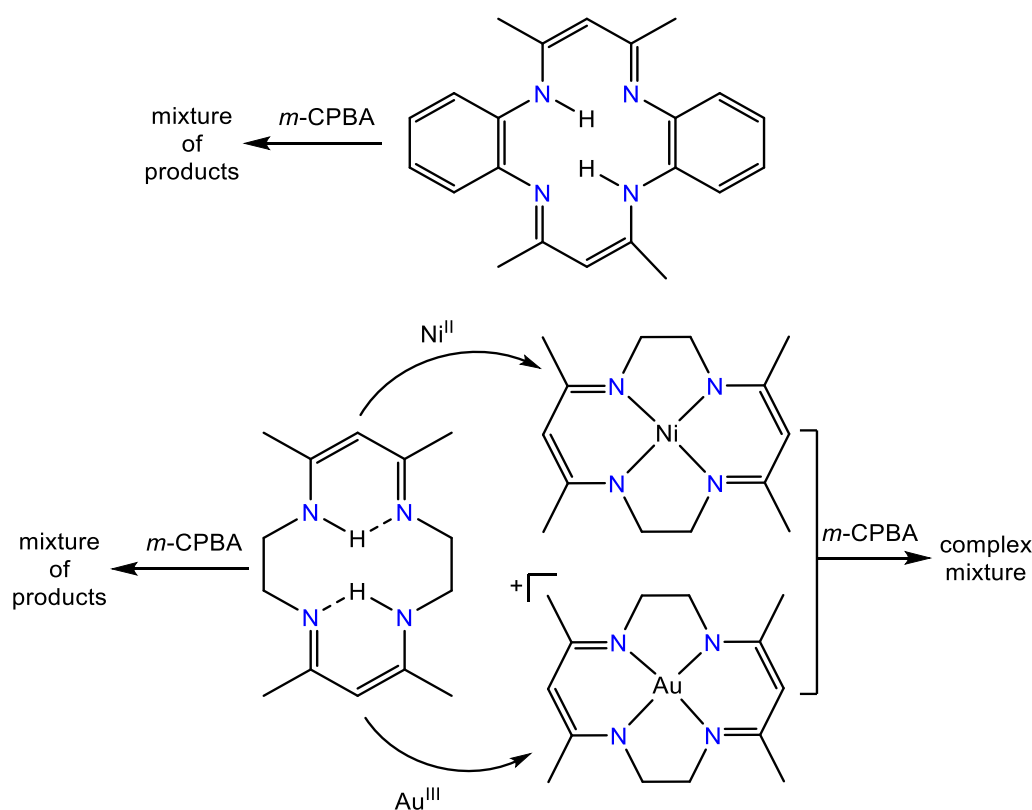
We also synthesized gold(III) complexes **52** and **53** by the condensation reaction of bis(1,2-ethanediamine)gold(III) with 2,4-pentanedione in aqueous-alkaline solution.⁴³ The presence of one or two six-membered β -diiminate rings in the complex depends on the ratio of reagents, pH and the reaction time. These complexes contained four donor nitrogen atoms, two five membered chelate ethylenediamine rings with the corresponding one or two six membered β -diiminate rings where the gold atom has a square planar coordination geometry around four nitrogens. The complexes were isolated as a form of the PF₆ salt after the addition of KPF₆ in the reaction mixture. Note that the complexes of ethylenediamine are usually not acidic enough to allow the condensation reaction with ketones. The pK_a of chelating amine complexes of Au(III)

comparatively have low values⁴⁴ (for example $\text{pK}_a \approx 6.5$ for $\text{Au}(\text{en})_2^{3+}$) which permits direct template synthesis of the complex.



Scheme 41: Synthesis to obtain gold(III) complexes

Unfortunately, here again, all reactions of direct oxidation of macrocyclic ligand **50**, as well as its Ni(II) and Au(III) complexes **51**, **52** and **53** using *m*-CPBA afforded complicated mixtures of products. In particular, no evidence was found in ¹³C NMR for the formation of a C-O or C=O bond and the mixtures remained EPR silent. Therefore, we failed to generate the expected keto-macrocyclic compounds with the selected macrocyclic ligand and their metal complexes.



Scheme 42: *m*-CPBA oxidation of macrocyclic ligands and its metal complexes

We assumed that the struggle in studying the coordination chemistry of bis-imine ketones may be due to the very weak electron-donating properties of these ligands. Hence, we considered incorporating electron-rich dimethylamino groups at R positions hoping the corresponding bis-imine ketone to be a better ligand.

II.3 Conclusion

Bis-imine ketones (α -Keto- β -diimines) **45** were previously described as fragile ligands and it was suggested to use them as soon as they are synthesized but following the oxidation procedure using *m*-CPBA as an oxidant, the obtained products are stable forms of bis-imine ketone ligands (with hydration product in few cases). This method was straightforward, fast and simple as compared to the other methods reported before for the oxidation of vinamidines. This methodology is promising since the low availability of α -keto- β -diimines has clearly hampered further developments. However, the oxidation by *m*-CPBA to obtain the respective bis-imine ketones may be dependent on the substitution pattern of the vinamidines.

II.4 Experimental

General considerations: All the reactions were performed under an inert atmosphere using standard Schlenk techniques or an argon filled glovebox unless otherwise stated. Dichloromethane and diethylether were dried and freshly distilled over calcium hydride and sodium/benzophenone respectively. The chemicals were purchased from Acros, Alfa Aesar and Sigma-Aldrich (now Merck) and were used without further purifications.

Melting point: mp were measured with a Büchi B-545 melting point apparatus system.

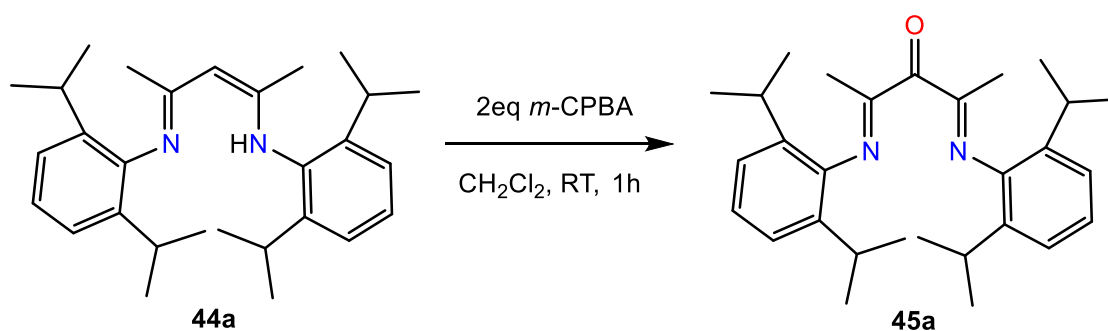
High Resolution Mass Spectrometry: HRMS spectra were obtained by electrospray ionization method on Brüker Esquire 3000 or a Thermo Scientific LTQ Orbitrap XL.

Infra-Red: IR spectra were recorded on a Perkin-Elmer GS2000 IR spectrophotometer with a Golden-Gate ATR unit.

Nuclear Magnetic Resonance: NMR spectra were performed on the NMR-ICMG platform of Grenoble with Avance III 300, 400 and 500 MHz Bruker spectrometers at room temperature. ^1H NMR and ^{13}C NMR chemical shifts (δ) are reported in parts per million (ppm) relative to TMS and were referenced to the solvent residual peak. NMR multiplicities are abbreviated as follows: s = singlet, d = doublet, t = triplet, sept = septuplet, br = broad, m = multiplet signal.

Electrochemical measurements: They were conducted using a BioLogic SP300 potentiostat in an argon filled glovebox. Cyclic voltammetry experiments were performed in a standard three-electrode electrochemical cell in dichloromethane or acetonitrile solutions of 0.1 M tetrabutylammonium hexafluorophosphate (TBAPF₆) as supporting electrolyte with a carbon disk ($\Phi = 3$ mm) as a working electrode, an Ag/0.01M AgNO₃ as reference electrode and a platinum wire as an auxiliary electrode. Ferrocene was used as standard and all reduction potentials are reported with respect to the $E_{1/2}$ of the Fc/Fc⁺ redox couple.

Crystal structure analysis: Crystallographic studies were performed on the RX-ICMG platform of Grenoble with a Bruker AXF-APEXII X-ray diffraction instrument equipped with graphite monochromated Mo/K α -radiation ($\lambda = 0.71073$ Å) and a cryostream cooler.



45a: *m*-CPBA [60 wt% with H₂O] (8.25 g, 28.68 mmol) was dissolved in CH₂Cl₂ (90 mL), dried over Na₂SO₄, 60 mL of this solution was added into the solution of vinamidine **44a** (4.0 g, 9.55 mmol) in CH₂Cl₂ (200 mL). The reaction mixture was stirred for one hour. The mixture was washed with saturated aqueous solution of NaHCO₃ (3 X 300 mL), with water (300 mL), then dried over Na₂SO₄, filtered & concentrated in vacuo yielding a yellow powder of **45a** (4.06 g, 98 % yield). The product was purified by crystallization at room temperature using cyclohexane (80 % yield).

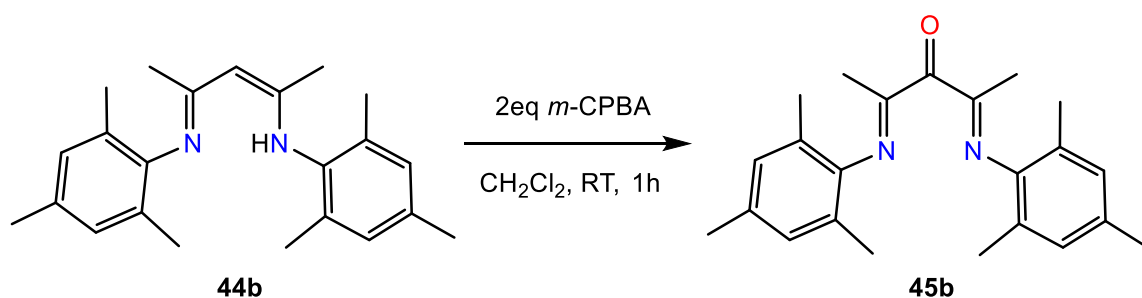
mp: 108-109 °C.

HRMS: *m/z* calcd for C₂₉H₄₁O₁N₂ (M+H⁺), 433.3213; found, 433.3217.

IR (ATR): $\nu = 1700 \text{ cm}^{-1}$ (C=O).

¹H NMR (400 MHz, CDCl₃) δ : 7.18-7.11 (m, 6H), 2.82 (sept, *J* = 7 Hz, 4H), 1.99 (s, 6H), 1.14 (two d, *J* = 7 Hz, 24H) ppm.

¹³C NMR (100 MHz, CDCl₃) δ : 193.5, 168.4, 144.6, 135.9, 124.8 (CH), 123.3 (CH), 28.2 (CH), 23.7 (CH₃), 23.2 (CH₃), 17.3 (CH₃) ppm.



45b: The general procedure of above described *m*-CPBA oxidation was followed, starting from vinamidine **44b** (820 mg, 2.5 mmol), affording **45b** as an oil, which crystallized upon trituration in cyclohexane. (640 mg, 75 % yield).

mp: 95-101 °C (dec.).

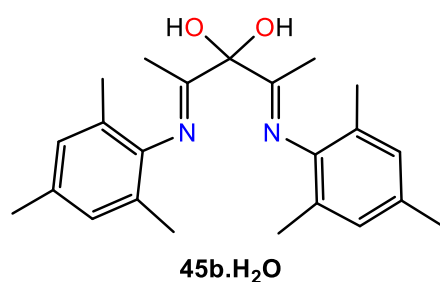
HRMS: m/z calcd for $\text{C}_{23}\text{H}_{29}\text{O}_1\text{N}_2$ ($\text{M}+\text{H}^+$), 349.2280; found, 349.2270.

IR (ATR): $\nu = 1702 \text{ cm}^{-1}$ (C=O).

^1H NMR (500 MHz, CDCl_3) δ : 6.90 (s, 4H), 2.29 (s, 6H), 2.01 (s, 12H), 1.79 (s, 6H) ppm.

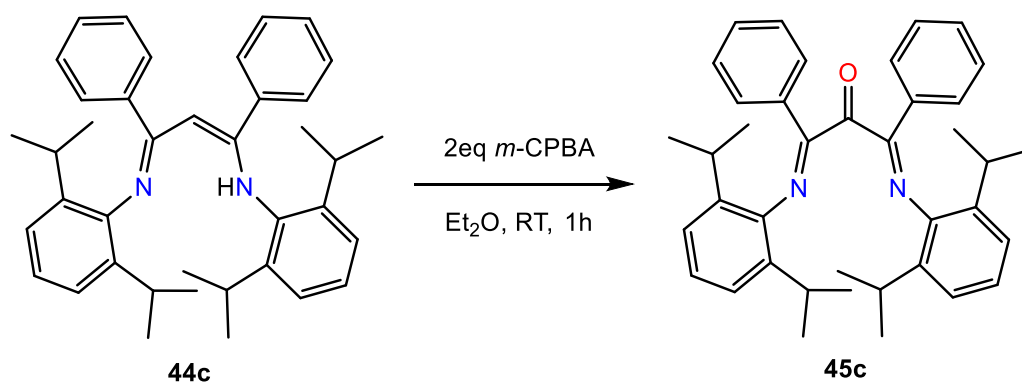
^{13}C NMR (125 MHz, CDCl_3) δ : 193.8, 168.5, 144.6, 133.3, 128.8 (CH), 125.0, 20.8 (CH_3), 17.9 (CH_3), 16.7 (CH_3) ppm.

45b.H₂O was always present as an impurity:



^1H NMR (400 MHz, CDCl_3) δ : 6.88 (s, 4H), 2.29 (s, 6H), 2.01 (s, 12H), 1.96 (s, 6H) ppm.

^{13}C NMR (100 MHz, CDCl_3) δ : 169.9, 143.3, 133.5, 129.0 (CH), 126.0, 94.3, 20.8 (CH_3), 18.0(CH_3), 14.8 (CH_3) ppm.



45c: Following the general procedure on precursor **44c** (1.65 g, 2.8 mmol) in Et₂O (40 mL), the product was synthesized which was further purified by chromatography on a short silica column using CH₂Cl₂ as eluent (1.37 g, 87 % yield). Single crystals in good quality were formed upon crystallization in cyclohexane for X-ray diffraction analysis.

mp: 160-162°C.

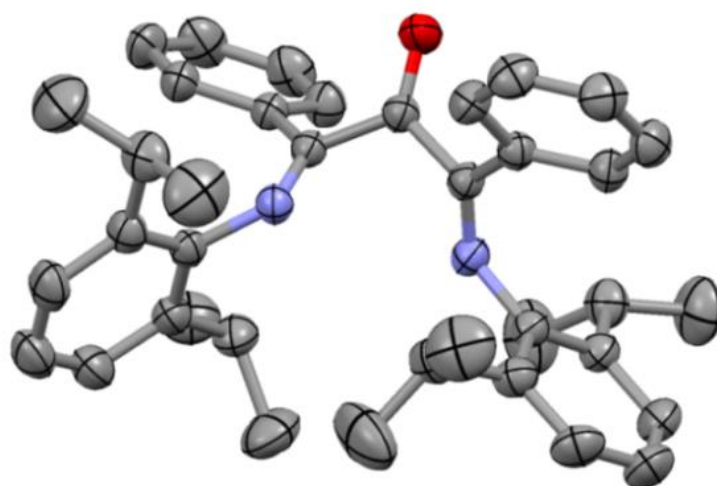
HRMS: *m/z* calcd for C₃₉H₄₅O₁N₂ (M+H⁺), 557.3532; found, 557.3533.

IR (ATR): $\nu = 1700 \text{ cm}^{-1}$ (C=O).

¹H NMR (300 MHz, CDCl₃) δ : 7.33 (d, *J* = 7 Hz, 2H), 7.25 (d, *J* = 7 Hz, 8H), 7.06 (s, 6H), 2.84 (sept, *J* = 7 Hz, 4H), 1.01 (d, *J* = 7 Hz, 12H), 0.75 (d, *J* = 7 Hz, 12H) ppm.

¹³C NMR (75 MHz, CDCl₃) δ : 192.5, 165.2, 144.3, 135.9, 131.9, 130.5 (CH), 129.2 (CH), 128.4 (CH), 124.9 (CH), 123.4(CH), 28.3 (CH) 24.1 (CH₃), 22.5 (CH₃) ppm.

Crystallographic data:



Formula: C₃₉ H₄₄ N₂ O

Space Group: P -1

Cell lengths (Å): a = 10.525(2); b = 12.498(7); c = 13.969(6)

Cell Angles (°): α = 69.67(5); β = 86.47(3); γ = 73.49(3)

Cell Volume: 1650.59

R-Factor (%): 6.04

Bond length

Selected Angle

C2O1 1.205(3)

C3C2C1 117.1(2)

C2C3 1.507(4)

O1C2C1 122.1(2)

C3C10 1.482(3)

C2C1C4 116.9(2)

C10C11 1.382(4)

C1N1C16 122.4(2)

C11C12 1.368(4)

N1C16C17 116.8(2)

C3N2 1.268(3)

C17C22C23 114.5(3)

N2C3 1.268(3)

C23C22C24 110.9(3)

N2C28 1.421(4)

C17C16C21 122.2(2)

C28C33 1.395(4)

C18C17C22 122.3(2)

C33C32 1.386(5)

N1C1C4 129.7(2)

C32C31 1.375(4)

C9C4C5 118.5(2)

C33C37 1.516(4)

C9C4C1 123.0(2)

C37C38 1.510(5)

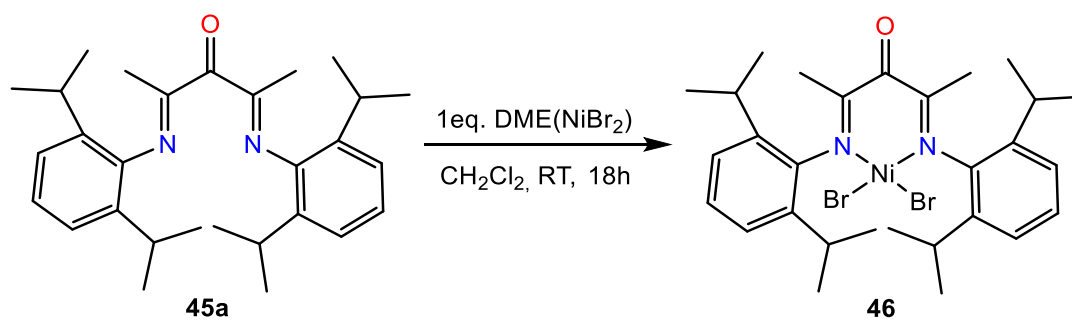
H6C6C5 120.0

C11H11 0.930

H22C22C24 106.9

C37H37 0.98

H24AH24BC24 35.3



46: The ligand **45a** (0.25 g, 0.578 mmol) was suspended with DME(NiBr₂) (0.241 g, 0.781 mmol) in CH₂Cl₂ (12 mL). This suspension was stirred for 18 hours at room temperature. The solvent was evaporated and the resulting residue was washed twice with diethyl ether (2 x 12 mL). The residue was redissolved in dichloromethane (12 mL), filtered and evaporated to give out red-brown solid product (yield = 0.094 g, 25 %).

mp: 179.2°C.

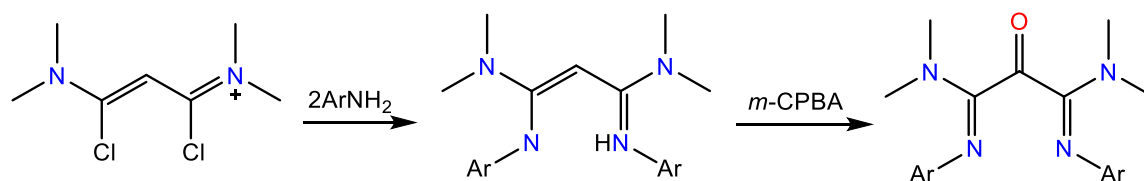
IR (ATR): $\nu = 1700$ (C=O), 1635 (C=N) cm⁻¹.

¹H NMR (400 MHz, CDCl₃) δ : 21.4 (s, 4H), 11 (br, 4H), 3.4 (s, 24H), -14.9 (s, 2H), -25.4 (s, 6H) ppm.

The characterization data was in good agreement with the reported results.^{34c}

**CHAPTER III: BIS-
IMINE KETONES
INTEGRATING
DIMETHYLAMINO
GROUPS**

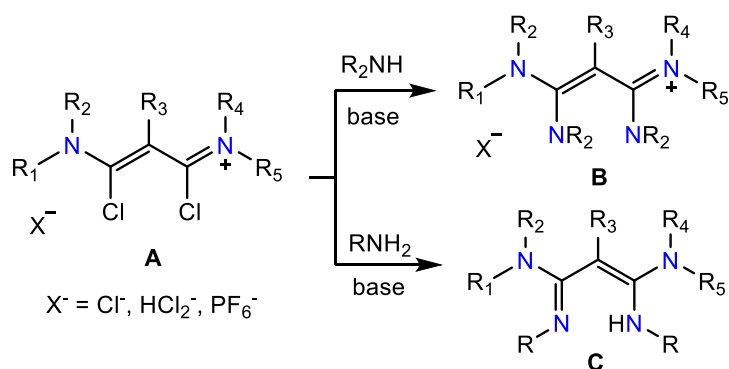
As we assumed that the weak electron-donating property of the previously synthesized bis-imine ketone ligands was problematic, we considered incorporating electron-rich dimethylamino groups into these ligands. In principle, such compounds could be synthesized from the reaction of anilines with 1,3-dichlorovinamidinium salts followed by *m*-CPBA oxidation.



Scheme 43: Step-wise synthesis of electron-enriched bis-imine ketones

III.1 1,3-dichlorovinamidinium precursors

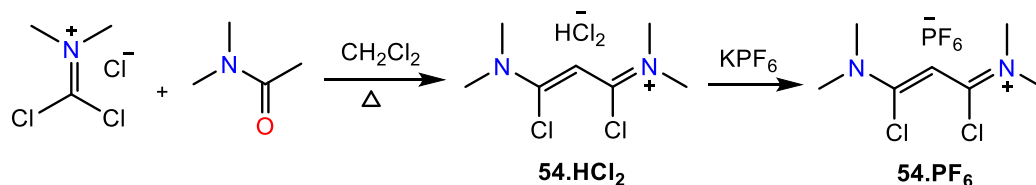
1,3-Dichlorovinamidinium salts⁴⁵ **A** have been studied since 1970s. They are the precursors for different kinds of electron-rich allenes⁴⁶, cyanines and heterocyclic structures.⁴⁷ According to the literature, the reaction of vinamidinium salts with secondary amines can result in the formation of tetra(amino)vinamidinium salts **B** whereas with primary amines, the corresponding vinamidines **C** can be obtained (Scheme 44).



Scheme 44: Reaction of 1,3-dichlorovinamidinium salts A with amines

The synthesis of 1,3-dichlorovinamidinium salt **54**⁺ was done by reacting the commercial available phosgene iminium chloride with 0.5 equivalents of dimethylacetamide following a procedure^{48a} which was recently modified by the Martin group.^{48b} Contrarily to previous reports, we discovered that the vinamidinium was generated in the form of its hydrogendichloride salt **54.HCl₂** and could be solubilized in

an ice cold water with no significant hydrolysis. The treatment of this aqueous solution with potassium hexafluorophosphate resulted in the counter-anion exchange from HCl₂ to PF₆ in good 72 % overall yield.



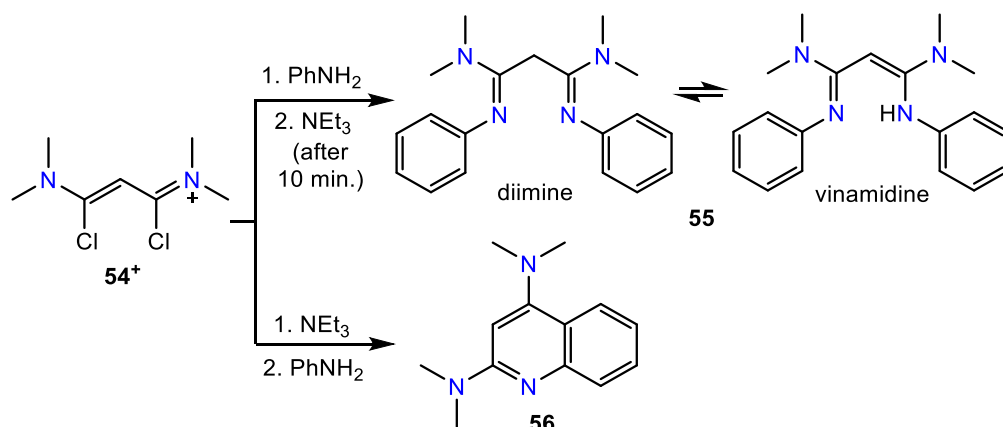
Scheme 45: Preparation of 1,3-dichlorovinamidinium salt 54⁺

III.2 Selectivity in the reaction of aniline with 1,3-dichlorovinamidinium salt

In 1971, Viehe *et al* reported the reaction of primary amines with vinamidinium **54⁺**.^{45b} As reported experimental procedures were not clearly detailed by the author, we directly added two equivalents of aniline to the solution of **54⁺** in dichloromethane (Scheme 46). The three equivalents of triethylamine (NEt₃) were also added as the reaction was expected to form two equivalents of HCl. However, we observed the quantitative formation of 2,4-(dimethylamino)quinoline **56** resulting from an intramolecular electrophilic aromatic substitution of the N-phenyl component after the addition of the first equivalent of aniline. This already known quinoline **56**⁴⁹ was isolated in 42 % yield and fully characterized. Nevertheless, we noticed that 1,3-diimine **55**, the tautomer of the desired vinamidine, was formed by delaying the addition of NEt₃ to a mixture of vinamidinium **54⁺** and aniline.

We tested different reaction conditions in order to optimize the formation of **55** (Table 1). When aniline was added to the solution of vinamidinium salt **54.PF₆** in presence of NEt₃, the only observed product according to ¹H NMR spectroscopy was quinoline **56** along with the triethylammonium salts, regardless of stoichiometry (Table 1: entry 1 and 2). Interestingly, a very small amount of diimine **55** was observed when we delayed the addition of NEt₃ to a mixture of aniline and vinamidinium by 2 minutes (entry 3). Increasing this delay upto 10 minutes boosted the **55** : **56** ratio to 80 : 20 (entry 4). Furthermore, using the hydrogendichloride salt of vinamidinium **54.HCl₂** enhanced the same **55** : **56** ratio to 85 : 15 (entry 5). The reaction was also attempted with one equivalent of aniline (entry 6) and we found that there was no formation of the

quinoline **56** instead only the diimine **55** was formed in almost 50 % conversion. Finally, adding aniline in excess and delaying the addition of NEt₃ by 10 minutes, ¹H NMR monitoring indicated the full conversion of **54.PF₆** into desired the diimine **55** that was recovered in 68 % yield as colorless crystals after the work-up (entry 7).



Scheme 46: Preparation of 1,3-dimethylamino-N,N-diphenylpropane-1,3-diimine **55 & 2,4-(dimethylamino)quinoline **56****

Table 1: Different reactions of vinamidinium **54⁺ with aniline in presence of triethylamine**

Experiment No.	54⁺ : PhNH ₂	54⁺ : NEt ₃	Delay before adding NEt ₃	55 : 56^a
1	1 : 2	1 : 3	b	0 : 100
2	1 : 6	1 : 3	b	0 : 100
3	1 : 2	1 : 3	2 min	8 : 92
4	1 : 2	1 : 3	10 min	80 : 20
5	1 : 2	1 : 3	10 min	85 : 15
6	1 : 1	1 : 3	10 min	50 : 0
7	1 : 6	1 : 6	10 min	100 : 0

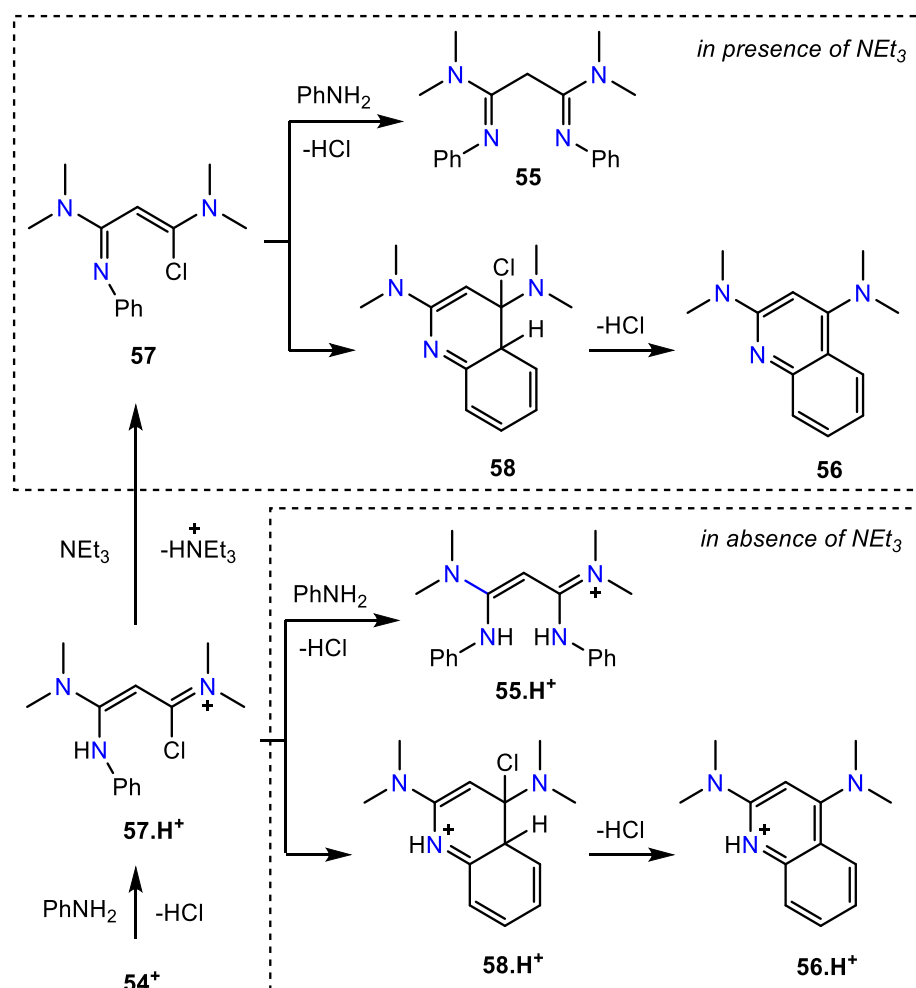
^a Measured from ¹H NMR spectra of the crude product in CDCl₃; ^b Aniline was added to vinamidinium in presence of NEt₃.

In conclusion, the addition of aniline (even in excess) to a solution of 1,3-dichlorovinamidinium salt **54⁺** in the presence of NEt₃ invariably leads to the formation of quinoline **56**. In contrast, delaying (by 10 minutes) the addition of NEt₃ forms 1,3-diimine **55**, even when a substoichiometric amount of aniline is used.

III.3 Investigation by DFT calculations

The reversal of selectivity in the reaction of vinamidinium **54⁺** to form two different products **55** and **56** in similar experimental conditions was rationalized through DFT calculations at the B3LYP/6-311g(d,p) level of theory (Dr. David Martin).⁵⁰

We considered that the reaction of the first equivalent of aniline with vinamidinium **54⁺** leads to the formation of either intermediate **57** or **57.H⁺** in the presence or absence of base respectively (Scheme 47). These intermediates can either react with the second equivalent of aniline to form the corresponding vinamidines **55/55.H⁺** or experience an intramolecular electrophilic substitution to give out cyclic dihydroquinoline products **58/58.H⁺** followed by the formation of final quinolines **56/56.H⁺**.



Scheme 47: Reaction track of vinamidinium **54⁺ with aniline in presence and absence of NEt_3**

For intermediate **57**, the amidine and enamine components are nearly orthogonal at the optimized minima. The C₂-C₃ bond (149 pm) is longer than the C₁-C₂ bond (134 pm) that indicated the weak conjugation between their respective π -systems. It has four diastereomeric conformers due to the non-symmetrical enamine and imine moieties which were found to be close in energy with the similar structural and electronic properties. On the contrary, the other intermediate **57.H⁺** has eight different isomers due to the *E/Z* isomerism around C₁-C₂, C₂-C₃ and C₃-NPh bonds because of its moderately twisted form and the whole conjugated π -system. They feature similar characteristics with similar energies (6 kcal mol⁻¹). The most stable conformers among all the diastereomeric forms of **57** and **57.H⁺** are shown in Figure 15.

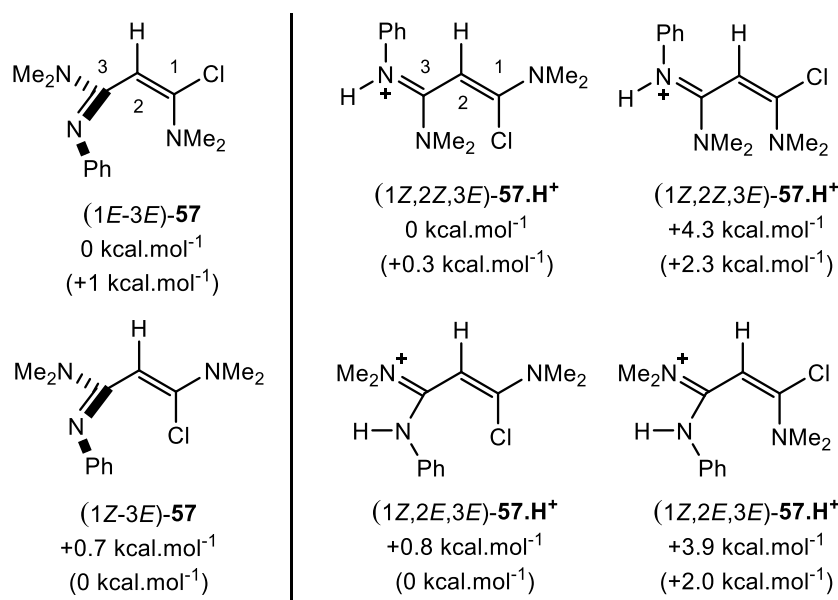


Figure 15: The most stable among the relative free enthalpies of diastereomeric conformers of **57 (left) & **57.H⁺** (right) at 298 K. Only 3*E* isomers are suitable for intramolecular cyclisation. Default optimizations were performed ‘*in vacuo*’**

In both the intermediates **57** and **57.H⁺**, the highest occupied molecular orbital (HOMO) is the π -orbital of the phenyl group whereas the lowest unoccupied molecular orbital (LUMO) is the expected electrophilic C₁ center for the enamine moieties (Figure 16; for simplicity, the discussion focuses only on the most stable conformers (1*E*, 3*E*)-**57** and (1*Z*, 2*Z*, 3*E*)-**57.H⁺**) according to the experimentally observed formation of **56**. The generation of **56** goes through the formation of a dihydroquinoline **58** by the intramolecular cyclisation of **57** which is probably the rate-determining step of the process. In the absence of base, the corresponding protonated intermediate **57.H⁺**

results in the less nucleophilic aryl center (the energy of the HOMO for **57** = -0.2 eV; for **57.H⁺** = -0.35 eV) and an increase in the electrophilicity at the C₁ center (the energy of the LUMO for **57** = -0.017 eV; for **57.H⁺** = -0.19 eV). Hence, with these two opposing effects, it isn't possible to determine qualitatively the relative rate of cyclisation of **57** and **57.H⁺**.

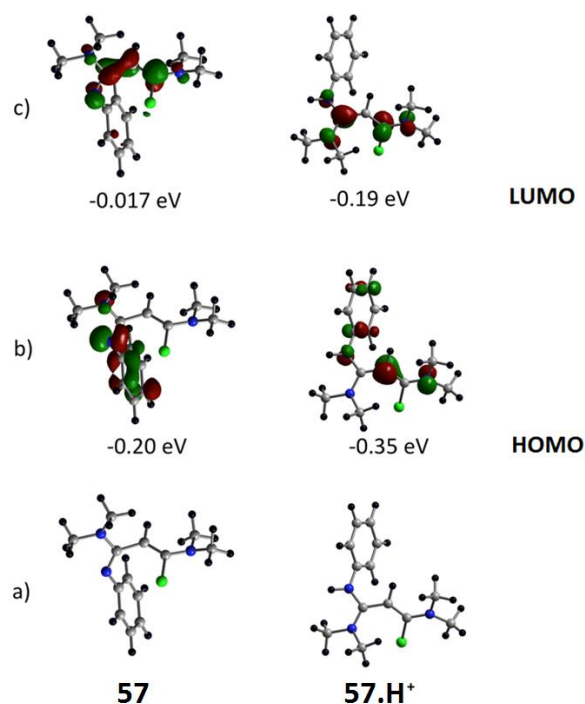


Figure 16: (a) The optimized geometry of the most stable diastereomer; (b) the highest occupied molecular orbital (HOMO) and (c) the lowest unoccupied molecular orbital (LUMO) of **57 and **57.H⁺** intermediates**

The only stable conformers of **57** has a significant configuration of *3E* as it is mandatory for the *N*-phenyl to be in the region of the responsive C₁ center for the formation of dihydroquinoline **58** obtained after the cyclisation. The evolution of the dihydroquinoline **58** was found to be endergonic with the value of +8 kcal mol⁻¹ for the *cis* isomer whereas +21 kcal mol⁻¹ for its *trans* isomer (in blue, Figure 17). The generation of **58.H⁺** was more thermodynamically disfavored (formation of *cis*-**58.H⁺** = +15 kcal mol⁻¹; *trans*-**58.H⁺** = +40 kcal mol⁻¹). All the processes correspond to late transition states as expected for the aromatic substitutions with the relatively milder electrophiles. Depending upon the initial conformations of **57** and **57.H⁺**, all the activation energy barriers are in the 32-43 kcal mol⁻¹ range that further suggested that the rates of cyclisation of **57** and **57.H⁺** were similar. Consequently, the development of

55 in the absence of NEt_3 would have resulted from the deactivated phenyl ring of **57.H⁺** that was further compensated by aniline as nucleophile. The fast formation of quinoline **55** occurred within minutes at room temperature in the presence of NEt_3 , therefore the estimated high value of activation barriers (above 30 kcal mol^{-1}) for the formation of **58** or **58.H⁺** are not in accordance with the experimental results.

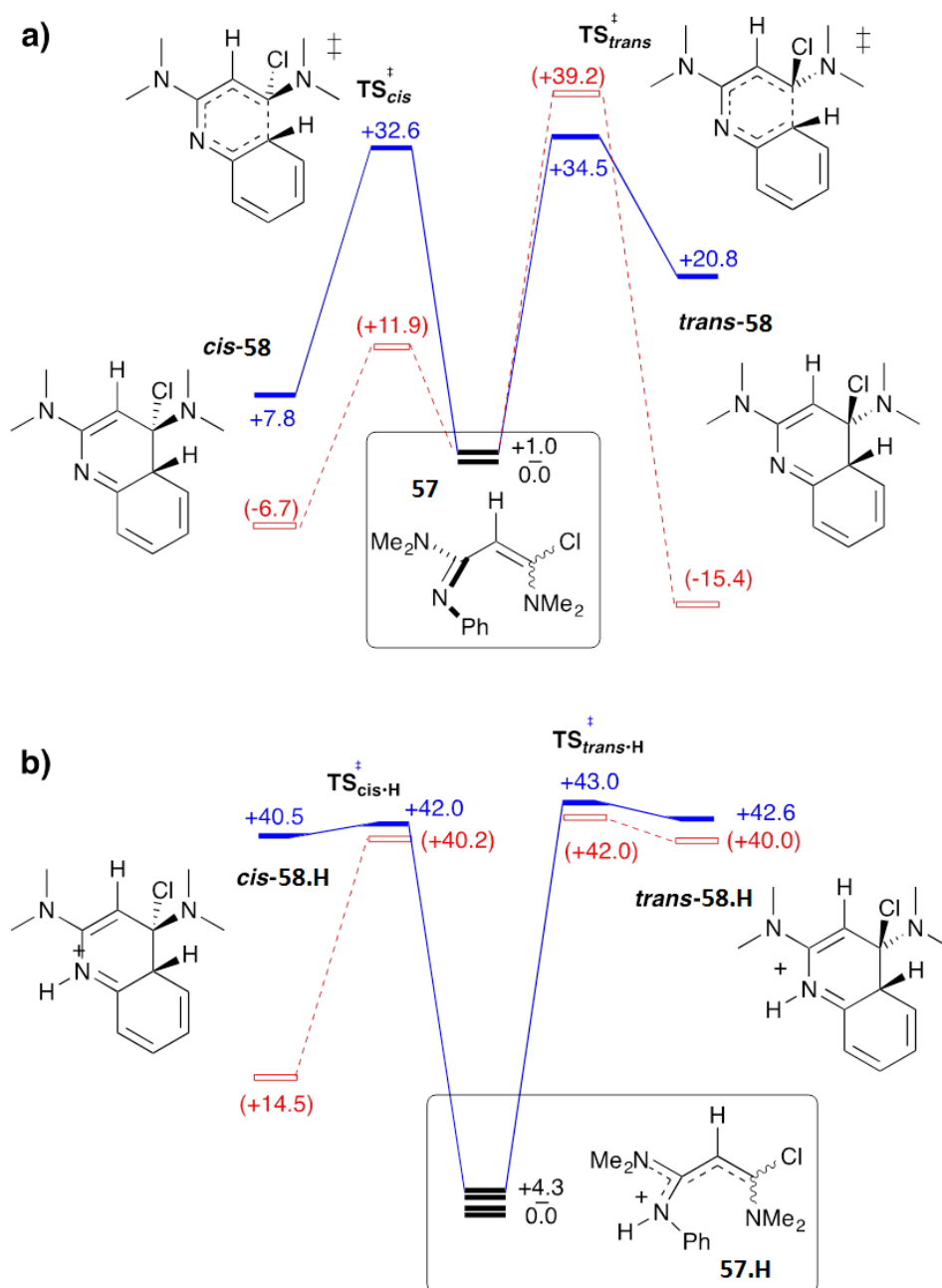


Figure 17: Energy diagram for the cyclisation of (a) **57** (top) and (b) **57.H⁺** (bottom). Energies are in kcal.mol^{-1} . Default optimizations were performed ‘*in vacuo*’ (blue). Optimization in ‘dichloromethane’ using the default polarizable continuum model corresponds to dashed lines with energies in parentheses (red)

Significantly, the optimized structure of intermediate *cis*-**58** has a noteworthy elongated C-Cl bond (297 pm) as compared to the other parented intermediates (*trans*-**58** = 192 pm; *cis*-**58.H**⁺ = 195 pm; *trans*-**58.H**⁺ = 185 pm). Further, similar features were noticeable in other transition states (**TS**[‡]_{*cis*} = 227 pm; **TS**[‡]_{*trans*} = 187 pm; **TS**[‡]_{*cis.H*} = 185 pm; **TS**[‡]_{*trans.H*} = 181 pm). The HOMO of the **TS**[‡]_{*cis*} resulted from the combination of π -system of the obtained dihydroquinoline **58** and the σ^* orbital of the C-Cl bond (Figure 18). The stabilizing interaction weakened and elongated the C-Cl bond. This effect was not significant in the case of the more electron-poor **TS**[‡]_{*cis.H*} because its π -system was lower in energy. Finally this factor was negligible in **TS**[‡]_{*trans*} and **TS**[‡]_{*trans.H*} because the relevant molecular orbitals did not overlap properly as the C-Cl bond was nearly orthogonal to the π -system.

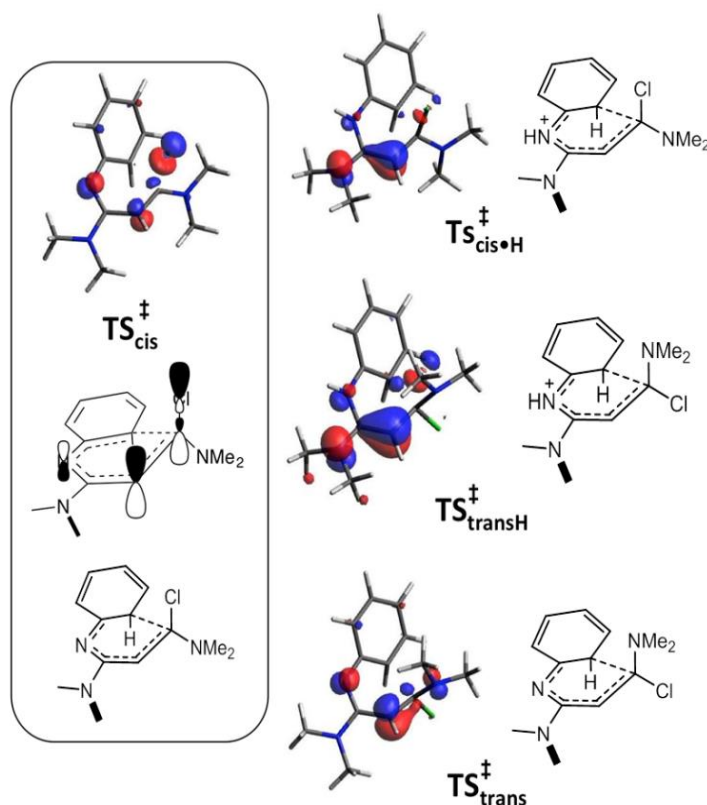


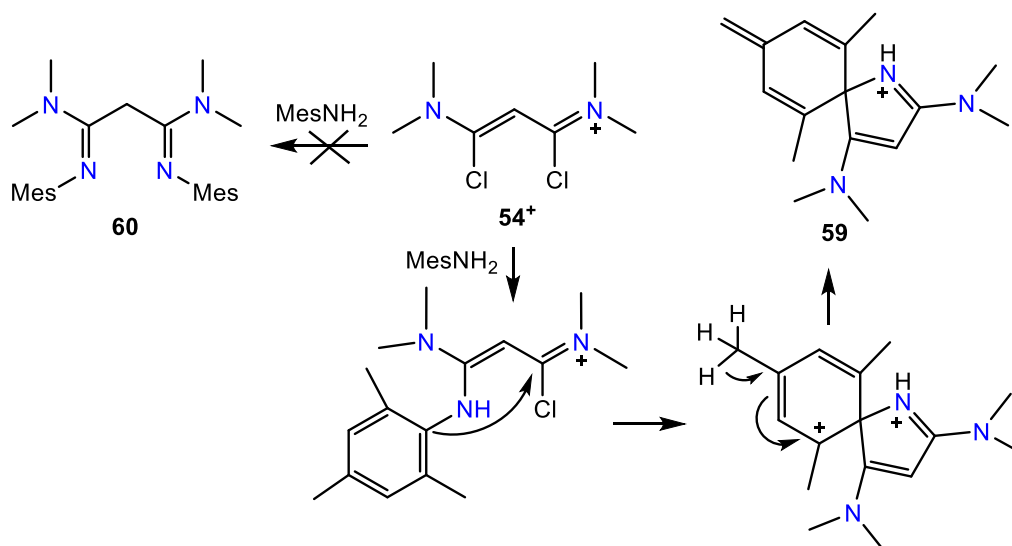
Figure 18: HOMO level representation of *cis*-58**, **TS**[‡]_{*cis*}, **TS**[‡]_{*trans*}, **TS**[‡]_{*cis.H*} and **TS**[‡]_{*trans.H*}**

Considering the role of the solvent for the ionization of C-Cl bond, the optimization of all the key intermediates and transition states was repeated using the polarizable continuum solvation model for dichloromethane (in red, Figure 17) and we found that the energy of **TS**[‡]_{*cis*} dropped to +12 kcal mol⁻¹ whereas the relative energies of **TS**[‡]_{*trans*}, **TS**[‡]_{*cis.H*} and **TS**[‡]_{*trans.H*} were not affected by solvent effects (39-43 kcal mol⁻¹).

Therefore, when considering solvent effects, the low-lying $\text{TS}^{\ddagger}_{cis}$ could account for the preferred formation of **56** in basic media at room temperature, as observed experimentally.

III.4 Limitations in the reaction of 1,3-dichlorovinamidinium with bulky anilines

During the course of this work, S. Aldridge and co-workers published the synthesis and coordination chemistry of several amino-functionalized vinamidines.⁵¹ Their synthetic methodology involved the reaction of anilines with 1,3-dichlorovinamidinium **54**⁺ but in different conditions (reflux for a day in chloroform followed by quenching with aqueous KOH). In the case of 2,4,6-trimethylaniline (MesNH_2), they observed the formation of only one product, an unexpected spirocyclic compound **59** which was fully characterized including X-ray analysis. The authors proposed that after the addition of the first equivalent of aniline, the *para*-methyl of the resulting product is deprotonated, thus triggering a nucleophilic attack of the *ipso*-position to the chloro-iminium moiety. We believed that a more likely mechanism involves the electrophilic attack of the chloro-iminium moiety to form a spiro Wheland-type intermediate (Scheme 48).



Scheme 48: Proposed mechanism for the reaction of vinamidinium with MesNH_2

In the case of 2,6-diisopropylaniline (DippNH_2), they reported the isolation of the desired diimine **61** in 33 % yield. We followed their procedure⁵¹ by refluxing the dichlorovinamidinium salt **54**⁺ with 2.4 equivalent of DippNH_2 in the presence of 3.5 equivalent of Hünig base (*N*-ethyl diisopropyl amine) in chloroform. But in these

experimental conditions, the desired diimine **61** was formed as a 5 % impurity. We could isolate the major product in 65 % yield that was fully characterized. Its ^1H NMR spectrum featured signals for five aromatic protons at $\delta = 6$ to 8 ppm which were reminiscent of quinoline **56**. X-ray diffraction study further confirmed the formation of the quinoline derivative **62** (Figure 19). We assumed that the reaction proceeds through an intramolecular electrophilic aromatic substitution involving the elimination of an isopropyl carbocation and the formation of isopropyl chloride.

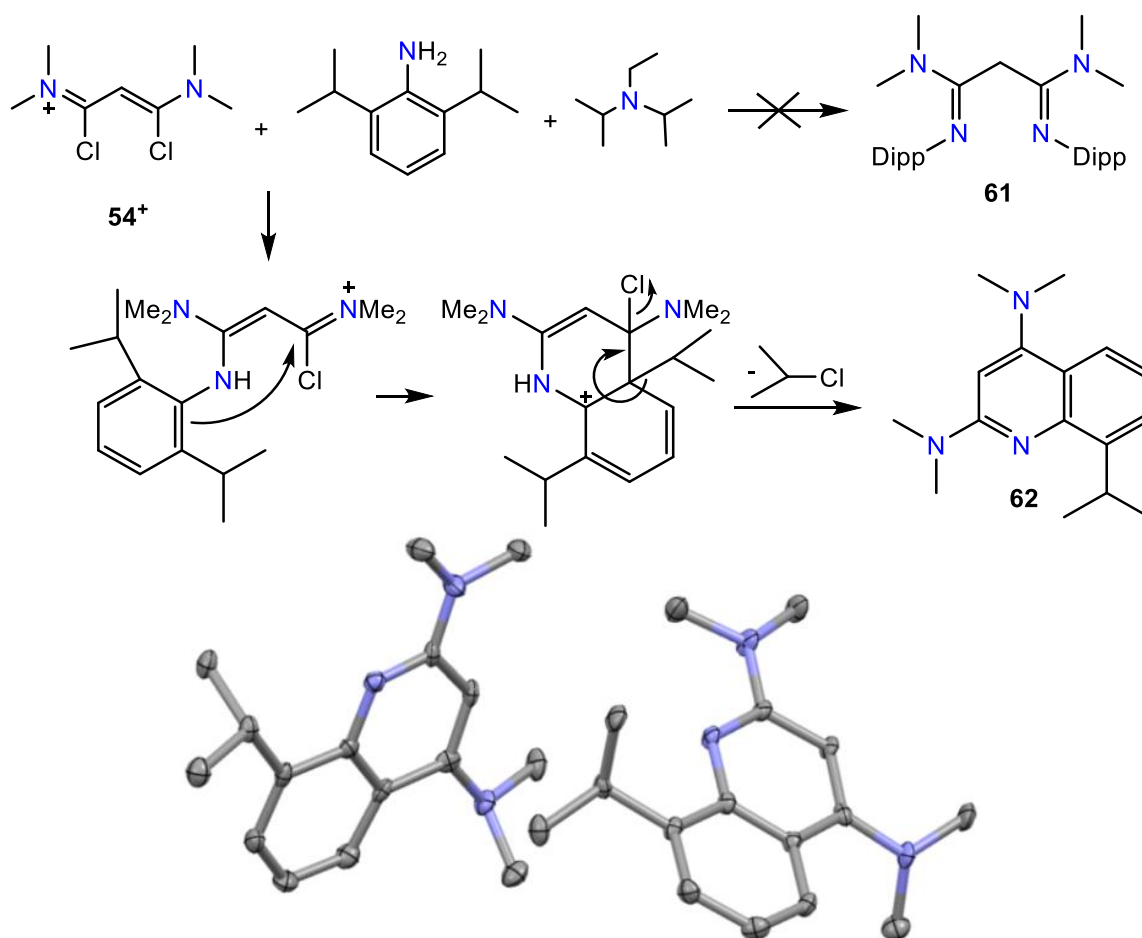
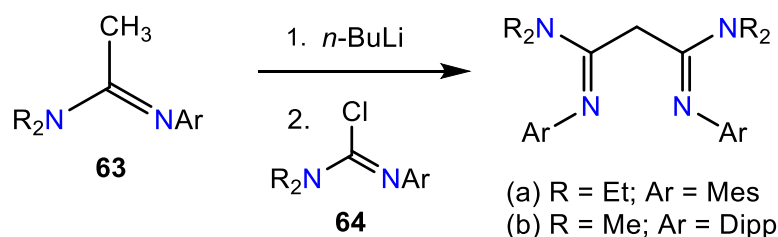


Figure 19: The reaction mechanism and the crystal structure (twin) for quinoline derivative **62 (H-atoms are omitted for clarity)**

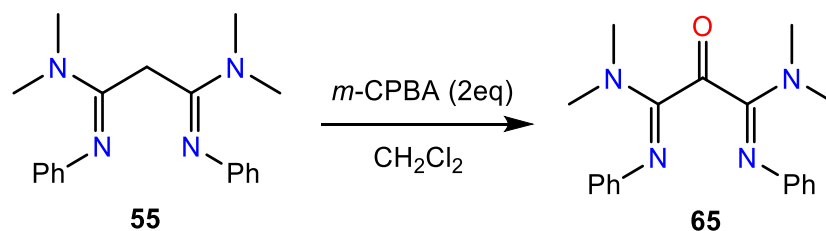
S. Aldridge and co-workers proposed an alternative method for the synthesis of diimines **60** and **61** featuring bulky N-substituents (Scheme 49). They reported that the reaction of lithiated 2-(methyl)vinamidines **63** with 2-(chloro)vinamidines **64** afforded the desired diimines in 35-66 % yield. However, we found that the preparation of precursors **63** and **64** was too inefficient (10-15 % yields) and irrelevant for the synthesis of diimines on a gram-scale.



Scheme 49: Alternative method for the synthesis of diimines

III.5 Synthesis and study of an electron-enriched bis-imine ketone

The designed diimine **55** was oxidized with *m*-CPBA in dichloromethane at room temperature according to our methodology (see chapter II). The previously unknown bis-imine ketone ligand **65** was isolated in 86 % yield.



Scheme 50: *m*-CPBA oxidation of vinamidine **65**

The oxidized product **65** was fully characterized. The presence of the ketone moiety was evidenced by a characteristic peak at $\delta = 191.0$ ppm in ^{13}C NMR as well as a band at $\nu = 1704$ cm^{-1} in IR spectroscopy. The structure was further ascertained by X-ray diffraction experiment (Figure 20).

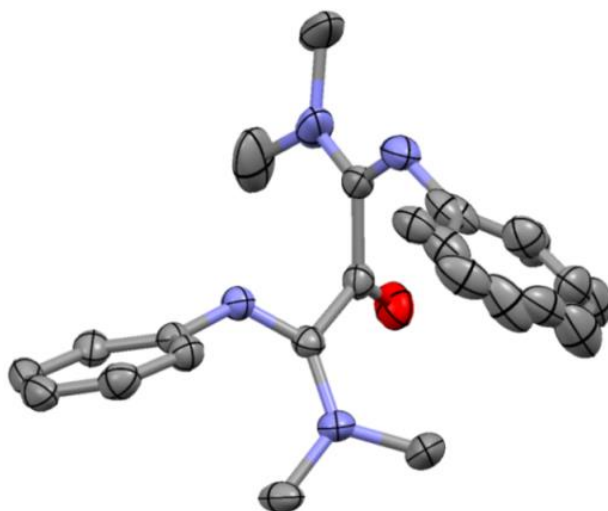


Figure 20: Crystal structure of ligand **65 (H-atoms are hidden for clarity)**

The reduction of **65** was studied by cyclic voltammetry. When the experiment was performed at the scan rate of $100 \text{ mV}\cdot\text{s}^{-1}$, an irreversible wave was observed. Electrochemical reversibility was ultimately achieved at $10,000 \text{ mV}\cdot\text{s}^{-1}$ scan rate ($E_{1/2} = -1.7 \text{ V}$). These experiments indicated the formation of the ketyl radical anion **65** \cdot^- which undergoes a fast chemical transformation (Figure 21).

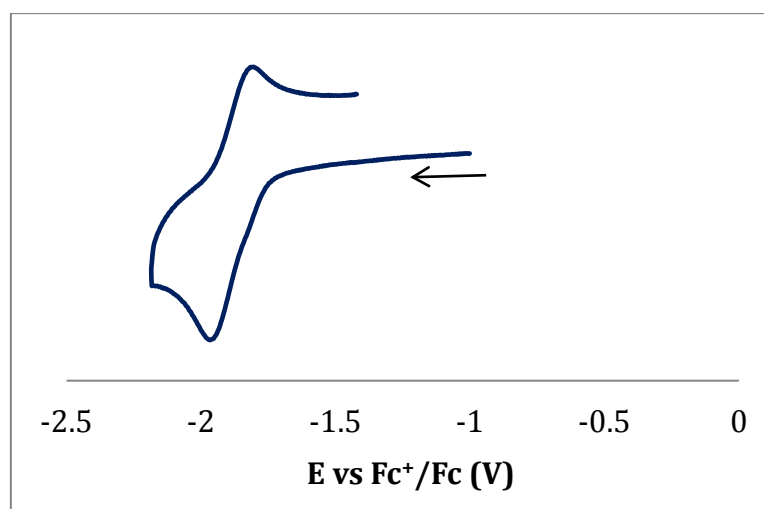
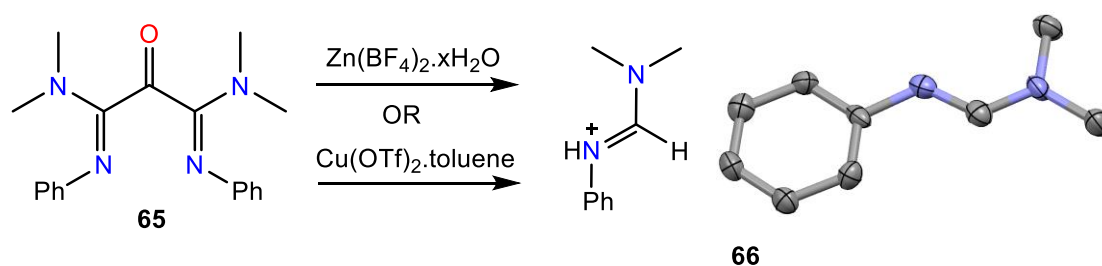


Figure 21: Cyclic voltammogram of ligand 65 in 0.1 M solution of TBAPF₆ in acetonitrile with a scan rate of $10,000 \text{ mV}\cdot\text{s}^{-1}$

We attempted several coordination reactions of diimine **65** with transition metal precursors. Complex reaction mixtures were obtained with $(\text{DME})\text{NiBr}_2$, ZnCl_2 or $\text{K}_2[\text{PtCl}_4]$. Despite all our efforts, no well-defined compound could be separated by crystallization.

Ligand **65** partially reacted with $\text{Zn}(\text{BF}_4)_2\cdot x\text{H}_2\text{O}$ and $\text{Cu}(\text{OTf})_2\cdot\text{toluene}$ metal salts. However, besides the free ligand, the main reaction product turned out to be an amidine **66** which was fully characterized, including X-ray analysis (Scheme 51). Amidine **66** is likely the result of a metal-promoted hydrolysis.



Scheme 51: Formation of the hydration product 66

Eventually, ligand **65** was reacted with one equivalent of diethylzinc (ZnEt_2) in dichloromethane at room temperature (Figure 22). Note that a gentle gas evolution was observed during the reaction. The crude solid was washed with pentane and crystals (15-20 % yield) were formed at -20°C by the layering of pentane over concentrated dichloromethane solution. X-ray analysis revealed that the resulting Zn-complex **67** consists of a zinc(II) chloride center which is O-coordinated by three (NNO)EtZn(II) units where (NNO) is a L2X scorpionate (diimine)(alkoxy) ligand (Figure 22). IR (no ν_{CO} , only $\nu_{\text{CN}} = 1559 \text{ cm}^{-1}$) and ^{13}C NMR ($\delta_{\text{CN}} = 157.1$, $\delta_{\text{CO}} = 78.2 \text{ ppm}$) spectroscopy were also in line with the formation of the R-CH-O moiety in the complex.

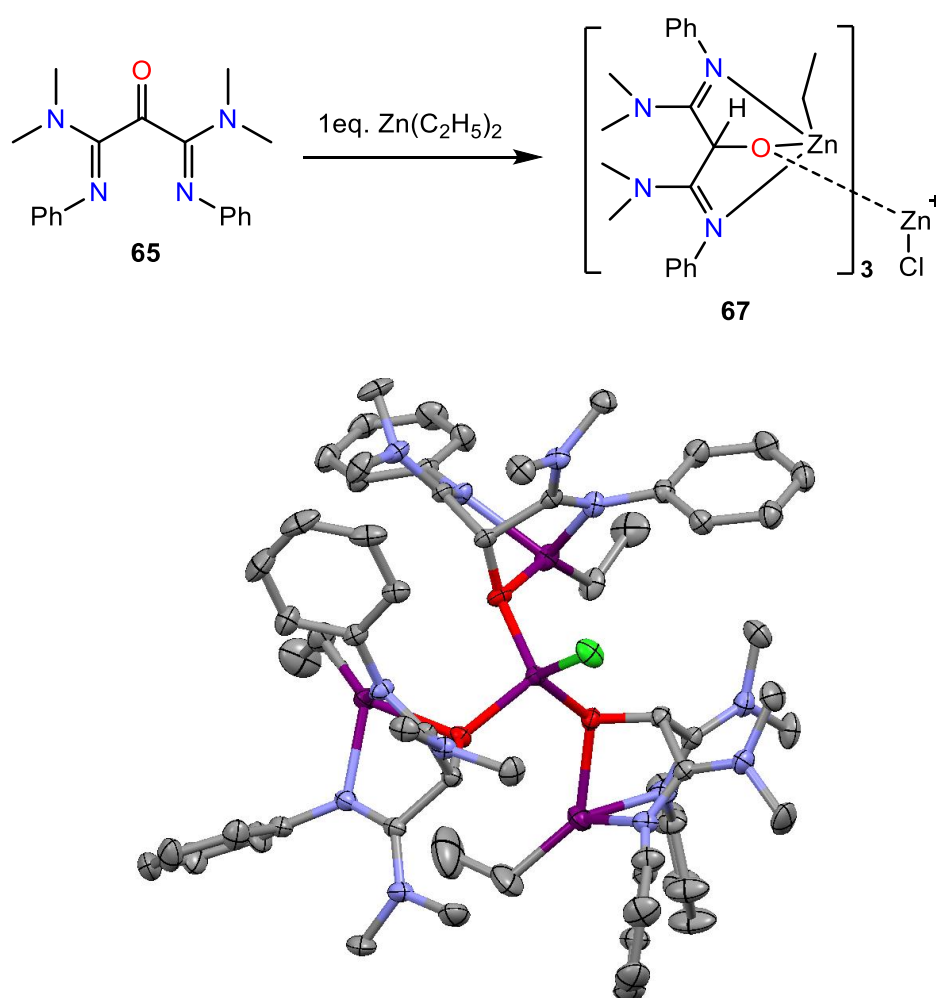
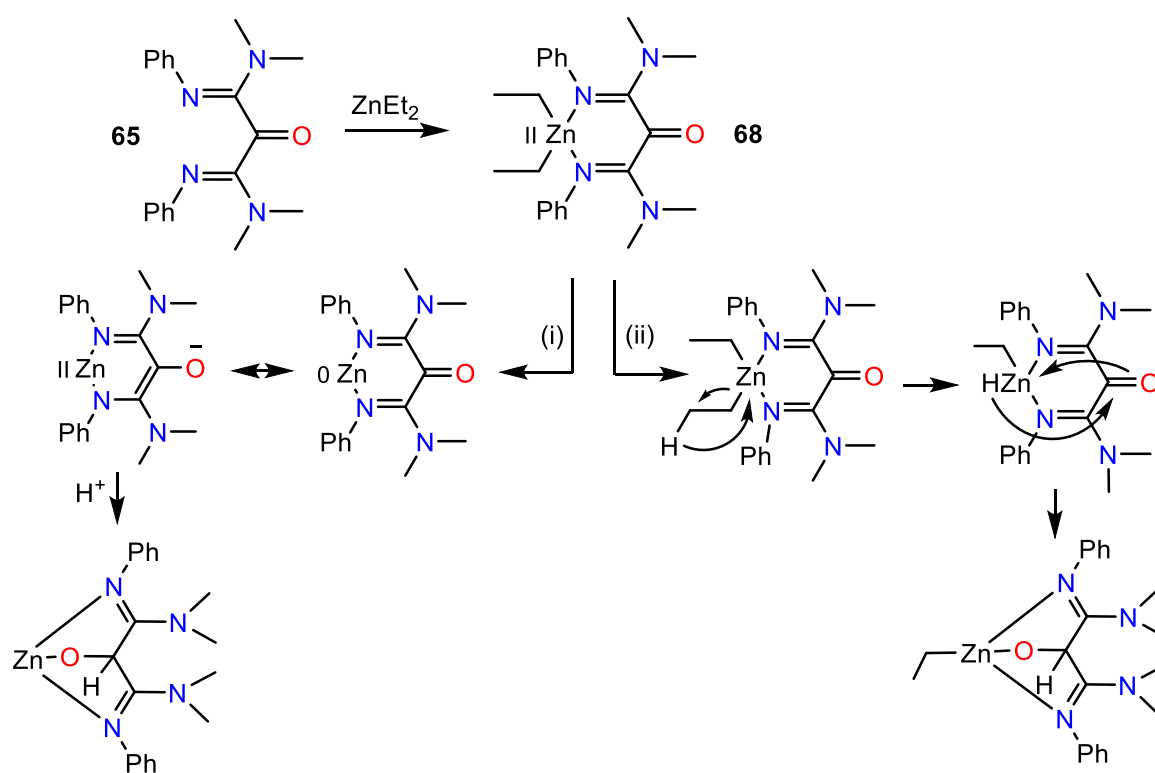


Figure 22: Synthesis and X-ray structure of complex 67 (H-atoms & counter-anions are omitted for clarity)

During this reaction, ligand **65** underwent a formal reduction. We proposed that ligand **65** first reacts with ZnEt_2 to afford complex **68**, then two possible processes could account for the formation of complex **67**:

(i) a reductive elimination of the ethyl groups to form butane gas and a complex that can be seen as Zn(0)-**65** or Zn(II)-**65**²⁻ due to the redox non-innocent behavior of the ligand. In that case, the formation of **67** would be the result of further protonation by an external source, possibly dichloromethane which can also be the source for the chloride anions (Scheme 52).

(ii) a β -hydride elimination of the ethyl group with the formation of ethylene. In that case, the reduction of the keto moiety is simply the result of a hydride migration with no need for an external source of protons. However, it does not account for the formation of the chloride anion.



Scheme 52 : Proposed mechanisms for the formation of complex 67

Such β -H elimination in zinc(II) compounds may have important implications in group transfer reactions in synthetic chemistry or for the understanding of Zn-based metalloenzymes.⁵² Indeed, it is not a very common pathway for organozinc compounds and can only be observed under extreme conditions⁵³ either by thermal treatment or IR laser pyrolysis at 600-650°C. Note that there are scarce reports of hydride reduction of electron-poor tri(fluoro)methyl ketones by ZnEt_2 ⁵⁴ which could be related to the formation of complex **67**.

III.6 Conclusion

The formation of the desired electron-rich diimine **55** was performed by delaying the addition of triethylamine to the reaction mixture of aniline and vinamidinium **54**⁺. On the other hand, the addition of aniline to vinamidinium **54**⁺ in the presence of base formed the quinoline **56**, regardless of stoichiometry. It is possible to rationalize the experimental results with a simple qualitative consideration of intermediates **57** and **57.H**⁺. Indeed, **57.H**⁺ bears both, a less electrophilic iminium and a more nucleophilic aryl center than in the case of intermediate **57**. DFT calculations are in line with experimental results, providing solvent effects are taken into account. Among the various transition states for the cyclisation process, only **TS**[‡]_{cis} derived from **57** allows for a fast intramolecular reaction at room temperature. The synthesis of diimine **55** cannot be extended towards bulkier anilines. The electron-enriched bis-imine ketone ligand **65** was formed by the *m*-CPBA oxidation of diimine **55**. The reaction of ligand **65** with diethylzinc afforded complex **67**. This reaction implies an unusual reductive process (either a reductive elimination or a β-hydride elimination from ethyl group) promoted by the ligand **65**.

III.7 Experimental

General considerations: 1,3-dichlorovinamidinium salt **54**⁺ was prepared according to literature procedures.⁴⁸ All the solvents and commercially available amines were freshly distilled before use and the reactions were performed under an inert atmosphere. Other commercial chemicals were used without further purifications.

DFT calculations were carried at the B3LYP/6-311g(d,p) level of theory using the program package Gaussian09.⁵⁰ Optimized structures were identified as energy minima by calculating the vibrational frequencies. E is the absolute electronic energy with zero point energy correction; H and G are the sum of electronic (in hartrees). Transition states were examined by vibrational analysis and then submitted to intrinsic reaction coordinate calculations.

Melting points: A Büchi B-545 melting point apparatus system was used to determine mp.

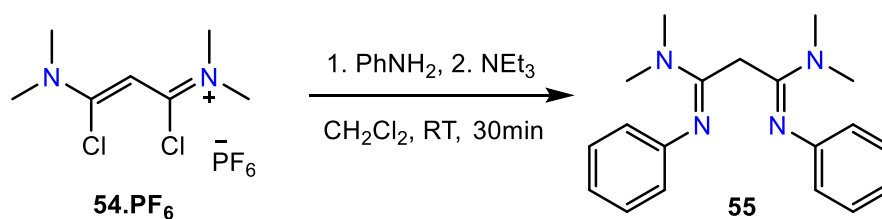
High Resolution Mass Spectrometry: HRMS were carried by electrospray ionization method on Brüker Esquire 3000 or a Thermo Scientific LTQ Orbitrap XL.

Infra-Red: IR spectra were measured on a Thermo Scientific Nicolet iS10 FT-IR ATR spectrometer.

Nuclear Magnetic Resonance: ¹H NMR (at 300, 400 or 500 MHz) and ¹³C NMR (at 75, 100 or 125 MHz) spectra were performed on the NMR-ICMG platform of Grenoble with Bruker Avance 300, 400 and 500 spectrometers at 298 K and reported in parts per million (ppm) relative to TMS. NMR multiplicities are abbreviated as follows: s = singlet, d = doublet, t = triplet, sept = septuplet, m = multiplet, br = broad signal.

Crystallographic studies were performed on the RX-ICMG platform of Grenoble with a Bruker AXF-APEXII X-ray diffraction instrument (with Mo/K α -radiation).

Electrochemical measurement of ligand **65:** It was carried out using a Bio-logic SP-300 potentiostat. Cyclic voltammetry experiment was performed in 0.1 M TBAPF₆ + CH₃CN at a scan rate of 10,000 mV.s⁻¹ with a vitreous carbon disk (3 mm in diameter) as a working electrode, Ag/0.01 M AgNO₃ as a reference electrode and a platinum wire as an auxiliary electrode. All reduction potentials are reported with respect to the E_{1/2} of the Fc/Fc⁺ redox couple.



55: Aniline (6.63 g, 0.071 mol) was added in once to a solution of vinamidinium salt **54.PF₆** (3.85 g, 0.011 mol) in CH₂Cl₂ (5 mL) at 0°C. After 10 minutes, a white suspension was observed and then NEt₃ (6.90 g, 0.068 mol) was added drop wise. After 30 minutes of stirring, volatiles were evaporated under vacuum. The resulting residue was triturated and washed twice with Et₂O and then dissolved in CH₂Cl₂. The organic solution was washed three times with 1 M aqueous solution of K₂CO₃, once with water and dried over Na₂SO₄. Evaporation under vacuum yielded a sticky oil. Addition of few drops of cyclohexane initiated the crystallization whereby crystals were isolated as colorless needles (2.37 g, 68 % yield). Single crystals suitable for X-ray diffraction analysis were obtained by recrystallization in cyclohexane at room temperature.

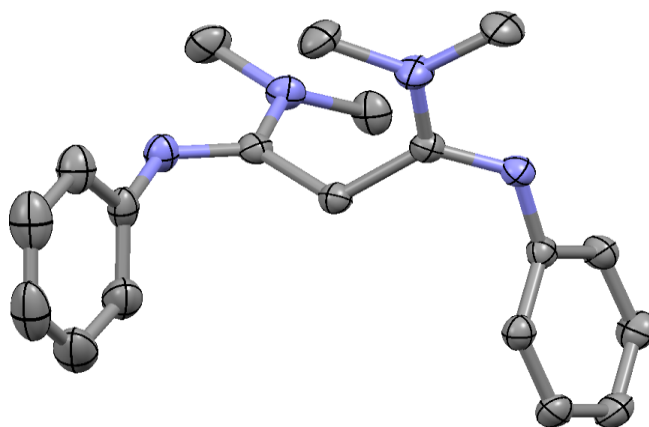
mp: 135°C.

HRMS: m/z calcd for [C₁₉H₂₅N₄]⁺, 309.2079; found, 309.2083.

¹H NMR (400 MHz, CDCl₃) δ: 7.35 (t, *J* = 8 Hz, 4H), 7.06 (t, *J* = 8 Hz, 2H), 6.73 (d, *J* = 8 Hz, 4H), 3.54 (s, 2H), 3.00 (s, 12H) ppm.

¹³C NMR (100 MHz, CDCl₃) δ: 155.7, 150.8, 129.0 (CH), 122.7 (CH), 121.9 (CH), 38.6 (CH₃), 29.4 (br, CH₂) ppm.

Crystallographic data:



Formula: C₁₉ H₂₄ N₄

Space Group: R -3

Cell lengths (Å): a = 16.0329(19); b = 16.0329(19); c = 16.0329(19)

Cell Angles (°): α = 113.029(17); β = 113.029(17); γ = 113.029(17)

Cell Volume: 2674.61

R-Factor (%): 4.01

Bond length

Selected Angle

C7H7B 0.990

C7C8N1 124.1(1)

C7C8 1.527(2)

C1N4C8 117.9(2)

C8N1 1.290(1)

N4C8N1 117.5(1)

N1C5 1.405(2)

C8N1C5 123.3(1)

C9C5 1.396(3)

N1C5C9 121.9(1)

C12C9 1.387(2)

C10C5C9 118.5(2)

C9H9 0.950

C1N4C14 116.4(2)

C8N4 1.363(2)

C8C7C6 118.3(1)

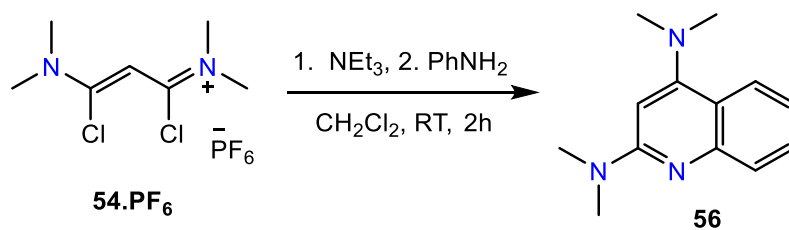
N4C1 1.456(3)

C7H7AH7B 36.48

C1H1A 0.980

H7AC7C8 107.7

N4C1 1.456(3)

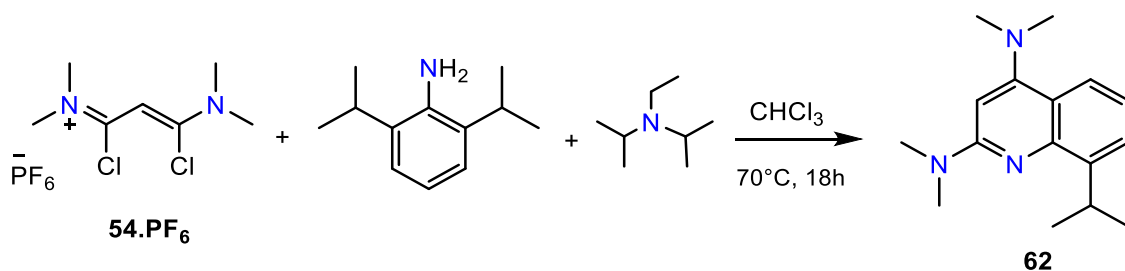


56: Under air, aniline (0.66 g, 7 mmol) was added drop wise to a solution of vinamidinium **54.PF₆** (1.0 g, 3 mmol) and NEt₃ (1.20 g, 12 mmol) in CH₂Cl₂ (20 mL). After two hours of stirring, the resulting mixture was washed once with aqueous NaHCO₃, once with water and dried over Na₂SO₄. After evaporation under vacuum, purification by flash column chromatography (silica, eluent: CH₂Cl₂, then ethyl acetate) yielded a colorless oil. (Yield = 265 mg, 42 %).

HRMS: m/z calcd for [C₁₃H₁₈N₃]⁺, 216.1501; found, 216.1504.

¹H NMR (500 MHz, CDCl₃) δ: 7.86 (d, *J* = 8 Hz, 1H), 7.69 (d, *J* = 8 Hz, 1H), 7.47 (t, *J* = 8 Hz, 1H), 7.15 (t, *J* = 8 Hz, 1H), 6.26 (s, 1H), 3.21 (s, 6H), 2.96 (s, 6H) ppm.

¹³C NMR (125 MHz, CDCl₃) δ: 158.4, 128.8 (CH), 126.8 (CH), 124.0 (CH), 120.2 (CH), 118.1, 94.9 (CH), 43.7 (CH₃), 37.9 (CH₃) ppm.



62: To a solution of vinamidinium salt **54.PF₆** (0.5 g, 1.47 mmol) in CHCl₃, 2,6-diisopropylaniline (0.61 g, 3.45 mmol, 2.4 eq) and *N*-ethyl diisopropyl amine (0.67 g, 5.17 mmol, 3.5 eq) were added. The reaction mixture was then refluxed overnight at 70°C. After cooling to room temperature, saturated KOH solution was added at 0°C until the pH reached 10, followed by water. The aqueous layer was washed twice with CHCl₃ and the organic layers were combined and washed with brine (NaCl) and dried over MgSO₄. The resulting solution was filtered and after evaporation, the obtained residue was purified by flash chromatography (eluent: DCM/MeOH/NEt₃ = 97/2/1) on silica gel yielded a reddish-oily product (231 mg, 61 % yield). The compound was recrystallized at -20 °C from a saturated pentane solution. Single crystals suitable for X-ray diffraction analysis were obtained from a saturated pentane solution at room temperature.

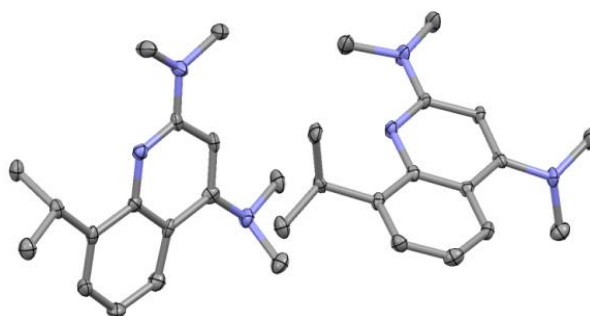
mp: 65.1°C.

HRMS (ESI): *m/z* calcd for [C₁₆H₂₄N₃]⁺, 258.1970; found 258.1969.

¹H NMR (500 MHz, CDCl₃) δ: 7.73 (d, *J* = 8 Hz, 1H), 7.39 (d, *J* = 8 Hz, 1H), 7.12 (t, *J* = 8 Hz, 1H), 6.29 (s, 1H), 4.15 (sept, *J* = 7 Hz, 1H), 3.21 (s, 6H), 2.94 (s, 6H), 1.36 (d, *J* = 7 Hz, 6H) ppm.

¹³C NMR (125 MHz, CDCl₃) δ: 159.3, 157.4, 147.1, 144.7, 124.7 (CH), 121.7 (CH), 120.3 (CH), 118.3, 95.1 (CH), 44.3 (CH₃), 38.2 (CH₃), 28.0 (CH), 23.2 (CH₃) ppm.

Crystallographic data (twin structure):



Formula: C₁₆H₂₃N₃

Space Group: P -1

Cell lengths (Å): a = 8.3549(10); b = 11.8139(12); c = 15.0527(17)

Cell Angles (°): α = 105.598(9); β = 93.257(9); γ = 90.138(9)

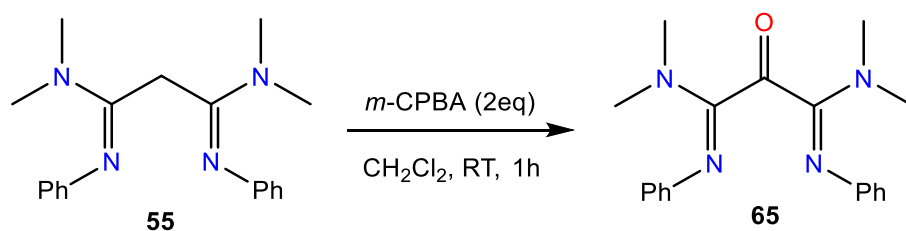
Cell Volume: 1428.49

R-Factor (%): 8.28

Bond length

Selected Angle

C3N3 1.405(7)	C3C2 1.351(6)	C8C14C15 114.2(4)
N3C12 1.450(6)	C2C1 1.450(7)	C16C14C15 109.5(4)
C1N2 1.361(6)	C2H2 0.930	C8C9N1 117.6(4)
C9N1 1.359(5)	C11H11C 0.960	C9N1C1 119.0(4)
C4C9 1.427(7)	C13H13B 0.960	C1C2C3 119.2(4)
C1N1 1.318(5)	C4C3 1.430(6)	N1C1N2 118.1(4)
C8C14 1.524(7)	C14H14 0.980	C11N2C10 115.7(4)
N2C11 1.436(6)	C6H6 0.930	C11N2C1 123.7(4)
C14C15 1.531(6)		C3N3C12 117.7(4)
C9C8 1.430(6)		C12N3C13 111.1(4)
C4C5 1.407(6)		C9C4C5 118.4(4)
C5C6 1.364(7)		C9C8C7 118.6(4)
C6C7 1.397(8)		C5C6C7 119.4(5)
C7C8 1.372(6)		C4C3N3 118.5(4)
C16H16B 0.960		C9C8C14 118.4(4)



65: *m*-CPBA [60 wt% with H₂O] (7.46 g, 25.94 mmol) was dissolved in CH₂Cl₂ (40 mL), dried over Na₂SO₄, 20 mL of this solution was added into a solution of 1,3-diimine **55** (2.0 g, 6.48 mmol) in CH₂Cl₂ (30 mL). The reaction mixture was stirred for one hour. The mixture was washed three times with saturated aqueous solution of NaHCO₃, once with water, dried over Na₂SO₄, filtered & concentrated in vacuo to give the solid product (1.8 g, 86 % yield). Single crystals suitable for X-ray diffraction analysis were obtained by crystallization in cyclohexane at room temperature.

mp: 111.2°C.

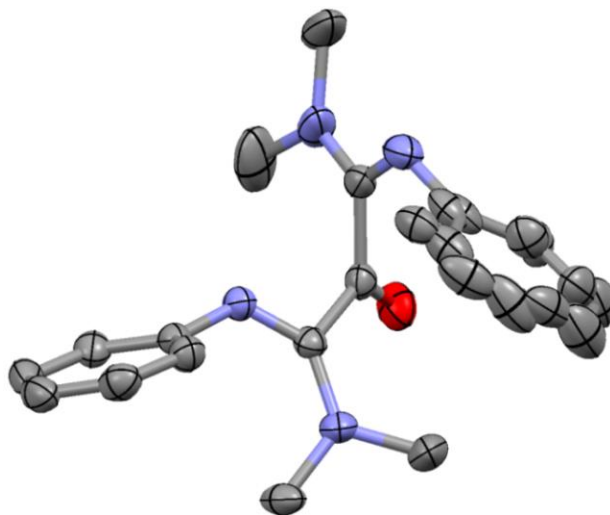
HRMS: *m/z* calcd for C₁₉H₂₃O₁N₄ (M+H⁺), 323.1872; found, 323.1881.

IR (ATR): $\nu = 1704 \text{ cm}^{-1}$ (C=O).

¹H NMR (300 MHz, CDCl₃) δ : 7.23 (t, *J* = 8 Hz, 4H), 6.95 (t, *J* = 8 Hz, 2H), 6.8 (d, *J* = 8 Hz, 4H), 2.59 (br s, 12H) ppm.

¹³C NMR (75 MHz, CDCl₃) δ : 191.2, 148.7, 129.1, 128.6 (CH), 122.6 (CH), 122.2 (br, CH), 38.7 (br, CH₃) ppm.

Crystallographic data:



Formula: C₁₉ H₂₂ N₄ O

Space Group: P n a 2₁

Cell lengths (Å): a = 12.168(2); b = 21.152(4); c = 6.9588(14)

Cell Angles (°): α = 90.00; β = 90.00; γ = 90.00

Cell Volume: 1791.04

R-Factor (%): 4.52

Bond length

Selected Angle

C6O1 1.203(2)

C3C6C8 115.9(1)

C6C3 1.515(2)

O1C6C3 123.5(1)

C3N4 1.347(2)

N4C3N2 132.1(1)

N4C6AA 1.459(3)

C3N2C5 126.4(1)

C3N2 1.283(2)

C6AAN4C1AA 114.3(2)

N2C5 1.409(2)

N2C5C10 119.2(1)

C5C12 1.391(2)

C12C5C10 119.2(1)

C12C9 1.382(2)

C5C10C1 119.9(2)

C9H9 0.951

C1AAN4C3 122.3(1)

C9H9 0.951

N2C3C6 108.5(1)

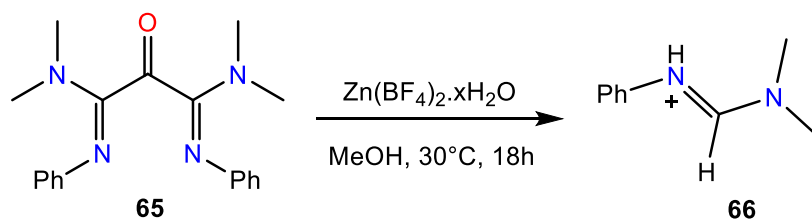
C12H12 0.950

H6ACC6AAN4 109.5

C6AAH6AB 0.980

H6AAC6AAH6AB 109.5

H1C1C13 119.7

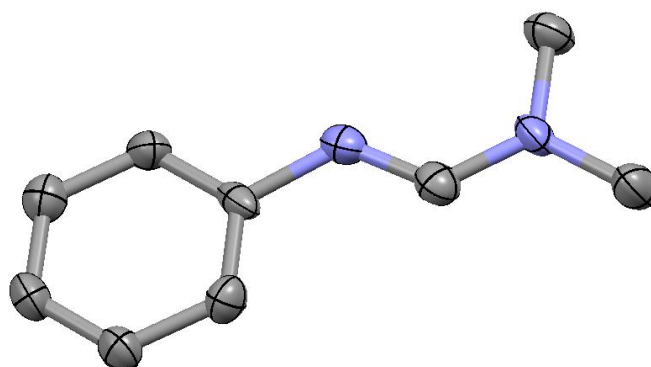


66: To the solution of ligand **65** (0.212 g, 0.658 mmol) in MeOH (8 mL), a solution of zinc fluoroborate (0.075 g, 0.314 mmol) in MeOH (7 mL) was added and the reaction mixture was stirred for 18 hours at 30°C. The solvent was evaporated and the residue was crystallized by layering ether over a CH₂Cl₂ solution at -20°C.

¹H NMR (400 MHz, CDCl₃) δ: 7.30 (d, *J* = 6 Hz, 8H), 7.04 (d, *J* = 6 Hz, 2H), 6.88 (s, 5H), 3.59 (s, 2H), 3.06 (s, 6H), 2.64 (br s, 12H) ppm.

¹³C NMR (100 MHz, CDCl₃) δ: 190.8, 152.7, 149.8, 148.5, 129.7 (CH), 128.6 (CH), 122.6 (CH), 121.7 (CH), 51.8 (CH), 38.6 (br, CH₃), 37.1 (br, CH₃) ppm.

Crystallographic data:



Formula: C₉H₁₃N₂

Space Group: P 2₁/c

Cell lengths (Å): a = 6.7152(8); b = 15.0642(17); c = 11.3605(14)

Cell Angles (°): α = 90; β = 105.270(11); γ = 90

Cell Volume: 1108.65

R-Factor (%): 7.63

Bond length

C1N1 1.445(4)

N1C7 1.296(5)

C7N2 1.323(4)

N2C8 1.439(5)

C1C6 1.383(5)

C6C5 1.407(5)

C8H8B 1.02(5)

C7H7 1.00(3)

C6H6 0.92(5)

C5H5 1.04(4)

N1H1 1.06(4)

Selected Angle

N1C7N2 123.8(4)

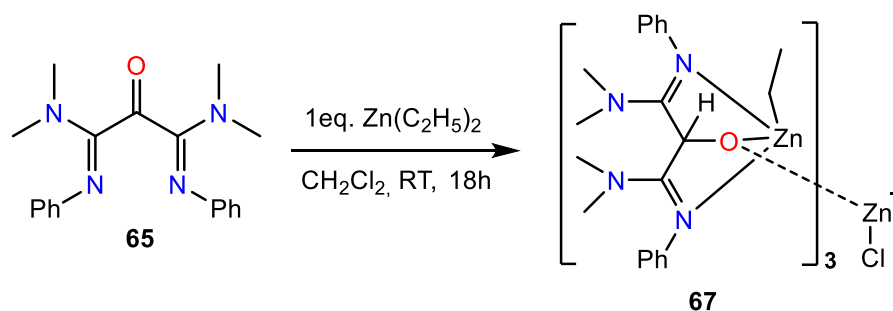
C8N2C9 117.1(3)

C7N1C1 123.8(3)

N1C1C6 123.1(3)

C1C6C5 119.2(4)

H8CC8H8B 128(4)



67: To the solution of the ligand **65** (0.5 g, 1.551 mmol) in CH₂Cl₂ (20 mL), 1 M diethyl zinc (1.6 mL, 1.6 mmol) was added and the reaction mixture was stirred for 18 hours. The solvent was evaporated and the residue was crystallized by layering pentane over minimum CH₂Cl₂ solution at -20°C. (Yield 15-20 %)

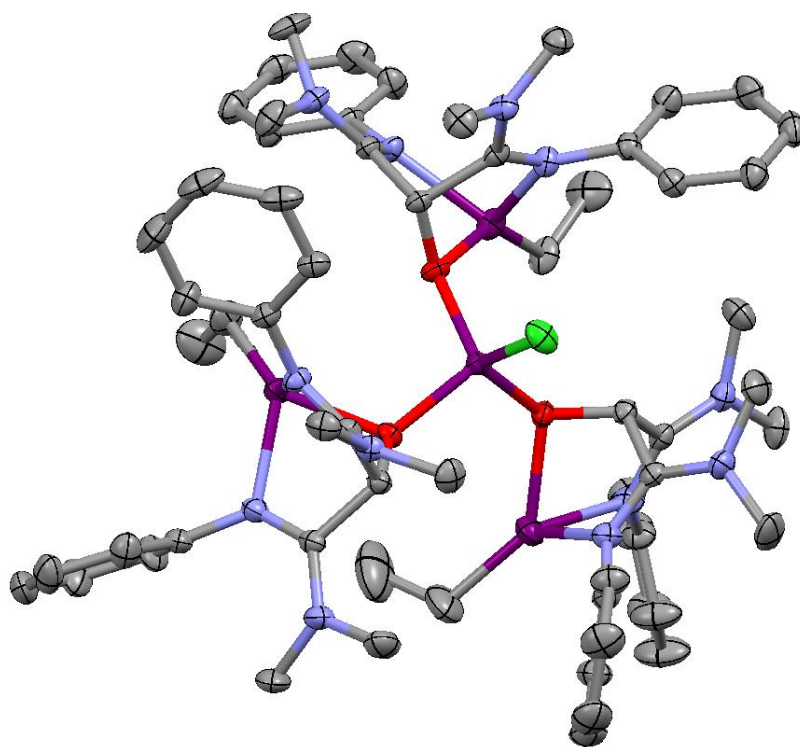
mp: 146-149°C.

IR (ATR): $\nu = 1559 \text{ cm}^{-1}$ (C-O).

¹H NMR (400 MHz, CDCl₃) δ : 7.3-6.8 (m, 10H), 3.7 (s, 2H), 2.8 (s, 12H), 1.28 (s, 3H) ppm.

¹³C NMR (100 MHz, CDCl₃) δ : 157.1, 127.5, 121.5 (CH), 120.3 (CH), 120 (CH), 78.2 (CH), 40.8 (CH₃), 30.7 (CH₂), 6.9 (CH₃) ppm.

Crystallographic data:



Formula: C₆₃ H₈₄ Cl N₁₂ O₃ Zn₄

Space Group: P -1

Cell lengths (Å): a = 13.603(3); b = 14.637(3); c = 21.903(4)

Cell Angles (°): α = 70.62(3); β = 76.87(3); γ = 63.02(3)

Cell Volume: 3650.94

R-Factor (%): 3.74

Bond length

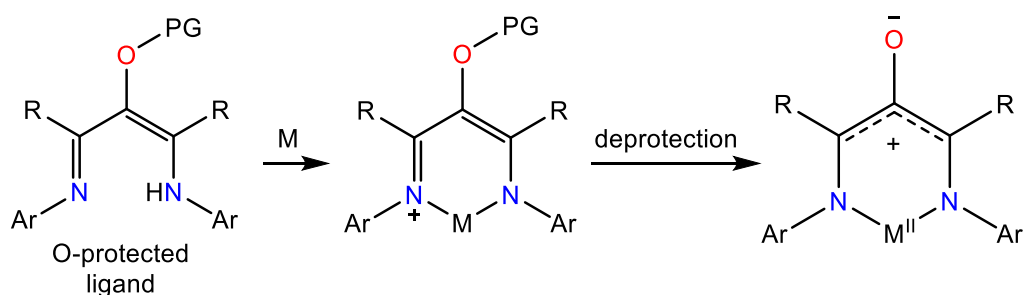
Selected Angle

Zn1Cl1 2.2378(9)	C29H29 0.949	Zn1O5Zn4 121.02(9)	C8C11O5 107.4(2)
Zn1O5 1.937(2)	C23H23B 0.990	Cl1Zn1O5 113.82(6)	N10C10N12 128.3(3)
O5Zn4 2.032(2)	H59CC59 0.980	Cl1Zn1O6 115.09(6)	Zn4O5C11 99.5(1)
Zn4C23 1.955(5)	C6H6C 0.980	O4Zn1Cl1 113.69(6)	N10C10C11 118.9(2)
C23C59 1.462(9)		O6Zn1O5 103.18(8)	
Zn4N12 2.089(2)		O5Zn4C23 138.3(1)	
N12C35 1.415(3)		Zn4C23C59 117.7(4)	
C35C29 1.382(3)		O5Zn4N12 78.49(8)	
C29C40 1.383(4)		Zn4N12C10 109.2(2)	
N12C10 1.293(3)		C20N10C10 121.7(3)	
C10N10 1.340(4)		C6N10C20 114.8(3)	
N10C6 1.450(4)		N12C35C29 118.5(3)	
C11C10 1.552(3)		C52C35C29 118.7(3)	
C11O5 1.391(4)		C23Zn4N12 128.2(2)	
C11H11 1.000			

**CHAPTER IV:
ALTERNATIVE
SYNTHETIC DESIGN
& STRATEGIES**

IV.1 O-protected ligands

In our group, an alternative synthesis of organic oxyallyl patterns have been developed which relies on the use of O-protecting groups. We wondered whether this could be applied to metal-based versions (Scheme 53).



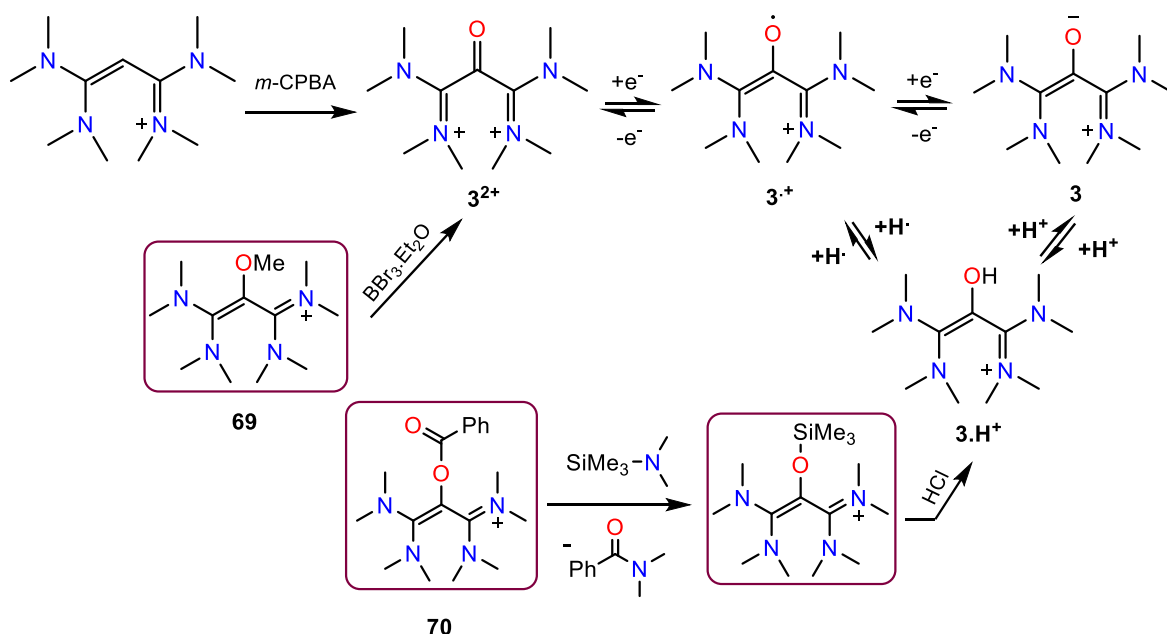
Scheme 53: The use of O-protected ligand for designing desired complexes

As mentioned before, the oxidation of tetrakis(di-methylamino) vinamidinium using *m*-CPBA as an oxidant formed di(amidinium)ketone **3**²⁺ that can be written in different redox forms in order to obtain the oxyallyl structure **3** (Scheme 54). These redox forms can also be accessible by using O-protected vinamidiniums (unpublished results).

For instance, di(amidinium)ketone **3**²⁺ was obtained by the deprotection of methyl group on vinamidinium **69** using boron bromide etherate complex (BBr₃.Et₂O). However, the last step was performed in poor yields.

Alternatively, vinamidinium **70** that feature a benzoyl O-protecting group was also synthesized. Dimethyltrimethylsilylamine (NMe₂SiMe₃) was used for the deprotection process followed by the acidic treatment. Not only **3H**⁺, the protonated form of oxyallyl **3**, was isolated in good yield (62%) but this method could be applied to a variety of novel organic oxyallyl derivatives (PhD thesis of V. Regnier, unpublished results).

Therefore, we considered the synthesis of ligands with benzoyl O-protecting groups.



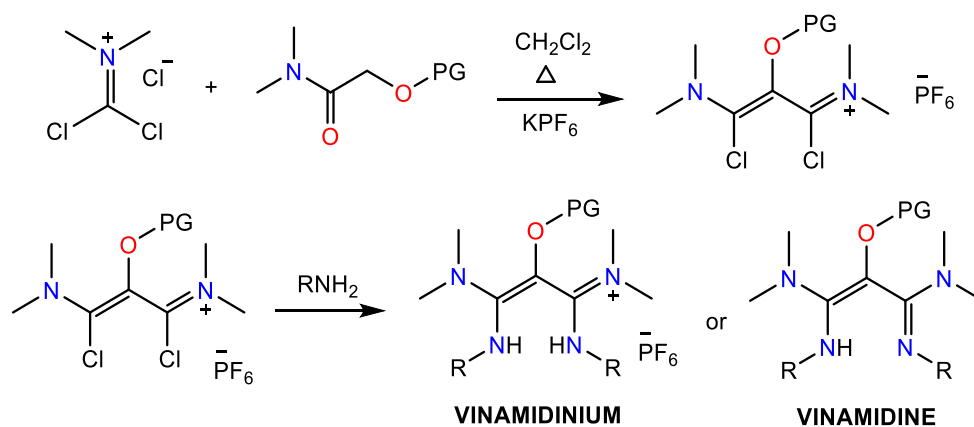
Scheme 54: Examples of O-protected vinamidiniums

IV.1.1 Preparation of O-protected ligands: preliminary considerations

The synthesis of O-protected ligands can be done following two different approaches:

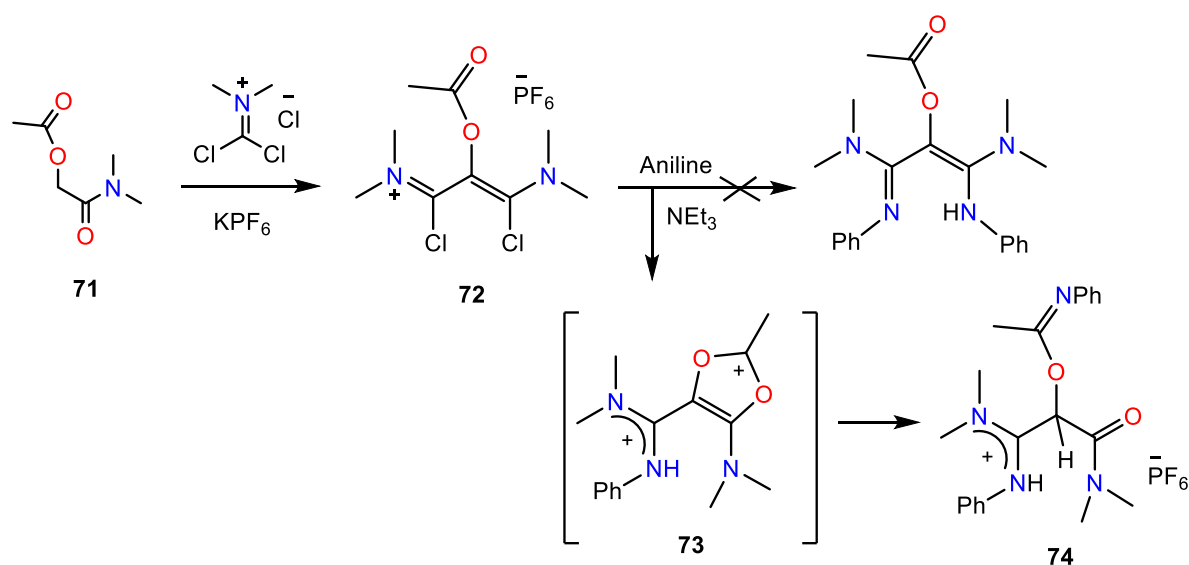
(i) from O-protected 1,3-dichlorovinamidinium salts

O-protected 1,3-dichlorovinamidinium salts can be synthesized according to previously described reaction⁵⁵ between phosgene iminium chloride and an acetamide (Scheme 55). In principle, these dichlorovinamidinium salts can be further treated with amines to give rise to O-protected vinamidiniums or vinamidines.



Scheme 55: Synthesis of O-protected vinamidiniums or vinamidines

We synthesized dichlorovinamidinium salt **72** with O-acetyl group in 43 % yield by the reaction of acetamide derivative **71** with phosgene iminium chloride. However, the addition of excess aniline in the presence of NEt₃ to vinamidinium **72** did not lead to the expected vinamidine but to benzimidate **74** which was fully characterized. This reaction likely goes through the transient formation of dicationic 1,3-dioxolium **73** followed by aminolysis with aniline. A parallel work of Marc Devillard (post doc) who synthesized a range of dioxolium salts featuring an ancillary vinamidinium pattern, is in line with this hypothesis.⁵⁶

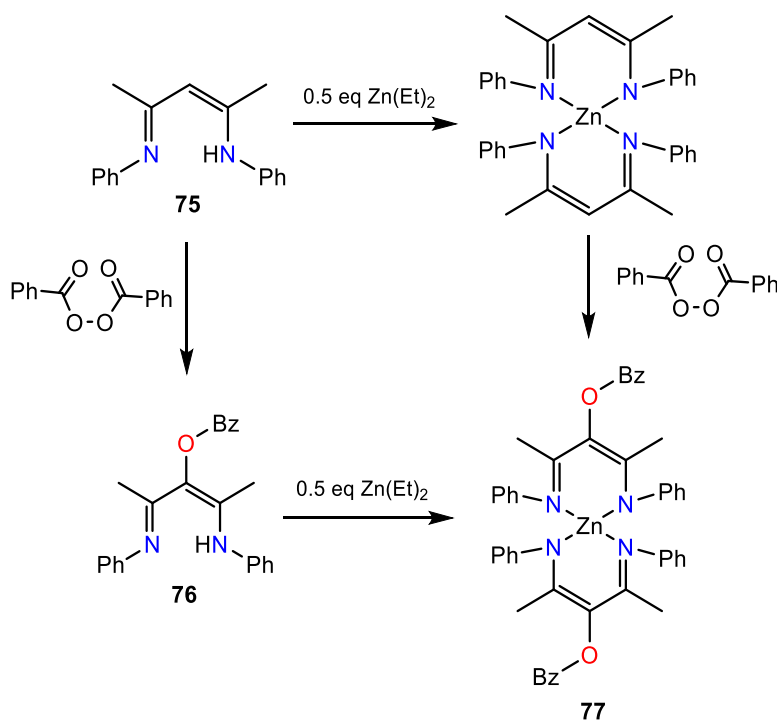


Scheme 56: Synthesis of benzimidate 74

(ii) from direct oxidation of vinamidines with benzoyl peroxide (BPO)

This method is similar to the method of direct oxidation using *m*-CPBA but instead of using *m*-CPBA, BPO was used as an oxidizing agent.

The synthesis to obtain O-protected Zn(II) complex **77** was already done by the Martin group (Scheme 57). The first step was the oxidation of vinamidine **75** with BPO to produce free O-protected vinamidine **76** that was treated with ZnEt₂ to undergo metal complexation to form O-protected complex **77**. The complex could also be prepared by reversing the order of reaction. Vinamidine **75** could be treated with ZnEt₂ first to form the corresponding complex followed by the oxidation with BPO to obtain O-protected complex **77**.



Scheme 57: Example of an O-protected ligand and the corresponding Zn(II) complex

IV.1.2 Bis(oxazoline)-based model

We chose to illustrate route (ii) further by synthesizing O-protected bis(oxazoline)-based ligands and their metal complexes. Bis-oxazolines (BOXs) have been considered as “privileged ligands”⁵⁷ due to their ability to quickly emerge as high-performance ligand platform that are used in many catalyzed stereo-controlled reactions⁵⁸ and have enormous use in catalysis. The metal complexes of bis-oxazolines have been used to prepare chiral Lewis acids where the role of the metal is to activate electrophiles in free coordination sites in order to attack nucleophiles or the enolate part.⁵⁹ Structures of bis-oxazolines with $R' = R'' = H$ are related to vinamidines and are precursors for the corresponding bidentate β -diketiminato (NacNac) ligands (Figure 23).⁶⁰

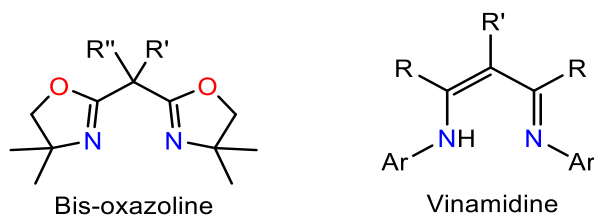
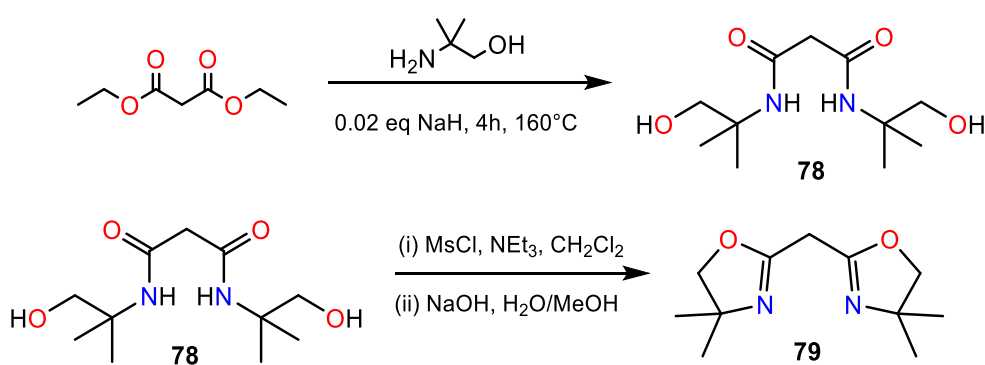


Figure 23: General structure of bis-oxazolines and vinamidines

We first synthesized bishydroxy malonamide **78** by the reaction of diethyl malonate with 2 equivalents of 2-amino-2-methyl-1-propanol in the presence of NaH at 160°C. After the removal of ethanol in vacuo, the solid product **78** was recovered and used further without purification (99 % yield).

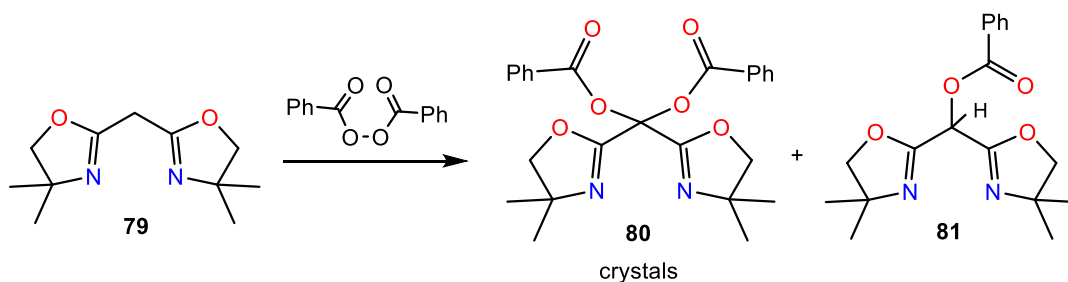
A solution of diamide **78** in dichloromethane was then treated with 2.5 equivalents of methanesulfonyl chloride at 0°C in the presence of 5 equivalents of triethylamine. After washing it with a saturated solution of ammonium chloride, the solvent was removed. The resulting crude mesylate was refluxed with 5 equivalents of sodium hydroxide in methanol/water mixture. The final product **79** was purified by bulb to bulb vacuum distillation and was isolated in 65 % yield (Scheme 58).⁶¹



Scheme 58: Synthesis of the selected bis-oxazoline **79**

The oxidation of bis-oxazoline **79** with *m*-CPBA did not work out well. ¹³C NMR and ¹H NMR indicated the formation of a complex mixture of unknown products and no formation of the expected bis-imine ketone structure was observed.

Therefore, bis-oxazoline **79** was reacted with BPO in the similar conditions. Layering pentane over a concentrated solution of the crude material in dichloromethane led to the crystallization of minor impurity **80** resulting from the reaction of a second molecule of BPO with bis-oxazoline **79**. It was fully characterized, including an X-ray analysis (see the crystal structure in Figure 24). After flash column chromatography of the remaining mother liquor, the desired O-protected preligand **81** was isolated in 75 % yield.



Scheme 59: Synthesis of O-protected bis-oxazoline ligand 81

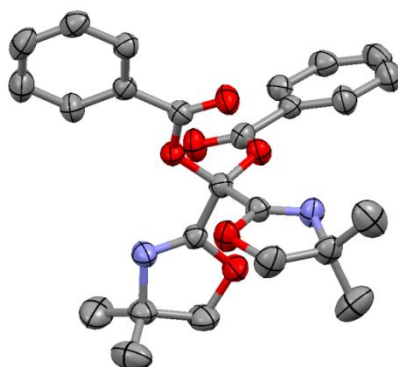


Figure 24: Crystal structure of the impurity 80

In both products **80** and **81**, there is a difference in the oxazoline and methyl hydrogens according to ^1H NMR (Figure 25). They are magnetically equivalent in **80** whereas they become diastereotopic in **81** due to the presence of the prochiral central carbon.

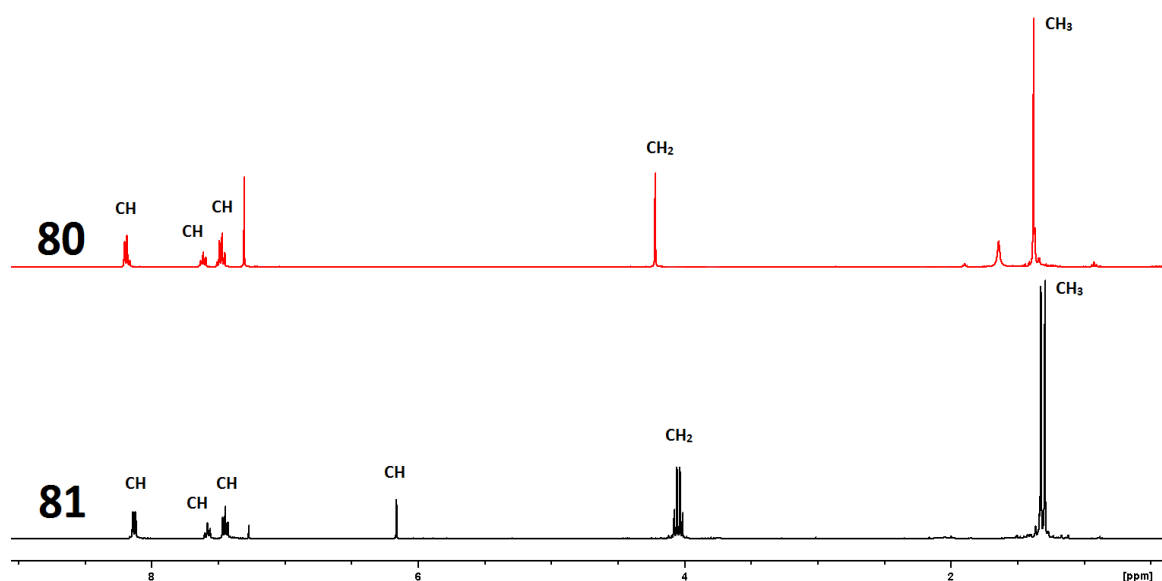
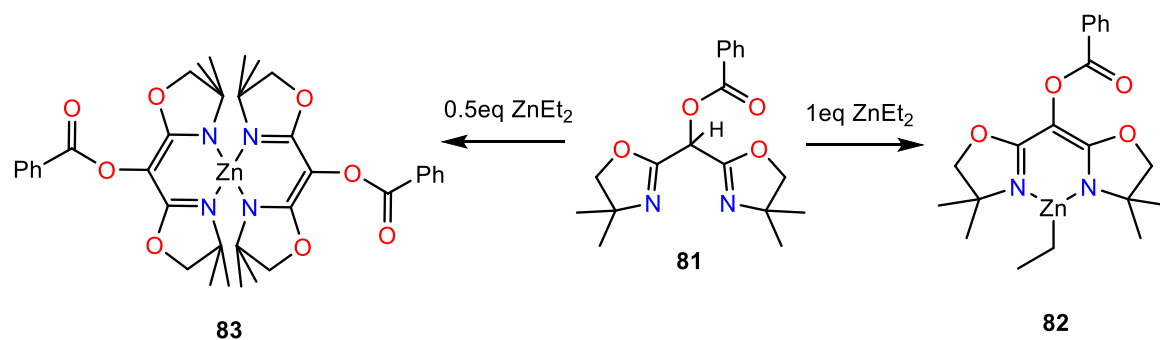


Figure 25: ^1H NMR spectra of ligands 80 and 81

The treatment of ligand **81** with one equivalent of ZnEt_2 afforded ethylzinc(II) complex **82**. The presence of one ethyl group attached to Zn was observed by ^1H NMR [CH_3 (t, $\delta = 1.28$ ppm) and CH_2 (q, $\delta = 0.4$ ppm)]. The addition of two equivalents of **81** to ZnEt_2 yielded zinc(II) complex **83**. The structure of Zn(II) complex **83** was confirmed by X-ray diffraction study (Figure 26) and featured the following structural data (IR (ATR): $\nu = 1773$ (C=O), 1619 (C-O) cm^{-1} ; ^{13}C NMR: $\delta_{\text{CO}} = 166.9$ ppm).



Scheme 60: Synthesis of Zn(II) complexes 82 and 83

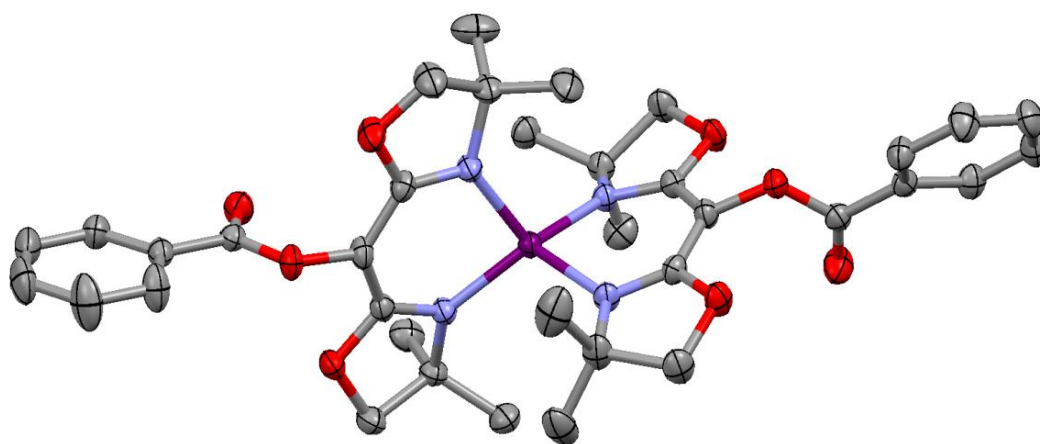


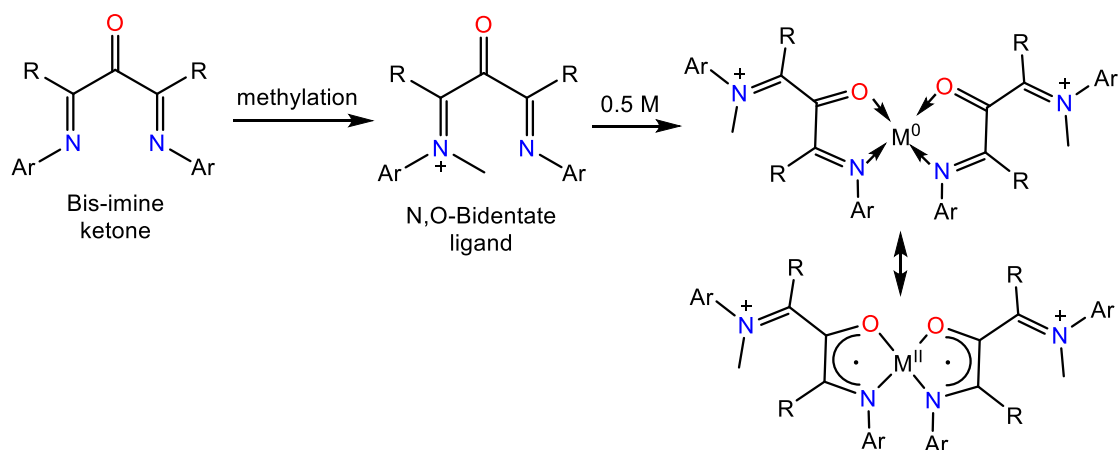
Figure 26: Crystal structure of Zn(II) complex 83 (H-atoms are omitted for clarity)

We attempted the deprotection of benzoyl groups in zinc complexes **77** and **83** with *N,N*-dimethyltrimethylsilylamine ($\text{NMe}_2\text{SiMe}_3$) and *n*-butyllithium (*n*-BuLi). However, no reaction was observed according to NMR spectroscopy. The formation of radical was also excluded, as the solutions remained EPR-silent. Hence, we could not go further with such type of O-protected ligands.

IV.2 Perspectives: alternative design for metal-based oxyallyls?

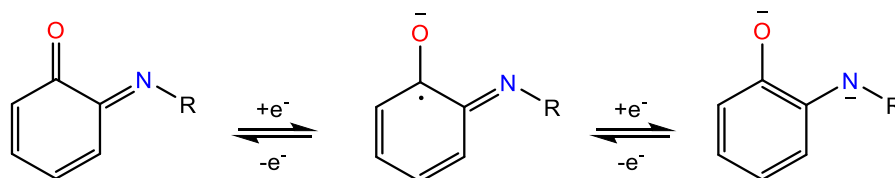
The bis-imine ketone ligands have the ability to coordinate themselves through all the coordinating sites present in the structure i.e., one oxygen and two nitrogens. This rich coordination chemistry may be at the source of difficulty to isolate well-defined metal complexes.

Therefore, as a perspective for future work, an alternative model for a metal-based oxyallyl featuring a bidentate ligand was proposed. The bidentate ligands would formally result from the N-alkylation of parented diimine ketones (Scheme 61).



Scheme 61: Alternative redox-active N,O-bidentate ligands and corresponding complexes

These N,O-bidentate ligands are reminiscent of *o*-aminophenolate ligands⁶² (previously discussed in chapter I) but featuring the capto-dative substitution of oxyallyl patterns which is expected to stabilize radical forms.

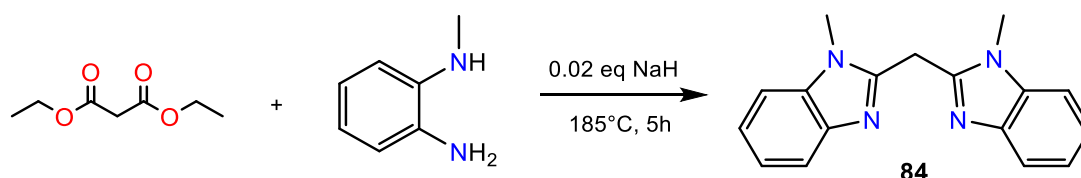


Scheme 62: Different oxidation states in *o*-aminophenolate ligand

IV.2.1 Bis(methylbenzimidazolyl)ketone

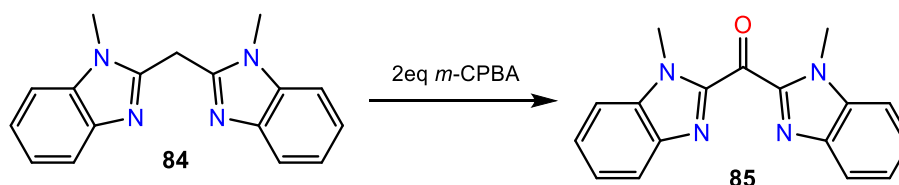
We considered a model based on bis(methylbenzimidazolyl)ketone **85**. The only reported synthesis for this compound involved the inconvenient reaction of N-methylbenzimidazole with diethyl carbonate under extreme experimental conditions.⁶³ Therefore, we decided to implement our previous strategy based on *m*-CPBA oxidation.

We first synthesized bis(N-methylbenzimidazol-2-yl)methane **84** using a modification of the method described by S. Elgafi *et al* [63]. The mixture of diethyl malonate with two equivalents of N-methyl-1,2-phenylenediamine was heated at 185°C for 5 hours in presence of NaH. The pure product **84** (mp = 201°C) was simply recovered by washing the formed solid with diethylether and drying under vacuum (69 % yield).



Scheme 63: Synthesis of bis(N-methylbenzimidazol-2-yl)methane **84**

Benzimidazole **84** was oxidized with *m*-CPBA to form ligand **85** in 92 % yield. The structure was asserted by IR and ¹³C NMR spectroscopy ($\nu = 1658 \text{ cm}^{-1}$ (C=O); $\delta_{\text{CO}} = 179 \text{ ppm}$).



Scheme 64: Synthesis of bis(methylbenzimidazolyl)ketone **85**

The cyclic voltammetry experiment for ligand **85** was performed (Figure 27). It showed a reversible reduction first at $E_{1/2} = -1.7 \text{ V}$ which is assigned to the formation of the ketyl radical anion followed by a further irreversible reduction at $E_{\text{pc}} = -2.1 \text{ V}$.

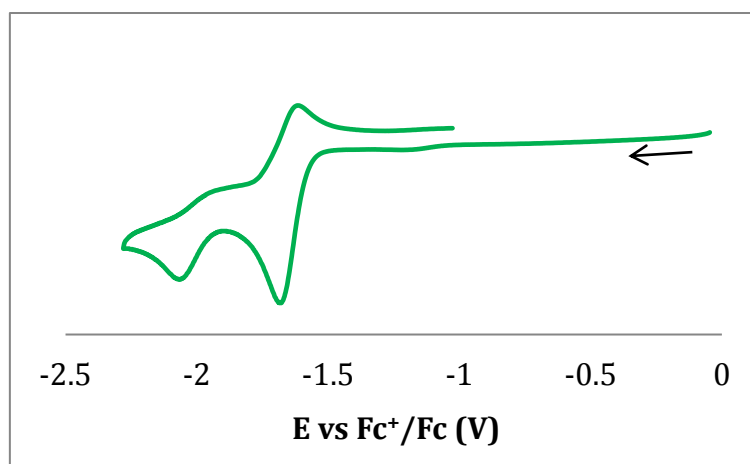
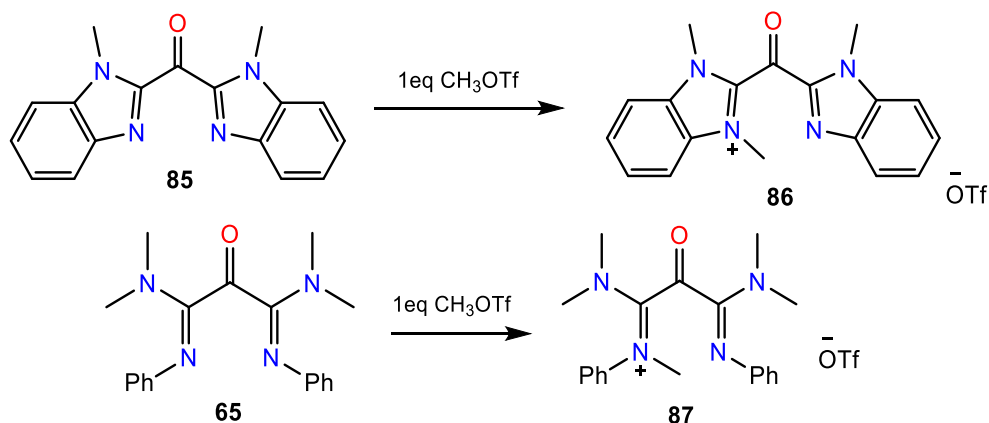


Figure 27: Cyclic voltammogram of ligand 85 in 0.1 M solution of TBAPF₆ in acetonitrile with a scan rate of 100 mV.s⁻¹

IV.2.2 N,O-bidentate ligands

N,O-bidentate ligand **86** was obtained by the reaction of ligand **85** with one equivalent of methyl triflate at room temperature. The product **86** was purified by washing with diethylether and was isolated in 76 % yield (Scheme 65). Ligand **86** was fully characterized including IR and ¹³C NMR spectroscopy (**86**: $\nu = 1680 \text{ cm}^{-1}$ (C=O); $\delta_{\text{CO}} = 172.7 \text{ ppm}$).

The same strategy of alkylation was applied to the previously synthesized bis-imine ketone ligands. Only, the electron-enriched ligand **65** was able to react with methyl triflate to form the corresponding N,O-bidentate ligand **87**. Ligand **87** was obtained in 60 % yield and the structure was confirmed by the characteristic CO signals in IR and ¹³C NMR spectroscopy (**87**: $\nu = 1735 \text{ cm}^{-1}$ (C=O); $\delta_{\text{CO}} = 180.1 \text{ ppm}$).



Scheme 65: Synthesis of N,O-bidentate ligand 86 and 87

According to cyclic voltammetry experiments, ligand **86** featured an irreversible reduction at $E_{pc1} = -1.1$ V. Ligand **87** showed two reductions at $E_{1/2} = -0.9$ V (for the formation of corresponding radical) and at $E_{pc} = -1.3$ V.

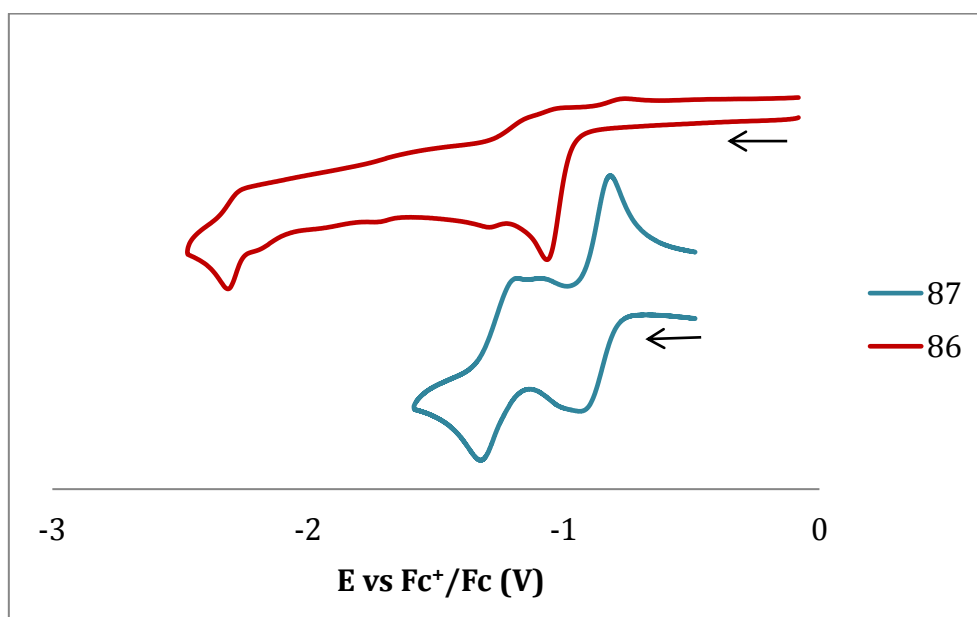
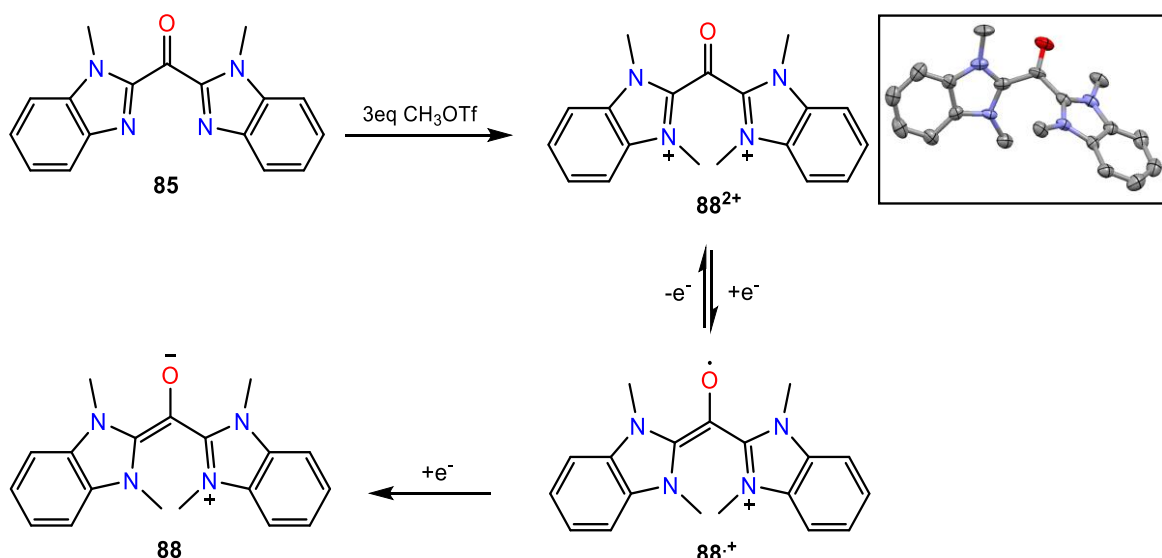


Figure 28: Cyclic voltammogram of ligands 86 and 87 in 0.1 M solution of TBAPF₆ in acetonitrile with a scan rate of 100 mV.s⁻¹

Prior to the study of the coordination with ligand **85**, we synthesized di-cation **88²⁺** which can be seen as an organic model for the targeted complexes. We performed the di(methylation) of di(imine)ketone **85** using methyl triflate in chloroform at 60°C. The corresponding bis(triflate) salt **88²⁺** was isolated in 88 % yield. The structure of **88²⁺** was confirmed by X-ray diffraction analysis (Scheme 66). In addition, it featured the typical CO signals in IR ($\nu = 1690$ cm⁻¹) and ¹³C NMR spectroscopy ($\delta = 166.8$ ppm).

Note that ligand **87** did not react with methyl triflate in similar conditions.



Scheme 66: Synthesis, redox transformation and X-ray structure of di-cation 88^{2+} (H-atoms & counter-anions are omitted for clarity)

According to cyclic voltammetry experiments, di-cation 88^{2+} undergoes a first reversible reduction at $E_{1/2} = -0.12$ V which is attributed to the formation of corresponding radical cation $88^{+\cdot}$. A second reduction at $E_{pc} = -0.9$ V to afford the corresponding zwitterionic oxallyl 88 seems to be coupled with a chemical transformation.

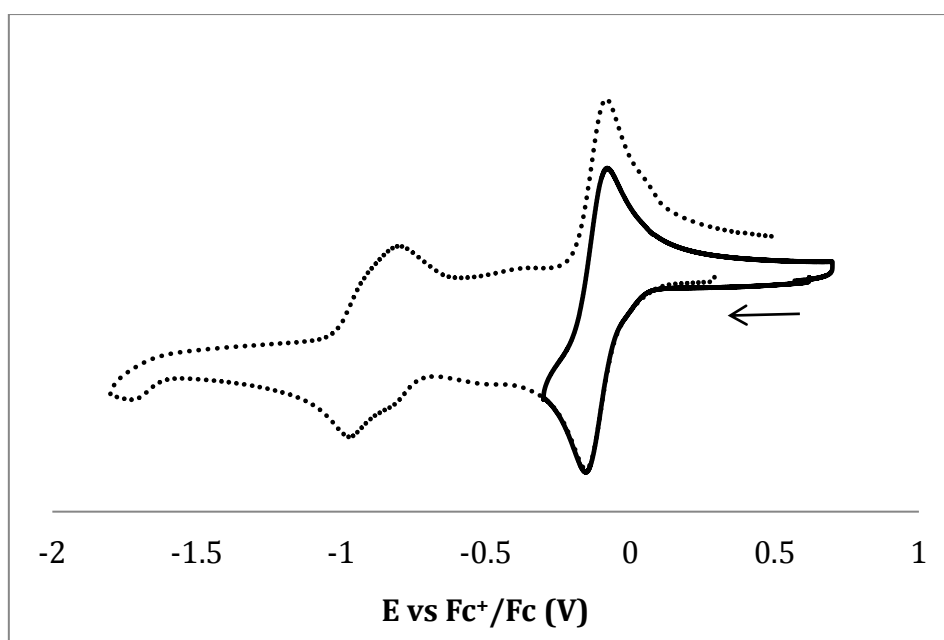


Figure 29: Cyclic voltammogram of di-cation 88^{2+} in 0.1 M solution of TBAPF₆ in acetonitrile with a scan rate of 100 mV.s⁻¹

The electrochemical reduction of **88**²⁺ was also performed in acetonitrile at E = -0.5 V. The stoichiometry (one coulomb per mole of substrate), the observation of a strong EPR signal at room temperature and an excellent fit between experimental and theoretical hyperfine coupling constants confirmed the formation of persistent **88**^{•+} that finally decayed after few hours at room temperature (Figure 30).

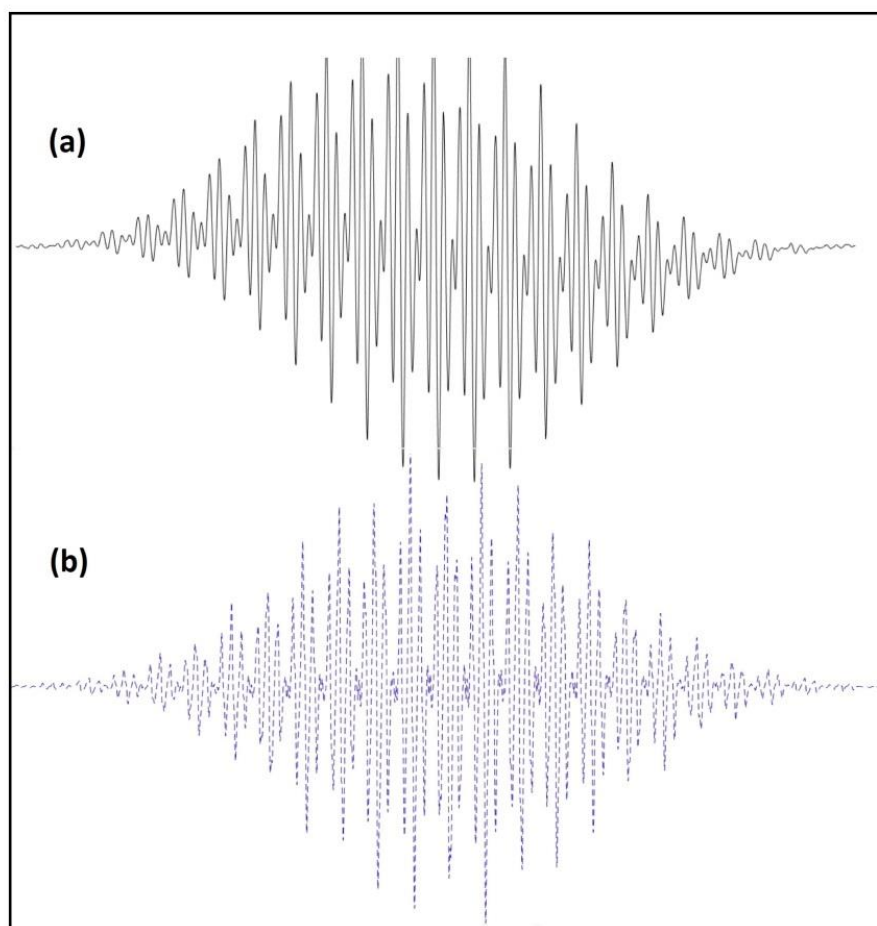


Figure 30: X-band EPR spectrum confirming the presence of **88^{•+}. (a) Experimental spectra, (b) simulated spectra with a Lorentzian line-broadening parameter of 0.37 and the following set of hyperfine constants: $a(^{14}\text{N}) = 3.1$ MHz (4 nuclei), $a(^1\text{H}) = 6.5$ MHz (12 nuclei) and $a(^1\text{H}) = 0.86$ MHz (4 nuclei)**

The addition of magnesium turnings to a solution of ligand **86** was accompanied by a color change of the solution from yellow to very dark red color. An EPR signal was observed at room temperature that indicated the presence of an organic radical moiety. Note that ¹H NMR and ¹³C NMR peaks could also be evidenced for a N-CH₃ substituent and some aromatic positions.

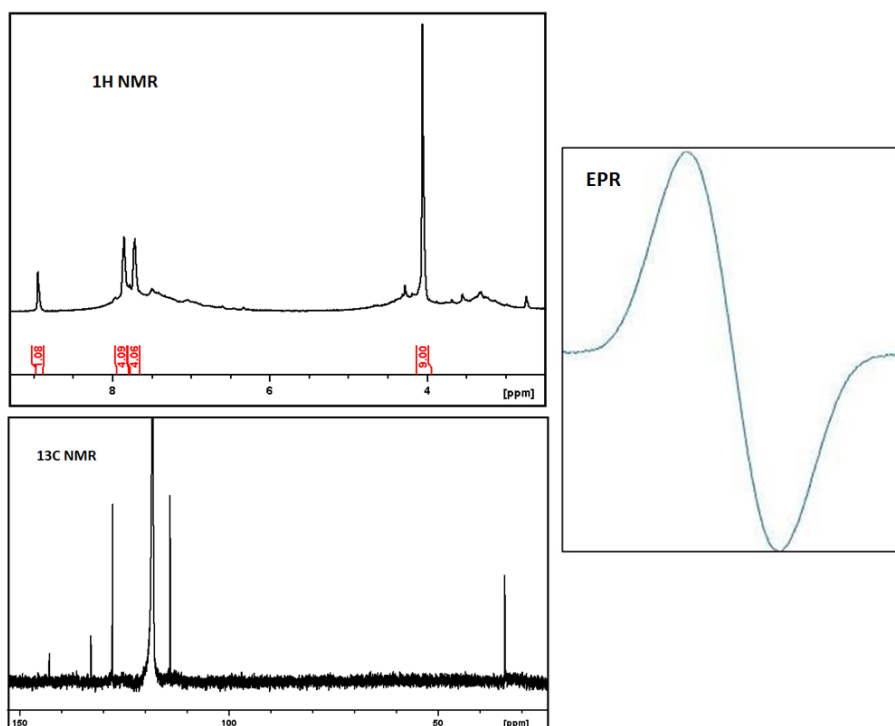


Figure 31: ^1H NMR, ^{13}C NMR and EPR spectra of **89**

Two reduction processes at $E_{1/2} = -1.1$ V and $E_{pc} = -1.5$ V were observed in the cyclic voltammetry experiment of the solution of **89**. The reversibility of the first reduction suggests that the reaction product **89** contains a coordinated magnesium. Indeed, the reduction of free ligand **86** is irreversible and leads to a product which does not undergo further reduction.

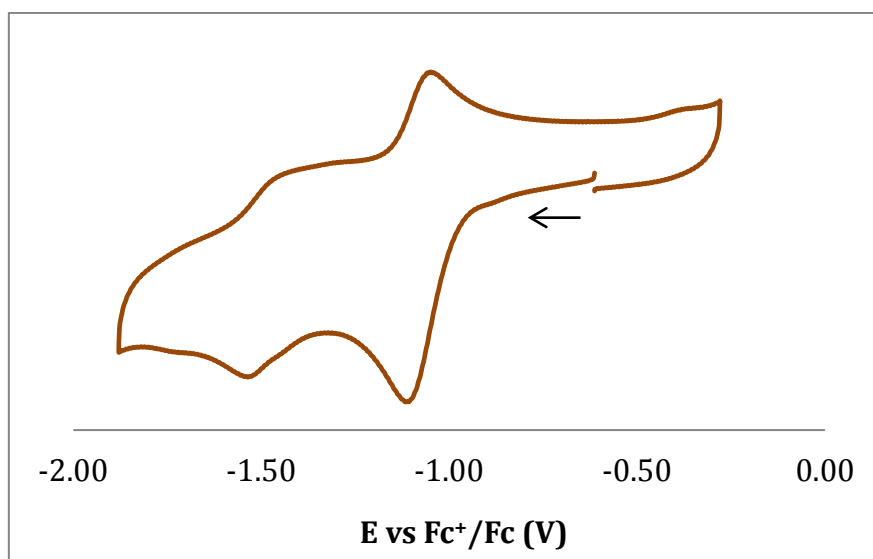
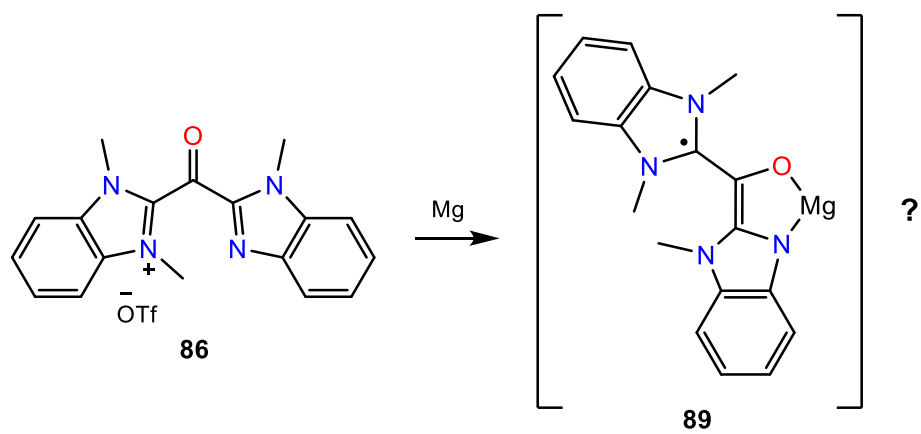


Figure 32: Cyclic voltammogram of product **89 in 0.1 M solution of TBAPF_6 in acetonitrile with a scan rate of $100 \text{ mV}\cdot\text{s}^{-1}$**



Scheme 67: Possible structure for 89

IV.3 Conclusion

The preparation of O-protected ligands was described by two methods: (i) from O-protected 1,3-dichlorovinamidium salts and (ii) from direct oxidation of vinamidines with benzoyl peroxide (BPO). The oxidation of free bis-oxazoline **79** using BPO gave rise to the formation of new O-protected ligand that further used for the formation of O-protected Zn(II) complexes. The deprotection of the benzoyl groups failed using $\text{NMe}_2\text{SiMe}_3$ and $n\text{-BuLi}$.

The oxidation of benzimidazole precursor was done successfully using *m*-CPBA to form bis(2-benzooxazolyl)ketone ligand **85**. The formation of two different N,O-bidentate ligands **86** and **87** was achieved by methylation and preliminary results suggested the formation of Mg(II) complex **89** with ligand **86**. The organic version of complex compounds of ligand **85** in the form of di-cation **88**²⁺ was formed and fully characterized.

IV.4 Experimental

General considerations: All the reactions were performed under an inert atmosphere. The solvents were freshly distilled before use. Dichloromethane, chloroform and acetonitrile were distilled over CaH_2 whereas diethyl ether was distilled by sodium/benzophenone. Reagent methyl trifluoromethanesulfonate was freshly dried before experiments. Other chemicals were purchased from Alfa Aesar and Sigma-Aldrich (now Merck) and were used without purifications.

Electron Paramagnetic Resonance: Isotropic EPR spectra were obtained at room temperature on a X-band Bruker EMX Plus spectrometer.

High Resolution Mass Spectrometry: HRMS spectra were obtained by electrospray ionization method on Bruker Esquire 3000 or a Thermo Scientific LTQ Orbitrap XL.

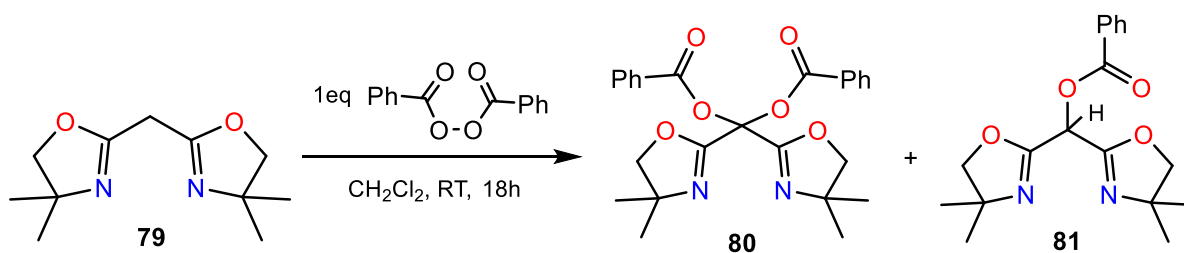
Melting points (mp) were recorded with a Büchi B-545 melting point apparatus system.

Infra-Red (IR) spectra were measured on a Thermo Scientific Nicolet iS10 FT-IR ATR spectrometer.

Nuclear Magnetic Resonance: NMR spectra were done on the NMR-ICMG platform of Grenoble with Bruker Avance 300, 400 and 500 MHz spectrometers at 298 K. ^1H NMR and ^{13}C NMR chemical shifts (δ) are reported in parts per million (ppm) relative to TMS. NMR multiplicities are abbreviated as follows: s = singlet, d = doublet, t = triplet, q = quadruplet, br = broad signal, m = multiplet.

Electrochemical measurements were conducted in a standard one-compartment and three electrode electrochemical cell with a Bio-logic SP300 potentiostat. Cyclic voltammetry experiments were performed in 0.1M $\text{TBAPF}_6 + \text{CH}_3\text{CN}$ at a scan rate of $100 \text{ mV}\cdot\text{s}^{-1}$ with a carbon disk of 3 mm in diameter as a working electrode, $\text{Ag}/0.01 \text{ M AgNO}_3$ as a reference electrode and a platinum wire as an auxiliary electrode. Ferrocene was used as standard, and all reduction potentials are reported with respect to the $E_{1/2}$ of the Fc/Fc^+ redox couple.

Crystallographic studies were performed on the RX-ICMG platform of Grenoble with a Bruker AXF-APEXII X-ray diffraction instrument (with $\text{Mo}/\text{K}\alpha$ -radiation).

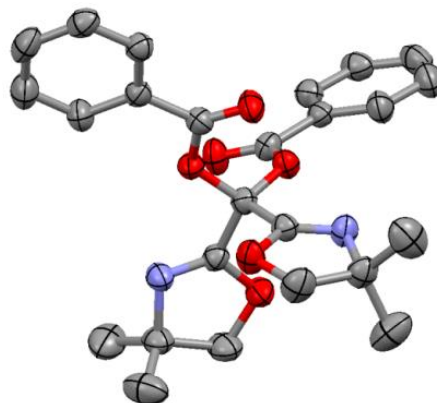


Benzoyl peroxide [BPO-70%] (1.81 g, 5.231 mmol) was dissolved in CH_2Cl_2 (20 mL), dried over Na_2SO_4 of which 10 mL solution was added into the solution of bis-oxazoline **79** (0.5 g, 2.378 mmol) in CH_2Cl_2 (5 mL). The reaction mixture was stirred overnight. The mixture was washed three times with saturated aqueous solution of NaHCO_3 , once with water, dried over Na_2SO_4 , filtered and concentrated in vacuo to get the solid product.

80: It was crystallized by layering pentane over CH_2Cl_2 solution of solid product at 0°C .

$^1\text{H NMR}$ (300 MHz, CDCl_3) δ : 8.15 (d, $J = 8$ Hz, 4H), 7.57 (t, $J = 8$ Hz, 2H), 7.42 (t, $J = 8$ Hz, 4H), 4.17 (s, 4H), 1.33 (s, 12H) ppm.

Crystallographic data:



Formula: $\text{C}_{25}\text{H}_{26}\text{N}_2\text{O}_6$

Space Group: C 2/c

Cell lengths (\AA): $a = 20.008(4)$; $b = 7.8835(16)$; $c = 15.899(3)$

Cell Angles ($^\circ$): $\alpha = 90$; $\beta = 107.36(3)$; $\gamma = 90$

Cell Volume: 2393.57

R-Factor (%): 9.99

<u>Bond length</u>		<u>Selected Angle</u>	
C4C1 1.520	C7N1 1.502(5)	O2C1C4 113.1	H13AC13H13B 109.5
C1O2 1.356(5)	C3C6 1.384(5)	C1C4C1 106.8	H12AC12H12B 108.6
O2C12 1.449(5)	C6C8 1.380(6)	O1C4O1 112.3	
C12C7 1.526(6)	C12H12A 0.970	O2C1N1 120.6(3)	
C7C13 1.504(8)	C11H11A 0.960	C7N1C1 106.3(3)	
C1N1 1.251(5)		C12O2C1 104.0(3)	
C4O1 1.412		C13C7C12 111.9(4)	
O1C2 1.354(4)		O1C2O3 122.7(3)	
C2O3 1.203(4)		C2O1C4 118.7	
C2C3 1.481(5)		C2C3C6 118.1(3)	

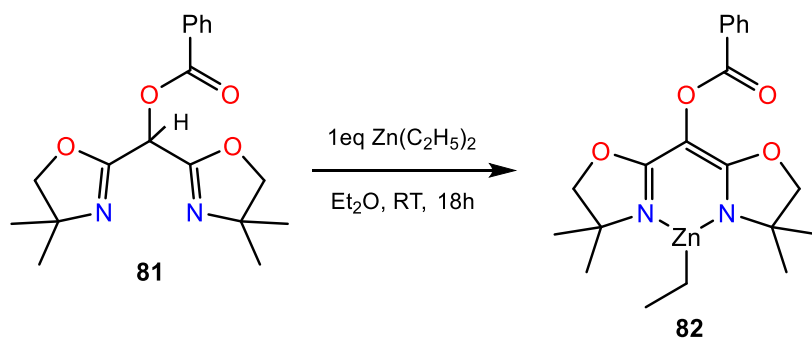
81: It was obtained by flash column chromatography of the remaining mother liquor after crystallization (eluent: CH₂Cl₂) (yield = 0.589 g, 75 %).

mp: 100.2°C.

HRMS: m/z calcd for [C₁₈H₂₃O₄N₂]⁺, 331.1652; found, 331.1650.

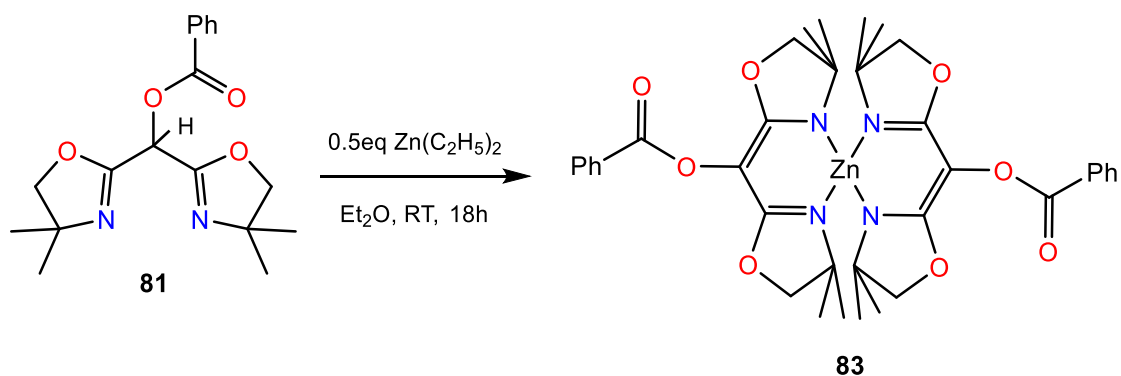
¹H NMR (400 MHz, CDCl₃) δ: 8.12 (d, *J* = 8 Hz, 2H), 7.57 (t, *J* = 8 Hz, 1H), 7.44 (t, *J* = 8 Hz, 2H), 6.15 (s, 1H), 4.06 (d, *J* = 8 Hz, 2H), 4.01 (d, *J* = 8 Hz, 2H), 1.31 (s, 6H), 1.28 (s, 6H) ppm.

¹³C NMR (100 MHz, CDCl₃) δ: 164.9, 159.2, 133.5 (CH), 130.2 (CH), 128.9, 128.4 (CH), 79.8 (CH₂), 67.8, 65.1 (CH), 28 (CH₃) ppm.



82: 1M diethylzinc (0.35 mL, 0.35 mmol) was added drop wise to the solution of O-protected ligand **81** (0.103 g, 0.313 mmol) in Et₂O (20 mL) and the mixture was stirred for 18 hours. The solvent was evaporated and washed with ether to obtain the dried white powder. (Yield = 0.062 g, 47 %)

¹H NMR (300 MHz, CDCl₃) δ : 8.17 (d, $J = 8$ Hz, 2H), 7.56 (t, $J = 8$ Hz, 1H), 7.44 (t, $J = 8$ Hz, 2H), 4.02 (s, 4H), 1.40 (s, 12H), 1.28 (t, $J = 8$ Hz, 3H), 0.39 (q, $J = 8$ Hz, 2H) ppm.



83: To the solution of ligand **81** (0.2 g, 0.605 mmol) in Et₂O (12 mL), 1M diethyl zinc (0.3 mL, 0.3 mmol) was added drop wise and the mixture was stirred for 18 hours. The solvent was evaporated to obtain the dried product which was further crystallized by layering ether over CH₂Cl₂ solution. Yield = 0.136 g, 31 %.

mp: 263.3°C.

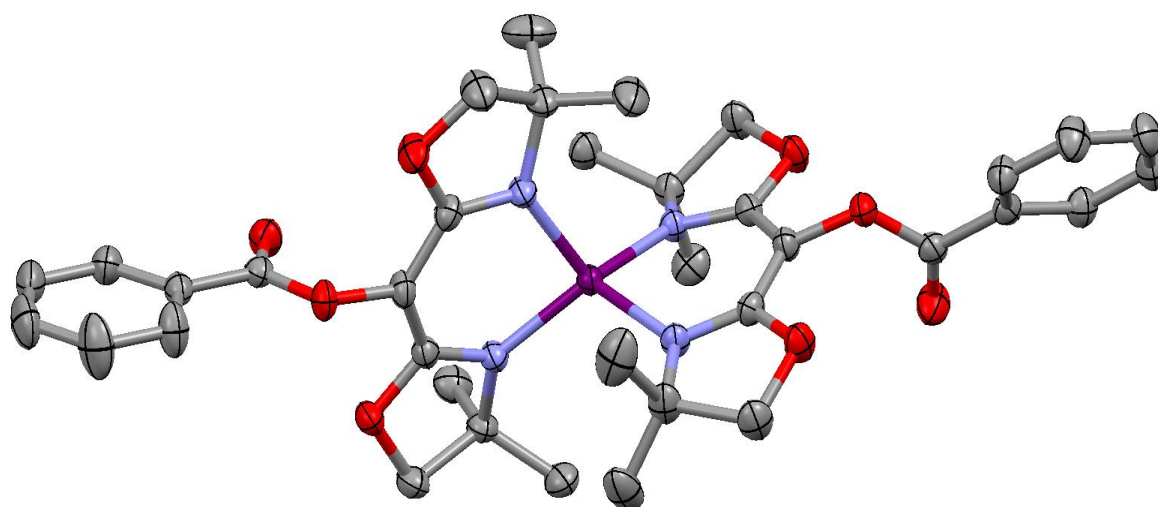
HRMS: m/z calcd for C₃₆H₄₃O₈N₄Zn (M+H⁺), 723.2367; found, 723.2369.

IR (ATR): $\nu = 1773$ (C=O), 1619 (C-O) cm⁻¹.

¹H NMR (500 MHz, CDCl₃) δ : 8.18 (d, $J = 7$ Hz, 4H), 7.55 (t, $J = 7$ Hz, 2H), 7.44 (t, $J = 7$ Hz, 4H), 3.93 (s, 8H), 1.42 (s, 24H) ppm.

¹³C NMR (125 MHz, CDCl₃) δ : 167, 165.5, 133 (CH), 130.3 (CH), 128.4 (CH), 93.3, 79.6 (CH₂), 66, 28.2 (CH₃) ppm.

Crystallographic data:



Formula: C₃₆H₄₂N₄O₈Zn

Space Group: P 2₁/n

Cell lengths (Å): a = 9.1888(18); b = 25.889(5); c = 16.153(3)

Cell Angles (°): α = 90; β = 91.33(3); γ = 90

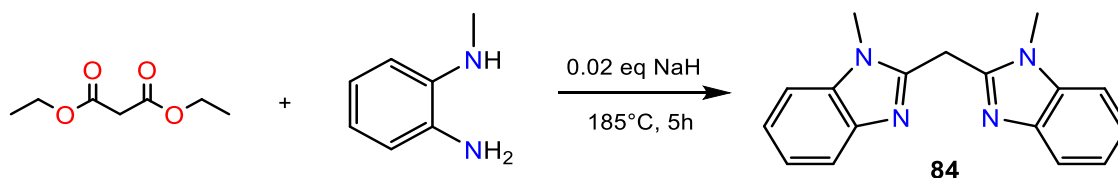
Cell Volume: 3841.58

R-Factor (%): 3.21

Bond length

Selected Angle

Zn1N3 1.980(2)	C19C8 1.530(3)	N3Zn1N2 94.70(6)
Zn1N2 2.017(2)	Zn1N1 1.983(1)	N1Zn1N4 93.91(6)
N3C2 1.318(2)	Zn1N4 2.023(2)	O5C6O3 123.7(2)
C2C5 1.390(3)	C34H34 0.949	C6O3C5 115.0(1)
C5O3 1.420(2)		C2O9C19 105.9(1)
O3C6 1.357(2)		C18C8C30 110.7(2)
C6O5 1.200(2)		C2N3Zn1 120.2(1)
C2O9 1.360(2)		C2C5C7 124.6(2)
O9C19 1.453(2)		O5C6C13 124.3(2)
N3C8 1.487(2)		C22C13C34 119.7(2)
C8C30 1.519(3)		C19C8N3 100.9(1)
C6C13 1.488(3)		H19AC19H19B 109.0
C13C34 1.380(3)		
C30H30A 0.980		
C19H19A 0.990		

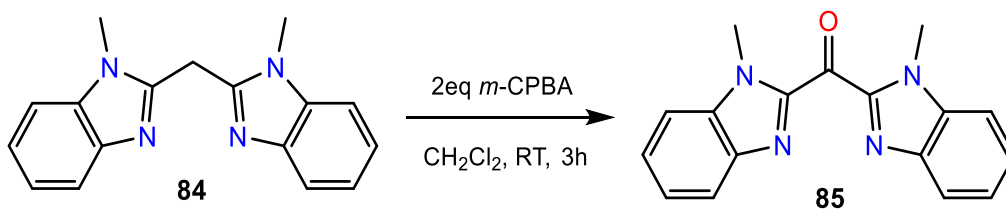


84: Diethyl malonate (2.532 g, 15.808 mmol) was mixed with N-methyl-1,2-phenylenediamine (3.948 g, 32.316 mmol) and NaH (0.008 g, 0.333 mmol). The mixture was heated at 185°C for 5 hours with the distillation set-up (as the reaction will release ethanol and water). After cooling to room temperature, pure product **84** was simply recovered by washing several times with diethylether and drying under vacuum (3 g, 69 % yield).

mp: 201.3 °C.

¹H NMR (400 MHz, CDCl₃) δ: 7.73-7.71 (m, *J* = 2H), 7.24-7.23 (m, 6H), 4.61 (s, 2H), 3.84 (s, 6H) ppm.

¹³C NMR (100 MHz, CDCl₃) δ: 149.2, 142.4, 136.2, 122.7 (CH), 122.2 (CH), 119.5 (CH), 109.4 (CH), 30.5 (CH₂), 28.6 (CH₃) ppm.



85: *m*-CPBA-60% (3.13 g, 10.88 mmol) was dissolved in CH₂Cl₂ (45 mL), dried over Na₂SO₄ of which 30 mL solution was added into the solution of 1,1-bis(1-methylbenzimidazol)methane (1.0 g, 3.62 mmol) in CH₂Cl₂ (15 mL). The reaction mixture was stirred for 3 hours and washed 3 times with saturated aqueous solution of NaHCO₃, once with water, dried by Na₂SO₄, filtered & concentrated in vacuo to get the solid product (0.97 g, 92 % yield). The compound was purified by crystallization in methanol (0.42 g, 40 % yield).

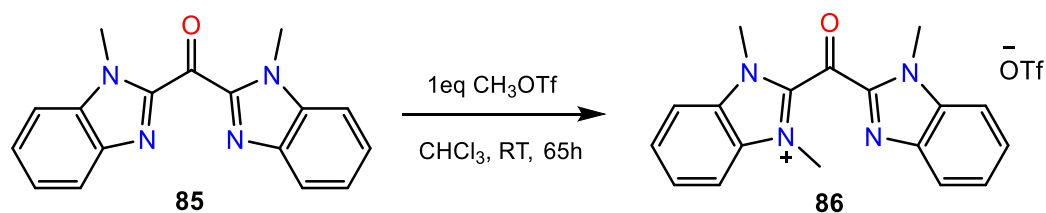
mp: 186.9°C.

HRMS: *m/z* calcd for [C₁₇H₁₅ON₄]⁺, 291.1240; found, 291.1239.

IR (ATR): ν = 1658 cm⁻¹ (C=O).

¹H NMR (500 MHz, CDCl₃) δ : 7.98 (d, *J* = 8 Hz, 2H), 7.47-7.46 (m, 4H), 7.38-7.35 (m, 2H), 4.14 (s, 6H) ppm.

¹³C NMR (125 MHz, CDCl₃) δ : 179, 146.9, 142.5, 136.9, 126.3 (CH), 123.8 (CH), 123 (CH), 110.3 (CH), 32.1 (CH₃) ppm.



86: At room temperature methyl triflate (0.04 mL, 0.353 mmol) was added into the solution of ligand **85** (0.1g, 0.344 mmol) in CHCl₃ (7 mL). The reaction mixture was stirred over weekend. The solution was filtered, residue was dried under vacuum and stored as a yellow solid (0.12 g, 76 % yield).

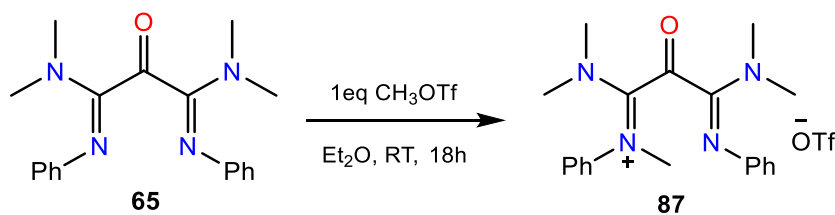
mp: 201.5°C.

HRMS: m/z calcd for [C₁₈H₁₇ON₄]⁺, 305.1397; found, 305.1385.

IR (ATR): $\nu = 1680 \text{ cm}^{-1}$ (C=O).

¹H NMR (400 MHz, CD₃CN) δ : 8.0-7.97 (m, 2H), 7.87-7.84 (m, 2H), 7.79 (t, $J = 8 \text{ Hz}$, 2H), 7.66 (t, $J = 8 \text{ Hz}$, 1H), 7.48 (t, $J = 8 \text{ Hz}$, 1H), 4.31 (s, 3H), 4.06 (s, 6H) ppm.

¹³C NMR (100 MHz, CD₃CN) δ : 172.7, 145.5, 145.1, 144.0, 139.1, 132.7, 130 (CH), 129.4 (CH), 126.4 (CH), 123.4 (CH), 114.8 (CH), 113.1 (CH), 34.9 (CH₃), 33.2 (CH₃) ppm.



87: Methyl triflate (0.4 mL, 3.534 mmol) was added to the solution of the selected ligand **65** (1 g, 3.102 mmol) in Et₂O (50 mL). The reaction mixture was stirred overnight at room temperature. The solution was filtered, washed twice with ether and dried under vacuum to get the desired solid product (0.9 g, 60 % yield).

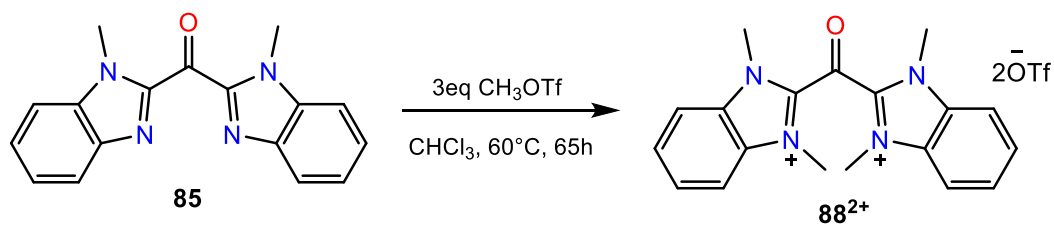
mp: 98.3°C.

HRMS: *m/z* calcd for [C₂₀H₂₅ON₄]⁺, 337.2023; found, 337.2017.

IR (ATR): $\nu = 1735\text{ cm}^{-1}$ (C=O).

¹H NMR (400 MHz, CDCl₃) δ : 7.47-7.36 (m, 5H), 7.28 (t, *J* = 7 Hz, 2H), 7.03 (t, *J* = 7 Hz, 1H), 6.82 (d, *J* = 7 Hz, 2H) 3.63 (s, 3H), 3.23 (s, 6H), 2.55 (s, 6H) ppm.

¹³C NMR (100 MHz, CDCl₃) δ : 180.1, 165, 147.7, 146.3, 140.7, 130.5 (CH), 130 (CH), 128.8 (CH), 124.2 (CH), 122.3 (CH), 120.8 (CH), 119.2 (CH), 44.3 (CH₃), 43.4 (CH₃), 42.9 (CH₃), 40.2 (CH₃) ppm.



88²⁺: Methyl trifluoromethanesulfonate (87 mg, 0.53 mmol) was added dropwise into the solution of (benzimidazol-2-yl)ketone **85** (50 mg, 0.17 mmol) in CHCl₃ (5 mL). A precipitate/solid appeared upon stirring over weekend at 60°C. The supernatant was removed by filtration. The resulting residue was washed several times with diethyl ether and dried under vacuum (94 mg, 88 % yield). The product was crystallized from a concentrated solution of acetonitrile at -20 °C.

mp: 260-262°C.

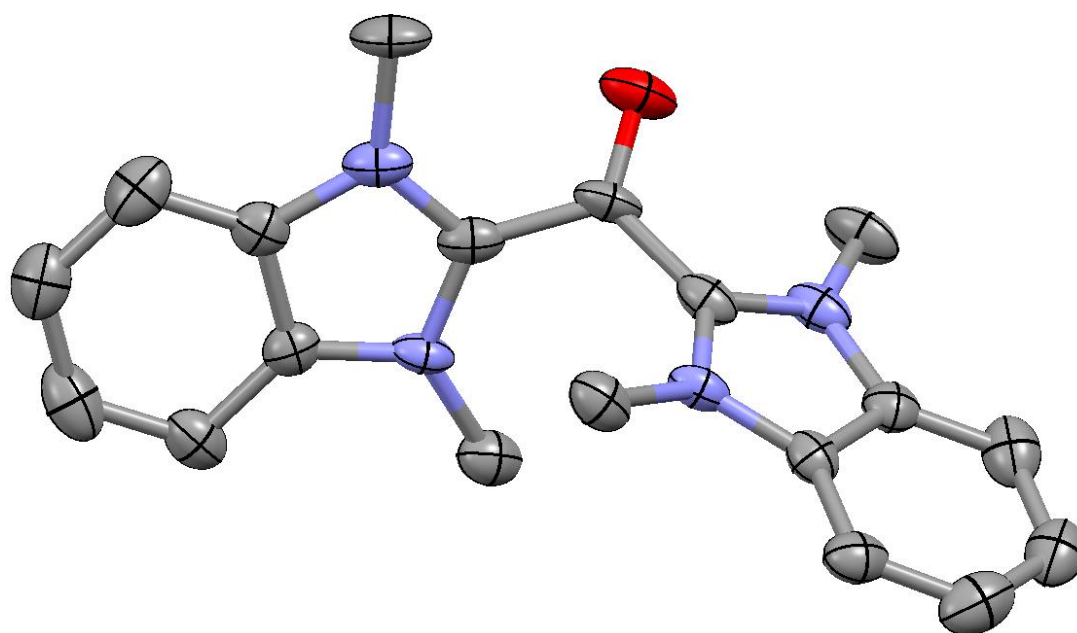
HRMS: m/z calcd for C₁₈H₁₇N₄O (M-CH₃⁺), 305.1397; found, 305.1385.

IR (ATR): $\nu = 1690 \text{ cm}^{-1}$ (C=O).

¹H NMR (400 MHz, CD₃CN) δ : 8.10-8.07 (m, 4H), 7.99-7.97 (m, 4H), 4.16 (s, 12H) ppm.

¹³C NMR (100 MHz, CD₃CN) δ : 166.8, 139.2, 134.0, 131.7 (CH), 115.7 (CH), 35.7 (CH₃) ppm.

Crystallographic data:



Formula: C₁₉ H₂₀ N₄ O

Space Group: C 2/c

Cell lengths (Å): a = 16.142(3); b = 6.5629(13); c = 24.162(5)

Cell Angles (°): α = 90; β = 101.12(3); γ = 90

Cell Volume: 2511.62

R-Factor (%): 12.56

Bond length

Selected Angle

C10O5 1.21

O5C10C12 120.8

C10C12 1.477

N9C12N6 110.6(7)

C12N6 1.34(1)

C18N9C12 127.8(7)

N6C17 1.47(1)

C12N6C17 127.9(7)

C12N9 1.335(9)

C12N6C11 107.2(6)

N9C18 1.47(1)

C14N9C12 108.3(6)

N9C14 1.40(1)

C16C14C11 124.1(8)

C14C11 1.39(1)

C12C10C12 118.3

C11C13 1.40(1)

H18BC18H18A 109.5

C14C16 1.36(1)

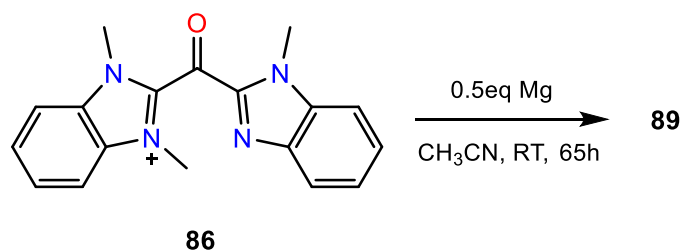
H17CC17H17A 109.4

C16C20 1.41(1)

C17H17C 0.959

C18H18A 0.96

C16H16 0.929



89: Magnesium turnings (0.008 g, 0.329 mmol) were added to the solution of bidentate ligand **86** (0.304 g, 0.669 mmol) in CH₃CN (15 mL). The solution was stirred over weekend at room temperature until all the Mg was dissolved completely that turned the solution into dark red color. The solution was filtered and the solvent was evaporated to yield dark red solid product (0.124 g, 59 % yield).

¹H NMR (400 MHz, CDCl₃) δ: 8.94 (s, 1H), 7.85 (s, 4H), 7.71 (s, 4H), 4.05 (s, 9H) ppm.

¹³C NMR (100 MHz, CDCl₃) δ: 143, 133, 127.9 (CH), 114.1 (CH), 34.1 (CH₃) ppm.

CONCLUSION & PERSPECTIVES

The formation of different ligands featuring bis-imine ketone backbone was synthesized using *m*-CPBA as an oxidant (Figure 33). This methodology is simpler, faster and easier as compared to Cu-oxidation method of vinamidines. In addition, we were able to study structural variation in bis-imine ketone ligands with the introduction of various substituents.

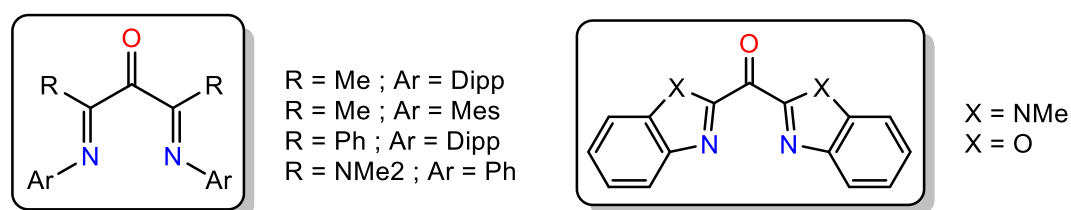


Figure 33: Ligands formed by *m*-CPBA oxidation

The investigation of the full reversal of selectivity in the reaction of aniline with 1,3-dichloro-1,3-bis(dimethylamino)vinamidinium salt was studied by DFT calculations that accounted for two different products. The formation of electron-enriched vinamidine was successfully obtained by delaying the addition of base (triethylamine). However, the incorporation of bulky aniline derivatives (Dipp, Mes) could not be achieved following the similar procedure.

Benzoyl O-protected ligands and Zn(II) complexes were obtained but deprotection of the benzoyl groups could not be done. Two N,O-bidentate ligands were synthesized to avoid the possibility of tri-coordination in the metal-oxyallyl complexes.

The genuine structure of oxyallyl substituted Mg(II) complex **89** is still uncertain. Indeed, we have not obtained suitable crystals of this complex for single crystal X-ray diffraction analysis. These preliminary results are encouraging for further study of the metal-reduction and coordination chemistry of N,O-bidentate ligands.

REFERENCES

-
- ¹ «Reactive intermediate Chemistry» (Eds.: R. A. Moss, M. S. Platz, M. Jones), *Wiley Interscience*, Hoboken, 2004.
- ² (a) M. Gomberg, *J. Am. Chem. Soc.*, 1900, **22**, 757; (b) M. Gomberg, *Chem. Rev.*, 1924, **1**, 91.
- ³ W. Schlenk and M. Brauns, *Ber. Dtsch. Chem. Ges.*, 1915, **48**, 661.
- ⁴ (a) A. Rajca, *Chem. Rev.*, 1994, **94**, 871; (b) A. Rajca, *Adv. Phys. Org. Chem.*, 2005, **40**, 153; (c) N. M. Shishklov, *Russ. Chem. Revs.*, 2006, **75**, 863; (d) T. Sugawara, H. Komatsu and K. Suzuki, *Chem. Soc. Rev.*, 2011, **40**, 3105; (e) I. Ratera and J. Veciana, *Chem. Soc. Rev.*, 2012, **41**, 303.
- ⁵ A. Igau, H. Grutzmacher, A. Baceiredo and G. Bertrand, *J. Am. Chem. Soc.*, 1988, **110**, 6463.
- ⁶ A. J. Arduengo, III, R. L. Harlow, and M. Kline, *J. Am. Chem. Soc.*, 1991, **113**, 361.
- ⁷ (a) M. Ballester, C. Molinet and J. Castañer, *J. Am. Chem. Soc.*, 1960, **82**, 4254; (b) M. Ballester, J. Riera, J. Castañer, C. Badía, and J. M. Monsó, *J. Am. Chem. Soc.*, 1971, **93**, 2215; (c) M. Ballester, J. Castañer, J. Riera, A. Ibáñez, and J. Pujadas, *J. Org. Chem.*, 1982, **47**, 259; (d) A. Rajca, *Chem. Rev.*, 1994, **94**, 871; (e) D. Martin, M. Melaimi, M. Soleilhavoup and G. Bertrand, *Organometallics*, 2011, **30**, 5304; (f) T. Sugawara, H. Komatsu and K. Suzuki, *Chem. Soc. Rev.*, 2011, **40**, 3105; (g) I. Ratera and J. Veciana, *Chem. Soc. Rev.*, 2012, **41**, 303; (h) M. Soleilhavoup and G. Bertrand, *Acc. Chem. Res.*, 2015, **48**, 256.
- ⁸ J. C. Garrison and W. J. Youngs, *Chem. Rev.*, 2005, **105**, 3978.
- ⁹ R. Hoffmann, *J. Am. Chem. Soc.*, 1968, **90**, 1475.
- ¹⁰ (a) M. H. J. Cordes and J. A. Berson, *J. Am. Chem. Soc.*, 1992, **114**, 11010; (b) M. H. J. Cordes and J. A. Berson, *J. Am. Chem. Soc.*, 1996, **118**, 6241; (c) T. S. Sorensen and F. Sun, *J. Chem. Soc. Perkin Trans.*, 1998, **2**, 1053.
- ¹¹ (a) N. J. Turro, S. S. Edelson, J. R. Williams T. R. Darling and W. B. Hammond, *J. Am. Chem. Soc.*, 1969, **91**, 2283; (b) F. G. Bordwell, T. G. Scamehorn and W. R. Springer, *J. Am. Chem. Soc.*, 1969, **91**, 2087; (c) F. G. Bordwell and J. G. Strong, *J. Org. Chem.*, 1973, **38**, 579; (d) N. Tsuchida, S. Yamazaki and S. Yamabe, *Org. Biomol. Chem.*, 2008, **6**, 3109; (e) M. Harmata, *Chem. Commun.*, 2010, **46**, 8904; (f) A. G. Lohse and R. P. Hsung, *Chem. Eur. J.*, 2011, **17**, 3812; (g) N. Shimada, C. Stewart and M. A. Tius, *Tetrahedron*, 2011, **67**, 5851; (h) W. T. Spencer, III, T. Vaidya and A. J. Frontier, *Eur. J. Org. Chem.*, 2013, 3621; (i) H. Li and J. Wu, *Synthesis*, 2015, **47**, 22.
- ¹² (a) T. Hirano, T. Kumagai and T. Miyashi, *J. Org. Chem.*, 1991, **56**, 1907; (b) A. P. Masters, M. Parvez, T. S. Sorensen and F. Sun, *J. Am. Chem. Soc.*, 1994, **116**, 2804; (c) S. Bhargava, J. Hou, M. Parvez and T. S. Sorensen, *J. Am. Chem. Soc.*, 2005, **127**, 3704; (d) V. Regnier and D. Martin, *Org. Chem. Front.*, 2015, **2**, 1536.
- ¹³ G. Kuzmanich, F. Spänig, C.-K. Tsai, J. M. Um, R. M. Hoekstra, K. N. Houk, D. M. Guldi and M. A. Garcia-Garibay, *J. Am. Chem. Soc.*, 2011, **133**, 2342.

-
- ¹⁴ (a) D. Martin, C. E. Moore, A. L. Rheingold and G. Bertrand, *Angew. Chem. Int. Ed.* 2013, **52**, 7014; (b) T. Schulz, C. Färber, M. Leibold, C. Bruhn, W. Baumann, D. Selent, T. Porsch, M. C. Holthausen and U. Siemeling, *Chem. Commun.*, 2013, **49**, 6834; (c) V. Regnier, F. Molton, C. Philouze and D. Martin, *Chem. Commun.*, 2016, **52**, 11422.
- ¹⁵ J. K. Mahoney, D. Martin, F. Thomas, C. E. Moore, A. L. Rheingold and G. Bertrand, *J. Am. Chem. Soc.*, 2015, **137**, 7519.
- ¹⁶ (a) M. Tian, S. Tatsuura, M. Furuki, Y. Sato, I. Iwasa and L. S. Pu, *J. Am. Chem. Soc.*, 2003, **125**, 348; (b) K. Yesudas and K. Bhanuprakash, *J. Phys. Chem. A*, 2007, **111**, 1943.
- ¹⁷ (a) S. Tatsuura, M. Tian, M. Furuki, Y. Sato, I. Iwasa and H. Mitsu, *Appl. Phys. Lett.*, 2004, **84**, 1450; (b) S. Tatsuura, T. Matsubara, M. Tian, H. Mitsu, I. Iwasa, Y. Sato and M. Furuki, *Appl. Phys. Lett.*, 2004, **85**, 540.
- ¹⁸ R. G. Hicks, *Org. Biomol. Chem.*, 2007, **5**, 1321.
- ¹⁹ (a) R. W. Baldock, P. Hudson, A. R. Katritzky and F. Soti, *J. Chem. Soc., Perkin Trans. 1*, 1974, 1422; (b) A. T. Balaban, M. T. Caproiu, N. Negoita and R. Baican, *Tetrahedron*, 1977, **33**, 2249; (c) A. R. Katritzky, M. C. Zerner and M. M. Karelson, *J. Am. Chem. Soc.*, 1986, **108**, 7213; (d) F. G. Bordwell and T. -Y. Lynch, *J. Am. Chem. Soc.*, 1989, **111**, 7558.
- ²⁰ T. H. Koch, J. A. Olesen and J. DeNiro, *J. Am. Chem. Soc.*, 1975, **97**, 7285.
- ²¹ J. K. Mahoney, D. Martin, C. E. Moore, A. L. Rheingold and G. Bertrand, *J. Am. Chem. Soc.*, 2013, **135**, 18766.
- ²² (a) K. Ehrlich and G. F. Emerson, *J. Am. Chem. Soc.*, 1972, **94**, 2464; (b) R. M. Bullock, R. T. Hembre and J. R. Norton, *J. Am. Chem. Soc.*, 1988, **110**, 7868; (c) A. Ohsuka, T. Hirao, H. Kurosawa and I. Ikeda, *Organometallics*, 1995, **14**, 2538; (d) A. M. Oertel, V. Ritleng, A. Busiah, L. F. Veiros and M. J. Chetcuti, *Organometallics*, 2011, **30**, 6495.
- ²³ R. Eisenberg and H. B. Gray, *Inorg. Chem.*, 2011, **50**, 9741.
- ²⁴ J. Stubbe and W. A. Van der Donk, *Chem. Rev.*, 1998, **98**, 706.
- ²⁵ (a) M. M. Whittaker and J. W. Whittaker, *Biophys. J.*, 1993, **64**, 762; (b) Y. Wang, J. L. Dubois, B. Hedman, K. O. Hodgson and T. D. P. Stack, *Science*, 1998, **279**, 537.
- ²⁶ (a) W. Sato, K. Okamoto, Y. Saito, M. Kawashima and T. Kaneda, 2006, *WO 2006118277*; (b) D. M. Connor, K. A. Keller and J. G. Lever, 2007, *US 200701139*
- ²⁷ (a) V. Lyaskovskyy and B. de Bruin, *ACS Catal.*, 2012, **2**, 270; (b) J. I. van der Vlugt, *Eur. J. Inorg. Chem.*, 2012, 363; (c) V. K. K. Praneeth, M. R. Ringenberg and T. R. Ward, *Angew. Chem. Int. Ed.*, 2012, **51**, 10228; (d) O. R. Luca and R. H. Crabtree, *Chem. Soc. Rev.*, 2013, **42**, 1440.
- ²⁸ J. P. Chirik, K. Weighardt, *Science*, 2010, **327**, 794.
- ²⁹ (a) K. J. Blackmore, J. W. Ziller and A. F. Heyduk, *Inorg. Chem.*, 2005, **44**, 5559; (b) C. Mukherjee, T. Weyhermüller, E. Both and P. Chaudhuri, *Inorg. Chem.*, 2008, **47**, 2740; (c) A. L.

Smith, K. I. Hardcastle and J. D. Soper, *J. Am. Chem. Soc.*, 2010, **132**, 14358; (d) J. L. Wong, R. H. Sánchez, J. G. Logan, R. A. Zarkesh, J. W. Ziller and A. F. Heyduk, *Chem. Sci.*, 2013, **4**, 1906.

³⁰ (a) L. Bourget-Merle, M. F. Lappert and J. R. Severn, *Chem. Rev.*, 2002, **102**, 3031; (b) D. J. Emslie and W. E. Piers, *Coord. Chem. Rev.*, 2002, **233–234**, 131; (c) D. J. Mindiola, *Acc. Chem. Res.*, 2006, **39**, 813; (d) C. J. Cramer and W. B. Tolman, *Acc. Chem. Res.*, 2007, **40**, 601; (e) P. L. Holland, *Acc. Chem. Res.*, 2008, **41**, 905; (f) Y. C. Tsai, *Coord. Chem. Rev.*, 2012, **256**, 722.

³¹ M. M. Khusniyarov, E. Bill, T. Weyhermüller, E. Bothe and K. Wieghardt, *Angew. Chem. Int. Ed.*, 2011, **50**, 1652.

³² (a) S. Fortier, O. G. Moral, C-H Chen, M. Pink, J. J. Le Roy, M. Murugesu, D. J. Mindiola and K. G. Caulton, *Chem. Commun.*, 2012, **48**, 11082; (b) J. Takaichi, K. Ohkubo, H. Sugimoto, M. Nakano, D. Usa, H. Maekawa, N. Fujieda, N. Nishiwaki, S. Seki, S. Fukuzumia and S. Itoh, *Dalton Trans.*, 2013, **42**, 2438.

³³ (a) C. M. Byrne, S. D. Allen, E. B. Lobkovsky and G. W. Coates, *J. Am. Chem. Soc.*, 2004, **126**, 11404; (b) R. Jiao, X. Shen, M. Xue, Y. Zhang, Y. Yao and Q. Shen, *Chem. Commun.*, 2010, **46**, 4118; (c) M. M. Rodriguez, E. Bill, W. W. Brennessel and P. L. Holland, *Science*, 2011, **334**, 780; (d) K. Grubel, W. W. Brennessel, B. Q. Mercado and P. L. Holland, *J. Am. Chem. Soc.*, 2014, **136**, 16807; (e) L. A. Harris, E. C. Y. Tam, M. P. Coles and J. R. Fulton, *Dalton Trans.*, 2014, **43**, 13803; (f) A. Kalita, V. Kumar and B. Mondal, *RSC Adv.*, 2015, **5**, 643.

³⁴ (a) J. D. Azoulay, R. S. Rojas, A. V. Serrano, H. Ohtaki, G. B. Galland, G. Wu and G. C. Bazan, *Angew. Chem., Int. Ed.*, 2009, **48**, 1089; (b) J. D. Azoulay, G. C. Bazan and G. B. Galland, *Macromolecules*, 2010, **43**, 2794; (c) A. Sokolohorskyj, O. Zeleznik, I. Cisarova, J. Lenz, A. Lederer and J. Merna, *J. Polym. Sci., Part A: Polym. Chem.*, 2017, **55**, 2440.

³⁵ (a) J. D. Azoulay, Y. Schneider, G. B. Galland and G. C. Bazan, *Chem. Commun.*, 2009, 6177; (b) J. D. Azoulay, H. Y. Gao, Z. A. Koretz, G. Kehr, G. Erker, F. Shimizu, G. B. Galland and G. C. Bazan, *Macromolecules*, 2012, **45**, 4487.

³⁶ (a) M. C. Weiss and V. L. Goedken, *J. Am. Chem. Soc.*, 1976, **98**, 3389; (b) B. Durham, T. J. Anderson, J. A. Switzer, J. F. Endicott and M. D. Glick, *Inorg. Chem.*, 1977, **16**, 271; (c) J. A. Switzer and F. J. Endicott, *J. Am. Chem. Soc.*, 1980, **102**, 1181; (d) D. P. Riley and D. H. Busch, *Inorg. Chem.*, 1983, **22**, 4141; (e) D. B. MacQueen, C. Lange, M. Calvin, J. W. Otvos, L. O. Spreer, C. B. Allan, A. Ganse and R. B. Frankel, *Inorg. Chim. Acta*, 1997, **263**, 125; (f) J. Zhang, Z. Zhang, Z. Chen and X. Zhou, *Dalton Trans.*, 2012, **41**, 357; (g) B. Liu, V. Dorcet, L. Maron, J. F. Carpentier and Y. Sarazin, *Eur. J. Inorg. Chem.*, 2012, 3023.

³⁷ (a) S. Yokota, Y. Tachi and S. Itoh, *Inorg. Chem.*, 2002, **41**, 1342; (b) M. S. Hill, R. Pongtavornpinyo and P. B. Hitchcock, *Chem. Commun.*, 2006, 3720; (c) M. L. Scheuermann, U. Fekl, W. Kaminsky and K. I. Goldberg, *Organometallics*, 2010, **29**, 4749.

-
- ³⁸ (a) P. H. M. Budzelaar, A. B. van Oort, and A. G. Orpen, *Eur. J. Inorg. Chem.*, 1998, 1485; (b) S. Yokota, Y. Tachi, N. Nishiwaki, M. Ariga and S. Itoh, *Inorg. Chem.*, 2001, **40**, 5316; (c) B. A. Jazdzewski, P. L. Holland, M. Pink, Jr., V. G. Young, D. J. E. Spencer and W. B. Tolman, *Inorg. Chem.*, 2001, **40**, 6097; (d) L. -M. Tang, Y. -Q. Duan, X. -F. Li and Y. -S. Li, *J. Organomet. Chem.*, 2006, **691**, 2023; (e) M. Arrowsmith, M. R. Crimmin, M. S. Hill and G. Kociok-Köhn, *Dalton Trans.*, 2013, **42**, 9720.
- ³⁹ V. Regnier, F. Molton, C. Philouze and D. Martin, *Chem. Commun.*, 2016, **52**, 11422.
- ⁴⁰ M. Tripathi, V. Regnier, Z. Ziani, M. Devillard, C. Philouze and D. Martin, *RSC Adv.*, 2018, **8**, 38346.
- ⁴¹ (a) V. L. Goedken, M. C. Weiss, D. Place and J. Dabrowiak, *Inorg. Synth.*, 1980, **20**, 115; (b) J. R. Chipperfield and S. Woodward, *J. Chem. Educ.*, 1994, **71**, 75.
- ⁴² (a) T. J. Truex and R. H. Holm, *J. Am. Chem. Soc.*, 1972, **94**, 4529; (b) S. C. Tang, S. Koch, G. N. Weinstein, R. W. Lane and R. H. Holm, *Inorg. Chem.*, 1973, **12**, 2589.
- ⁴³ (a) S. A. Brawner, I. J. B. Lin, J. -H. Kim and G. W. Everett, *Inorg. Chem.*, 1978, **17**, 1304; (b) J. -H. Kim and G. W. Everett, *Inorg. Chem.*, 1979, **18**, 3145.
- ⁴⁴ (a) B. P. Block and J. C. Bailar, *J. Am. Chem. Soc.*, 1951, **73**, 4722; (b) C. F. Weick and F. Basolo, *Inorg. Chem.*, 1966, **5**, 576.
- ⁴⁵ (a) H. G. Viehe, Z. Janousek and M. A. Defrenne, *Angew. Chem., Int. Ed.*, 1971, **10**, 575; (b) Z. Janousek and H. G. Viehe, *Angew. Chem., Int. Ed.*, 1971, **10**, 574; (c) R. Gompper, G. Maas, E.-U. Würthwein, H. G. Viehe, H. Hartmann, E. Vilsmaier, J. C. Jochims, M. Hitzler, Q. Wang, J. Liebscher and W. Kantlehner, *J. Prakt. Chem.*, 1994, **336**, 390.
- ⁴⁶ (a) V. Lavallo, C. A. Dyker, B. Donnadiou and G. Bertrand, *Angew. Chem., Int. Ed.*, 2008, **47**, 5411; (b) C. A. Dyker, V. Lavallo, B. Donnadiou and G. Bertrand, *Angew. Chem., Int. Ed.*, 2008, **47**, 3206; (c) M. Melaimi, P. Parameswaran, B. Donnadiou, G. Frenking and G. Bertrand, *Angew. Chem., Int. Ed.*, 2009, **48**, 4792; (d) A. DeHope, B. Donnadiou and G. Bertrand, *J. Organomet. Chem.*, 2011, **696**, 2899; (e) C. Pranckevicius and D. W. Stephan, *Organometallics*, 2013, **32**, 2693; (f) W.-C. Chen, Y.-C. Hsu, C.-Y. Lee, G. P. A. Yap and T.-G. Ong, *Organometallics*, 2013, **32**, 2435; (g) W.-C. Chen, C.-Y. Lee, B.-C. Lin, Y.-C. Hsu, J.-S. Shen, C.-P. Hsu, G. P. A. Yap and T.-G. Ong, *J. Am. Chem. Soc.*, 2014, **136**, 914.
- ⁴⁷ (a) H. G. Viehe, Z. Janousek, R. Gompper and D. Lach, *Angew. Chem.*, 1973, **85**, 581; (b) G. J. de Voghel, T. L. Eggerichs, Z. Janousek and H. G. Viehe, *J. Org. Chem.*, 1974, **39**, 1233; (c) R. Weiss, H. Wolf, U. Schubert and T. Clark, *J. Am. Chem. Soc.*, 1981, **103**, 6142; (d) G. Toth, I. Bitter, G. Bigam and O. Strausz, *Magn. Reson. Chem.*, 1986, **24**, 137; (e) S. Ehrenberg, R. Gompper, K. Polborn and H.-U. Wagner, *Angew. Chem., Int. Ed.*, 1991, **30**, 334; (f) G. Toth, A. Kovacs, I. Bitter and H. Duddeck, *Liebigs Ann. Chem.*, 1991, 1215.

-
- ⁴⁸ (a) A. Fürstner, M. Alcazaro and H. Krause, *Org. Synth.*, 2009, **86**, 298; (b) V. Regnier, Y. Planet, C. E. Moore, J. Pecaut, C. Philouze and D. Martin, *Angew. Chem. Int. Ed.*, 2017, **56**, 1031.
- ⁴⁹ E. B. Pedersen, *Tetrahedron*, 1977, **33**, 217.
- ⁵⁰ DFT calculations were carried out with the Gaussian09 software package: M. J. Frisch, G. W. Trucks, H. B. Schlegel, G. E. Scuseria, M. A. Robb, J. R. Cheeseman, G. Scalmani, V. Barone, B. Mennucci, G. A. Petersson, H. Nakatsuji, M. Caricato, X. Li, H. P. Hratchian, A. F. Izmaylov, J. Bloino, G. Zheng, J. L. Sonnenberg, M. Hada, M. Ehara, K. Toyota, R. Fukuda, J. Hasegawa, M. Ishida, T. Nakajima, Y. Honda, O. Kitao, H. Nakai, T. Vreven, J. A. Montgomery, Jr., J. E. Peralta, F. Ogliaro, M. Bearpark, J. J. Heyd, E. Brothers, K. N. Kudin, V. N. Staroverov, R. Kobayashi, J. Normand, K. Raghavachari, A. Rendell, J. C. Burant, S. S. Iyengar, J. Tomasi, M. Cossi, N. Rega, J. M. Millam, M. Klene, J. E. Knox, J. B. Cross, V. Bakken, C. Adamo, J. Jaramillo, R. Gomperts, R. E. Stratmann, O. Yazyev, A. J. Austin, R. Cammi, C. Pomelli, J. W. Ochterski, R. L. Martin, K. Morokuma, V. G. Zakrzewski, G. A. Voth, P. Salvador, J. J. Dannenberg, S. Dapprich, A. D. Daniels, Ö. Farkas, J. B. Foresman, J. V. Ortiz, J. Cioslowski and D. J. Fox, *Gaussian 09, Revision 4.2.0*, Gaussian, Inc., Wallingford CT, 2009.
- ⁵¹ D. C. H. Do, A. Keyser, A. V. Protchenko, B. Maitland, I. Pernik, H. Niu, E. L. Kolychev, A. Rit, D. Vidovic, A. Stasch, C. Jones and S. Aldridge, *Chem. Eur. J.*, 2017, **23**, 5830.
- ⁵² G. Parkin, *Chem. Rev.*, 2004, **104**, 699.
- ⁵³ (a) Y. S. Kim, Y. S. Won, H. Hagelin-Weaver, N. Omenetto and T. Anderson, *J. Phys. Chem. A*, 2008, **112**, 4246; (b) R. E. Linney and D. K. Russell, *J. Mater. Chem.*, 1993, **3**, 587.
- ⁵⁴ (a) E. Hevia, A. R. Kennedy, J. Klett, Z. Livingstone and M. D. MacCall, *Dalton Trans.*, 2010, **39**, 520; (b) H. Huang, H. Zong, G. Bian and L. Song, *Tetrahedron: Asymmetry*, 2015, **26**, 835; (c) S. Tang, L. Zeng, Y. Liu, and A. Lei, *Angew. Chem. Int. Ed.*, 2015, **54**, 15850.
- ⁵⁵ V. Regnier, Y. Planet, C. E. Moore, J. Pecaut, C. Philouze and D. Martin, *Angew. Chem. Int. Ed.*, 2017, **56**, 1031.
- ⁵⁶ M. Devillard, V. Regnier, J. Pecaut and D. Martin, *Org. Chem. Front.*, 2019 (DOI: 10.1039/c9qo00298g)
- ⁵⁷ T. P. Yoon and E. N. Jacobsen, *Science*, 2003, **299**, 1691.
- ⁵⁸ A. Pfaltz, *Synlett*, 1999, 835.
- ⁵⁹ (a) D. A. Evans, M. C. Kozlowski, J. A. Murry, C. S. Burgey, K. R. Campos, B. T. Connell and R. J. Staples, *J. Am. Chem. Soc.*, 1999, **121**, 669; (b) D. A. Evans, D. M. Barnes, J. S. Johnson, T. Lectka, P. von Matt, S. J. Miller, J. A. Murry, R. D. Norcross, E. A. Shaughnessy and K. R. Campos, *J. Am. Chem. Soc.*, 1999, **121**, 7582; (c) D. A. Evans, T. Rovis, M. C. Kozlowski and J. S. Tedrow, *J. Am. Chem. Soc.*, 1999, **121**, 1994; (d) N. Gathergood, W. Zhuang and K. A. Jorgensen, *J. Am. Chem. Soc.*, 2000, **122**, 12517; (e) N. Nishiwaki, K. R. Knudsen, K. V. Gothelf and K. A. Jorgensen, *Angew. Chem. Int. Ed.*,

2001, **40**, 2992; (f) K. B. Jensen, J. Thorhauge, R. G. Hazell and K. A. Jorgensen, *Angew. Chem. Int. Ed.*, 2001, **40**, 160.

⁶⁰ J. E. Parks and R. H. Holm, *Inorg. Chem.*, 1968, **7**, 1408.

⁶¹ A. Walli, S. Dechert and F. Meyer, *Eur. J. Inorg. Chem.*, 2013, 7044.

⁶² A. I. Poddel'sky, V. K. Cherkasov and G. A. Abakumov, *Coord. Chem. Rev.*, 2009, **253**, 291.

⁶³ S. Elgafi, L. D. Field, B. A. Messerle, P. Turner and T. W. Hambley, *J. Organomet. Chem.*, 1999, **588**, 69.

APPENDIX

CONFERENCES

- Attended Stable Carbene Symposium in 2018 in Toulouse, FRANCE
- Oral presentation in ACS 2019 National Meeting & Exposition in Orlando, FL, USA
- Oral presentation in Semaine d'Etudes en Chimie Organique (SECO) 2019 in FRANCE
- Oral presentation in GECOM-CONCOORD 2019 in Erquy, FRANCE

PUBLICATIONS

- Investigation of the full reversal of selectivity in the reaction of aniline with 1,3-dichloro-1,3-bis(dimethylamino)vinamidinium salts - *New J. Chem.*, **2017**, *41*, 15016
- Metal free oxidation of vinamidine derivatives and a simple synthesis of α -keto- β -diimines ligands - *Rsc Adv.*, **2018**, *8*, 38346
- A computational study of the interplay of steric and electronic effects in the stabilization of 1,3-(diamino)oxyallyls - *Journal of Molecular Structure* **2018**, *1172*, 3.



Cite this: *New J. Chem.*, 2017, 41, 15016

Received 11th September 2017,
Accepted 2nd November 2017

DOI: 10.1039/c7nj03442c

rsc.li/njc

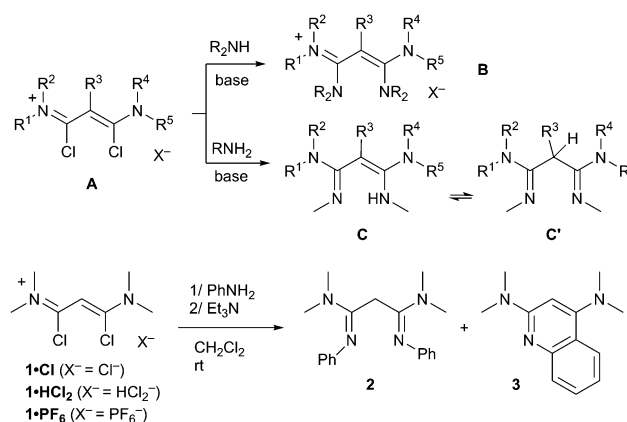
Investigation of the full reversal of selectivity in the reaction of aniline with 1,3-dichloro-1,3-bis(dimethylamino)vinamidinium salts†

Monika Tripathi, Vianney Regnier, Christophe Lincheneau and David Martin *

The addition of aniline, even in excess, to a solution of 1,3-dichloro-1,3-bis(dimethylamino)vinamidinium salt in the presence of triethylamine invariably leads to the formation of 2,4-bis(dimethylamino)quinoline. Conversely, delaying the addition of the base leads to the formation of 1,3-dimethylamino-*N,N'*-diphenylpropane-1,3-diimine, even when only a substoichiometric amount of aniline was used. A DFT study led to the consideration of factors that accounted for this reversal of reactivity. The role of a secondary orbital interaction in key transition states, as well as the role of solvent, is discussed.

The chemistry of 1,3-dichloro-vinamidinium salts **A** (Scheme 1) was essentially developed in the 1970s. These readily available compounds¹ have allowed the synthesis of some cyanines, allenes and a variety of heterocycles.^{2,3} More recently, several works on electron-rich allenes,^{4,5} so-called carbodicarbenes,⁶ have triggered a revival of interest in these versatile synthons.⁷ In turn, we decided to reinvestigate the reactivity of the long-known 1,3-dichloro-1,3-bis(dimethylamino)vinamidinium **1**⁺. In particular, we showed that this compound is not as moisture sensitive as previously suggested.⁸ On the contrary, its high persistence in aqueous solution allows for the metathesis of the counterion of the salt. We used the resulting (hexafluoro)phosphate salt **1**·PF₆ as the precursor for an isolable pyrimidinium-2-ylidene.⁸ Herein we report our findings on the simple reaction of **1**⁺ with aniline in the presence of triethylamine. We show that the timing of the addition of the base allows for switching the reaction towards the formation of either a quinoline or a malonamidine, in otherwise identical experimental conditions. DFT calculations allowed the rationalization of this full reversal of selectivity.

In the course of our work on atypical vinamidinium derivatives,^{8,9} we were interested in 1,3-bis(dimethylamino)-*N,N'*-diphenylpropane-1,3-diimine **2**. The reaction of 1,3-dichloro-vinamidinium salts **A** with amines has been reported many times.^{2,7} Secondary amines quantitatively afford tetra(amino)vinamidinium salts **B**, whereas primary amines usually yield the corresponding diketimine, either as tautomer **C** or **C'**. Half a century ago, Viehe *et al.* briefly described the synthesis of **2** from **1**⁺ and aniline. As the authors did not provide a detailed experimental procedure,



Scheme 1 1,3-dichloro-vinamidinium salts **A** and their reaction with amines.

we simply reacted two equivalents of aniline with **1**·PF₆. We also added three equivalents of triethylamine, as we anticipated the interception of two equivalents of HCl and deprotonation of **2**·H⁺. However, we observed the quantitative formation of quinoline **3**,³ which resulted from the addition of one equivalent of aniline followed by an intramolecular electrophilic aromatic substitution of an *N*-phenyl moiety. Even with an excess amount of aniline, **3** remained the only observed product, along with triethylammonium salts (Table 1, entries 1 and 2). Finally, the formation of a small amount of the desired 1,3-diimine **2** was achieved by delaying the addition of triethylamine for about two minutes (entry 3). Increasing this delay up to 10 minutes enhanced the 2:3 ratio to 85:15. The replacement of the PF₆[−] anion by HCl₂[−] is also slightly beneficial (entries 4 and 5). Importantly, with only one equivalent of aniline, only **2** is formed in nearly 50% conversion (entry 6). Conversely, the use of an excess amount of aniline allowed the total

Université Grenoble-Alpes, CNRS, DCM (UMR 5250), CS 40700, 38058 Grenoble Cedex 9, France. E-mail: david.martin@univ-grenoble-alpes.fr

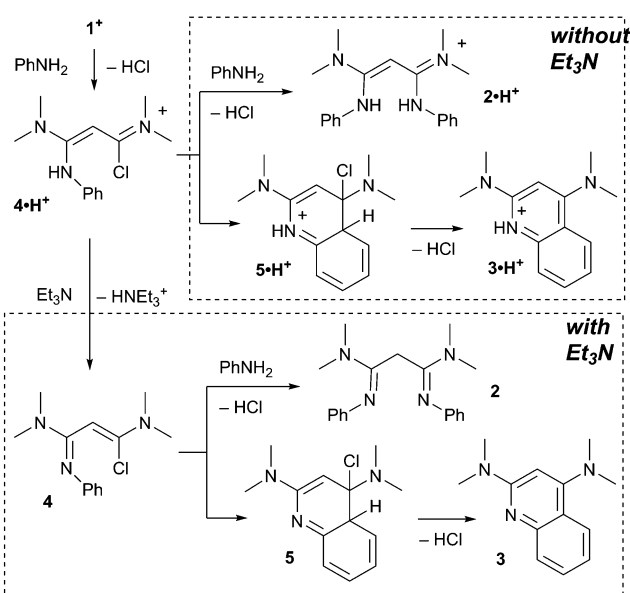
† Electronic supplementary information (ESI) available. See DOI: 10.1039/c7nj03442c

Table 1 Reaction of 1^+ with aniline in the presence of triethylamine (TEA)

Entry ^a	1^+ : aniline ratio	1^+ :TEA ratio	X ⁻	Delay before the addition of TEA	2:3 ratio ^b
1	1:2	1:3	PF ₆ ⁻	—	0:100
2	1:6	1:3	PF ₆ ⁻	—	0:100
3	1:6	1:3	PF ₆ ⁻	2 min	8:92
4	1:2	1:3	PF ₆ ⁻	10 min	80:20
5	1:2	1:3	HCl ₂ ⁻	10 min	85:15
6	1:1	1:3	PF ₆ ⁻	10 min	50:0 ^c
7	1:6	1:6	PF ₆ ⁻	10 min	100:0

^a A typical test reaction was performed on 1 mmol of 1^+ ; see also the experimental part. ^b Measured from the ¹H NMR spectra of the crude reaction in CDCl₃. ^c 1:1 ratio of only starting material **1** and product **2** was observed; no traces of **3** could be detected.

conversion of 1^+ into **2**, which was isolated as colorless crystals in 68% yield after work-up. Of note, during the preparation of this paper, Aldridge *et al.* also published the synthesis of **2**, which is in line with our findings that the reaction performs

**Scheme 2** Reaction pathways for the reaction of 1^+ with aniline.

well when the basic work-up is delayed. Indeed, *in situ* generated 1^+ and two equivalents of aniline were stirred in refluxing tetrahydrofuran for one night and late work-up with aqueous NaOH afforded **2** in 50–60% yield.¹⁰

We considered that the reaction of 1^+ with the first equivalent of aniline affords $4\cdot\text{H}^+$, which can either react with a second equivalent of aniline or undergo an intramolecular electrophilic substitution, to afford $2\cdot\text{H}^+$ or $3\cdot\text{H}^+$, respectively (Scheme 2). In the presence of a base, the key intermediate becomes **4**, from which the reaction pathway can similarly diverge to yield either **2** or **3**.

We first examined intermediate **4** with DFT computations at the B3LYP/6-311g(d,p) level of theory.¹¹ At the optimized minima, the amidine and enamine moieties are nearly orthogonal (Fig. 1). The weak conjugation between their respective π -systems is also indicated by the long C₂–C₃ bond (149 pm, to be compared to the C₁–C₂ bond length: 134 pm). Due to the non-symmetrical enamine and the imine moieties, **4** has four diastereomeric conformers, which were found to be close in energy and with similar electronic and structural properties. In contrast with its basic counterpart, the alternative intermediate $4\cdot\text{H}^+$ is only slightly twisted and its whole π -system is conjugated. As a result, eight isomers of $4\cdot\text{H}^+$ had to be considered, due to *E/Z* isomerism around C₁–C₂, C₂–C₃ and C₃–NPh bonds. They were found at similar energies within a 6 kcal mol⁻¹ range and featured similar characteristics.

For both $4\cdot\text{H}^+$ and **4**, the lowest unoccupied molecular orbital (LUMO, see Fig. 2; for clarity, the discussion focuses on the most stable conformers (1*E*,3*E*)-**4** and (1*Z*,2*Z*,3*E*)- $4\cdot\text{H}^+$) has a significant weight on C₁, which is the expected electrophilic center for the enamine moieties. The highest occupied molecular orbital (HOMO) is a π -orbital at the phenyl group, according with the experimentally observed formation of **3**. The intramolecular cyclisation of **4** first goes through the formation of dihydroquinoline **5**, which is very likely the rate-determining step of the process. The protonation of **4** clearly results in a less nucleophilic aryl group (the energy of the HOMO of **4**: -0.2 eV; $4\cdot\text{H}^+$: -0.35 eV). However, it also results in an increase in electrophilicity at C₁ (the energy of the LUMO of **4**: -0.02 eV;

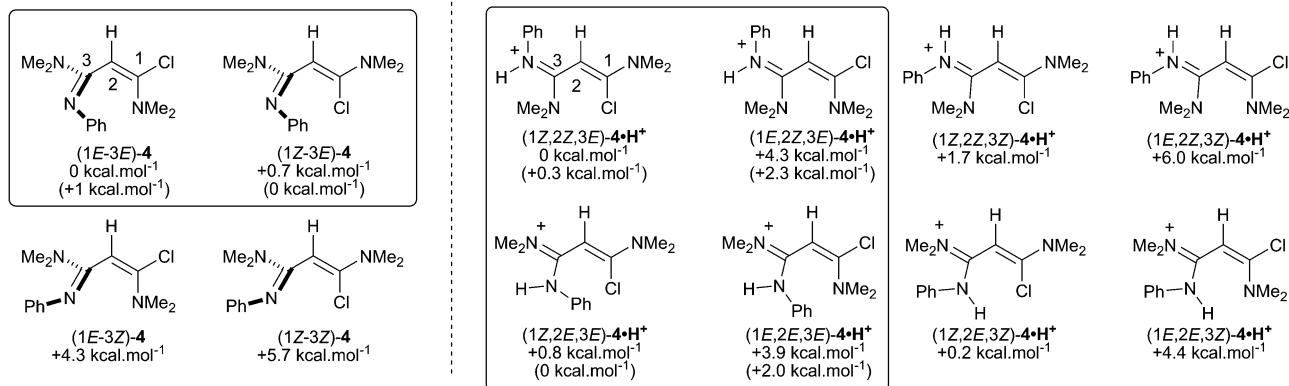


Fig. 1 Relative free enthalpies for diastereomeric conformers of **4** (left) and $4\cdot\text{H}^+$ (right) at 298 K. Default optimizations were performed “*in vacuo*”. Only 3*E* isomers are relevant for intramolecular cyclisation and are highlighted. Energies after optimization in “dichloromethane”, using the default polarizable continuum model, are in parentheses.

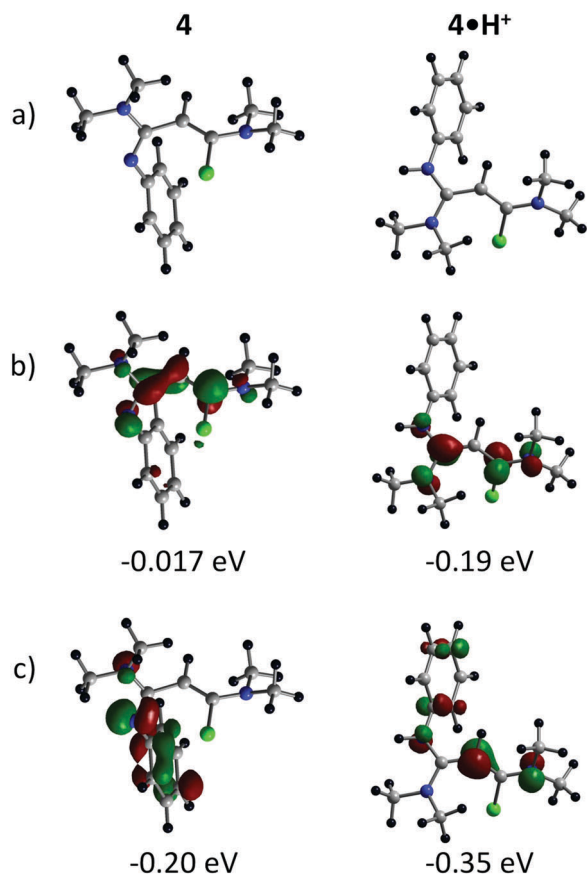


Fig. 2 Representations of (a) the optimized geometry of the most stable diastereomer; (b) lowest unoccupied molecular orbital; (c) the highest occupied molecular orbital of **4** (left) and **4·H⁺** (right).

4·H⁺: 0.2 eV). Therefore, the relative rate of cyclisation of **4** and **4·H⁺** cannot be qualitatively predicted, with the two effects being antagonist.

Note that only conformers of **4** with a 3*E* configuration are relevant for the formation of the intermediate dihydroquinoline **5**, as the latter requires the *N*-phenyl group to be in the vicinity of the reactive C1 center. The formation of **5** was found to be endergonic by +8 kcal mol⁻¹ for the formation of the *cis* isomer and by +21 kcal mol⁻¹ for *trans*-**5** (Fig. 3, in blue). The formation of **5·H⁺** is more thermodynamically disfavored (the formation of *cis*-**5·H⁺**: +15 kcal mol⁻¹; *trans*-**5·H⁺**: +40 kcal mol⁻¹). As expected for aromatic substitutions with relatively mild electrophiles, all processes correspond to late transition states. All activation barriers are in the 32–43 kcal mol⁻¹ range, depending on the initial conformation of **4** or **4·H⁺**. At this stage, this study suggested that the rates of cyclisation of **4** and **4·H⁺** were similar. Therefore, the formation of **2** in the absence of a base would only result from the deactivation of the phenyl ring in **4·H⁺**, which would then be outcompeted by aniline as a nucleophile. However, the predicted high activation barriers for the formation of **5** or **5·H⁺**, above 30 kcal mol⁻¹, were inconsistent with the experimentally observed fast formation of **3**, within minutes at room temperature in the presence of triethylamine.

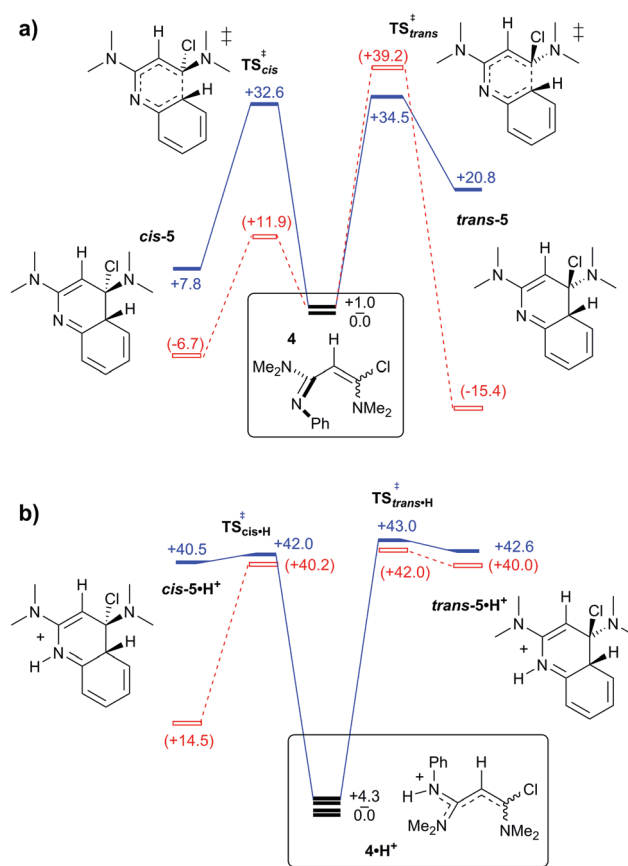


Fig. 3 Energy diagram for the cyclisation of (a) **4** (top) and (b) **4·H⁺** (bottom). Energies are in kcal mol⁻¹. Default optimizations were performed "in vacuo" (in blue). Optimization in "dichloromethane", using the default polarizable continuum model, corresponds to dashed lines, with energies in parentheses (in red).

Importantly, the optimized structure of intermediates *cis*-**5** features a significantly elongated C–Cl bond (297 pm) compared to the other parented intermediates (*trans*-**5**: 192 pm; *cis*-**5·H⁺**: 195 pm; *trans*-**5·H⁺**: 185 pm). A similar effect is discernible for the corresponding transition states (the C–Cl bond length in **TS_{cis}[‡]**: 227 pm; **TS_{trans}[‡]**: 187 pm; **TS_{cis-H}[‡]**: 185 pm; **TS_{trans-H}[‡]**: 181 pm). The HOMO of **TS_{cis}[‡]** results from the combination of the π -system of the formed dihydroquinoline and the σ^* of the C–Cl bond (see Fig. 4). This stabilizing interaction weakens and elongates the C–Cl bond. It is not significant in the case of the more electron-poor **TS_{cis-H}[‡]** because its π -system is lower in energy. It is negligible in **TS_{trans}[‡]** and **TS_{trans-H}[‡]** because the relevant molecular orbitals do not properly overlap, with the C–Cl bond being nearly orthogonal to the π -system.

Considering the key role of the solvent in the ionization of such a C–Cl bond, we re-optimized all key intermediates and transition states, taking dichloromethane into account with the polarizable continuum solvation model (Fig. 3, in red). The relative energies of **TS_{trans}[‡]**, **TS_{cis-H}[‡]** and **TS_{trans-H}[‡]** were not significantly affected by solvent effects (39–43 kcal mol⁻¹). In marked contrast, the energy of **TS_{cis}[‡]** dropped to +12 kcal mol⁻¹.

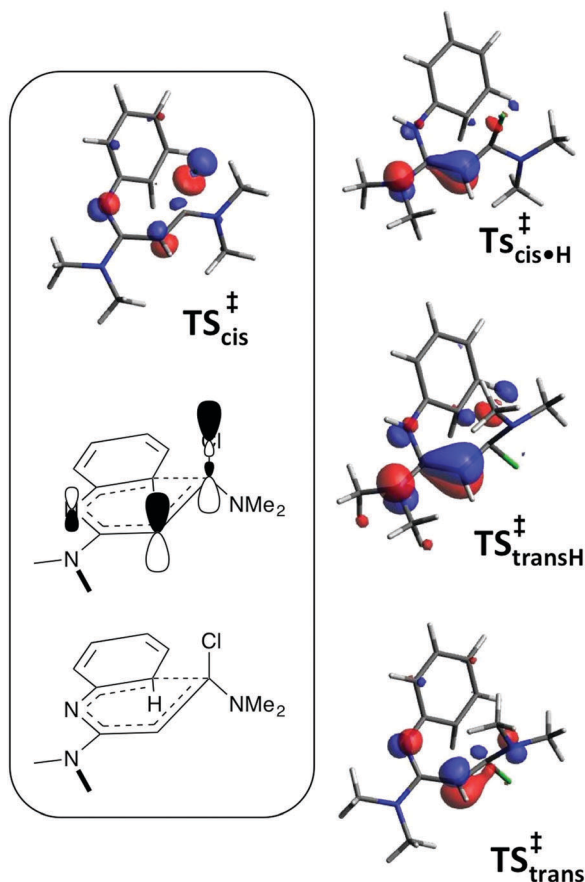


Fig. 4 Representation of the HOMO of *cis*-5, $\text{TS}_{\text{cis}}^{\ddagger}$, $\text{TS}_{\text{cis-H}}^{\ddagger}$, $\text{TS}_{\text{trans}}^{\ddagger}$ and $\text{TS}_{\text{trans-H}}^{\ddagger}$.

Conclusion

The addition of aniline to 1^+ in the presence of triethylamine leads to the formation of quinoline **3**, regardless of stoichiometry. Conversely, delaying the addition of the base switches the reaction towards the formation of malonamidine **2** only. Simple considerations on the key intermediates **4** and $4\cdot\text{H}^+$ do not allow a straightforward rationalization of these experimental results. Indeed, **4** bears a more nucleophilic arene moiety and at the same time it features a less electrophilic chloro-iminium center than that in the case of $4\cdot\text{H}^+$. Therefore, the relative rates of cyclisation of **4** and $4\cdot\text{H}^+$ through intramolecular electrophilic aromatic substitution cannot be predicted qualitatively.

Among the various transition states for the cyclisation of **4** or $4\cdot\text{H}^+$, only $\text{TS}_{\text{cis}}^{\ddagger}$, which stems from **4**, can account for a fast intramolecular reaction at room temperature, thus explaining the experimental results. The peculiar electronics and geometry of $\text{TS}_{\text{cis}}^{\ddagger}$ allow a significant stabilizing interaction of the π -system of the formed dihydroquinoline and the σ^* of the C–Cl bond. A polar solvent is critical to weaken the C–Cl bond, suggesting that the intramolecular process is unlikely in the gas phase.

Di(chloro)vinamidinium salts are key synthons in vinamidinium chemistry. In the context of the current renewal of the field, the in-depth understanding of their reactivity is critical. With respect to our specific research program, it provides valuable

guidelines for our ongoing work in the design and synthesis of novel derivatives.

Experimental section

General considerations on experiments

1,3-Dichloro-1,3-bis(dimethylamino)vinamidinium salts were prepared according to the literature.^{7c,8} Commercially available aniline and triethylamine were freshly distilled before use. NMR spectra were recorded on the NMR-ICMG platform of Grenoble with Bruker Avance 300, 400 and 500 MHz spectrometers at 298 K. ^1H NMR and ^{13}C NMR chemical shifts (δ) are reported in parts per million (ppm) relative to TMS and were referenced to the residual solvent peak. NMR multiplicities are abbreviated as follows: s = singlet, d = doublet, t = triplet, br = broad signal.

Synthesis of 2

Aniline (6.63 g, 0.071 mol) was added once to a solution of **1**· PF_6 (3.85 g, 0.011 mol) in dichloromethane (5 mL). After 10 minutes, a white suspension was observed and triethylamine (6.90 g, 0.068 mol) was added dropwise. After 30 minutes of stirring, volatiles were evaporated under vacuum. The resulting residue was washed twice with diethylether and then dissolved in dichloromethane. The organic solution was washed three times with 1 M aqueous solution of K_2CO_3 , once with water and dried over Na_2SO_4 . Evaporation under vacuum yielded a sticky oil. The addition of a few drops of cyclohexane initiated the crystallization of **2**, which was isolated as colorless needles (2.37 g, 68% yield). mp 135 °C. ^1H NMR (CDCl_3 , 400 MHz): δ = 7.35 (t, J = 8 Hz, 4H), 7.06 (t, J = 8 Hz, 2H), 6.73 (d, J = 8 Hz, 4H), 3.54 (s, 2H), 3.00 (s, 12 H); $^{13}\text{C}\{^1\text{H}\}$ NMR (CDCl_3 , 100 MHz): δ = 155.7 (C), 150.8 (C), 129.0 (CH), 122.7 (CH), 121.9 (CH), 38.6 (CH_3), 29.4 (br, CH_2). HRMS: m/z calcd for $\text{C}_{19}\text{H}_{25}\text{N}_4^+$ [$\text{M} + \text{H}$] $^+$: 309.2079, found: 309.2083.

Synthesis of 3

Aniline (0.66 g, 7 mmol) was added dropwise to a solution of **1**· PF_6 (1.0 g, 3 mmol) and triethylamine (1.2 g, 12 mmol) in dichloromethane (20 mL). After two hours of stirring, the resulting mixture was washed once with aqueous NaHCO_3 , once with water and dried over Na_2SO_4 . After evaporation under vacuum, purification by column chromatography (silica, eluent: dichloromethane, then ethyl acetate) yielded a colorless oil (265 mg, 42% yield). ^1H NMR (CDCl_3 , 400 MHz): δ = 7.84 (dd, J = 1 and 8 Hz, 1H), 7.69 (d, J = 8 Hz, 1H), 7.46 (dt, J = 1 and 8 Hz, 1H), 7.14 (dt, J = 1 and 8 Hz, 1H), 6.24 (s, 1H), 3.21 (s, 6H), 2.96 (s, 6H); $^{13}\text{C}\{^1\text{H}\}$ NMR (CDCl_3 , 100 MHz): δ = 158.8 (C), 158.6 (br, C), 149.6 (br, C), 129.1 (CH), 127.0 (CH), 124.2 (CH), 120.6 (CH), 118.5 (C), 95.2 (CH), 44.1 (CH_3), 38.3 (CH_3). HRMS: m/z calcd for $\text{C}_{13}\text{H}_{18}\text{N}_3^+$ [$\text{M} + \text{H}$] $^+$: 216.1501, found: 216.1504.

Conflicts of interest

There are no conflicts to declare.

Acknowledgements

This work was supported by the French National Agency for Research (ANR-14-CE06-0013-01 and ANR-17-ERC2-0015-01) and the AGIR-POLE fund of the University of Grenoble-Alpes. Work was performed on the ICMG Chemistry Nanobio Platform of Grenoble, as well as “Centre de Calcul Intensif en Chimie” (CECIC).

References

- (a) H. G. Viehe, Z. Janousek and M. A. Defrenne, *Angew. Chem., Int. Ed.*, 1971, **10**, 575; (b) Z. Janousek and H. G. Viehe, *Angew. Chem., Int. Ed.*, 1971, **10**, 574; (c) R. Gompper, G. Maas, E.-U. Würthwein, H. G. Viehe, H. Hartmann, E. Vilsmaier, J. C. Jochims, M. Hitzler, Q. Wang, J. Liebscher and W. Kantlehner, *J. Prakt. Chem.*, 1994, **336**, 390.
- (a) H. G. Viehe, Z. Janousek, R. Gompper and D. Lach, *Angew. Chem.*, 1973, **85**, 581; (b) G. J. de Voghel, T. L. Eggerichs, Z. Janousek and H. G. Viehe, *J. Org. Chem.*, 1974, **39**, 1233; (c) S. Brenner and H. G. Viehe, *Tetrahedron Lett.*, 1976, **16**, 1617; (d) B. Caillaux, P. George, F. Tataruch, Z. Janousek and H. G. Viehe, *Chimia*, 1976, **30**, 387; (e) G. J. De Voghel, T. L. Eggerichs, B. Clamot and H. G. Viehe, *Chimia*, 1976, **30**, 191; (f) M. Huys-Francotte, Z. Janousek and H. G. Viehe, *J. Chem. Res., Synop.*, 1977, 100; (g) J. Gorissen and H. G. Viehe, *Bull. Soc. Chim. Belg.*, 1978, **87**, 391; (h) A. Antus-Ercsenyi and I. Bitter, *Acta Chim. Acad. Sci. Hung.*, 1979, **99**, 29; (i) R. Weiss and H. Wolf, *Chem. Ber.*, 1980, **113**, 1746; (j) B. Kobel, H. G. Viehe, J. P. Declercq, G. Germin and M. Van Meerssche, *Tetrahedron Lett.*, 1980, **21**, 3799; (k) R. Weiss, H. Wolf, U. Schubert and T. Clark, *J. Am. Chem. Soc.*, 1981, **103**, 6142; (l) G. Toth, I. Bitter, G. Bigam and O. Strausz, *Magn. Reson. Chem.*, 1986, **24**, 137; (m) I. Shibuya and H. Nakanishi, *Bull. Chem. Soc. Jpn.*, 1987, **60**, 2686; (n) S. Ehrenberg, R. Gompper, K. Polborn and H.-U. Wagner, *Angew. Chem., Int. Ed.*, 1991, **30**, 334.
- The synthesis of quinolines from 1,3-di(chloro)vinamidinium and one equivalent of aniline has been reported: (a) H. G. Viehe, G. J. De Voghel and F. Smets, *Chimia*, 1976, **30**, 189; (b) G. Toth, A. Kovacs, I. Bitter and H. Duddeck, *Liebigs Ann. Chem.*, 1991, 1215; (c) S. Zouari, M. T. Kaddachi and P. H. Kahn, *Phys. Chem. News*, 2004, **15**, 120.
- (a) V. Lavallo, C. A. Dyker, B. Donnadiu and G. Bertrand, *Angew. Chem., Int. Ed.*, 2008, **47**, 5411; (b) C. A. Dyker, V. Lavallo, B. Donnadiu and G. Bertrand, *Angew. Chem., Int. Ed.*, 2008, **47**, 3206; (c) M. Melaimi, P. Parameswaran, B. Donnadiu, G. Frenking and G. Bertrand, *Angew. Chem., Int. Ed.*, 2009, **48**, 4792; (d) I. Fernández, C. A. Dyker, A. DeHope, B. Donnadiu, G. Frenking and G. Bertrand, *J. Am. Chem. Soc.*, 2009, **131**, 11875; (e) D. A. Ruiz, M. Melaimi and G. Bertrand, *Chem. – Asian J.*, 2013, **8**, 2940; (f) C. Prankevicus, L. Liu, G. Bertrand and D. W. Stephan, *Angew. Chem., Int. Ed.*, 2016, **55**, 5536.
- (a) A. DeHope, B. Donnadiu and G. Bertrand, *J. Organomet. Chem.*, 2011, **696**, 2899; (b) C. Prankevicus and D. W. Stephan, *Organometallics*, 2013, **32**, 2693; (c) W.-C. Chen, Y.-C. Hsu, C.-Y. Lee, G. P. A. Yap and T.-G. Ong, *Organometallics*, 2013, **32**, 2435; (d) W.-C. Chen, C.-Y. Lee, B.-C. Lin, Y.-C. Hsu, J.-S. Shen, C.-P. Hsu, G. P. A. Yap and T.-G. Ong, *J. Am. Chem. Soc.*, 2014, **136**, 914; (e) M. J. Goldfogel, C. C. Roberts and S. J. Meek, *J. Am. Chem. Soc.*, 2014, **136**, 6227; (f) Y.-C. Hsu, J.-S. Shen, B.-C. Lin, W.-C. Chen, Y.-T. Chan, W.-M. Ching, G. P. A. Yap, C.-P. Hsu and T.-G. Ong, *Angew. Chem., Int. Ed.*, 2015, **54**, 2420; (g) C. Prankevicus, L. Fan and D. W. Stephan, *J. Am. Chem. Soc.*, 2015, **137**, 5582; (h) C. C. Roberts, D. M. Matias, M. J. Goldfogel and S. J. Meek, *J. Am. Chem. Soc.*, 2015, **137**, 6488; (i) W.-C. Chen, J.-S. Shen, T. Jurca, C.-J. Peng, Y.-H. Lin, Y.-P. Wang, W.-C. Shih, G. P. A. Yap and T.-G. Ong, *Angew. Chem., Int. Ed.*, 2015, **54**, 15207.
- (a) R. Tonner and G. Frenking, *Angew. Chem., Int. Ed.*, 2007, **46**, 8695; (b) R. Tonner and G. Frenking, *Chem. – Eur. J.*, 2008, **14**, 3260; (c) R. Tonner and G. Frenking, *Chem. – Eur. J.*, 2008, **14**, 3273; (d) O. Kaufhold and F. E. Hahn, *Angew. Chem., Int. Ed.*, 2008, **47**, 4057; (e) C. A. Dyker and G. Bertrand, *Nat. Chem.*, 2009, **1**, 265; (f) S. Klein, R. Tonner and G. Frenking, *Chem. – Eur. J.*, 2010, **16**, 10160; (g) M. Alcarazo, *Dalton Trans.*, 2011, **40**, 1839; (h) G. Frenking, *Angew. Chem., Int. Ed.*, 2014, **53**, 6040.
- (a) A. Fürstner, M. Alcazaro, R. Goddard and C. W. Lehmann, *Angew. Chem., Int. Ed.*, 2008, **47**, 3210; (b) M. Alcazaro, C. W. Lehmann, A. Anoop, W. Thiel and A. Fürstner, *Nat. Chem.*, 2009, **1**, 295; (c) A. Fürstner, M. Alcazaro and H. Krause, *Org. Synth.*, 2009, 298; (d) A. El-Hellani, J. Monot, S. Tang, R. Guillot, C. Bour and V. Gandon, *Inorg. Chem.*, 2013, **52**, 11493.
- V. Regnier, Y. Planet, C. E. Moore, J. Pecaut, C. Philouze and D. Martin, *Angew. Chem., Int. Ed.*, 2017, **56**, 1031.
- V. Regnier, F. Molton, C. Philouze and D. Martin, *Chem. Commun.*, 2016, **52**, 11422.
- D. C. Huan, Do, A. Keyser, A. V. Protchenko, B. Maitland, I. Pernik, H. Niu, E. L. Kolychev, A. Rit, D. Vidovic, A. Stasch, C. Jones and S. Aldridge, *Chem. – Eur. J.*, 2017, **23**, 5830.
- DFT calculations were carried out with the Gaussian09 software package: M. J. Frisch, G. W. Trucks, H. B. Schlegel, G. E. Scuseria, M. A. Robb, J. R. Cheeseman, G. Scalmani, V. Barone, B. Mennucci, G. A. Petersson, H. Nakatsuji, M. Caricato, X. Li, H. P. Hratchian, A. F. Izmaylov, J. Bloino, G. Zheng, J. L. Sonnenberg, M. Hada, M. Ehara, K. Toyota, R. Fukuda, J. Hasegawa, M. Ishida, T. Nakajima, Y. Honda, O. Kitao, H. Nakai, T. Vreven, J. A. Montgomery, Jr., J. E. Peralta, F. Ogliaro, M. Bearpark, J. J. Heyd, E. Brothers, K. N. Kudin, V. N. Staroverov, R. Kobayashi, J. Normand, K. Raghavachari, A. Rendell, J. C. Burant, S. S. Iyengar, J. Tomasi, M. Cossi, N. Rega, J. M. Millam, M. Klene, J. E. Knox, J. B. Cross, V. Bakken, C. Adamo, J. Jaramillo, R. Gomperts, R. E. Stratmann, O. Yazyev, A. J. Austin, R. Cammi, C. Pomelli, J. W. Ochterski, R. L. Martin, K. Morokuma, V. G. Zakrzewski, G. A. Voth, P. Salvador, J. J. Dannenberg, S. Dapprich, A. D. Daniels, Ö. Farkas, J. B. Foresman, J. V. Ortiz, J. Cioslowski and D. J. Fox, *Gaussian 09, Revision 4.2.0*, Gaussian, Inc., Wallingford, 2009.




Cite this: *RSC Adv.*, 2018, 8, 38346

Received 4th October 2018
Accepted 8th November 2018

DOI: 10.1039/c8ra08220k

rsc.li/rsc-advances

Metal free oxidation of vinamidine derivatives: a simple synthesis of α -keto- β -diimine ligands†

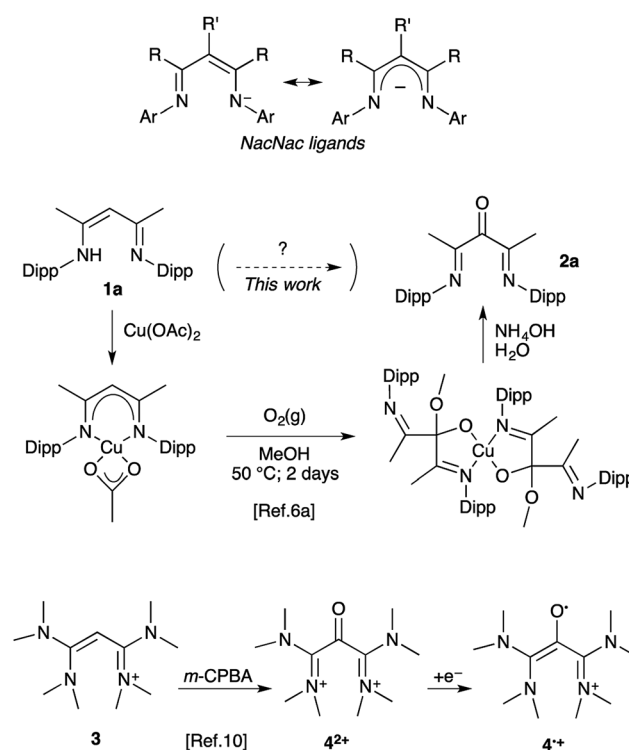
Monika Tripathi, Vianney Regnier, Zakaria Ziani, Marc Devillard, Christian Philouze and David Martin *

Oxidation of vinamidinium salts with *meta*-chloroperbenzoic acid is the key synthetic step towards new persistent 1,3-di(amino)oxyallyl radical cations. When applied to parent vinamidines, this protocol allows for a simple straightforward synthesis of α -keto- β -diimine ligands, for which no convenient synthesis was previously available.

β -Diketiminates, so-called NacNac ligands (Scheme 1), have been a focus in coordination chemistry for decades.¹ Structural modifications include a large variety of N-substituents, as well as bulky,² electron-withdrawing,³ or electron donating⁴ R groups. Substitution at the central carbon atom ($R' \neq H$) has also been explored as a strategy to tame this reactive position and enhance the chemical stability of the complex.⁵ The α -keto- β -diimines are among rare representatives with a more significant modification at the central carbon. These electron-deficient ligands have found applications in the design of highly active nickel(II) initiators for the synthesis of high molecular weight polyethylenes and poly- α -olefins.⁶ Interestingly, low-disperse semi-crystalline polymers could be obtained under living conditions and remarkable enantiomorphic site control could be achieved.⁷

The low availability of α -keto- β -diimines has clearly hampered further development. Their metal complexes have been known for long, but only as occasional by-products from the air-decomposition of unprotected NacNac complexes ($R' = H$).⁸ To date only a rare selective oxygen-degradation of copper(II) complexes allows for the synthesis of a handful of 2,4-di(arylimino)pentan-3-ones **2** from the corresponding vinamidines **1**.^{6a,d,9} The procedure requires (i) the synthesis of the NacNac-Cu(II) complex, (ii) oxidation at the ligand with dioxygen in a methanol/dichloromethane mixture, (iii) the decomplexation and hydrolysis of the resulting hemiacetal ligand (Scheme 1). In turn, we had to synthesize 2,4-bis((2,6-diisopropylphenyl)imino)pentan-3-one **2a** and experienced firsthand the length and limitations of this methodology. Among the three steps, the oxidation of the NacNac-copper complex is especially inconvenient and wasteful, as it consists of a continuous bubbling of pure dioxygen

in a warm solution for two days.^{6a} Recently, we released a patented, though in principle far simpler, oxidation of tetrakis(dimethylamino) vinamidinium **3** into di(amidinium)ketone **4**²⁺ with *meta*-chloroperbenzoic acid (*m*-CPBA) as oxidant. Our initial focus was on the corresponding radical **4**^{•+}, which was found remarkably air-persistent, despite minimal steric hindrance.¹⁰ Herein we report how further assessment of such 1,3-(diamino)oxyallyl radical cations ultimately led to a straightforward protocol for the synthesis of α -keto- β -diimines from NacNac precursors.



Scheme 1 Previously reported synthesis of α -keto- β -diimines and synthesis of air-persistent radical **4**^{•+} from vinamidinium **3**.

Univ. Grenoble Alpes, CNRS, DCM, 38000 Grenoble, France. E-mail: david.martin@univ-grenoble-alpes.fr

† Electronic supplementary information (ESI) available: ¹H and ¹³C spectra of all new compounds, computational and crystallographic (CCDC 1866491–1866494) details. For ESI and crystallographic data in CIF or other electronic format see DOI: 10.1039/c8ra08220k



Prior to 4^{+} , only two oxyallyl radical cations had been synthesized from the reaction of rare stable electrophilic carbenes with carbon monoxide.^{11–13} In principle, the oxidation of vinamidinium salts should provide for a more simple and general route, with no need of sophisticated N-substituents. To probe this assumption, we first considered the oxidative functionalization of the chloride salt of vinamidinium 5^{+} , which was synthesized from *N,N*-dimethyl-benzamide and 1-dimethylamino-1-phenylethene.¹⁴ Addition of *m*-CPBA at room temperature yielded 2-chlorovinamidinium **6** in 71% yield (Scheme 2). This result indicated the competitive formation of *meta*-chlorobenzoyl hypochlorite $\text{Cl}(\text{C}_6\text{H}_4)\text{CO}_2\text{Cl}$, from the reaction of chloride anions with *m*-CPBA.¹⁵ Therefore we proceeded to an anion metathesis. The resulting tetrafluoroborate salt reacted with *m*-CPBA, but this time to afford $7\cdot\text{H}^{+}$, which was fully characterized and isolated in 74% yield. Of note, the NMR spectra of vinamidiniums **6** and $7\cdot\text{H}^{+}$ mostly differ in the ^{13}C chemical shift of their central carbon: 94 and 127 ppm, respectively. They were unambiguously characterized by mass spectrometry analyses and X-ray diffraction studies (Fig. 1).

Solutions of $7\cdot\text{H}^{+}$ featured an EPR signal upon exposure to air. This slow reaction could be brought to fast completion in presence of potassium hydrogenocarbonate. The remarkable

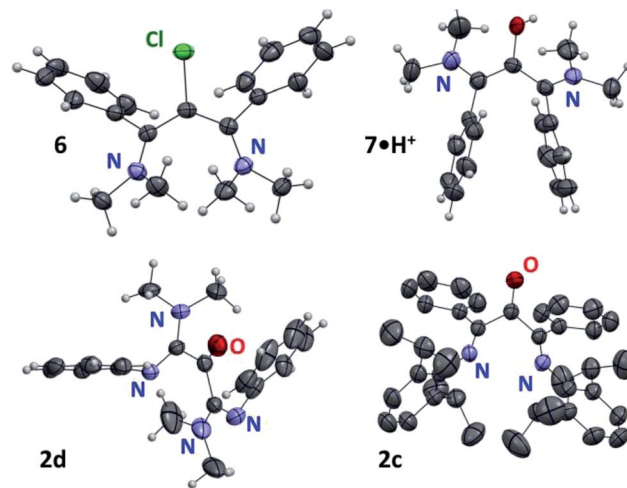
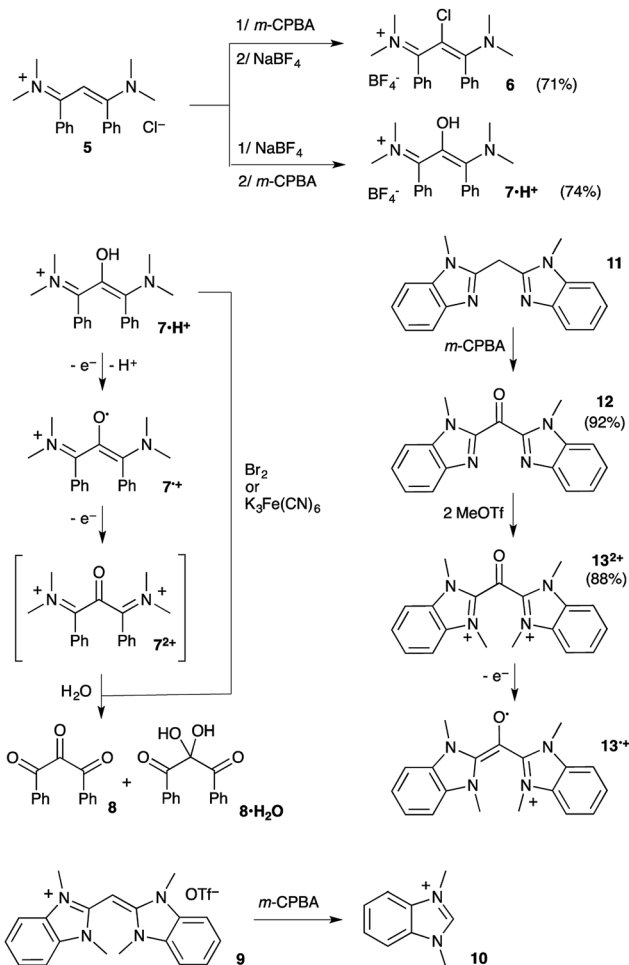


Fig. 1 X-ray structures of **6**, $7\cdot\text{H}^{+}$ and **2c,d** with thermal ellipsoids drawn at 50% probability level. Most hydrogen atoms, solvent molecules and counter-anions were omitted for clarity.

persistence under aerobic conditions of the resulting radical (in aerated solutions for several hours) was reminiscent of our previously reported stable oxyallyl radicals, some being similarly synthesized by auto-oxidation of parented enol-cations.^{11a} Therefore, we hypothesized the formation of radical 7^{+} . Although the radical ultimately decayed and couldn't be isolated, the excellent fit between the experimental EPR hyperfine coupling constants¹⁶ and the calculated values¹⁷ for 7^{+} strongly supported this reasonable assumption (Fig. 2a). The reaction of $7\cdot\text{H}^{+}$ with excess *meta*-chloroperbenzoic acid or stronger oxidants, such as dibromine or potassium ferricyanate, led to over oxidation and directly afforded EPR-silent mixtures of trione **8** and the corresponding hydrated *gem*-diol $8\cdot\text{H}_2\text{O}$,¹⁸ likely through the formation and subsequent hydrolysis of electron-poor di(iminium)ketone 7^{2+} .

We turned to mono(methine)cyanine **9** featuring electron-rich benzimidazole patterns.¹⁹ However, the reaction of **9** with *m*-CPBA afforded known²⁰ 1,3-dimethyl-benzimidazolium **10**, and not the expected di(benzimidazolium)ketone 13^{2+} (Scheme 2). Note that uncompleted, but clean, formation of **10** was still observed when adding sub-stoichiometric (one equivalent) *m*-CPBA over one hour at $-78\text{ }^{\circ}\text{C}$. Importantly, dication 13^{2+} could be finally synthesized by the oxidation of di(imine)methane **11**¹⁹ by *m*-CPBA, followed by di(alkylation) of the resulting di(imine)ketone **12**. Given that 13^{2+} was found almost unreactive towards water, the formation of **10** from **9** results from further oxidative cleavages of 13^{2+} , and not its hydrolysis.²¹ According to cyclic voltammetry experiments, 13^{2+} undergoes successive reductions at $E_{1/2} = -0.12\text{ V vs. Fc/Fc}^{+}$ (reversible) and $E_{\text{pc}} = -0.9\text{ V}$ (with further chemical evolution), which we attributed to the formation of radical cation 13^{+} and zwitterionic oxyallyl **13**, respectively (see ESI†). We performed the electrochemical reduction of a solution of 13^{2+} in acetonitrile at $E = -0.5\text{ V}$. The stoichiometry (one coulomb per mole of substrate), the observation of a strong EPR signal, as well as an excellent fit between experimental and theoretical hyperfine coupling constants, confirmed the formation of persistent 13^{+}



Scheme 2 Redox transformations of di(imidazole)methane and 1,3-di(phenyl)vinamidinium derivatives.



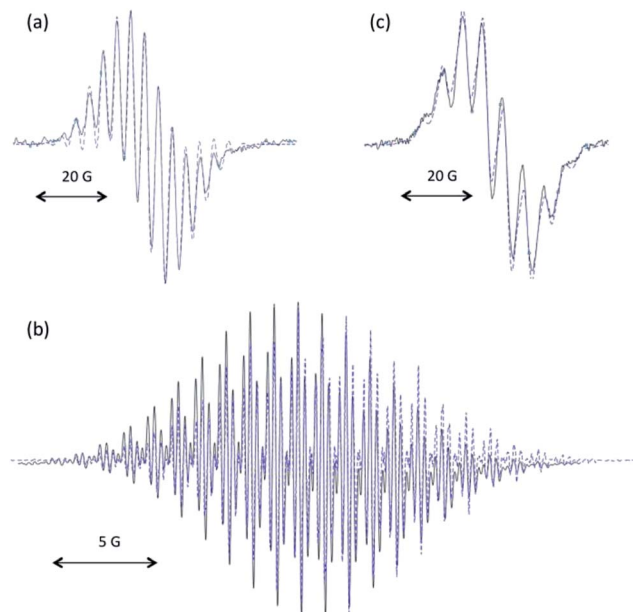
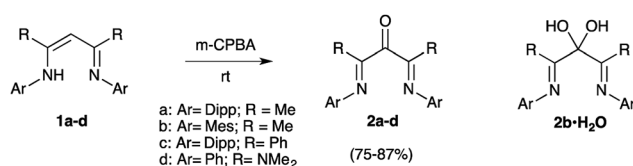


Fig. 2 Experimental isotropic X-band EPR spectra in dichloromethane at room temperature (plain black line) of $7^{+\bullet}$ (a), $10^{+\bullet}$ (b) and a crude reaction mixture of *m*-CPBA and **1a** (c). Simulated spectra (dashed blue line) were obtained with (a) a Lorentzian line-broadening parameter of 0.22 and the following set of hyperfine constants: $a(^{14}\text{N}) = 8.6$ MHz (2 nuclei) and $a(^1\text{H}) = 12.0$ MHz (12 nuclei); (b) with a Lorentzian line-broadening parameter of 0.013 and the following set of hyperfine constants: $a(^{14}\text{N}) = 3.1$ MHz (4 nuclei), $a(^1\text{H}) = 6.5$ MHz (12 nuclei) and $a(^1\text{H}) = 0.86$ MHz (4 nuclei); (c) with a Lorentzian line-broadening parameter of 0.37 and the following set of hyperfine constants: $a(^{14}\text{N}) = 7.8$ MHz (2 nuclei), $a(^1\text{H}) = 16.5$ MHz (1 nucleus) and $a(^1\text{H}) = 15.6$ MHz (6 nuclei).

(Fig. 2b), which ultimately decayed at room temperature after several hours.

The formation of di(imine)ketone **12** from **11** was so clean that it prompted us to explore further the direct oxidation of NaCNac precursors. To our delight, treatment of **1a**²² afforded **2a** in 98% yield. In contrast with the former long and tedious syntheses from literature, the one-step reaction was completed after one hour at room temperature on multigram scales. EPR monitoring of the reaction showed the formation of a paramagnetic intermediate. Simulation of the hyperfine structure of the spectra required significant coupling with a single proton, in addition to two equivalent nitrogen atoms and six protons (Fig. 2c). This suggested the transient formation of N-protonated radical **1a**· H^{\bullet} , parented to $4^{+\bullet}$, $7^{+\bullet}$ and $13^{+\bullet}$, thus implying closely related pathways for the *m*-CPBA oxidation of vinamidiniums and vinamidines **1a**.



Scheme 3 One-step synthesis of α -keto- β -diimines **2a–d** from vinamidines **1a–d**.

The only few reported β -di(imine)ketones were derivatives of acetylacetone and ortho-substituted anilines. Apart from **1a**, which can be stored for several days, they were described as unstable ligands, to be used as soon as synthesized.^{6d} We applied our protocol to vinamidines **1b**²¹ with 2,4,6-trimethylaryl *N*-substituents and, indeed, the resulting ketone **2b** decayed into a complex mixture within hours. Fast work-up allowed for its isolation in 75% yield (Scheme 3). However, even freshly crystallized **2b** contained an impurity with similar NMR chemical shifts, except for a ¹³C NMR signal (quarternary carbon) at 94 ppm in place of the CO band of **2b** at 194 ppm. Although the instability of **2b** limited further investigations, drying crystals *in vacuo* in presence of P₂O₅ decreased the amount of impurity, allowing us to assign this latter to the corresponding hydrated gem-diol **2b**· H_2O .^{23,24}

Finally, we considered vinamidines **1c**²⁵ and **1d**,^{4b,d} with phenyl and di(methyl)amino R groups, respectively. The corresponding di(imine)ketones **2c,d**, which are out of reach of previous methods, were isolated in 86–87% yield. They features similar key structural data (IR_{ATR}: $\nu = 1700$ cm⁻¹; ¹³C NMR $\delta_{\text{CO}} = 194$ –191 ppm). Their structures were asserted by a structural X-ray diffraction study (Fig. 1). Importantly, in ketones **2c,d** were found remarkably bench stable and have been stored for month with no noticeable degradation.

In conclusion, the synthesis and characterization of radicals $7^{+\bullet}$ and $13^{+\bullet}$ are further evidences that introducing 1,3-di(amino)oxyallyl patterns is a robust principle for the design of persistent radical cations. However, the outcome of the reaction of vinamidiniums with *m*-CPBA is too dependent of the substitution pattern to constitute a general route and over-oxidation is only manageable with extra electron-donating amino groups. In contrast, when applied to vinamidines, this protocol allows for a straightforward synthesis of α -keto- β -diimines. In addition to its simplicity, stable derivatives were isolated, with unprecedented bulky or electron-donating R groups. We are now evaluating these new ligands for nickel-initiated polymerization of ethylene.

Conflicts of interest

There are no conflicts to declare.

Acknowledgements

This work was supported by the French National Agency for Research (ANR-14-CE06-0013-01 and ANR-17-ERC2-0015). University of Grenoble-Alpes contributed through ICMG Chemistry Nanobio Platform, the LabEx ARCANE (ANR-11-LABX-0003-01), the “Centre de Calcul Intensif en Chimie de Grenoble” and AGIR-POLE (grant for MT).

Notes and references

- (a) L. Bourget-Merle, M. F. Lappert and J. R. Severn, *Chem. Rev.*, 2002, **102**, 3031; (b) D. J. Emslie and W. E. Piers, *Coord. Chem. Rev.*, 2002, **233–234**, 131; (c) H. W. Roesky, S. Singh, V. Jancik and V. Chandrasekhar, *Acc. Chem. Res.*,

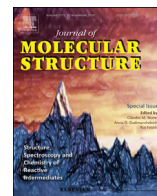


- 2004, **37**, 969; (d) D. J. Mindiola, *Acc. Chem. Res.*, 2006, **39**, 813; (e) C. J. Cramer and W. B. Tolman, *Acc. Chem. Res.*, 2007, **40**, 601; (f) P. L. Holland, *Acc. Chem. Res.*, 2008, **41**, 905; (g) Y. C. Tsai, *Coord. Chem. Rev.*, 2012, **256**, 722.
- 2 For examples with R = *tert*-butyl, see: (a) J. Vela, J. M. Smith, Y. Yu, N. A. Ketterer, C. J. Flaschenriem, R. J. Lachicotte and P. L. Holland, *J. Am. Chem. Soc.*, 2005, **127**, 7857; (b) Y. M. Badiei, A. Dinescu, X. Dai, R. M. Palomino, F. W. Heinemann, T. R. Cundari and T. H. Warren, *Angew. Chem., Int. Ed.*, 2008, **47**, 9961; (c) G. Zhao, F. Basuli, U. J. Kilgore, H. Fan, H. Aneetha, J. C. Huffman, G. Wu and D. J. Mindiola, *J. Am. Chem. Soc.*, 2006, **128**, 13575.
- 3 For some representative examples, see: (a) D. S. Laitar, C. J. N. Mathison, W. M. Davis and J. P. Sadighi, *Inorg. Chem.*, 2003, **42**, 7354; (b) S. Hong, L. M. R. Hill, A. K. Gupta, B. D. Naab, J. B. Gilroy, R. G. Hicks, C. J. Cramer and W. B. Tolman, *Inorg. Chem.*, 2009, **48**, 4514; (c) D. T. Carey, E. K. Cope-Eatough, E. Vilaplana-Mafé, F. S. Mair, R. G. Pritchard, J. E. Warren and R. J. Woods, *Dalton Trans.*, 2003, 1083; (d) H. A. Chiong and O. Daugulis, *Organometallics*, 2006, **25**, 4054; (e) A. G. M. Barrett, M. R. Crimmin, M. S. Hill, P. B. Hitchcock and P. A. Procopiou, *Angew. Chem., Int. Ed.*, 2007, **46**, 6339; (f) S. Kernbichl, M. Reiter, F. Adams, S. Vagin and B. Rieger, *J. Am. Chem. Soc.*, 2017, **139**, 6787; (g) S. Kundu, W. Y. Kim, J. A. Bertke and T. H. Warren, *J. Am. Chem. Soc.*, 2017, **139**, 1045; (h) K. S. Choung, M. D. Islam, R. W. Gou and T. S. Teets, *Inorg. Chem.*, 2017, **56**, 14326.
- 4 (a) V. Regnier, Y. Planet, C. E. Moore, J. Pecaut, C. Philouze and D. Martin, *Angew. Chem., Int. Ed.*, 2017, **56**, 1031; (b) D. C. H. Do, A. Keyser, A. V. Protchenko, B. Maitland, I. Pernik, H. Niu, E. L. Kolychev, A. Rit, D. Vidovic, A. Stasch, C. Jones and S. Aldridge, *Chem.–Eur. J.*, 2017, **23**, 5830; (c) I. Pernik, B. Maitland, A. Stasch and C. Jones, *Can. J. Chem.*, 2018, **96**, 513; (d) M. Tripathi, V. Regnier, C. Lincheneau and D. Martin, *New J. Chem.*, 2017, **41**, 15016.
- 5 (a) C. M. Byrne, S. D. Allen, E. B. Lobkovsky and G. W. Coates, *J. Am. Chem. Soc.*, 2004, **126**, 11404; (b) R. Jiao, X. Shen, M. Xue, Y. Zhang, Y. Yao and Q. Shen, *Chem. Commun.*, 2010, **46**, 4118; (c) M. M. Rodriguez, E. Bill, W. W. Brennessel and P. L. Holland, *Science*, 2011, **334**, 780; (d) L. A. Harris, E. C. Y. Tam, M. P. Coles and J. R. Fulton, *Dalton Trans.*, 2014, **43**, 13803; (e) K. Grubel, W. W. Brennessel, B. Q. Mercado and P. L. Holland, *J. Am. Chem. Soc.*, 2014, **136**, 16807; (f) A. Kalita, V. Kumar and B. Mondal, *RSC Adv.*, 2015, **5**, 643.
- 6 (a) J. D. Azoulay, R. S. Rojas, A. V. Serrano, H. Ohtaki, G. B. Galland, G. Wu and G. C. Bazan, *Angew. Chem., Int. Ed.*, 2009, **48**, 1089; (b) J. D. Azoulay, Y. Schneider and G. C. Bazan, US20090299020A1, 2009; (c) J. D. Azoulay, G. C. Bazan and G. B. Galland, *Macromolecules*, 2010, **43**, 2794; (d) A. Sokolohorskyj, O. Zeleznik, I. Cisarova, J. Lenz, A. Lederer and J. Merna, *J. Polym. Sci., Part A: Polym. Chem.*, 2017, **55**, 2440.
- 7 (a) J. D. Azoulay, Y. Schneider, G. B. Galland and G. C. Bazan, *Chem. Commun.*, 2009, 6177; (b) J. D. Azoulay, H. Y. Gao, Z. A. Koretz, G. Kehr, G. Erker, F. Shimizu, G. B. Galland and G. C. Bazan, *Macromolecules*, 2012, **45**, 4487.
- 8 For the reaction of dioxygen with NacNac–cobalt complexes, see: (a) M. C. Weiss and V. L. Goedken, *J. Am. Chem. Soc.*, 1976, **98**, 3389; (b) B. Durham, T. J. Anderson, J. A. Switzer, J. F. Endicott and M. D. Glick, *Inorg. Chem.*, 1977, **16**, 271; (c) J. A. Switzer and F. J. Endicott, *J. Am. Chem. Soc.*, 1980, **102**, 1181 NacNac–iron complexes: (d) D. P. Riley and D. H. Busch, *Inorg. Chem.*, 1983, **22**, 4141; (e) D. B. MacQueen, C. Lange, M. Calvin, J. W. Otvos, L. O. Spreer, C. B. Allan, A. Ganse and R. B. Frankel, *Inorg. Chim. Acta*, 1997, **263**, 125 For lanthanides: (f) J. Zhang, Z. Zhang, Z. Chen and X. Zhou, *Dalton Trans.*, 2012, **41**, 357 For alkaline earths: (g) B. Liu, V. Dorcet, L. Maron, J. F. Carpentier and Y. Sarazin, *Eur. J. Inorg. Chem.*, 2012, 3023.
- 9 S. Yokota, Y. Tachi and S. Itoh, *Inorg. Chem.*, 2002, **41**, 1342.
- 10 V. Regnier, F. Molton, C. Philouze and D. Martin, *Chem. Commun.*, 2016, **52**, 11422.
- 11 (a) D. Martin, C. E. Moore, A. L. Rheingold and G. Bertrand, *Angew. Chem., Int. Ed.*, 2013, **52**, 7014; (b) J. K. Mahoney, D. Martin, F. Thomas, C. Moore, A. L. Rheingold and G. Bertrand, *J. Am. Chem. Soc.*, 2015, **137**, 7519.
- 12 For the reaction of stable carbenes with CO, see also: (a) V. Lavallo, Y. Canac, B. Donnadieu, W. W. Schoeller and G. Bertrand, *Angew. Chem., Int. Ed.*, 2006, **45**, 3488; (b) T. W. Hudnall and C. W. Bielawski, *J. Am. Chem. Soc.*, 2009, **131**, 16039; (c) U. Siemeling, C. Färber, C. Bruhn, M. Leibold, D. Selent, W. Baumann, M. von Hopffgarten, C. Goedecke and G. Frenking, *Chem. Sci.*, 2010, **1**, 697; (d) T. Schulz, C. Färber, M. Leibold, C. Bruhn, W. Baumann, D. Selent, T. Porsch, M. C. Holthausen and U. Siemeling, *Chem. Commun.*, 2013, **49**, 6834; (e) T. Schulz, C. Färber, M. Leibold, C. Bruhn, P. Prochnow, J. E. Bandow, T. Schneider, T. Porsch, M. C. Holthausen and U. Siemeling, *Chem. Commun.*, 2014, **50**, 2341.
- 13 For the quest on stable 1,3-(diamino)oxyallyl derivatives, see: (a) V. Regnier and D. Martin, *Org. Chem. Front.*, 2015, **2**, 1536; (b) M. Devillard, V. Regnier, M. Tripathi and D. Martin, *J. Mol. Struct.*, 2018, **1172**, 3.
- 14 (a) H. Ahlbrecht, W. Raab and C. Vonderheid, *Synthesis*, 1979, 127; (b) R. Pajkert, T. Böttcher, M. Ponomarenko, M. Bremer and G.-V. Rösenthaler, *Tetrahedron*, 2013, **69**, 8943.
- 15 For the reaction of *m*-CPBA with halides see: (a) N. J. Bunce and D. D. Tanner, *J. Am. Chem. Soc.*, 1969, **91**, 6096; (b) M. Srebnik, *Synth. Commun.*, 1989, **19**, 197.
- 16 Experimental EPR spectra were fitted with the EasySpin simulation package: S. Stoll and A. Schweiger, *J. Magn. Reson.*, 2006, **178**, 42.
- 17 DFT calculations were performed using the program package Gaussian09: *Gaussian 09*, M. J. Frisch, G. W. Trucks, H. B. Schlegel, G. E. Scuseria, M. A. Robb, J. R. Cheeseman, *et al.*, Gaussian Inc., Wallingford CT, 2009. See ESI† for complete citation and further details.



- 18 The trione is usually isolated as a mixture with its hydrate: Z. L. Wang, X. L. An, L. S. Ge, J.-H. Jin, X. Luo and W.-P. Deng, *Tetrahedron*, 2014, **70**, 3788.
- 19 (a) C. A. Dyker, V. Lavallo, B. Donnadieu and G. Bertrand, *Angew. Chem., Int. Ed.*, 2008, **47**, 3206; (b) W.-C. Chen, Y.-C. Hsu, C.-Y. Lee, G. P. A. Yap and T.-G. Ong, *Organometallics*, 2013, **32**, 2435.
- 20 A. K. Diba, C. Noll, M. Richter, M. T. Gieseler and M. Kalesse, *Angew. Chem., Int. Ed.*, 2010, **49**, 8367.
- 21 We propose that further reaction of 13^{2+} with m-CPBA yields Bayer-Villiger type products, either (imidazolyl)-carbonates or carboxylate derivatives. These electrophiles being highly activated, they would readily undergo hydrolysis, affording 1,3-dimethylbenzimidazolium salts.
- 22 For a convenient protocole for the condensation of anilines with acetylacetone, see: L.-M. Tang, Y.-Q. Duan, X.-F. Li and Y.-S. Li, *J. Organomet. Chem.*, 2006, **691**, 2023.
- 23 Such compounds have been mentioned in patents: Y. Tang, Z. Chen, G. Ji, X. Sun, C. Xu and J. Li, WO 2015024517, 2015.
- 24 In parented Pt-complexes the ^{13}C chemical shift of the central carbon is in the 80–110 ppm range: M. L. Scheuermann, U. Fekl, W. Kaminsky and K. I. Goldberg, *Organometallics*, 2010, **29**, 4749.
- 25 M. Arrowsmith, M. R. Crimmin, M. S. Hill and G. Kociok-Köhn, *Dalton Trans.*, 2013, **42**, 9720.





A computational study of the interplay of steric and electronic effects in the stabilization of 1,3-(diamino)oxyallyls

Marc Devillard, Vianney Regnier, Monika Tripathi, David Martin*

UMR CNRS-UGA 5250, Département de Chimie Moléculaire, University of Grenoble-Alpes, CS 40700, 38058, Grenoble cedex 9, France

ARTICLE INFO

Article history:

Received 20 November 2017

Received in revised form

25 January 2018

Accepted 7 February 2018

Available online 8 February 2018

Keywords:

Substituent effects

DFT calculations

Cyclopropanones

Oxyallyls

ABSTRACT

Ring opening of cyclopropanones affords non-Kekulé oxyallyls, which are usually fleeting intermediates. However, recent experimental results showed that amino-substituted versions can be stable enough to be characterized in solution by NMR spectroscopy. Herein, the role of substituents in the stabilization of oxyallyls was examined by DFT calculations at the B3LYP/6-311g(d,p) level of theory. The stability of model compounds, relative to their cyclic structural isomers, was evaluated for simple substituents covering a broad range of electronic properties. The particular case of the model 1,3-bis(amino)oxyallyl (H₂N)CHCOCH(NH₂) has been examined from a conformational standpoint to shed light on the interplay of sterics and electronic influence of the amino substituents. Finally, model tetrasubstituted di(amino)oxyallyls were considered and provided few general guidelines for the design of new stable derivatives with oxyallyl patterns.

© 2018 Elsevier B.V. All rights reserved.

1. Introduction

Oxyallyls **A** (see Fig. 1) are non-Kekulé molecules, whose structure can be assigned to zwitterionic or biradical limit forms [1,2]. They are structural isomers of cyclopropanones **B**, along with other functional groups, such as methyleneoxiranes **C**, enones **D** and oxetenes **E**. Since the 1960s, they have been postulated as the key reactive intermediates in numerous [4 + 3] cycloadditions [3], rearrangement reactions, Nazarov-type cyclisations [4] and the biosynthesis of prostaglandins [5].

The cyclization of prototypical oxyallyls into the corresponding cyclopropanone is almost barrierless and had precluded their direct observations for decades. Measurements of the activation energy for the disrotatory ring opening of cyclopropanones, which can be approximated to the oxyallyl-cyclopropanone energy difference, demonstrated that steric effects can be used to destabilize cyclopropanones relatively to their oxyallyl isomer. For instance, this value is lowered from 30 kcal mol⁻¹ for the *trans*-di(tertbutyl) cyclopropanone [6], down to +9.8 kcal mol⁻¹ for **1**, which features very bulky *cis* substituents (Scheme 1) [7]. Even in this very favorable case, the oxyallyl remains the less stable form. In contrast, Lahti et al. predicted that the ring opening of strained bicyclo[2.1.0]

pentan-5-ones **2** should be thermodynamically favored [8]. However, despite several attempts, these compounds have eluded spectroscopic observation so far [9]. In 2011, the group of Garcia-Garibay reported the generation of di(cyclohexyl)oxyallyl **3** in the crystalline state [10]. The packed environment hindered the ring closure to the point that the half-life of **3** reaches 42 min at 298 K, allowing for the first time the direct observation of an oxyallyl intermediate.

In the recent years, several authors, including our team, reported the synthesis of amino-substituted oxyallyls **4a-c** (Scheme 2) [11]. These compounds are dramatically more persistent than their elusive alkyl-substituted counterparts. Species **4a-b** could be characterized by NMR in solution, but rearranged into **5a-b** above -10 °C [12]. The group of Siemeling reported the isolation and the X-Ray diffraction structure of a lithium chloride complex of oxyallyl **4c** [13]. Last year, we could generate metal-free **4c** and show that its half-life in acetonitrile is almost 1 h at room temperature [14].

Amino groups are strong π -donors and, of course, their introduction modifies significantly the electronic structure of the oxyallyl core. Because of the extension of the delocalized π -system, zwitterionic resonance structures are expected to outweigh the biradical ones (for canonical structures of **A**, see Fig. 1). Importantly, the influence of electronic effects of 1,3-substituents on the relative stability of oxyallyls hasn't been really assessed yet. Even the case of amino groups remains unclear. So far, only the parent 1,3-

* Corresponding author.

E-mail address: david.martin@univ-grenoble-alpes.fr (D. Martin).

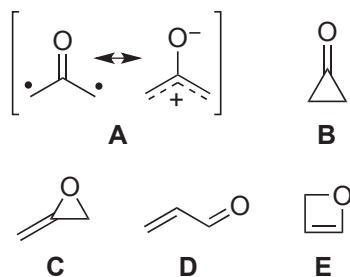
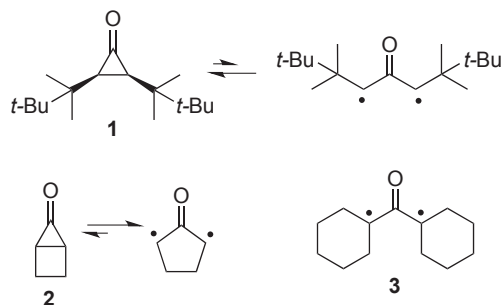
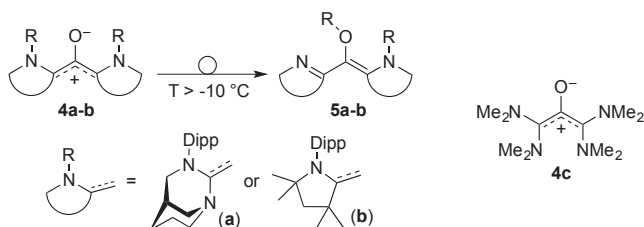


Fig. 1. Structural isomers of C_3H_4O .



Scheme 1. Influence of ring strain and steric hindrance on the cyclopropanone-oxallyl equilibrium.



Scheme 2. Reported amino-substituted oxallyls and related compounds; Dipp = 2,6-di(isopropyl)phenyl.

bis(dimethylamino)oxallyl has been briefly considered with computational methods. This unhindered di(amino)oxallyl features a planar π -system. As expected, it is a close-shell molecule with a high singlet-triplet energy gap [15]. However, in the experimentally generated compounds **4a–c** steric hindrance results in twisted C–N bonds. Such distortions blur the genuine electronic effect of the substituent. It is known from amide, ureas and iminium series that the $-I$ inductive effect of nitrogen atom becomes significant, as the $+M$ π -donation of the amino group is hampered. In extreme cases, it may even prevail, thus resulting in species with unusual properties and reactivity [16].

Herein we propose to probe the role of substituents in the stabilization of oxallyls. We considered model compounds with simple substituents covering a broad range of electronic properties. We evaluated their stability, relative to their cyclic structural isomers, with an emphasis on the interplay of steric and electronic effects in 1,3-di(amino)oxallyls.

2. Computational methods

We carried out calculations using the density functional theory as implemented in the program package Gaussian09 [21], with the B3LYP exchange–correlation functional [22] and the 6-311G(d,p)

basis set. Indeed **5a**, one of the very few observed di(amino)oxallyl, as well as related (amino)(carboxy)radicals, were previously studied at this level of theory and calculations well reproduced experimental data, including NMR chemical shifts [12a] or geometry from x-ray diffraction studies [12b]. The parent all-H substituted oxallyl was only considered out of curiosity. Indeed it is a well known problematic particular case for DFT [17], which fails to recognize the transition state nature of its singlet ground state [18].

Singlet oxallyls were investigated as open shell molecules with broken spin symmetry [keyword guess(mix, always) in Gaussian09; UB3LYP/6-311g(d,p) level of theory]. All structures were submitted to vibrational analysis and minima were characterized by the absence of imaginary frequencies. Relaxed optimized energy as a function of angles or torsions, were performed with 10° steps. A global scan was first performed. The results were smoothed with additional local scans around all local minima, in order to eliminate artefacts due to a single monodirectional scan.

3. Results

We first considered symmetric 1,3-disubstituted oxallyls **A_R**, as well as their corresponding cyclopropanone **B_R** and methyleneoxirane **C_R** isomers. Model substituents R were selected in order to cover a broad range of electronic effects and their size was kept as small as possible in order to minimize steric effects. In Table 1, the electron donating capability of R decreases from entry 1 to entry 12 [19]. Amino-substituted oxallyls (R = NMe₂ or NH₂, entries 1–2) have a close-shell singlet ground state. The first excited triplet state was found at more than $+20$ kcal mol⁻¹, the corresponding cyclopropanone and methyleneoxirane being even higher in energy. In marked contrast, classical oxallyls, with H or methyl substituents, are in the exact opposite situation. The corresponding cyclopropanone is the most stable isomer, followed by the methyleneoxirane, the oxallyl form being a high-energy biradicaloid (entries 6–7).

More generally, it can be stated that closed-shell ground states are achieved with strong donor substituents. Increased electron withdrawing effects generally destabilize **A_R** relatively to **B_R** and **C_R**. Entries 3 and 9 are the only clear exceptions. They correspond to vinylogous versions of NH₂ and COH substituents, respectively. The extension of the delocalized π -system by 4 carbon atoms results both in the stabilization of **A_R** and a significant decrease of the singlet-triplet gap. This result is especially interesting, as it indicates that biradicaloid linear ketocyanines dyes, which were recently proposed [20], could be viable targets.

Therefore any steric hindrance that induces twisting of an amino group is expected to be detrimental for the stability of 1,3-di(amino)oxallyls with respect to other isomers, as it results in decreased $+M$ donation. We considered energy as a function of symmetrical torsions θ_1 around the C–N bonds, for model compounds **ANH₂–CNH₂** (Fig. 2). As shown on Fig. 3, varying θ_1 doesn't modify the energy of cyclopropanone **B_{NH₂}** and methyleneoxirane **C_{NH₂}** by more than a few kcal.mol⁻¹. These small variations are likely resulting from subtle changes in steric interactions between substituents. In marked contrast, as expected, oxallyl **ANH₂** is critically destabilized when increasing θ_1 . Strikingly, no minimum of energy for an oxallyl form could even be found for $\theta_1 > 60^\circ$. When $\theta_1 = 0^\circ$, the lone pair of the nitrogen atom is fully conjugated with the π -system. Conversely, when $\theta_1 = 90^\circ$, there is no possible π -conjugation and the amino becomes a $-I$ inductive group. Therefore increasing θ_1 amount to increase electron-withdrawing properties of the N-substituent. In other words, the stability of 1,3-disubstituted oxallyls compared to their corresponding cyclopropanone isomers increases as the substituents are more

Table 1
Influence of substituents on the relative energies of oxyallyls A_R , cyclopropanones B_R and methyleneoxiranes C_R .

Entry	R	ΔE_{S-T}	E_B^a	E_C^a
1	NMe ₂	+22.3	+23.1	+23.9
2	NH ₂	+20.9	+27.5	+26.2
3	CHCHNH ₂	+5.1	+19.3	+20.5
4	OMe	+10.7	+3.0	+7.2
5	OH	+1.5	+1.9	+1.9
6	Me	+4.3	-13.7	-6.5
7	H	-1.0	-26.2	-15.3
8	CCH	+1.3	-3.1	+5.0
9	CHCHCOH	+0.5	+6.2	+9.3
10	COH	-1.5	-18.0	-11
11	CN	-0.5	-11.9	-3.2
12	NO ₂	-0.4	-33.3	-24.0

^a Energies are given with zero-point correction in kcal.mol⁻¹ and are relative to the corresponding singlet oxyallyl ¹A_R.

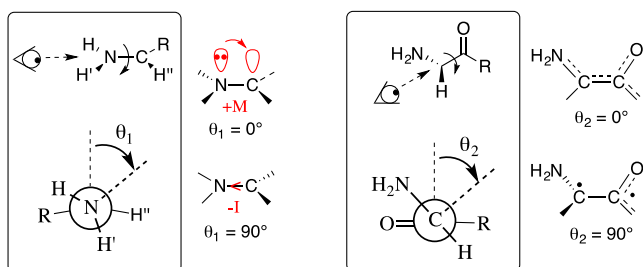
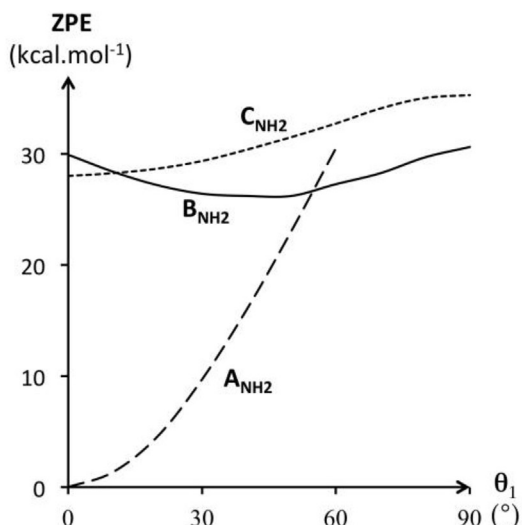


Fig. 2. Torsion angles θ_1 (left) and θ_2 (right).

electron-donor.

Steric hindrance also induces torsions (θ_2 and θ_2') around the two (N)C–C(O) bonds (see Fig. 2). Indeed, the optimized structures of **4a–c** are symmetrical with $\theta_2 = \theta_2' = 10, 13$ and 23° , respectively. Here again, as such twisting hampers an optimal conjugation of the π -system, it is expected to be detrimental for the stability of 1,3-di(amino)oxyallyls. We scanned the relaxed optimized energy of **A**_{NH₂} as a function of θ_2 and θ_2' (Fig. 4). The surface of energy can be delimited in areas, which correspond to as many isomers of **A**_{NH₂}.



As expected the lowest energy minimum corresponds to the planar all-*trans* oxyallyl ($\theta_2 = \theta_2' = 0^\circ$). This latter is destabilized when varying simultaneously θ_2 and θ_2' to ultimately favor the cyclopropanone isomer for $60^\circ < \theta_2, \theta_2' < 110^\circ$ (see sectional view 4a), whereas varying of θ_2 with $\theta_2 \approx 0^\circ$ will favor the cyclopropanone form for $80^\circ < \theta_2 < 120^\circ$ (see sectional view 4b).

Next, we considered model tetrasubstituted 1,3-di(amino)oxyallyls **A**_(NH₂,R) (see Table 2). Interestingly, in all cases, the oxyallyl was more stable than its cyclopropanone isomer by about 30–35 kcal mol⁻¹. In contrast, the singlet-triplet gap was significantly sensitive to the R substituent and decreased when increasing the electron-withdrawing capability of R (entries 1–5). In other words, capto-dative substitution stabilize the triplet diradical state of **A**_(NH₂,R). Importantly, the C–C bond length in cyclopropanones **B**_(NH₂,R) increases accordingly in the series, from 159 ppm (R = H) up to 178 pm (R = CN). The weakening of this bond by capto-dative substitution, is also evident from the resulting decreased stretching frequency of the bond (from 699 cm⁻¹ to 552 cm⁻¹). Note that for R = CHO, the cyclopropanone does not correspond to a minimum of energy. It is predicted to be a transition state for the *cis-trans* interconversion of the corresponding oxyallyl.

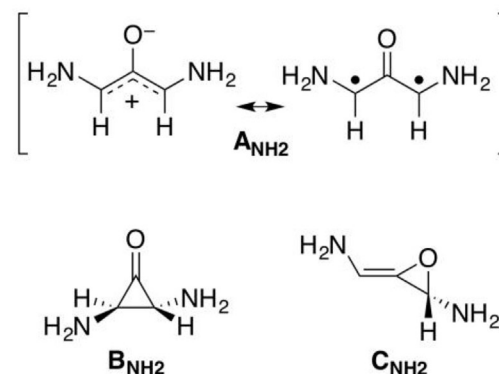


Fig. 3. Energy (with zero-point correction) of **A**_{NH₂}, **B**_{NH₂} and **C**_{NH₂} as a function of θ_1 . The C₂ axis of the molecule was maintained: torsions around the two C–N bonds are identical.

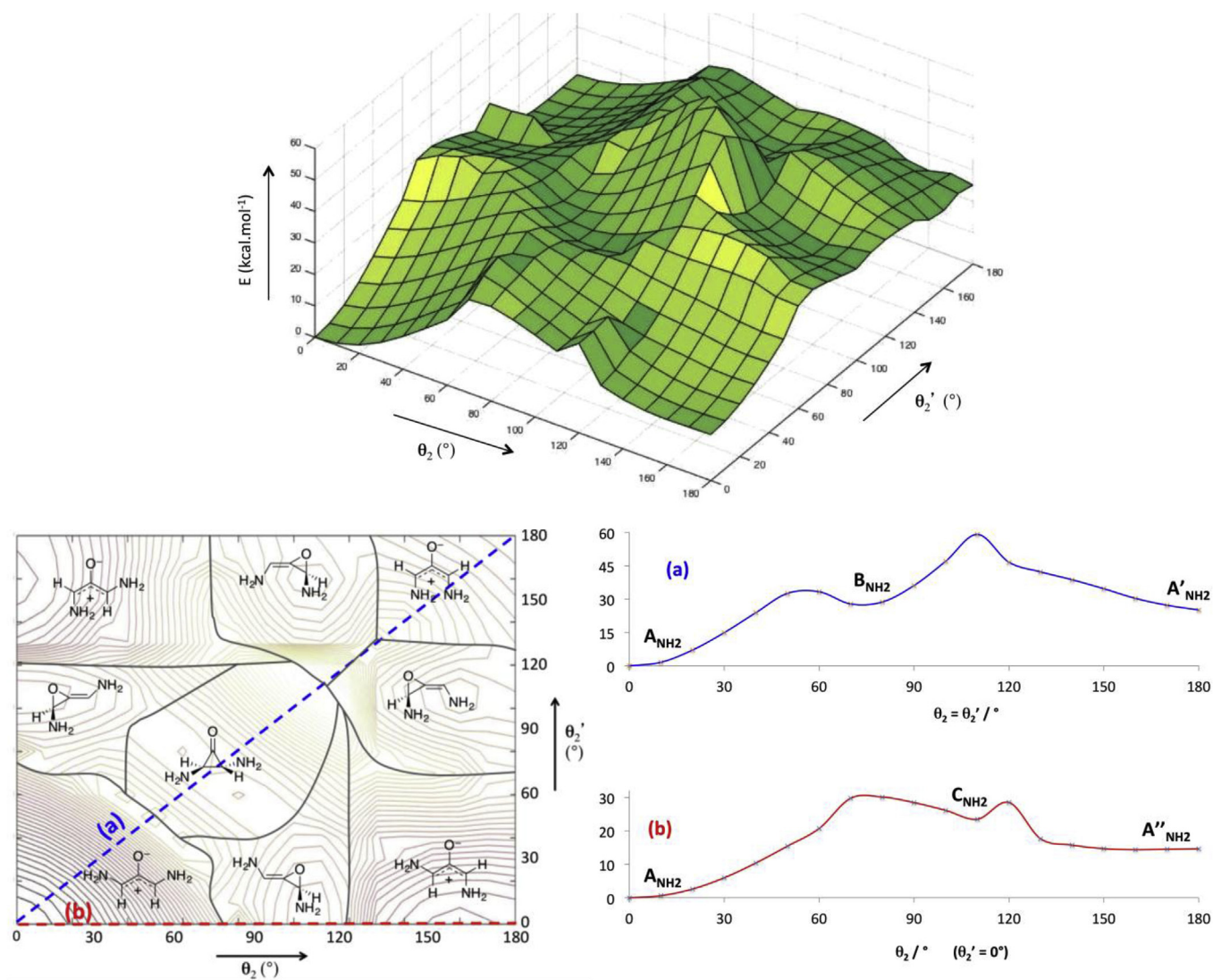
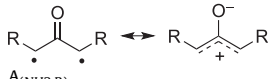
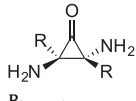


Fig. 4. 3D representation of the relaxed optimized energy of A_{NH_2} as a function of torsions θ_2 and θ_2' , and projection with demarcation of areas corresponding to the most stable isomer. Sectional view a (in blue) represents energy as a function of θ_2 , the C_2 axis of the molecule is maintained and torsions around the two C–C bonds are identical; in sectional view b (in red) only one C–C bond is twisted, the second being constant at $\theta_2' = 0^\circ$. (For interpretation of the references to colour in this figure legend, the reader is referred to the Web version of this article.)

Table 2

Relative energies of tetrasubstituted 1,3-di(amino)oxyallyls $A_{(NH_2,R)}$ and the corresponding cyclopropanones $B_{(NH_2,R)}$.

Entry	$A_{(NH_2,R)}$ 		$B_{(NH_2,R)}$ 		
	R	ΔE_{S-T}	E_B^a	d_{CC}^c	ω_{CC}^d
1	H	+20.9	+27.5	159	699
2	NH ₂	+23.8	+32.8	160	674
3	CCH	+12.2	+34.8	164	624
4	CHO	+6.0	+30.5 ^b	176	559
5	CN	+11.5	+31.7	178	552

^a Energies are given with zero-point correction in kcal.mol⁻¹ and are relative to the corresponding singlet oxallyl ¹A.

^b Optimized structure of cyclopropanone corresponds to a transition state.

^c Computed H₂NC–CNH₂ bond length of the cyclopropanone ring (in pm).

^d Computed stretching frequency of the H₂NC–CNH₂ bond (in cm⁻¹).

4. Conclusion

At least two strong electron-donors are required to favor 1,3-substituted oxyallyls over their cyclopropanone form, regardless of steric hindrance. In this context, amino groups should be ideal. However, examination of the interplay of sterics and electronic effect of the substituent reveals a more complex situation. Indeed, the stabilization of the corresponding 1,3-di(amino)oxyallyls is very sensitive to the conjugation of the lone pair of the nitrogen atom with the π -system of the oxyallyl moiety, any deviation from ideal planarity being detrimental.

Amino groups are among the most electron donating substituents. Given that known 1,3-di(amino)oxyallyls rearrange prior to isolation and cannot be isolated, it is clear that the design of bottle-able derivatives requires extra stabilizing features. This work indicates that the introduction of a second set of substituents in a captodative manner, as well as the extension of the conjugated skeleton, are always beneficial. These approaches are certainly complementary and allow the achievement of both a significantly stabilized oxyallyl and a low singlet-triplet energy gap. This suggests that the corresponding biradicaloids are viable synthetic targets. We are actually exploring the possibility to isolate such compounds in our laboratory.

Acknowledgements

This work was funded by the French National Agency for Research (ANR-14-CE06-0013-01 and ANR-17-ERC2-0015-01) and the University of Grenoble-Alpes (Agir-Pole). The author is grateful to the "Centre de Calcul Intensif en Chimie" of Grenoble (CECIC) for providing computational resources.

Appendix A. Supplementary data

Supplementary data related to this article can be found at <https://doi.org/10.1016/j.molstruc.2018.02.029>.

References

- [1] (a) R. Hoffmann, *J. Am. Chem. Soc.* 90 (1968) 1475; (b) M. Abe, *Chem. Rev.* 113 (2013) 7011.
- [2] (a) For an overview of the quest for observable oxyallyl derivatives, see V. Regnier, D. Martin, *Org. Chem. Front* 2 (2015) 1536; (b) For related reactive intermediates, see D.J. Tantillo, K.N. Houk, R.V. Hoffman, J. Tao, *J. Org. Chem.* 64 (1999) 3830.
- [3] For reviews, see: (a) A.G. Lohse, R.P. Hsung, *Chem. Eur J.* 17 (2011) 3812; (b) M. Harmata, *Chem. Commun.* 46 (2010) 8904; (c) M. Harmata, *Chem. Commun.* 46 (2010) 8886; (d) H.F. Bettinger, *Angew. Chem. Int. Ed.* 49 (2010) 670; (e) M. Harmata, *Adv. Synth. Catal.* 348 (2006) 2297; (f) M.A. Battiste, P.M. Pelphrey, D.L. Wright, *Chem. Eur J.* 12 (2006) 3438; (g) I.V. Hartung, H.M.R. Hoffmann, *Angew. Chem. Int. Ed.* 43 (2004) 1934; (h) M. Harmata, P. Rashatasakhon, *Tetrahedron* 59 (2003) 2371; (i) M. Harmata, *Acc. Chem. Res.* 34 (2001) 595; (j) J.H. Rigby, F.C. Pigge, *Org. React.* 51 (1997) 351; (k) M. Harmata, *Tetrahedron* 53 (1997) 6235; (l) A.R. Katritzky, N. Dennis, *Chem. Rev.* 89 (1989) 827.
- [4] (a) P.J. Chenier, *J. Chem. Educ.* 55 (1978) 286; (b) F.G. Bordwell, R.G. Scamehorn, W.R. Springer, *J. Am. Chem. Soc.* 91 (1969) 2087; (c) F.G. Bordwell, J.G. Strong, *J. Org. Chem.* 38 (1973) 579; (d) N. Tsuchida, S. Yamazaki, S. Yamabe, *Org. Biomol. Chem.* 6 (2008) 3109; (e) G. Liang, D. Trauner, *J. Am. Chem. Soc.* 126 (2004) 9544; (f) W. He, I.R. Herrick, T.A. Atesin, P.A. Caruana, C.A. Kellenberger, A.J. Frontier, *J. Am. Chem. Soc.* 130 (2008) 1003; (g) E. Lee, C.H. Yoon, *J. Chem. Soc. Chem. Commun.* (1994) 479; (h) G.D. Hamblin, R.P. Jimenez, T.S. Sorensen, *J. Org. Chem.* 72 (2007) 9439.
- [5] (a) E.J. Corey, S.P.T. Matsuda, R. Nagata, M.B. Cleaver, *Tetrahedron Lett.* 29 (1988) 2555; (b) R. Koljak, O. Boudaud, B.-H. Shieh, N. Samei, A.R. Brash, *Science* 277 (1997) 1994; (c) B.A. Hess Jr., L. Smentek, A.R. Brash, J.K. Cha, *J. Am. Chem. Soc.* 121 (1999) 5603.
- [6] (a) D.B. Sclove, J.F. Pazos, R.L. Camp, F.D. Greene, *J. Am. Chem. Soc.* 92 (1970) 7488; (b) J.F. Pazos, J.G. Pacifici, G.O. Pierson, D.B. Sclove, F.D. Greene, *J. Org. Chem.* 39 (1974) 1990.
- [7] T.S. Sorensen, F. Sun, *J. Chem. Soc. Perkin Trans. 2* (1998) 1053.
- [8] A.S. Ichimura, P.M. Lahti, A.R. Matlin, *J. Am. Chem. Soc.* 112 (1990) 2868.
- [9] (a) T. Hirano, T. Kumagai, T. Miyashi, K. Akiyama, Y. Ikegami, *J. Org. Chem.* 56 (1991) 1907; (b) A.P. Masters, M. Parvez, T.S. Sorensen, F. Sun, *J. Am. Chem. Soc.* 116 (1994) 2804; (c) A.R. Matlin, P.M. Lahti, D. Appella, A. Straumanis, S. Lin, H. Patel, K. Jin, K.P. Schrieber, J. Pauls, P. Raulerson, *J. Am. Chem. Soc.* 121 (1999) 2164.
- [10] G. Kuzmanich, F. Spänig, C.-K. Tsai, J.M. Um, R.M. Hoekstra, K.N. Houk, D.M. Guldi, M.A. Garcia-Garibay, *J. Am. Chem. Soc.* 133 (2011) 2342.
- [11] A ferrocene-based derivative was also isolated. However it is better described as a zwitterionic enol rather than an oxyallyl, because only one amidinium unit is conjugated with the carbonyl moiety, see U. Siemeling, C. Färber, C. Bruhn, M. Leibold, D. Selent, W. Baumann, M. von Hopffgarten, C. Goedecke, G. Frenking, *Chem. Sci.* 1 (2010) 697.
- [12] (a) D. Martin, C.E. Moore, A.L. Rheingold, G. Bertrand, *Angew. Chem. Int. Ed.* 52 (2013) 7014; (b) J.K. Mahoney, D. Martin, F. Thomas, C. Moore, A.L. Rheingold, G. Bertrand, *J. Am. Chem. Soc.* 137 (2015) 7519; (c) S.D. Ursula, U. Radius, *Organometallics* 36 (2017) 1398.
- [13] T. Schulz, C. Färber, M. Leibold, C. Bruhn, W. Baumann, D. Selent, T. Porsch, M.C. Holthausen, U. Siemeling, *Chem. Commun.* 49 (2013) 6834.
- [14] V. Regnier, F. Molton, C. Philouze, D. Martin, *Chem. Commun.* 52 (2016) 11422.
- [15] J. Fabian, R. Peichert, *J. Phys. Chem.* 23 (2010) 1137.
- [16] (a) H.K. Hall, A. El-Shekeil, *Chem. Rev.* 83 (1983) 549; (b) A. Berkessel, R.K. Thauer, *Angew. Chem. Int. Ed.* 34 (1995) 2247; (c) K. Tani, B.M. Stoltz, *Nature* 441 (2006) 731; (d) J. Clayden, W.J. Moran, *Angew. Chem. Int. Ed.* 45 (2006) 7118; (e) T. Ly, M. Krout, D.K. Pham, K. Tani, B.M. Stoltz, R.R. Julian, *J. Am. Chem. Soc.* 129 (2007) 1864; (f) D. Martin, N. Lassauque, B. Donnadiou, G. Bertrand, *Angew. Chem. Int. Ed.* 51 (2012) 6172; (g) D. Martin, N. Lassauque, F. Steinman, G. Manuel, G. Bertrand, *Chem. Eur J.* 19 (2013) 14895.
- [17] For discussions and recent calculations on the simplest oxyallyl, see: (a) L.V. Slipchenko, A.I. Krylov, *J. Chem. Phys.* 117 (2002) 4694; (b) L.V. Slipchenko, A.I. Krylov, *J. Chem. Phys.* 123 (2005), 084107; (c) J. Brabec, J. Pittner, *J. Phys. Chem. A* 110 (2006) 11765; (d) O. Demel, K.R. Shamasundar, L. Kong, M. Nooijen, *J. Phys. Chem. A* 112 (2008) 11895; (e) X.Z. Li, J. Paldus, *J. Chem. Phys.* 129 (2008), 174101.
- [18] (a) T. Ichino, S.M. Villano, A.J. Gianola, D.J. Goebbert, L. Velarde, A. Sanov, S.J. Blanksby, X. Zhou, D.A. Hrovat, W.T. Borden, W.C. Lineberger, *Angew. Chem. Int. Ed.* 48 (2009) 8509; (b) T. Ichino, S.M. Villano, A.J. Gianola, D.J. Goebbert, L. Velarde, A. Sanov, S.J. Blanksby, X. Zhou, D.A. Hrovat, W.T. Borden, W.C. Lineberger, *J. Phys. Chem. A* 115 (2011) 1634.
- [19] The σ Hammett parameters provide of measure of the electron donating ability of a substituent C. Hansch, A. Leo, R.W. Taft, *Chem. Rev.* 91 (1991) 165.
- [20] K. Yesudas, E.D. Jemmis, K. Bhanuprakash, *Phys. Chem. Chem. Phys.* 17 (2015) 12988.
- [21] M.J. Frisch, G.W. Trucks, H.B. Schlegel, G.E. Scuseria, M.A. Robb, J.R. Cheeseman, G. Scalmani, V. Barone, B. Mennucci, G.A. Petersson, H. Nakatsuji, M. Caricato, X. Li, H.P. Hratchian, A.F. Izmaylov, J. Bloino, G. Zheng, J.L. Sonnenberg, M. Hada, M. Ehara, K. Toyota, R. Fukuda, J. Hasegawa, M. Ishida, T. Nakajima, Y. Honda, O. Kitao, H. Nakai, T. Vreven, J.A. Montgomery Jr., J.E. Peralta, F. Ogliaro, M. Bearpark, J.J. Heyd, E. Brothers, K.N. Kudin, V.N. Staroverov, R. Kobayashi, J. Normand, K. Raghavachari, A. Rendell, J.C. Burant, S.S. Iyengar, J. Tomasi, M. Cossi, N. Rega, J.M. Millam, M. Klene, J.E. Knox, J.B. Cross, V. Bakken, C. Adamo, J. Jaramillo, R. Gomperts, R.E. Stratmann, O. Yazyev, A.J. Austin, R. Cammi, C. Pomelli, J.W. Ochterski, R.L. Martin, K. Morokuma, V.G. Zakrzewski, G.A. Voth, P. Salvador, J.J. Dannenberg, S. Dapprich, A.D. Daniels, Ö. Farkas, J.B. Foresman, J.V. Ortiz, J. Cioslowski, D.J. Fox, *Gaussian 09*, Gaussian Inc., Wallingford CT, 2009.
- [22] (a) A.D. Becke, *J. Chem. Phys.* 98 (1993) 5648; (b) C. Lee, W. Yang, R.G. Parr, *Phys. Rev. B* 37 (1988) 785; (c) S.H. Vosko, L. Wilk, M. Nusair, *Can. J. Phys.* 58 (1980) 1200; (d) P.J. Stephens, F.J. Devlin, C.F. Chabalowski, M.J. Frisch, *J. Phys. Chem.* 98 (1994) 11623.

